Microwave-Assisted Preparation of Inorganic Nanostructures in Liquid Phase

ARTICLE *in* CHEMICAL REVIEWS · JUNE 2014

Impact Factor: 46.57 · DOI: 10.1021/cr400366s · Source: PubMed

2 AUTHORS:

Ying-Jie Zhu
Chinese Academy of Sciences
215 PUBLICATIONS **6,862** CITATIONS
SEE PROFILE

Feng Chen
Chinese Academy of Sciences
93 PUBLICATIONS **1,556** CITATIONS
SEE PROFILE

CHEMICAL REVIEWS

Review

pubs.acs.org/CR

Microwave-Assisted Preparation of Inorganic Nanostructures in Liquid Phase

Ying-Jie Zhu* and Feng Chen

State Key Laboratory of High Performance Ceramics and Superfine Microstructure, Shanghai Institute of Ceramics, Chinese Academy of Sciences, Shanghai 200050, People's Republic of China

CONTENTS

1. INTRODUCTION

The heating effect of microwaves was accidentally discovered in 1945 by Percy LeBaron Spencer, an American engineer and inventor, at the Raytheon Co. While working on radar applications of microwaves, he found that a chocolate bar melted in his pocket. Microwaves are the electromagnetic waves with frequencies ranging from 0.3 to 300 GHz and with wavelengths of between 1 mm and 1 m, which are between infrared and radio frequency waves in the electromagnetic spectrum. Microwave radar equipment uses lower wavelengths of 0.01−0.25 m of the microwave band, and much of the microwave band is used for telecommunications. To avoid the interference with these uses, the wavelengths used by industrial and domestic microwave apparatuses are regulated at both national and international levels. The commonly used frequency in laboratories and homes for microwave heating is 2.45 GHz (with a wavelength of about 12.24 cm).

Time is invaluable; this is also true for science, especially in the field of synthetic chemistry where many time-consuming

Received: July 10, 2013
Published: June 4, 2014

   dx.doi.org/10.1021/cr400366s | *Chem. Rev.* 2014, 114, 6462−6555

trial-and-error experiments are needed. Rapid synthetic techniques will be extremely beneficial for scientists to perform more experiments within the same period of time to expand their scientific creativity. Hayes even used the figurative expression "microwave synthesis: chemistry at the speed of light".[1] Hayes also pointed out: "Microwave synthesis is a breakthrough technology for chemistry: an idea whose time has come. Its use has become more widespread, and as the technology continues to rapidly evolve, microwave synthesis will have a dramatic impact on the world of chemistry."[1] Microwave chemistry definitively fulfills the promise of being a fast synthetic technique.[2]

In today's world, researchers in both academia and industry are constantly challenged to consider more environmentally benign methods for the fabrication of the desired products. Among the 12 principles of green chemistry, the desire for utilizing "safer solvents" and to "design for energy efficiency" are two key principles of relevance to synthetic chemists.[3] The microwave energy is more efficient in selective heating in many processes, which is understood to be more environmentally friendly, requiring less energy than the conventional heating processes.[4] The American Chemical Society monograph on Green Chemistry[5] recommends that we "use methods that minimize the energy required for a reaction to take place. For example...catalysts or microwave radiation..." Patete et al.[6] published a review article entitled "Viable Methodologies for the Synthesis of High-Quality Nanostructures", and they listed the microwave-assisted synthesis as one of the environmentally friendly methods. Dahl et al.[7] published a review article entitled "Toward Greener Nanosynthesis", and they suggested that the microwave synthesis is a relatively new chemical method to facilitate reactions and could be another avenue for green synthesis of nanomaterials. Several attributes of microwave heating contribute to greener syntheses, including shorter reaction time, lower energy consumption, and higher product yield. The microwave-assisted technology can be combined with other green chemistry strategies to make it more appealing to green synthesis. For example, ionic liquids, solvent-free reactions, and nontoxic precursors can be easily utilized in conjunction with microwave heating.

The pioneering work on the microwave-assisted synthesis was carried out in the middle of the 1980s. The research work of Komarneni and Roy[8] in 1985 was the beginning of microwave-assisted inorganic synthesis in liquid phase, while Gedye et al.[9] and Giguere et al.[10] first reported the use of microwaves for the organic synthesis in 1986. In their pioneering work,[8] Komarneni and Roy reported the microwave-assisted synthesis of titania gel spheres by the dispersal of the polymerized titanium ethoxide solution into a two-phase liquid suspension in kerosene followed by heating in a microwave oven. Since these reports on the microwave-assisted synthesis, the microwave heating technology has been receiving increasing attention as a promising heating method.[11] The microwave heating technology is emerging as an alternative popular heat source for rapid chemical reactions and materials synthesis in minutes, instead of hours or even days usually required by the conventional heating methods. Over the past two decades, the microwave chemistry has rapidly developed from a laboratory curiosity to a well-established synthetic technique used in many academic and industrial laboratories around the world. This technology will open new synthetic pathways and allow the use of more environmentally friendly solvents, and it will also yield cleaner products that will not require as much purification.[12] The microwave-assisted preparation of inorganic nanostructured materials in liquid phase is currently a fast-growing area of research. It is expected that the related research activities will continue to grow rapidly in the coming years. Although most research on microwave-assisted synthesis is still performed on a laboratory (milliliter) scale, it is expected that this novel technology will soon be used on a larger, perhaps even production, scale.[13]

Nowadays, more laboratories of materials science as well as organic and pharmaceutical chemical laboratories have been equipped with microwave reactors. Many early publications on microwave-assisted synthesis were carried out in household microwave ovens, and experimental parameters like microwave power, reaction temperature, and pressure inside the vessel were not precisely known in household microwave ovens. These uncertainties led to poor control over the synthesis and a lack of reproducibility of experiments. Therefore, the use of commercially available specially designed microwave reactors with built-in magnetic stirrers, and direct temperature and pressure monitoring by various probes and sensors is strongly recommended. It is possible to combine microwave chemistry with the well-established liquid-phase synthesis techniques, and the possible combinations open unique and exciting opportunities for the preparation of inorganic nanostructures in liquid phase.[2]

In recent years, some review articles have been published on the microwave-assisted synthesis of nanostructured materials, such as metal nanostructures,[13,14] nanostructured carbon materials,[15] nanoporous nanomaterials,[4,16] colloidal nanocrystals,[17] inorganic nanomaterials,[2] metal oxide nanoparticles supported on carbon nanotubes,[18] and polymer nanocomposites.[19] Currently, timely and comprehensive review articles on microwave-assisted preparation of inorganic nanostructured materials in liquid phase are of great importance and significance for the future rapid development of the related research field.

In this Review, we do not give an exhaustive coverage of the microwave-assisted synthesis of inorganic nanostructures in liquid phase, but mainly cover the significant research progress in the past decade. Many inorganic nanostructured materials including metals, semimetals, alloys, metal oxides, metal sulfides, metal selenides, metal tellurides, calcium-based salts and other oxysalts, inorganic/inorganic nanocomposites, and inorganic/organic nanocomposites, prepared by microwave heating in various solvents including water, polyols, ionic liquids, and mixed solvents, are classified and reviewed. The microwave-assisted self-assembly of inorganic nanostructures in liquid phase is discussed. In addition, the differences between microwave heating and conventional heating in the formation of inorganic nanostructures in liquid phase are compared. Finally, future prospects and challenges for microwave-assisted preparation of inorganic nanostructures in liquid phase are discussed. For the microwave-assisted synthesis of metallic nanostructures, we will focus on the progress made from 2005 upward, covering the new results that are not included in a previous review.[14] For the microwave-assisted synthesis of nanostructured metal compounds, we will focus on metal oxides and metal chalcogenides for the reasons that they are very important functional materials both for the fundamental research and for practical applications and that there have been a large number of publications in the literature. However, fewer papers have been published on the microwave-assisted synthesis of other metal compounds such as metal halides

dx.doi.org/10.1021/cr400366s | Chem. Rev. 2014, 114, 6462−6555

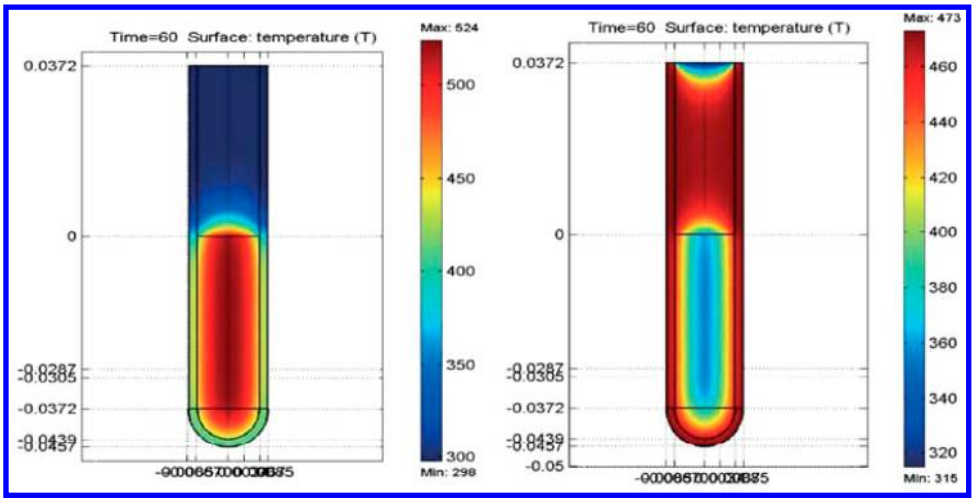

Figure 1. Temperature profile after 1 min as affected by microwave irradiation (left) as compared to treatment in an oil bath (right). Microwave irradiation raises the temperature of the whole reaction volume simultaneously, whereas in the oil heated tube, the reaction mixture in contact with the vessel wall is heated first. Temperature scale is in kelvin. "0" on the vertical scale indicates the position of the meniscus. Reproduced with permission from ref 28. Copyright 2003 Kluwer Academic Publishers.

and metal nitrides; thus, less coverage will be put on these nanostructured materials. The microwave-assisted synthesis of zeolite membranes and metal−organic frameworks has been reviewed by Li et al.[20] and Klinowski et al.,[21] respectively, and these will not be included. In addition, the microwave-plasma synthesis, microwave sintering, microwave processing,[22] and microwave-assisted functionalization of materials[23] are not the topics in this Review.

1.1. Microwave Chemistry and Microwave Effects

Microwave chemistry is the science of applying microwave irradiation to chemical reactions. The basic principles of microwave chemistry have been discussed in some review papers.[14,17,24−27] Nüchter et al.[24] discussed a critical overview of the microwave technology and focused mostly on the reaction engineering in the microwave field. Gabriel et al.[25] provided a thorough explanation of the underlying theory of the microwave dielectric heating. The microwave heating involves two main mechanisms, dipolar polarization and ionic conduction. Microwaves generally heat any material containing mobile electric charges such as polar molecules or conducting ions in a solvent or in a solid. During the microwave heating, polar molecules such as water molecules try to orientate with the rapidly changing alternating electric field; thus heat is generated by the rotation, friction, and collision of molecules (dipolar polarization mechanism). In the case of ions, any ions present in solution will move through the solution based on the orientation of the electric field, and because this is in constant fluctuation, the ion is moving in constantly changing directions through the solution, causing a local temperature rise due to friction and collision.[12] Semiconducting and conducting samples heat when ions or electrons within them form an electric current and energy is lost due to the electrical resistance of the material (ionic conduction mechanism).

The microwave heating technology is emerging as an alternative heat source for rapid volumetric heating with shorter reaction time and higher reaction rate, selectivity, and yield as compared to the conventional heating methods. As a result, microwave heating has opened the possibility of realizing fast chemical reactions and rapid materials preparation in very short time periods, usually in minutes, instead of hours or even days usually required by the conventional heating methods, leading to relatively low cost, energy saving, and high efficiency for materials production.

In contrast, the conventional heating usually involves the use of an electric furnace or oil bath, which heats the walls of the reactor and then the reactants by convection or conduction. The reactor acts as the intermediary to transfer thermal energy from the external heat source to the solvent, and ultimately to the reactants. The core of the sample takes much longer to achieve the target temperature. Such a pathway typically leads to thermal gradients throughout the bulk media, and to inefficient and nonuniform reactions, which may cause serious issues in the scale-up production. In contrast, the microwave heating is able to heat target materials without heating the entire furnace or oil bath, which saves time and energy. Figure 1 shows the comparison of temperature profiles by microwave heating and oil bath.[28]

The energies of microwaves are not high enough to break typical chemical bonds. For example, the energy of a microwave photon at a frequency of 2.45 GHz is only 1.0×10^{-5} eV, and the energies at 0.3 and 30 GHz are 1.2×10^{-6} and 1.2×10^{-3} eV, respectively.[24] These energies are too low to cleave chemical bonds, even lower than the Brownian motion, and can only affect molecular rotations.[29] Thus, microwave chemistry is based on efficient heating of materials, not inducing chemical reactions by direct absorption of electromagnetic radiation, as applied in photochemistry processes.[2] Jhung et al.[30] reported that microwave irradiation accelerated not only nucleation but also crystal growth.

The ability of microwave heating for a specific material or solvent at a given frequency and temperature is determined by the so-called loss tangent $\tan \delta = \delta''/\delta'$, where δ'' is the dielectric loss, representing the conversion efficiency of the electromagnetic radiation into heat, and δ' is the dielectric constant, describing the polarizability of molecules in the electric field.[17,25,26] The loss tangent value depends on the temperature and frequency, and these two parameters strongly affect the penetration depth, which is defined as the point where 37% of the initially irradiated microwave power is still present.[24]

dx.doi.org/10.1021/cr400366s | Chem. Rev. 2014, 114, 6462−6555

The microwave penetration depth is inversely proportional to the loss tangent. The solvents and materials with high loss tangents have short penetration depths. In the case of water, which is the most frequently used solvent, the penetration depth at room temperature is just a few centimeters, and this has far-ranging implications for the scale-up of microwave synthesis. For pure water and most of the organic solvents, the loss tangent decreases with temperature; that is, the absorption of microwave irradiation decreases with temperature, which means that microwave heating at high temperatures may become somewhat difficult.[2] Horikoshi et al.[31] reported that the dielectric loss factors decreased (~72% for a microwave frequency of 2.45 GHz and ~60% for 5.8 GHz) with increasing temperature of water from 22 to 99 °C. The penetration depth of the 2.45 GHz microwaves in water increased 2.7-fold from ~1.8 to 4.8 cm when the temperature increased from 22 to 99 °C, whereas the penetration was rather shallow for the 5.8 GHz microwaves (from 0.34 to 0.62 cm, i.e., a 1.8-fold increase), as shown in Figure 2. The penetration depth is proportional to the

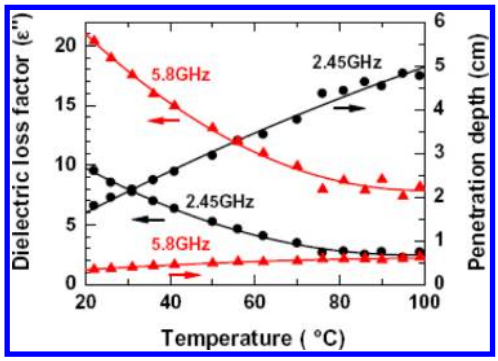

Figure 2. Temperature profiles of the changes in dielectric loss factor (δ'') and penetration depth (cm) of 2.45 and 5.8 GHz microwaves in water. Reproduced with permission from ref 31. Copyright 2009 Elsevier B.V.

wavelength of applied microwaves. For example, the penetration depths in water are ~1.8 and 0.34 cm at 22 °C for the 2.45 and 5.8 GHz microwaves, respectively,[31] and the penetration depths in oleylamine are 22.8 and 3.8 cm for 2.45 and 5.8 GHz microwaves, respectively.[32] The gap shown in Figure 2 for dielectric loss factors of the 2.45 and 5.8 GHz microwave frequencies in water is proportional to the difference in frequency. For low loss dielectric (i.e., δ''/δ' much smaller than 1), the depth (D_p, in cm) to which the microwave radiation penetrates the microwave absorbing media can be estimated from eq 1,[33] where λ_0 is the wavelength of the radiation ($\lambda_{0(2.45\ GHz)}$ = 0.122 m and $\lambda_{0(5.8\ GHz)}$ = 0.0517 m). D_p denotes the depth at which the power density of microwaves is reduced to 1/e of its initial value.

$$D_p = \left(\frac{\lambda_0}{2\pi}\right)\left(\frac{\sqrt{\varepsilon'}}{\varepsilon''}\right) \quad (1)$$

Horikoshi et al.[32] investigated the effect of microwave frequency (5.8 and 2.45 GHz) on the formation of Au nanoparticles in ethylene glycol (EG) and oleylamine. Oleylamine has a low dielectric constant and is not dielectrically heated by 2.45 GHz microwaves. They found that a change in microwave frequency from 2.45 to 5.8 GHz at equal microwave power levels led to the formation of Au nanoparticles in the nonpolar solvent of oleylamine; however, a change in the microwave frequency had almost no effect on the size and shape of Au nanoparticles obtained in the polar solvent of EG at identical microwave power levels. It is usually assumed that the microwave-assisted synthesis does not occur in nonpolar solvents because they are not microwave absorbers. However, this study has shown that it is possible to form Au nanoparticles even in a nonpolar solvent at the same microwave power and solution composition using microwaves with a higher frequency (e.g., 5.8 GHz). In contrast, in a polar solvent such as EG, the size and shape of Au nanoparticles showed little frequency-dependent effect.

There is a significant difference between the variable-frequency and fixed-frequency microwave heating. Microwaves can penetrate a solvent with different depths by varying frequencies (wavelengths). During a variable-frequency microwave heating process, a selected bandwidth is swept around a central frequency in a specified time, which keeps the microwave energy from remaining focused at any given location for more than a fraction of a second. In the presence of standing waves of electric fields during constant frequency microwave heating, the arcing occurs from a charge buildup in conductive materials. Arcing problems and localized heating can be eliminated using the variable-frequency microwave heating.[34] Jiang et al.[35] prepared Ag nanoparticles with a narrow size distribution and with a high yield by the variable-frequency microwave heating. The Suib group reported microwave-assisted two-step hydrothermal synthesis of cryptomelane-type manganese oxides (OMS-2) at different microwave frequencies and also using the variable-frequency heating. They found that OMS-2 prepared at a high-frequency limit of 5.5 GHz showed the highest conversion (50%) for the oxidation of 2-thiophenemethanol to 2-thiophenecarboxaldehyde among all of the tested OMS-2 samples.[34] The Suib group also investigated the effect of microwave frequency on the microwave-hydrothermal product of nanocrystalline tetragonal $BaTiO_3$ with particle sizes ranging from 30 to 100 nm.[36] They systematically investigated the effects of microwave frequency, microwave bandwidth sweep time, and aging time on the microstructure, particle size, phase purity, surface area, and porosity of the as-prepared $BaTiO_3$ nanostructures. They found that the particle size, morphology, and surface area of the products were influenced by the microwave frequency and bandwidth sweep time. High microwave frequency (5.5 GHz) and variable frequency (3−5.5 GHz to 1 s) led to spherical $BaTiO_3$ nanoparticles with a narrow and unimodal particle size distribution. However, the products prepared via the conventional heating under similar conditions exhibited bimodal particle size distributions with irregular grain sizes. $BaTiO_3$ prepared using the standard 2.45 GHz microwaves yielded nanoparticles with a cubic structure. The surface areas of the prepared powders decreased with the processing time using 4.0 and 5.5 GHz microwaves, but increased gradually with extended processing time in variable frequency (3−5.5 GHz to 1 s) microwaves. The dependence of properties of $BaTiO_3$ on microwave frequency may be due to different transverse magnetic modes at different frequencies.[36]

The effect of microwave power on the formation of nanostructured materials has also been investigated. Seol et al.[37] investigated the effect of applied microwave power on the formation of Au nanoparticles using $HAuCl_4$ and sodium citrate as reactants in aqueous solution. Using a high microwave power to increase the temperature ramping rate led to homogeneous nucleation, smaller average size, and narrower size distribution

dx.doi.org/10.1021/cr400366s | Chem. Rev. 2014, 114, 6462−6555

of Au nanoparticles. Yang et al.[38] investigated the effect of microwave power on the morphology of Ag nanostructures. The results showed that a medium microwave power of ~320 W × 3−4 min produced Ag nanowires of 6−8 μm in length, while Ag nanowires were shortened to 2−4 μm at a lower power. At a higher microwave power, Ag particles dominated the product with short nanowires of ~3−4 μm. In addition, the combination of 800 W × 0.5 min + 320 W × 2.5 min resulted in mainly uniform Ag nanowires up to 10 μm in length with a small quantity of Ag particles. However, prolonged treatment at 800 W during the first heating stage and the reversed combination of 320 W + 800 W led to a high yield of Ag particles.

The microwave heating has two types: pulsed microwave heating and continuous microwave heating. Shen et al.[39] investigated the difference between the pulsed microwave heating and continuous microwave heating in the synthesis of WC nanoparticles using $(NH_4)_6H_2W_{12}O_{40}\cdot xH_2O$ in mixed solvents of 2-propanol and water. The pulsed microwave heating produced WC nanoparticles with an average particle size of 21.4 nm with a 15 s-on and 15 s-off heating mode for 20 times; however, the particle size increased to 35.7 nm by the continuous microwave heating for 5 min.

Gedye et al.[40,41] reported the effects of several factors, such as sample volume, solvent, homogeneous and heterogeneous reactions, size of reaction vessel, and power level, on the rate enhancements in microwave-assisted organic synthesis. Bonaccorsi and Proverbio[42] investigated the microwave synthesis of NaA zeolite using two reaction flasks with sizes of 100 and 500 mL. If the penetration depth is much less than the thickness of the bulk material, only the external part is dielectrically heated, while the remaining part is heated by convection. The reaction mixture (50 g) was treated in two spherical glass reactors. In such a way, the same amount of reaction mixture had different surface to volume ratios exposed to microwaves. The product with a lower crystallization and higher level of impurities was obtained in the reactor with a volume of 500 mL, indicating an excess of energy transferred to the mixture. Conner et al.[43] investigated the synthesis of silicalite in either an 11 mm diameter microwave reactor or a 33 mm diameter microwave reactor. They found from simulation that the distributions of microwave energies within the reactors were different, and the morphology and yield of the resultant zeolite also differed. Larger uniform silicalite crystals were obtained in the larger reactor in which the variation in microwave energy distribution was greater.

Panzarella et al.[44] investigated several microwave synthesis parameters such as the reaction vessel size, precursor volume, microwave power delivery, and microwave cavity design. The syntheses of NaY zeolite and β-zeolite were carried out under a number of different conditions to determine the influence of these parameters on the nucleation rate, crystallization rate, particle size, and morphology. They found that the nucleation and crystallization rates of NaY and β-zeolite were more rapid in the multimode CEM MARS-5 oven as compared to the single-mode CEM Discover oven. The higher synthesis rate in the MARS-5 oven may result from the multimode microwave electric field distribution. Lower formation rates of NaY and β-zeolite observed in the Discover oven with a circular waveguide may be the result of a more uniform microwave electric field distribution. Changes in the reaction vessel size and precursor volume were found to influence the formation rate of zeolite. They also reported that the microwave reactor engineering could lead to different variations in spatial or temporal variations in microwave exposure, and different extents of rate enhancement. The reactor geometry significantly influenced the reaction rate. The larger diameter reactor (33 mm) yielded a faster crystallization for the synthesis of zeolites in the MARS-5 microwave oven. They suggested that future studies of microwave rate enhancements must specify the reactor engineering parameters for the experiments.[44]

The in situ stirring in the reaction system plays an important role in the microwave-assisted synthesis of inorganic nanostructures.[45,46] The stirring is important for achieving uniform microwave irradiation of the reaction system especially in a large vessel. Komarneni et al.[45] reported that stirring under microwave-hydrothermal conditions in the temperature range of 150−200 °C led to enhanced yields as well as smaller and more uniform $BaTiO_3$ nanoparticles as compared to those obtained in the static environment under otherwise similar conditions. Well-dispersed $BaTiO_3$ nanoparticles with smaller sizes of ~30 nm were synthesized at 180 °C under stirring, while aggregated and larger particles with sizes of 60−100 nm were obtained without stirring. Katsuki et al.[46] prepared cubic $BaTiO_3$ nanoparticles using commercial TiO_2 and $Ba(OH)_2$ in distilled water at 90 °C by a home-built single-mode semicontinuous microwave reactor. The conversion ratio of TiO_2 to $BaTiO_3$ was 97.6% and 100% for 5 and 15 min under stirring, respectively. In comparison, the conversion ratio was only 62−65% at 90 °C for 15 min without stirring.

1.2. Rate Accelerations by Microwave Heating

Many experiments have shown that the microwave heating can significantly increase the rates of chemical reactions by several orders of magnitude. Chemical reactions that otherwise take hours or even days to complete by using the conventional heating methods can be completed in very short periods of time (minutes) under microwave irradiation. Even chemical reactions that do not occur under the conventional heating conditions can be performed under similar conditions by the microwave heating. These experimental results cannot be well explained by the effect of rapid microwave heating alone, leading to the interpretation of the existence of the "specific microwave effects" or "nonthermal microwave effects".

The synthesis of materials involves the processes of nucleation and crystal growth. The question arises as to which stage is selectively accelerated under microwave irradiation. Jhung et al.[30] synthesized microporous materials of silicalite-1 and VSB-5 molecular sieves by the conventional electric heating and microwave irradiation to estimate the relative accelerations at the stages of nucleation and crystal growth. They found that microwave irradiation accelerated not only nucleation but also crystal growth. However, the effect of microwave irradiation appeared to be much more significant on nucleation relative to crystal growth. Because of the accelerations in both stages, the overall synthesis times for silicalite-1 and VSB-5 decreased by ~30- and 12-fold, respectively, by using microwave heating. The microwave nucleated precursors had higher population of nuclei with smaller sizes than the precursors nucleated by the conventional heating.

The studies on the mechanisms of microwave heating are even complicated by the fact that the rate enhancements of chemical reactions are dependent on many complex factors. Gedye et al.[40,41] reported the effects of several factors, such as sample volume, solvent, homogeneous and heterogeneous

reactions, size of reaction vessel, and power level, on rate enhancements in microwave-assisted organic synthesis. The rate enhancements of between 5 and 1240 were found for several classes of organic reactions. They proposed that the rate enhancements were caused predominantly by the rapid superheating of the solvent by microwaves. They also found that the presence of ions in the reaction mixture increased the microwave heating rate. When ions were present in solution, the maximum heating rate was observed at the smallest volume. Scaling up the chemical reaction led to a slightly lower reaction rate and a lower yield of the product for the same reaction time. Although the reaction rate was reduced when the reaction was scaled up, large rate enhancement was still observed. Robinson et al.[47] investigated the experimental phenomena in the single-mode microwave reactor. They highlighted several situations where experimental observations were often misinterpreted as "specific microwave effects". The simulations and heating experiments were used to investigate the quantitative effects of the solvent type and volume, vessel materials and internals, and stirring rate on the distribution of the electric field, power density, and heating rate. They found that significant concentrations of the electric field and power density existed around the edges of stirrers, internal temperature probes, and other protruding objects, which could cause large thermal gradients and local heating. The volume of solvent and vessel material had a significant impact upon the electric field distribution. The temperature recorded during microwave heating experiments depended upon both the measurement method and the position of the measuring device within the system.

The current debate on rate accelerations by microwave heating focuses on whether there are the "specific microwave effects" or "nonthermal microwave effects".[17,20,29,48−54] Baghbanzadeh et al.[17] gave a thoughtful discussion about the nonthermal effects of microwave heating. They have proposed that, in addition to the thermal/kinetic effects, microwave effects that are caused by the uniqueness of the microwave dielectric heating mechanisms must also be considered. These effects should be termed as "specific microwave effects", which are defined as "rate accelerations that cannot be achieved or duplicated by the conventional heating, but are essentially still thermal effects". However, the "nonthermal microwave effects" should be classified as rate accelerations that can be rationalized by neither purely thermal/kinetic nor specific microwave effects. They proposed that nonthermal effects are supposed to result from direct interaction of microwaves with specific molecules or materials in the reaction medium, which is not related to a macroscopic temperature effect.

Examples of "specific microwave effects" include the superheating effect, selective heating of polar species in a microwave transparent (or at least less absorbing) medium, formation of "molecular radiators" by direct coupling of microwave energy to specific reagents in homogeneous solution, and elimination of vessel wall effects caused by inverted temperature gradients.[2] Microwave heated liquids may have boiling points of 10−20 °C higher than the conventional boiling point at the atmospheric pressure, and this superheating effect makes the comparison of the reaction rates under the conventional heating and microwave heating rather difficult. However, superheating can be strongly suppressed by stirring.[2] "Hot spots" are a thermal effect that arises as a consequence of the inhomogeneity of the applied microwave field and selective heating. In a heterogeneous reaction system composed of different reactants, the microwave selective heating of different components of the system may occur, leading to inhomogeneous energy dissipation and temperature gradients. The heat transfer processes take place from zones with a higher temperature (hot spots) to those with a lower temperature. If the heat conduction rate is high between zones, hot spots disappear as the components rapidly reach the thermal equilibrium. In a system where the heat transfer is slow, the presence of steady-state hot spots may exist and enhance the rate of the chemical reaction within that hot zone. The size of hot spots was estimated to be as large as 100 μm.[52] Washington and Strouse[55] investigated the growth of CdSe and CdTe nanocrystals by selective heating of the chalcogenide precursor in microwave nonabsorbing alkane solvents. The chalcogenide precursor selectively absorbed the microwave energy, resulting in the instantaneous nucleation and growth upon microwave irradiation.

Two models of the mechanism have been proposed for microwave-induced reaction rate enhancements.[49] The first proposed mechanism assumes that, although the reaction time is drastically reduced for a microwave-induced reaction, the kinetics or mechanism of the chemical reaction is not altered; that is, the reaction rate enhancement is simply due to the thermal heating effect. The rapid heating rate and superheating/"hot spots" of the reaction system under microwave irradiation result in a dramatically increased reaction rate. Another proposal assumes that there are "nonthermal microwave effects" in addition to the thermal effects discussed above. It was proposed that the effects of microwave irradiation in chemical reactions are a combination of the thermal effects and nonthermal effects.[52] Nonthermal effects result from direct interaction of microwaves with specific molecules or materials in the reaction medium. In this regard, the microwave heating strongly interferes with possible nonthermal effects, and these are difficult to separate in the mechanism studies.[52] The reported "nonthermal microwave effects" include varied activation energy, increased collision efficiency by mutual orientation of polar molecules, and possible excitement of rotational or vibrational transitions.[27,50,52] Perreux and Loupy[50] proposed a rationalization of microwave effects in organic synthesis based on medium effects and mechanistic considerations. They proposed that under microwave irradiation the pre-exponential factor A in the Arrhenius law $k = A \exp(-\Delta G/RT)$, which is representative of the probability of molecular impacts, increases. The collision efficiency can be effectively influenced by mutual orientation of polar molecules involved in the reaction. Godinho et al.[53] prepared Gd-doped CeO_2 nanorods by the microwave-assisted method; they postulated that the growth process under microwave irradiation increased the effective collision rate due to the increase in the collision cross-section of the particle. However, the effect of microwave heating on the activation energy of chemical reactions has been under debate, and some conflicting results have been reported, and this topic will be discussed in section 8.

Jacob et al.[49] published a review article to discuss thermal and nonthermal interactions of microwaves with materials. They discussed some comparative examples of organic reactions performed both by the microwave heating and by the conventional heating, and concluded that the rate enhancements under microwave irradiation were purely due to thermal reasons. They classified reaction rate enhancements into the following categories: (1) The first is reaction rate enhancement due to "hot spots"/localized heating effect. The acceleration of

the chemical reaction by microwave heating was suggested to be due to either of the following reasons: superheating effect due to the presence of a large number of ions, superheating effect at the boundary between nonmiscible liquids along with efficient mixing of reactants, and rapid temperature ramping of the reaction system caused by microwave dielectric heating. (2) The second is reaction rate enhancement due to molecular agitation. Microwaves cause rapid shift of the dipoles in the molecules. The intermolecular bonds hinder the rotation of the dipoles, causing a lag in the dipoles following the electromagnetic radiation. This process may also be viewed as molecular agitation or stirring, which may account for the nonthermal effects of microwaves. (3) Third is reaction rate enhancement due to improved transport properties of molecules. The slowest step in solid-state reactions is the diffusion of reactants. Because the rate of a reaction is controlled by the slowest step, any process that can enhance the diffusion of reactants will lead to a significant rate enhancement. Microwave irradiation can enhance the diffusion of reactants as compared to the conventional heating at the same temperature. (4) The final category is reaction rate enhancement due to other reasons.

Kuhnert[51] discussed whether there are "nonthermal microwave effects" in organic synthesis. Two representative examples of microwave chemistry were provided to illustrate the confusion caused by an uncritical consideration of published results. Both examples showed the differences between the reaction conditions of the conventional thermal and microwave heating methods, and demonstrated the difficulties in such a comparison. They cautiously concluded that all speculation of special and nonthermal effects in microwave heating has no basis. Kappe[29] and Baghbanzadeh et al.[17] proposed that in most cases the observed rate enhancements under microwave irradiation are simply a thermal/kinetic effect, resulting from high reaction temperatures that can be rapidly attained by microwave heating. Naturally, such temperature profiles of microwave heating are very difficult if not impossible to reproduce by the conventional thermal heating. Therefore, the comparisons of the microwave heating processes with the conventional heating ones under exactly the same conditions are inherently challengeable. Baghbanzadeh et al.[17] emphasized that practical difficulties in accurate measurement of reaction temperature during microwave heating often contribute to misinterpretations of the experimental results. Langa et al.[48] also ascribed the temperature measurement of the reaction system as one reason for the controversies over the "nonthermal microwave effects". However, the effect of the microwave frequency on the nanocrystal formation at the constant temperature would be a genuine indication of the involvement of the nonthermal microwave effects.[17] Baghbanzadeh et al.[17] pointed out that extreme care must be taken in the interpretation of published data. The readers must be aware that it is probable that in the next few years the majority of claimed "specific microwave effects" and "nonthermal microwave effects" involved in the nanocrystal synthesis will have to be reinterpreted as the result of erroneous temperature measurements.

To tackle this problem, the Kappe group has done inspiring work on the comparisons between microwave heating and conventional heating, as they designed smart experiments to discriminate the thermal and nomthermal effects.[54] They used the reaction vessel made from silicon carbide (SiC) and a single-mode microwave reactor that allows simultaneous temperature monitoring by the external infrared and internal fiber optic probes. SiC is a strongly microwave-absorbing and chemically inert ceramic material with a very low thermal expansion coefficient that can be used at extremely high temperatures (melting point ~2700 °C). Microwave irradiation induces a flow of electrons in the semiconducting SiC that heats the reaction vessel very efficiently through the resistance heating mechanism. They proposed that because of the high microwave absorptivity of SiC, any material contained within the SiC vial will be effectively shielded from the electromagnetic field. For this purpose, custom-made 10 mL reaction vials made from sintered SiC and standard microwave-transparent Pyrex vials with the exact same geometry were used. Their experiments provided a good method to heat a reaction system by the conventional heat transfer mechanism and not by dielectric heating effects, although using microwave irradiation. Eighteen previously published microwave-assisted organic chemical reactions were investigated in comparison with the conventional heating; however, they did not find any significant differences in terms of the conversion, purity, and product yield between experiments performed in SiC vials and microwave-transparent Pyrex vials. They proposed that only bulk temperature effects were responsible for the observed rate enhancements and that the electromagnetic field had no direct influence on the reaction pathway.

Conner and Tompsett[56] proposed that microwaves can change the energies and/or "effective temperature" of individual species at interfaces. Species sorbed or formed on a surface are more susceptible to microwave interactions. The sorbed species with different permittivities exhibit different effective temperatures. Microwave exposure can change the relative energies of the intermediate species in a given sequence, which will influence the overall kinetics. The overall reaction rate for a sequence of metastable intermediates in a reaction can be increased significantly even if the activation energy maxima do not decrease. They simulated the kinetic consequences for a series of reactions due to changes in the effective temperature of a single reaction-intermediate species. They drew the following conclusions from these simulations: (1) Increases in the relative effective temperatures of reaction intermediates due to microwave exposure can increase the overall reaction rate by orders of magnitude with photon energies much less than those required to break specific bonds. (2) The reaction profile does not need to be changed permanently to produce rate enhancement. (3) Variation of reaction intermediate energies can give rise to greater overall reaction rates than either reaction path alone at moderate conversions. (4) Product/reactant ratios can exceed those normally attainable during the periodic energy variations of the reaction intermediates. They proposed that the most significant influence of microwave enhancement of chemical reactions is that microwaves can change the reaction profile (or relative temperatures) instantaneously and often periodically. These changes are due to the significant differences in microwave absorption by molecular species, particularly at interfaces. Microwave exposure can thus increase reaction rates significantly by periodically providing a more favorable reaction coordinate (selective heating: changing the reaction profile). Microwave enhancement would often be more evident in a multimode cavity wherein favorable reaction paths might be present even for short times.

In summary, on the basis of thorough literature search and analysis, we can get an overall picture that in many cases reports

on the "specific microwave effects" or "nonthermal microwave effects" were based on inaccurate comparisons of the microwave heating with conventional heating; that is, the syntheses were not carried out under exactly the same conditions. Baghbanzadeh et al.[17] pointed out that most scientists agree that in the majority of cases the observed rate enhancements should originate from a purely thermal/kinetic effect, that is, a consequence of the high reaction temperatures that can be rapidly attained when irradiating polar materials in a microwave field. No clear and unequivocal evidence has been found for the existence of "specific microwave effects" or "nonthermal microwave effects".[2] Up to now, a large volume of experimental data on microwave-assisted syntheses has been documented in the literature; however, the detailed mechanisms of the chemical reaction, nucleation, and crystal growth of inorganic nanostructures in liquid phase under microwave irradiation have still not been fully understood. The existence of "nonthermal effects" or "specific microwave effects" of microwave heating has been controversial for years, and the debate on the exact mechanisms of rate accelerations by microwave heating will still be continuing until unambiguous conclusions have been reached. Therefore, a large number of carefully designed comparative studies between the microwave heating and conventional heating are necessary for further understanding of the microwave heating mechanisms. However, the fundamental difficulties facing all comparative studies between the microwave heating and conventional heating are the discrepancies of experimental conditions between different experiments. Unfortunately, in many cases, the microwave-assisted syntheses were often compared to the literature data from those that were performed under completely different conditions such as different reaction temperatures and reaction times, and the conclusions drawn from these comparisons are usually inaccurate and speculative. Therefore, it is strongly recommended that the comparative studies between the microwave heating and conventional heating should be conducted under exactly identical experimental conditions. However, one main challenge is that the rapid and unique temperature profiles of the microwave heating are very difficult if not impossible to be duplicated by the conventional heating methods. As a result, the comparisons of the microwave heating processes with conventional heating ones under exactly the same conditions are inherently challenging.

1.3. Microwave-Assisted Preparation in Different Solvents

Solvents play important roles in microwave-assisted synthesis in liquid phase. Therefore, the solvent is a crucial factor for the microwave-assisted formation of inorganic nanostructures. The unavoidable choice of a specific solvent for a desired chemical reaction can have profound economical, environmental, and societal implications.[3] One of the most important properties of a solvent is its polarity. The more polar a solvent is, the higher its ability to couple with the microwave energy, leading to a rapid increase in temperature and fast reaction rate.[1] The heating rate and efficiency of the microwaves strongly depend on the properties of the reaction system. The use of excellent microwave absorbing solvents results in high heating rates. The solvents used in microwave heating can be classified on the basis of their loss tangent (tan δ): high (tan $\delta > 0.5$), medium (tan $\delta \approx 0.1-0.5$), and low (tan $\delta < 0.1$).[29]

Table 1 shows loss tangent (tan δ) values at 2.45 GHz and 20 °C[17,29] and boiling points of some typical solvents. Among the solvents commonly used for the microwave-assisted preparation of inorganic nanostructures, water (tan δ = 0.123) and alcohols are good solvents for microwave heating. Ethylene glycol (tan δ = 1.350) has a high boiling point (~198 °C) and reductive ability, allowing relatively high temperatures for the preparation of inorganic nanostructures in an open reaction system.

Table 1. Loss Tangent (tan δ) Values at 2.45 GHz and 20 °C[17,29] and Boiling Points of Different Solvents

solvent	boiling point (°C)	tan δ
ethylene glycol	~198	1.350
ethanol	78	0.941
2-propanol	82	0.799
methanol	65	0.659
1,2-dichlorobenzene	180.5	0.280
N-methyl-2-pyrrolidone	202	0.275
1-butyl-3-methylimidazolium hexafluorophosphate		0.185
acetic acid	118−119	0.174
N,*N*-dimethylformamide	153	0.161
1,2-dichloroethane	84	0.127
water	100	0.123
chlorobenzene	131	0.101
acetone	56−57	0.054
tetrahydrofuran	66	0.047
dichloromethane	39.8	0.042
toluene	111	0.040
hexane	68−69	0.020

The dielectric properties of most solvents change significantly with temperature.[47] For example, ethanol is a good microwave absorber at room temperature with a tan δ of 0.941. However, the tan δ of ethanol decreases to 0.270 at 100 °C, and further decreases to 0.080 at 200 °C.[17] Most organic solvents such as ethanol are microwave-heated by the dipolar polarization mechanism, and their ability to absorb microwaves decreases with increasing temperature due to decreased bulk viscosity and reduced molecular friction. In contrast, the ionic liquid such as 1-butyl-3-methylimidazolium hexafluorophosphate ([bmim][PF_6]) is heated by the ionic conduction mechanism, so its ability to absorb microwaves increases with increasing temperature.[47] The tan δ of [bmim][PF_6] increases sharply from 0.185 at 20 °C to 1.804 at 100 °C and 3.592 at 200 °C.[17] Therefore, ionic liquids are excellent microwave absorbers at low and especially at high temperatures, and their applications in microwave-assisted synthesis of inorganic nanostructures will be discussed in detail in section 4.

In addition to the single-solvent microwave-assisted synthesis, mixed solvents are also frequently used in the microwave-assisted synthesis with more freedom of control over the formation of nanostructures. In the mixed solvent reaction systems, different kinds of solvents can be selected and volume ratios of solvents can be varied; that is, more experimental parameters can be adjusted to control the chemical composition, structure, size, and morphology of the product. Different temperatures can be obtained by microwave heating in a binary solvent system comprising a polar solvent and a nonpolar solvent. For example, for a microwave-assisted phase transfer reaction in a binary system of water and chloroform, the water phase can reach 100 °C while the chloroform phase can retain a low temperature below its boiling point (~61 °C), allowing the extraction of the reactants from one phase to the other.

dx.doi.org/10.1021/cr400366s | *Chem. Rev.* 2014, 114, 6462−6555

One clever stragety for microwave heating a nonpolar solvent is adding a small amount of an excellent microwave absorber such as an ionic liquid into the nonpolar solvent; in this way, nonpolar solvents can be used as the media for microwave-assisted chemistry. An example was reported by Leadbeater et al.[57] on the use of an ionic liquid as an aid for microwave heating of nonpolar solvents. They found that the addition of a small quantity of an ionic liquid to a nonpolar solvent greatly increased the rate and yield of chemical reactions. By adding a small amount of 1,3-dialkylimidazolium iodide in hexane, the temperature reached 217 °C after microwave heating at 200 W for 10 s; in comparison, the temperature was only 46 °C after microwave heating at 200 W for 10 s in the absence of the ionic liquid.

1.4. Microwave-Assisted Preparation in an Open Reaction System

The microwave-assisted preparation of inorganic nanostructures in liquid phase can be carried out in an open reaction system under the atmospheric pressure, in which high boiling-point solvents are usully adopted to enable chemical reactions at relatively high temperatures. The advantages of the microwave-assisted preparation in an open reaction system are relatively simple, safe, and low-cost as compared to those in an closed reaction system. Among various solvents, polyols with high boiling points such as ethylene glycol (boiling point ∼198 °C) and glycel (boiling point ∼290 °C) are typical solvents for carrying out the microwave-assisted preparation in an open reaction system. The boiling points of many ionic liquids that are considered as green solvents are very high, and they can also be adopted. Refluxing is also a choice for performing microwave-assisted reactions at the boiling point of a solvent in an open reaction system.

The temperatures for the preparation in an open reaction system can be selected in the range from room temperature to the boiling point of the solvent. For example, the reaction temperatures can be adopted from room temperature to ∼100 °C by using water as the solvent. The reaction temperatures can be greatly widened from room temperature to ∼198 °C by using ethylene glycol as the solvent. When glycel is used as the solvent in an open reaction system, the reaction temperatures can vary in a wide range from room temperature to ∼290 °C, even higher than those of many conventional hydrothermal/solvothermal reactions in a closed reaction system.

However, the range of reaction temperature is narrow by using low boiling point solvents; for example, the highest temperature that can be reached is about 65 °C by adopting methanol as the solvent, at which temperature many chemical reactions cannot be performed.

1.5. Microwave-Assisted Preparation in a Closed Reaction System – Microwave-Assisted Hydrothermal/Solvothermal Method

The microwave dielectric heating is an ideal method for accelerating chemical reactions and materials synthesis under pressurized conditions in a closed reaction system. It is possible to increase the temperature of a reaction system in water or in an organic solvent higher than the conventional boiling point of the solvent under pressurized conditions in a closed reaction system. For example, ethanol has a conventional boiling point of ∼78 °C, and microwave heating in a closed vessel could rapidly increase the temperature to 164 °C and a pressure of 12 atm, leading to a thousand-fold acceleration of the reaction rate.[25] In contrast, the reaction temperature usually cannot exceed the boiling point of the solvent in an open reaction system.

In a sealed reaction system, solvents can be brought to temperatures well above their boiling points by increasing autogenous pressures resulting from heating. Performing a chemical reaction in liquid solvents in a closed system is referred to as "solvothermal processing", or in the case of water as the only solvent, "hydrothermal processing". The hydrothermal or solvothermal reactions take advantage of increased solubility and reactivity of reactants at elevated temperatures and pressures. The solvothermal/hydrothermal processing allows many inorganic materials to be prepared at temperatures substantially below those required by traditional solid-state reactions. Unlike coprecipitation and sol−gel methods, which also allow for substantially reduced reaction temperatures, the products of solvothermal/hydrothermal reactions are usually crystalline and do not require postannealing treatment. It should be noted that the pressures generated in a sealed vessel should always be estimated beforehand, and the pressures should be monitored during the solvothermal/hydrothermal experiments for the sake of safety.[58] If the pressure is too high in a closed solvothermal/hydrothermal reaction system, an explosion will occur.

The traditional hydrothermal and solvothermal syntheses of inorganic materials in closed reaction systems have been intensively investigated in the past decades.[59] The combination of the hydrothermal and solvothermal processes with microwave heating has greatly contributed to significant progress in the rapid synthesis of materials[60] due to its remarkably reduced processing time usually by orders of magnitude as compared to the traditional hydrothermal/solvothermal processes.[61] Microwave-assisted hydrothermal/solvothermal techniques employ autoclaves made from high-strength polymeric materials that are transparent to microwaves, but the reaction systems are rapidly heated to a temperature that is in turn governed by the pressure.[62]

In recent years, microwave-assisted hydrothermal or solvothermal methods have been intensively adopted for the rapid preparation of inorganic nanostructures in closed reaction systems at elevated temperatures and pressures. The pressurized environment at an elevated temperature in a closed system is favorable for many chemical reactions. In a closed reaction system, the preparation temperatures are not limited by and can be much higher than the boiling points of solvents. In contrast, the highest temperature that can be reached in an open reaction system is determined by the boiling point of the solvent. On the basis of the solvent used, the preparation in a closed system is classified as "microwave-assisted hydrothermal" and "microwave-assisted solvothermal" methods. In the microwave-assisted hydrothermal method, water is used as the only solvent in a closed system by microwave heating. In contrast, the microwave-assisted solvothermal method adopts an organic solvent or mixed solvents in a closed system by microwave heating.

One striking feature of the microwave-assisted hydrothermal or microwave-assisted solvothermal synthesis of inorganic nanostructures is its rapidness as compared to the conventional hydrothermal or solvothermal method. In the convetional hydrothermal or solvothermal method, a long period of time (usually one to several days) is needed. In contrast, the preparation time can be significantly reduced to minutes instead of days in the microwave-assisted hydrothermal or microwave-assisted solvothermal synthesis.

2. MICROWAVE-ASSISTED PREPARATION OF NANOSTRUCTURES IN AQUEOUS SOLUTION

Water is the most commonly used solvent for the synthesis of inorganic nanostructures. About 70% of the earth's surface is composed of water, making water the most abundant liquid. In fact, water was the only solvent available to chemists to carry out chemical reactions for hundreds of years.[3] Water is cheap, widely available, and environment-friendly. Naturally abundant water is a good sustainable alternative because of its nontoxic, noncorrosive, nonflammable nature, and relatively low vapor pressure as compared to organic solvents.[63] Water is also a polar solvent and a good microwave absorber.

A simplified schematic illustration of the microwave heating mechanism of water molecules is shown in Figure 3. During the microwave heating, polarized water molecules try to orientate with the rapidly changing alternating electric field; thus heat is generated by the rotation, friction, and collision of water molecules. The loss tangents of the solvents, which are related to the ability of the solvent to absorb microwave energy, depend on the relaxation times of the molecules. These relaxation times depend critically on the nature of the functional groups and the volume of the molecule. Functional groups capable of hydrogen bonding have a particularly strong influence on the relaxation time. The relaxation times of solvents decrease as the temperature of the solvent increases. Water has a relaxation time of 9×10^{-12} s at 20 °C; that is, it has a relaxation frequency of ~18 GHz, and the most effective conversion of microwave energy into thermal energy will occur in this frequency region.[25] However, the majority of commercial and household microwave appliances use a frequency of 2.45 GHz, which is displaced from this maximum. It is fortunate that even when the relaxation time is 1 or 2 orders of magnitude different from that which corresponds to the microwave frequency operating in the cavity, the solvent is still capable of acting as an effective medium for microwave dielectric heating because its loss tangent is sufficiently large. The loss tangent of water at 2.45 GHz and room temperature is 0.123, which is much higher than those at lower frequencies (0.045 at 900 MHz, 0.001 at 27.12 MHz), and the heating rates are sufficiently high at this frequency for the food processing industry.[25]

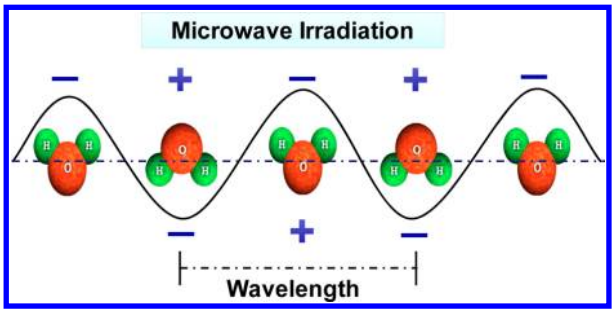

Figure 3. Water molecules in an alternating electrical field under microwave irradiation.

The structure of water is influenced when ionic salts are dissolved in it and the relaxation time decreases at low concentrations and then increases. It has been proposed that the presence of the ions causes a hydrogen bonding breakage in water. Those water molecules that are coordinated to the ions are rotationally fixed, but those that are not coordinated do not experience such strong intermolecular hydrogen-bonding effects, and consequently in this free state they have lower relaxation times.[64] At higher concentrations, the effects are reversed, and the relaxation time of water in concentrated salt solutions is higher than that of pure water, presumably due to a greater ordering of the water molecules when a large number of ions are present.[25]

Because of the advantages of water as the solvent, a large number of research activities have been devoted to the microwave-assisted synthesis of inorganic nanostructures in aqueous solution, and the related experimental data have been well documented in the literature. In this section, the recent main progress in microwave-assisted synthesis of inorganic nanostructures in aqueous solution will be reviewed and discussed on the basis of the classification of different kinds of materials.

2.1. Metals, Semimetals, Nonmetals, and Alloys

The preparation of metal nanostructures has been the topic of intensive research during the past several decades, mainly because of their unique properties and promising applications from a technological point of view. The principle for the formation of metal nanostructures in aqueous solution is based on the reduction of metallic ions with a reducing reagent under microwave irradiation. A soluble metal salt is usually used as the metal source. In many reaction systems, an additive or a surfactant is also used. The properties of metal nanostructures depend on their size and morphology, which are determined by their preparation methods. Nanostructures of noble metals such as Au, Pt, and Ag are of particular interest due to their close conduction and valence bands in which electrons move freely. These free electrons generate surface plasmon bands that depend on their size and shape. The fascinating color of noble metal nanocrystals depends on both the size and the shape of nanocrystals as well as the refractive index of the surrounding medium.[65]

In 2005, Tsuji et al.[14] published a review article entitled "Microwave-Assisted Synthesis of Metallic Nanostructures in Solution". This article covered the research work made on the microwave-assisted preparation of metallic nanostructures in solution before 2005. They discussed some typical examples of Ag, Au, Pt, and AuPd nanostructures prepared using water-soluble metal salt, reductant, and surfactant. The metallic nanostructures with various morphologies including spheres, polygonal plates, sheets, rods, wires, tubes, and dendrites were rapidly prepared within minutes by microwave heating. The morphology and size of metallic nanostructures could be controlled by adjusting various experimental parameters, such as the concentration of metal salt, chain length of the surfactant, solvent, and reaction temperature. Polshettiwar et al.[66] reviewed microwave-assisted preparation of noble metal nanostructures via reduction of noble metal salts with glucose, sucrose, and maltose. Recently, Nadagouda et al.[13] published a review paper entitled "Microwave-Assisted Green Synthesis of Silver Nanostructures", covering some of their own recent research work along with others in the production of Ag nanostructures using microwave irradiation. Readers can also refer to a review paper by Meng et al. entitled "A Review on Diverse Silver Nanostructures".[67] In this section, we focus on the research progress made in the microwave-assisted preparation of metallic nanostructures in aqueous solution from 2005 upward, which has been published after the review article by Tsuji et al. in 2005.[14]

dx.doi.org/10.1021/cr400366s | Chem. Rev. 2014, 114, 6462−6555

Among a variety of metals, the microwave-assisted preparation of Au nanostructures has been most intensively investigated due to their interesting properties and promising applications in various fields such as catalysis and biomedicine. Some examples will be discussed below to highlight the recent research progress. In almost all cases, $HAuCl_4$ was used as the gold source, and a reductant was adopted to reduce Au(III) in aqueous solution. In some reaction systems, an additive or a surfactant was utilized to adjust the size and morphology of Au nanostructures.

In a few cases, no reductant was used in the reaction system. Vargas-Hernandez et al.[68] prepared Au nanoparticles using $HAuCl_4$ in aqueous solution by microwave heating without any reducing agent. However, due to the absence of any protecting agent, Au particle aggregation and rapid growth were also observed. To prevent aggregation, dodecanethiol was added, and Au nanostructures with well-defined shapes and sizes were obtained. Two mechanisms were proposed to explain the reducing ability of water: first, the effect of superheated water was proposed, and second, a purely electrochemical reaction was considered to calculate the Gibbs free energy for the overall redox reaction. The theoretical prediction was in good agreement with the experimental data. At pH 3, the Gibbs free energy changed from positive to negative values at temperatures higher than 100 °C. This method opens the possibility of producing noble metal nanostructures without using reducing reagents that are frequently used for metal ion reduction.

In most cases, a variety of reducing reagents were adopted for the microwave-assisted preparation of Au nanostructures in aqueous solution, including $NaBH_4$,[69] hydrazine hydrate,[70] poly(vinylpyrrolidone) (PVP),[71] citric acid or sodium citrate,[72−75] α-D-glucose, sucrose, and maltose,[76] amino acid,[77] 2-naphthol,[78] poly allylamine hydrochloride,[79] and 2,7-dihydroxy naphthalene.[80] In some reaction systems, an additive or a surfactant such as cetyltrimethylammonium bromide (CTAB),[74,78,80] PVP,[71] PVP/sodium dodecyl sulfate (SDS),[73] Triton X-100,[77] and pluronic[81] was used. Au nanostructures with various shapes have been reported, such as nanoparticles,[69−72,74,77,79,81−88] prisms/cubes/hexagons,[76] polygonal/triangular/prisms,[78,80] ginger-like nanobranches,[73] hexagon-shaped Au nanoplates,[75] and triangular/hexagonal structures.[89]

Significant effort has been devoted to the control over the morphology and size of Au nanostructures. For example, Kundu et al.[78] prepared Au nanostructures using $HAuCl_4 \cdot 3H_2O$, 2-naphthol, NaOH, and CTAB in aqueous solution by microwave heating for 1−1.5 min. The morphologies of Au nanostructures (spherical, polygonal, or triangular/prisms, etc.) were dependent on the molar ratio of surfactant to metal ion and the concentration of 2-naphthol, and the size and shape of Au could be tuned simply by varying the molar ratio of the reactants. Kundu et al.[79] prepared aggregates of Au nanoparticles in an aqueous solution containing $HAuCl_4$ and poly(allylamine hydrochloride) in the presence or in the absence of Au seed particles by microwave heating for ∼0.5−1 min. The growth of Au nanoparticles could be controlled by aligning them on the polymeric chain, and Au nanoparticles subsequently self-assembled to form aggregated nanostructures. Au nanoparticles were stable for at least 6 months under ambient conditions. The same research group reported fast microwave-assisted preparation of Au nanostructures using CTAB as a surfactant in the presence of 2,7-dihydroxy naphthalene as a reducing agent in aqueous solution for 1−1.5 min, and Au nanostructures with different shapes (spherical, polygonal, rod, and triangular/prisms) could be obtained by adjusting the surfactant/metal molar ratio and the concentration of 2,7-dihydroxy naphthalene.[80] Wang et al.[75] obtained hexagon-shaped Au nanoplates using $HAuCl_4$ and sodium citrate in aqueous solution by the microwave-hydrothermal method. They found that the morphology and size of Au nanostructures were dependent on both the heating method and the molar ratio of $HAuCl_4$ to sodium citrate. At a molar ratio of 5:4, Au hexagonal nanoplates with a large Au (111) crystallographic facet were obtained. Uppal et al.[72] used the concentration of trisodium citrate to control the size of Au nanoparticles; smaller Au nanoparticles were obtained with increasing citrate concentration. Different methods (thermal, microwave, 254 nm hard ultraviolet light, and sonication), using reagent solutions with equal concentrations, were used to prepare Au nanoparticles. The experiments showed marked differences in the final colloids, with variance in the monodispersity, size, and shape of Au nanostructures by different methods. However, the experimental parameters such as the reaction temperature and reaction time were not the same in the four methods, making the experimental results difficult to compare. Kundu et al.[71] found that the size of Au nanoparticles could be controlled through varying the molar ratio of PVP to Au^{3+} and by using PVP with different molecular weights.

The microwave energy is highly efficient and energy-saving in many chemical processes, which is considered to be environmentally friendly for green synthesis of nanomaterials.[4,6,7] Several merits of microwave heating contribute to environmentally friendly synthesis of nanostructured materials, including short reaction time, low energy consumption, and high product yield. The microwave-assisted technology can be combined with other green chemistry strategies to make it more appealing for green synthesis, which should be greatly advocated and encouraged because it represents a promising future research trend.

In recent years, exciting progress has been made in developing environmentally friendly microwave-assisted approaches for the preparation of Au nanostructures by using biocompatible natural materials, for example, bovine serum albumin (BSA),[84,86,87] human serum albumin,[87] chicken egg white lysozyme,[85] red wine or grape pomace extract,[65] beet juice,[88] and black seed extract.[89] These rapid microwave-assisted green methods provide great potential for applications of as-prepared biocompatible Au nanostructures in various biomedical fields. Baruwati et al.[65] reported a green microwave-assisted method for the fabrication of noble metal nanoparticles, such as Au, Ag, Pd, and Pt, using red wine or preferably grape pomace extract as the only source of green solvent, reducing agent, and stabilizing agent. Red grape pomace was chosen as a three-in-one reagent because it contains numerous polyphenolic compounds that can act as capping and reducing agents. Microwave irradiation was used to produce highly crystalline metal nanoparticles within a few seconds. Because red grape pomace contains much higher amounts of polyphenolics, they used the major winery waste, rather than the wine itself, for this high-value product generation. When the optimized conditions for generating nanoparticles with red wine were used with pomace, they were able to produce highly dispersed Au nanoparticles with a narrow size distribution and a yield of more than 80%. The Au

nanoparticles were in the size range of 5−10 nm with a spherical morphology, as shown in Figure 4. Kou et al.[88]

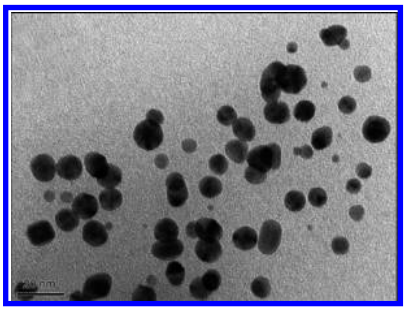

Figure 4. Transmission electron microscopy (TEM) micrograph of Au nanoparticles prepared using grape pomace extract at 50 W microwave power and 60 s exposure time. Reproduced with permission from ref 65. Copyright 2009 Wiley VCH.

reported a rapid microwave-assisted green preparation method for a variety of noble metal nanoparticles (Ag, Au, Pt, and Pd) in aqueous solutions using beet juice, an abundant sugar-rich agricultural product, which served as both a reducing and a capping reagent at 100 °C for 20 min with a maximum pressure of 280 psi. Fragoon et al.[89] reported a green microwave-assisted method for the preparation of Au nanostructures using black seed extract. The shape and size of Au nanostructures were found to be sensitive to the amount of the extract, and the reaction temperature had a significant effect on the morphology of Au nanostructures. The as-prepared Au nanocrystals were mainly triangular and hexagonal in shape.

Functional folic acid-conjugated Au nanoparticles with sizes of 15 ± 5 nm were prepared using folic acid, $HAuCl_4$, and NaOH by a rapid microwave hydrothermal process at 100 °C for 2 h; the product could target tumor cells overexpressing the folate receptors, and thus could be used for the sensitive and selective detection of human HeLa cells.[83] Dihydrolipoic acid capped fluorescent Au nanoclusters were prepared using $HAuCl_4$, lipoic acid, NaOH, and $NaBH_4$ in aqueous solution by microwave heating at 180 W for 4 min. The product was capable of sensing Hg^{2+} through the specific interaction between Hg^{2+} and Au^+ on the surface of Au nanoclusters, and the application of the as-prepared product for monitoring Hg^{2+} in living cells was demonstrated.[69] Protein-protected Au nanoclusters were prepared from an aqueous solution of BSA−$HAuCl_4$−NaOH by microwave heating.[86,87] The as-prepared BSA-protected Au nanoclusters could be used as a fluorescence enhanced sensor for detection of Ag^+ ions with a high selectivity and sensitivity.[86] A similar procedure was also applied for the preparation of human serum albumin-protected Au nanoclusters with a strong red emission, which could be efficiently quenched by nitrogen oxides (NO_x), demonstrating its great potential in determining the intracellular concentration of NO_x.[87]

In addition to the intensive research on the microwave-assisted preparation of Au nanostructures, nanostructures of other noble metals prepared by the microwave-assisted aqueous solution method, such as Pt,[65,88,90,91] Ag,[65,70,88,92−111] Au−Ag,[70] Pd,[65,88,112] Pd−Pt,[113] Cu,[106,114] Cu−Ag,[106] and Rh,[115] have also been reported, and some examples of the related research work are discussed below.

The microwave-assisted preparation of Ag nanostructures in aqueous solution has been intensively investigated. Ag nanostructures with various morphologies, such as nanoparticles,[65,88,94,95,97,99,100,102−104,106−109,111] nanorods and nanowires,[96,98,101,104] nanocubes,[93] pearl-necklace-like and nanochains,[104,105,108] and prisms,[110] have been prepared by the microwave-assisted methods. In most cases, water-soluble $AgNO_3$ was adopted as the silver source.

Similar to the research work on microwave-assisted green preparation of Au nanostructures, it is very encouraging that some researchers have explored microwave-assisted environmentally friendly preparation methods for Ag nanostructures in aqueous solution using a variety of biocompatible natural materials, such as red wine or grape pomace extract,[65] beet juice,[88] guava leaf extract,[95] leaf extract of saccharum officinarum (sugar cane),[109] starch,[94] starch/ascorbic acid,[106] amino acids,[99] glutathione,[102] sucrose and glucose,[101,104] and carboxymethyl cellulose sodium.[100] Some examples are discussed below.

The rapid production of inorganic nanomaterials from plant extracts under microwave irradiation is a promising green method for industrial applications. Baruwati et al.[65] reported the microwave-assisted fabrication of Ag nanoparticles using red wine or preferably grape pomace extract as the only source of solvent, reducing agent, and stabilizing agent. Kou et al.[88] prepared Ag nanoparticles in aqueous solution using beet juice, an abundant sugar-rich agricultural product, by microwave heating at 100 °C for 20 min. Ag nanoparticles prepared using beet juice exhibited higher catalytic activity and durability than those prepared using $NaBH_4$ in the transformation of 4-nitrophenol to 4-aminophenol. Chaudhari et al.[109] prepared Ag nanoparticles using fresh leaf extract of *Saccharum officinarum* (sugar cane) within a few minutes under microwave irradiation. Raghunandan et al.[95] reported the microwave-assisted rapid fabrication of Ag nanoparticles with sizes of 26 ± 5 nm from guava leaf extract in aqueous solution for ∼1.5 min.

Hu et al.[99] prepared monodisperse Ag nanoparticles via the rapid microwave-assisted method in a $AgNO_3$ aqueous solution, using basic amino acids such as L-lysine or L-arginine as a reducing agent and soluble starch as a protecting agent, at 150 °C for a very short period of time (only 10 s), and the TEM micrograph of the product is shown in Figure 5. The as-prepared Ag nanoparticles had a spherical shape and a mean particle diameter of 26.3 nm with a standard deviation of 2.1 nm, and were readily redispersed in water, exhibiting a

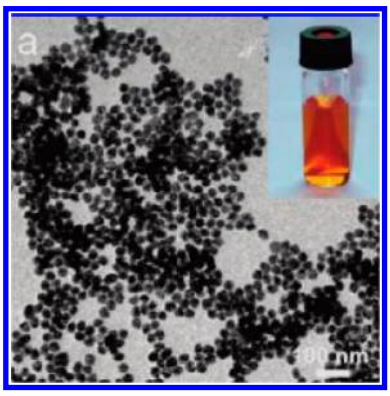

Figure 5. Typical TEM micrograph of Ag nanoparticles prepared in an aqueous system using $AgNO_3$ as the silver source, L-lysine as a reducing agent, and soluble starch as a capping agent via microwave irradiation at 150 °C for only 10 s. Reproduced with permission from ref 99. Copyright 2008 American Chemical Society.

transparent light brown suspension of well-dispersed Ag nanoparticles (the inset of Figure 5). The aqueous dispersion of Ag nanoparticles was stable without precipitate for more than 2 months at room temperature.

Valodkar et al.[106] prepared Cu, Ag, and Cu−Ag nanoparticles by microwave-assisted chemical reduction in aqueous solution using ascorbic acid as a reducing agent and starch as a stabilizing agent. Sreeram et al.[94] adopted starch as a template and reducing agent for the microwave-assisted preparation of Ag nanoparticles with an average size of 12 nm. Filippo et al.[101] adopted sucrose as a green reducing reagent for the formation of Ag nanostructures under pulsed microwave irradiation at 800 W. Ag nanoparticles were formed, and then self-assembled and fused with each other to form nanowires and further branched nanowires. In addition, different Ag nanostructures including spherical nanoparticles, necklace, and nanowires were rapidly prepared under microwave irradiation from aqueous solutions of $AgNO_3$ and β-D-glucose.[104] Baruwati et al.[102] developed a rapid and green microwave-assisted protocol for the preparation of Ag nanoparticles ranging from 5−10 nm in size using a benign antioxidant biomolecule of glutathione as both a reducing and a capping agent without using any organic solvent. This method yielded Ag nanoparticles within 0.5−1 min at a power level as low as 50 W. Chen et al.[100] employed carboxymethyl cellulose sodium (CMS) as both a reducing and a stabilizing reagent. Although the hydrolysis of CMS in aqueous solution without the help of a catalyst was almost impossible using the conventional heating method, it could be achieved by microwave heating. Ag^+ ions could be reduced by the hydrolyzate of CMS to form Ag nanoparticles. The as-prepared Ag nanoparticles were stable and could be stored at room temperature for 2 months without any visible change.

Very interesting work has been done for the preparation of metal nanoparticles using microorganisms; however, this process was usually slow, but the use of microwave irradiation will significantly accelerate this process. Saifuddin et al.[107] described a novel approach for the preparation of noble metal nanostructures such as Ag using culture supernatant of *Bacillus subtilis* under microwave irradiation in water in the absence of any surfactant. The reaction mixture was subjected to several short bursts of microwave irradiation at power output of about 100 W in a cyclic mode (on 15 s, off 15 s, 5−15 cycles). Ag nanoparticles with sizes in the range of 5−60 nm were obtained. The formation of nanoparticles by this method is rapid, requires no toxic chemicals, and the nanoparticles are stable for several months.

Liu et al.[103] prepared highly fluorescent Ag nanoclusters in the presence of polymethacrylic acid sodium salt in aqueous solution via microwave heating at 200 W for 70 s. The as-prepared Ag nanoclusters were monodisperse and uniform with an average size of 2 nm, and exhibited a strong fluorescence emission at 575 nm with an excitation at 510 nm. Furthermore, these nanoclusters were stable, and the fluorescence quenching did not occur even after 1 month of storage in the dark at 4 °C. In contrast, when the conventional heating was used, Ag nanoclusters with a weak fluorescence were not formed until 2 h with unhomogeneous sizes and a low quantum yield. The as-prepared Ag nanoclusters were explored as a novel fluorescence probe for the determination of Cr^{3+} ions with high sensitivity and selectivity.

Kundu et al.[108] reported the microwave-assisted preparation of Ag nanoparticles in the presence of poly(oxyethylene isooctyl phenyl ether) (TX-100) and 2,7-dihydroxy naphthalene as a reducing agent for 1 min. They found that the size of Ag nanoparticles could be controlled by changing the molar ratio of Ag^+ ion to surfactant, concentration of the reductant, and pH value of the reaction medium. This method could also prepare Ag nanochains in a strongly basic medium and at a lower concentration of TX-100. Kundu et al.[93] prepared Ag nanocubes using an aqueous solution containing $AgNO_3$ and poly(styrenesulfonate) in the presence of Au seeds by pulsed microwave heating for 1−2 min. The nanocubes were stable for at least 2 months under ambient conditions. Ag nanorods were prepared using silver salt and sodium citrate in the absence of a surfactant or polymer in water by the microwave-hydrothermal method.[96] Liu et al.[98] found that the concentration of Au seeds played an important role in the formation of Ag nanorods using $AgNO_3$, sodium citrate, and Au seeds in aqueous solution by a microwave-assisted process at 100 °C for 10 min. Luo et al.[97] prepared dendrimer-protected Ag nanoparticles using $AgNO_3$ and poly(propyleneimine) dendrimer in aqueous solution by microwave heating at 100 °C for 8 min.

The scaling up of microwave-assisted chemical reactions is very important for the industrial scale production and applications of nanostructured materials, and we expect that this topic will be an important future research trend. Using continuous flow-type microwave reactors is a promising strategy, and exciting progress has been made in recent years. Horikoshi et al.[111] reported a continuous-flow reactor system consisting of a Pyrex pipe (length = 135 mm; internal diameter = 8 mm) placed horizontally in the microwave waveguide through which the carboxymethyl cellulose (CMC)/$[Ag(NH_3)_2]^+$ aqueous solution was circulated by a peristaltic pump, as shown in Figure 6. Microwave irradiation of 1200 W was obtained from a microwave generator (maximum power 3000 W). In the photograph of Figure 6, the microwaves were generated from the back toward the reactor with the maximum of the microwave electric field positioned at the center of the reactor. A metal mesh closed the waveguide to prevent microwave leakage and to observe the reaction situation in

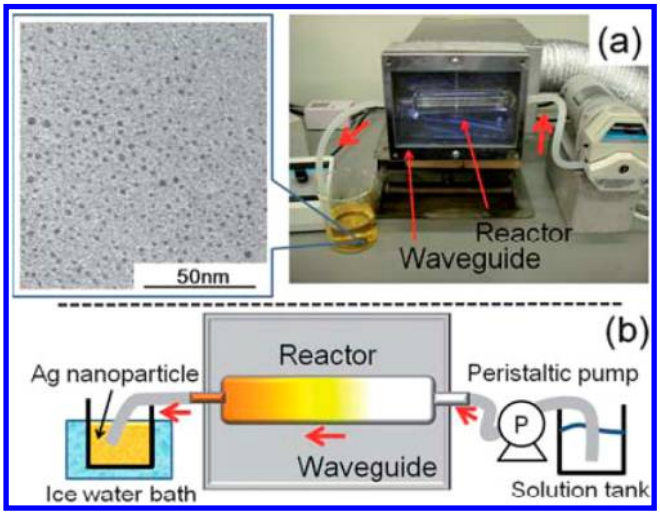

Figure 6. (a) Photograph of the continuous flow reactor system for the microwave-assisted synthesis of Ag nanoparticles; the TEM micrograph of the as-prepared Ag colloid is also displayed. (b) Schematic illustration of the overall experimental setup. Concentrations: 0.05% w/v CMC, and 60 mM $[Ag(NH_3)_2]^+$ aqueous solution. Reproduced with permission from ref 111. Copyright 2010 The Royal Society of Chemistry.

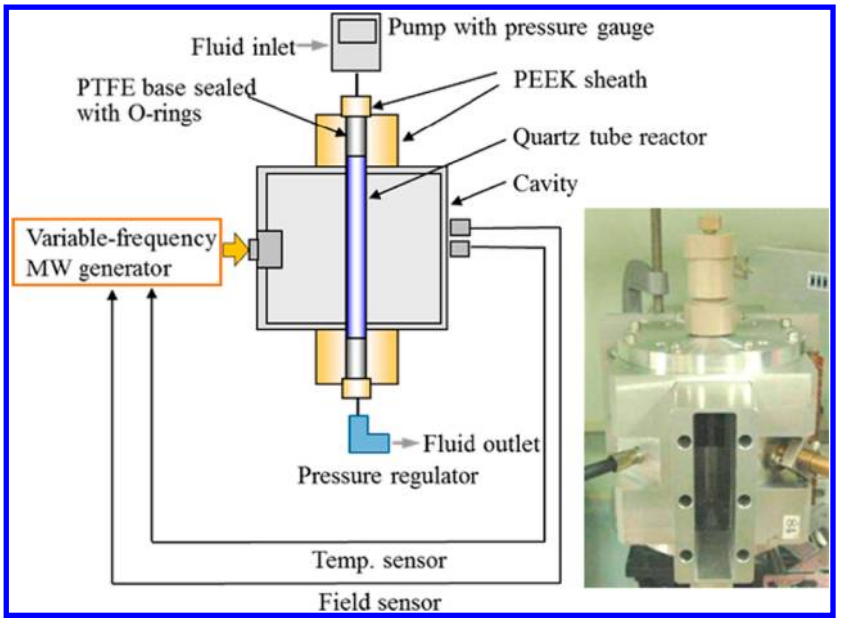

Figure 7. Experimental setup of the microwave-assisted continuous flow reactor system and a photograph of the microwave cavity part. The quartz reactor tube is connected with the PEEK sheath, which is designed to resist up to a pressure of 10 MPa. Reproduced with permission from ref 116. Copyright 2013 American Chemical Society.

the reactor. For maximal heating efficiency, the flow rate of the peristaltic pump was fixed at 600 mL min^{-1}, and the residence time of the precursor solution in the microwave reactor was ~0.7 s. The solution temperature rapidly increased to 100 °C under microwave irradiation to yield Ag nanoparticles, which were then collected in the receiver flask and rapidly cooled with an ice−water bath to prevent any further reaction. The TEM image in Figure 6 shows the formation of Ag nanoparticles with a narrow size distribution (0.7−2.8 nm, average size 1.5 nm). The cartoon in Figure 6 summarizes the reactor setup and the experimental observations. Interestingly, the internal reactor walls had no visible evidence of a yellow stain even after 7 min of microwave irradiation.

The continuous flow-type microwave reactor with a pressurized function allowing homogeneous heating of the reaction solution flow is desirable for rapid and scaling up synthesis of nanostructured materials. This kind of innovative work has been demonstrated by Nishioka et al.[116] They reported a continuous flow-type single-mode microwave reactor equipped with an elevated-pressure attachment; this microwave reactor could form a uniform electromagnetic field along a tubular reactor (quartz glass, 1.5 mm × 100 mm) located in the center of a cylindrical microwave cavity, as shown in Figure 7. This microwave reactor system was characterized by a variable frequency microwave generator (2.5 GHz ± 200 MHz, 100 W), pressure pump, and a TM_{010} single-mode cavity in which a quartz tubular reactor was mounted along the central axis. The key feature of the microwave reactor system was the automatic detection and compensation of the resonance frequency shift. The temperature of the reaction solution was measured using a radiation thermometer through the open slit (width, 8 mm) of the cavity. The reaction fluid was pressurized by a pump and was guided to the quartz reactor tube inlet (1.5 mm × 100 mm). The pressure was controlled manually using a pressure regulator; it was measured using the pressure gauge. The quartz reactor tube was connected with the PEEK sheath as designed to tolerate up to 10 MPa and was sealed with either a Viton or a Kalrez O-ring. Continuous flows of polar solvents including water, EG, and ethanol were heated instantaneously beyond their boiling points by the application of pressure. Acceleration of the reaction was exemplified in continuous synthesis of Cu nanoparticles at the reaction temperature beyond the boiling point of the solvent of EG at 2 MPa.

As discussed above, among noble metals, the microwave-assisted preparation of Au and Ag nanostructures has been intensively investigated. In contrast, other noble metal nanostructures prepared by microwave heating have been less reported in the literature. Colloidal Pt nanoparticles were prepared using an aqueous solution containing H_2PtCl_6 and 3-thiophenemalonic acid by microwave heating at 300 W for 8 min, and the particle size could be controlled by the molar ratio of the reactants.[90] By microwave heating an aqueous solution containing K_2PtCl_4 and 2-[4-(2-hydroxyethyl)-1-piperazinyl]-ethanesulfonic acid for only 12 s, Pt nanoclusters with a porous interconnected nanostructure were obtained.[91] Mehta et al.[112] prepared Pd nanoparticles using $PdCl_2$, glucose, and poly-(ethylene glycol) (PEG) as a capping agent in aqueous solution by microwave heating for only 20 s. Pd@Pt core−shell nanostructures were prepared in aqueous solution containing K_2PtCl_4, $PdCl_2$, and CTAB (pH 9) by microwave heating in a homemade microwave refluxing synthesis system at 200 W for 3 min, and the morphology of Pd@Pt nanostructures could be controlled by adjusting the molar ratio of Pt to Pd precursor.[113] Pradhan et al.[115] reported the microwave-assisted gram quantity production of one-dimensional (1-D) nanostructures composed of Rh(0) and Rh(I) using CTAB as a reducing agent as well as a soft template. Reduction of Rh(III) to Rh(0)/Rh(I) occurred on the glass surface as a result of decomposition of CTAB upon microwave heating without any other reducing agent. In contrast, the conventional hydrothermal process produced only spherical Rh(0) nanoparticles. Liu et al.[114] prepared single-crystalline Cu nanowires using $CuCl_2$, ascorbic acid, and hexadecylamine in deionized water by microwave heating at 120 °C for 2 h. The as-prepared Cu nanowires had an average diameter of 50 ± 10 nm and lengths of longer than 10 μm, that is, an aspect ratio of greater than 300. Both ascorbic

dx.doi.org/10.1021/cr400366s | Chem. Rev. 2014, 114, 6462−6555

acid and hexadecylamine played important roles in the morphology and aspect ratio of Cu nanowires. In addition to noble metal nanostructures, other metal nanostructures have also been prepared by microwave heating, but less reported. For example, Sb dendrites composed of well-crystallized nanoflakes with sizes of 20−40 nm were prepared from an aqueous solution containing antimony sodium tartrate and Zn powder in ambient air by microwave heating at 280 W for 30 min.[117]

Fluorescent Si quantum dots were rapidly prepared using Si nanowires and glutaric acid via a microwave-assisted process at 185 °C for 15 min. The as-prepared Si quantum dots had good aqueous dispersibility, high photo- and pH-stability, and strong photoluminescence, which are promising for the application in immunofluorescent cellular imaging.[118] Zhong et al.[119] reported the microwave-assisted preparation of fluorescent Si nanoparticles using the protein as a hydrophilic ligand. Si nanowires, which were prepared by an established HF-assisted etching method, first broke up into Si nanoparticles in aqueous suspension in a microwave reactor at 180−200 °C. The resultant Si nanoparticles were further modified with immunoglobulin G (IgG, a typical protein) as a hydrophilic ligand by mild microwave heating (30 °C, 5−10 min).

Te nanowires with a diameter of 20 nm and lengths of tens of micrometers were rapidly prepared using Na_2TeO_3, aqueous ammonia, hydrazine hydrate, and PVP in aqueous solution by the microwave-assisted hydrothermal method at 150 °C for 15 min. The experimental results demonstrated that the amount of PVP, pH value, a suitable surfactant, and reaction time were key factors for the formation of high-quality Te nanowires with a high aspect ratio.[120] A microwave-assisted monosaccharide reduction approach was reported for the preparation of Te nanotubes with diameters of 50−100 nm and lengths of a few micrometers using H_2TeO_3, glucose, and sodium dodecylbenzenesulfonate in distilled water at 160 °C for 6 h.[121] With the assistance of sugars or their derivatives, 1-D nanostructures of Te and Se with different sizes were obtained under microwave-hydrothermal conditions.[122]

Among nanostructures of nonmetals, the microwave-assisted preparation of carbon nanostructures has been most intensively investigated. A variety of carbon nanostructures have been prepared, including carbon dots,[123−130] nanoparticles,[131,132] nanospheres,[133] and graphene sheets.[134−138] Wang et al.[123] prepared photoluminescent carbon dots using a carbohydrate (glycerol, glycol, glucose, sucrose, etc.) and a tiny amount of an inorganic ion by a one-step microwave method for just a few minutes. In a typical experiment, glycerol (70% (v/v)) was mixed with 7.1 mM phosphate solution (pH 7.4) and heated in a household microwave oven (750 W) for 14 min. The as-prepared carbon dots exhibited blue, yellow, and red photoluminescence under ultraviolet, blue, and green light excitation. Mitra et al.[124] prepared highly fluorescent carbon dots with average sizes of 1−3 nm embedded in the carbon matrix using an aqueous solution of PEG, poly(vinyl alcohol) (PVA), and H_3PO_4 under microwave irradiation at 750 W for 55−57 s. Puvvada et al.[125] prepared water-dispersible carbon dots through microwave-assisted pyrolysis of an aqueous solution of dextrin in the presence of H_2SO_4 at 800 W for 2.5 min. Wang et al.[126] obtained fluorescent carbon dots using graphite oxide, candle soot, conductive carbon black, and lampblack in HNO_3 solution by three different heating methods: conventional reflux heating for 12 h, microwave reflux heating for 8 h, and microwave-hydrothermal treatment at 800 W for 15−60 min. As compared to the conventional reflux heating, the microwave-assisted reflux heating and microwave-hydrothermal method both shortened the reaction time. Carbon dots prepared using the microwave-assisted techniques exhibited increased absorption, higher quantum yield, and longer fluorescence lifetime than those prepared by the conventional reflux heating. Jaiswal et al.[128] used PEG to prepare amorphous carbon dots with an average size of 4.5 ± 0.9 nm. The synthesis is based on a rapid one-step microwave-mediated caramelization of aqueous PEG-200 solution. Irradiation of the aqueous PEG solution by microwave in a 900 W domestic microwave oven for 10 min resulted in the formation of golden-yellow colored solution, indicating the formation of carbon dots. Experiments with higher than 600 Da molecular weight PEG did not yield any discernible carbon dots. Prolonging the microwave irradiation time resulted in the formation of larger fluorescent carbon dots. Wang et al.[129] prepared carbon dots with a diameter of ∼5 nm from the eggshell membrane ash in NaOH solution by microwave heating in a domestic microwave oven for only 5 min. This method is low-cost because the eggshell membrane is a common protein-rich waste in daily life and can be obtained easily and cheaply. Jiang et al.[127] prepared carbon dots by microwave heating an amino acid in the presence of an acid or alkali. Carbon dots with an average size of 2 nm were obtained from a 20 mL H_3PO_4 (0.5 mol L^{-1}) solution containing 2 g of histidine by microwave heating in a 700 W household microwave oven for 160 s. Song et al.[130] prepared fluorescent carbon dots with sizes in the range of 2−7 nm from an aqueous solution containing glucose and 4,7,10-trioxa-1,13-tridecanediamine by microwave pyrolysis at 500 W for 10 min. Chandra et al.[131] prepared carbon nanoparticles with average sizes of 3−10 nm by microwave heating sucrose as the carbon source with H_3PO_4 as an oxidizing agent at 100 W for 220 s. Zhu et al.[132] obtained fluorescent carbon nanoparticles with an average diameter of ∼2.75 nm using PEG-200 and saccharide (glucose, fructose, etc.) in aqueous solution at 500 W for 2−10 min. Cui et al.[133] reported the rapid microwave-hydrothermal preparation of carbon nanospheres using glucose as the carbon source in aqueous solution at 170 °C for 20 min.

Janowska et al.[135] prepared graphene sheets consisting mostly of mono-, bi-, or few-layer (less than 10 layers) by exfoliation of expanded graphite in aqueous solution of ammonia under microwave irradiation, with an overall yield of ∼8 wt %. Reduction of graphite oxide with ascorbic acid in aqueous solution under microwave refluxing within 30 min was also reported for production of graphene sheets.[134] Long et al.[137] prepared water-dispersible polymer-grafted graphene sheets with a thickness of about 3.5 nm from a reaction system containing graphite oxide, NaOH, acrylamide monomer, azodiisobutyronitrile, and hydrazine hydrate by microwave heating involving prereduction, grafting, and postreduction. Polyacrylamide chains were rapidly grafted onto the graphene sheets via free-radical polymerization under sequential microwave irradiations. Vadahanambi et al.[138] reported a rapid microwave route to graphene nanosheets and those decorated with metal nanoparticles (Fe, Pt, and Pd) by using a chemical foaming agent (azodicarbonamide), an oxidizer (H_2O_2), and a radical initiator (ammonium peroxydisulfate). Under microwave irradiation, an intercalated foaming agent between graphite oxide layers led to rapid exfoliation, accompanied by lightening and release of gases. Sufficient care must be taken because this microwave reaction may cause violent explosions.

Pt decorated graphene exhibited a highly sensitive biosensor for glucose even in a neutral phosphate buffer solution.

2.2. Metal Oxides

Considerable effort has been devoted to microwave-assisted synthesis of nanostructures of various metal oxides due to their interesting properties, high stability, and wide applications in many fields. In many cases of microwave-assisted synthesis of metal oxide nanostructures, a water-soluble metal salt is used as the metal source, an alkaline reagent is used to create an alkaline environment, and an additive or a surfactant is often adopted to control the morphology and size of the product. Nanostructures of metal oxides with various morphologies have been prepared in aqueous solution by microwave-assisted methods; some examples of metal oxides include MgO,[139] PdO,[140] PtO_2,[141] ZnO,[142−154] SnO,[155,156] SnO_2,[157−161] $Ti_xSn_{1-x}O_2$,[162] α-Fe_2O_3,[163−170] γ-Fe_2O_3,[171] Fe_3O_4,[163,172−175] Co_3O_4,[176−181] CuO,[182−189] Mn_3O_4,[190] MnO_2,[191−196] TiO_2,[197−213] $TiO_{2-x}C_x$,[214] ZrO_2,[215−219] WO_3,[220−223] MoO_3,[224] CeO_2,[53,225−233] Nd_2O_3,[234] Y_2O_3,[235] $(Y,Gd)_2O_3$,[236] V_2O_5,[237] MWO_4 (M = Ca, Sr, Ba, Fe, Co, Ni, Mn, Zn, Ag/In),[238−244] Bi_2WO_6,[245−247] $NaY(WO_4)_2$,[248] $Y_3Al_5O_{12}$,[249−251] Zn_2SnO_4,[252] $ZnGa_2O_4$,[253,254] MFe_2O_4 (M = Mg, Zn, Ni, Mn, Co),[255−260] MAl_2O_4 (M = Zn, Co),[261−263] $BiFeO_3$,[264−266] $Bi_2Fe_4O_9$,[265] $Bi_{1.8}Y_{1.2}Fe_5O_{12}$,[267] $MnCo_2O_4$,[268] $MTiO_3$ (M = Ba, Sr, Pb),[45,269−278] $Li_4Ti_5O_{12}$,[279] $K_2Ti_6O_{13}$,[280] $MMoO_4$ (M = Ba, Ca),[281,282] γ-Bi_2MoO_6,[283] $Cd_2Ge_2O_6$,[284] $Na_2Ta_2O_6$,[285] $SnNb_2O_6$,[286] and MVO_4 (M = Bi, Ce, Y, La).[287−291]

ZnO nanostructures with various morphologies have aroused much interest due to their interesting properties and wide applications in various fields. Hu et al.[142] prepared linked ZnO rods with various morphologies such as bipods, tripods, and tetrapods using $Zn(NO_3)_2{\cdot}6H_2O$ and hexamethylenetetramine (HMTA) in aqueous solution by microwave heating at 90 °C for 2 min. The oriented attachment mechanism was proposed for the formation of linked ZnO rods. Unalan et al.[143] reported the rapid synthesis of ZnO nanowires on various substrates (such as poly(ethylene terephthalate), silicon, and glass) using a commercial microwave oven. Vertical ZnO nanowires were grown by dipping the substrates in an aqueous solution of $Zn(NO_3)_2{\cdot}6H_2O$ and HMTA under microwave irradiation at different powers (120, 385, and 700 W) at atmospheric pressure for 1−30 min. The average growth rate of ZnO nanowires was as high as 100 nm min^{-1}, depending on microwave power. Cho et al.[152] prepared density-controlled ZnO nanorod arrays on a flexible Teflon substrate using inductively coupled plasma etching with anodic aluminum oxide (AAO) membranes in an aqueous solution containing $Zn(CH_3COO)_2{\cdot}2H_2O$ and ammonia under microwave irradiation at 90 °C for 40 min. The average interpore distances of the Si surface etched with an AAO membrane anodized in 0.3 M oxalic acid and an AAO membrane anodized in 0.1 M phosphoric acid were ∼100 and ∼450 nm, respectively. During the microwave irradiation, ZnO nanorods grew from Si pores. Thus, the density of ZnO nanorods could be controlled by changing the interpore distance of the AAO membrane mask. ZnO porous nanoplates were synthesized using an aqueous solution containing zinc salt and an alkali (urea or ammonia) through microwave irradiation and subsequent thermal heating of the nanoplate precursor.[144,150] ZnO nanotubes were prepared using an aqueous solution containing $Zn(NO_3)_2{\cdot}6H_2O$ and urea under microwave irradiation at 180 W for 40 min.[154] ZnO nanostructures including nanorods, nanocandles, nanoneedles, nanodisks, and nanonuts were obtained at 90 °C with a low microwave power (∼50 W) and a subsequent aging process. In addition, more complex ZnO structures including ZnO bulky stars, cakes, and jellyfishes were also obtained.[153] ZnO micro-/nanostructured materials with different morphologies were synthesized using aqueous solutions containing $ZnCl_2$ and ammonia via the microwave-hydrothermal method for 1−2.5 min, and fork-like, hollow shuttle-like, multiwalled tube-like, flower-like, and lamella-like morphologies were obtained by simply varying the reaction time.[145] Hexagonal ZnO nanostructured flowers composed of spear-shaped nanorods with diameters of 50 nm were synthesized from an aqueous solution containing a 1:15 molar ratio of $Zn(CH_3COO)_2{\cdot}2H_2O$ to KOH under 180 W microwave irradiation for 20 min.[147] ZnO nanostructures with various morphologies (nanoparticles, nanorods, and flowers) were synthesized using $Zn(CH_3COO)_2{\cdot}2H_2O$, NaOH, and guanidinium carbonate or acetyl acetone in aqueous solution via the fast microwave-assisted method for 2 min.[148] ZnO rods with hierarchical nanostructures were prepared using the micowave-hydrothermal method. The thorn-like nanostructures were grown on the surface of rods in high density with lengths from ∼10 to 80 nm.[149]

Iron oxides are important functional materials and have wide applications in many fields. Considerable effort has been devoted to microwave-assisted synthesis of iron oxide nanostructures, and some examples are discussed below. Amorphous Fe_2O_3 nanoparticles with sizes of ∼3−5 nm were synthesized by pulsed microwave heating an aqueous solution containing $FeCl_3{\cdot}6H_2O$, PEG-2000, and urea at 650 W for 10 min.[292] α-Fe_2O_3 nanoparticles of 23−25 nm in diameter were prepared using 0.02 M $Fe(NO_3)_3{\cdot}9H_2O$ solution by a microwave-hydrothermal process at 100 °C for 4 h.[164] α-Fe_2O_3 nanoparticles with sizes of ∼5 nm were prepared using $Fe(NO_3)_3$ and urea in aqueous solution by a microwave-assisted hydrothermal route at 120 °C for 30 min.[166] α-Fe_2O_3 nanoparticles were prepared using $FeCl_3$, PEG, $N_2H_4{\cdot}H_2O$, and H_2O_2 in aqueous solution by rapid microwave heating at 100 °C for 10 min. The morphology of α-Fe_2O_3 was affected by the heating method. Ellipsoidal α-Fe_2O_3 nanoparticles formed following the oriented attachment mechanism by microwave heating, while a mixture of irregular α-Fe_2O_3 nanoparticles and rods was obtained by oil bath.[163] α-Fe_2O_3 nanorods with an average diameter of ∼60 nm were prepared using $FeCl_3{\cdot}6H_2O$ and PVP in aqueous solution through the microwave-assisted hydrothermal method at 120−180 °C for 2 h.[165] Hu et al.[168] prepared α-Fe_2O_3 nanorings using $FeCl_3{\cdot}6H_2O$ and $NH_4H_2PO_4$ in aqueous solution by a microwave-hydrothermal process at 220 °C for 25 min. The TEM micrographs of the as-prepared α-Fe_2O_3 nanorings are shown in Figure 8; the sample consisted of more than 90% ringlike structures. Figure 8B shows a high-magnification TEM image of a single α-Fe_2O_3 nanoring with a circular shape, and its corresponding electron diffraction pattern (Figure 8C) indicates that the nanoring was single-crystalline. α-Fe_2O_3 nanorings had an average outer diameter of ∼100 nm and inner diameters ranging from 20 to 60 nm. Because the hydrolysis of Fe^{3+} ions is pH-dependent, and the equilibrium between phosphate anions and Fe^{3+} ions determines both the availability of free phosphate ions and the dissolution degree of solid α-Fe_2O_3, the growth of α-Fe_2O_3 can be thermodynamically controlled by adjusting the reactant concentration. The sensors made of α-Fe_2O_3 nanorings exhibited high sensitivity not only for biosensing of H_2O_2 in

dx.doi.org/10.1021/cr400366s | Chem. Rev. 2014, 114, 6462−6555

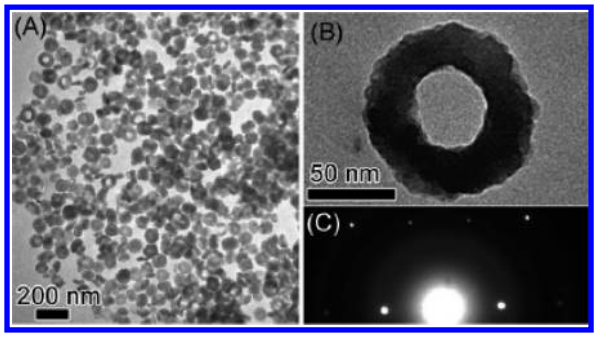

Figure 8. (A) Low-magnification TEM image of α-Fe_2O_3 nanorings; (B) high-magnification TEM image of a single α-Fe_2O_3 nanoring; and (C) electron diffraction pattern indicating the single-crystalline nature of the nanoring. Reproduced with permission from ref 168. Copyright 2007 Wiley-VCH.

a physiological solution but also for gas-sensing of alcohol vapor at room temperature.

Hu et al.[167] reported the rapid microwave-hydrothermal synthesis of monodisperse α-Fe_2O_3 nanocrystals using an aqueous solution containing $FeCl_3$ and $NH_4H_2PO_4$ at 220 °C for 10−25 min, and a variety of morphologies, including ellipsoids/spindles with aspect ratios ranging from 1.1 to 6.3, nanosheets, nanorings, and spheres, were obtained. A microwave-assisted hydrothermal process was adopted for the fast synthesis of α-Fe_2O_3 hierarchically nanostructured architectures using an aqueous solution containing $K_3[Fe(CN)_6]$. It was found that the reactant concentration and reaction temperature, instead of the reaction time, had a great influence on the morphology of the product. Several kinds of nanostructures, such as nanoparticles, dendritic crystals, plates, and self-organized nanorods, could be obtained under different experimental conditions.[169] α-Fe_2O_3 hierarchical microspheres formed by self-assembly of 30−50 nm nanoparticles were obtained using $FeCl_3{\cdot}6H_2O$, urea, and polyacrylamide in aqueous solution by microwave refluxing for 20 min, followed by thermal treatment at 550 °C for 4 h.[170] Sreeja et al.[171] prepared γ-Fe_2O_3 nanoparticles with an average particle size of 10 nm from an aqueous solution containing $FeSO_4{\cdot}7H_2O$, $FeCl_3{\cdot}6H_2O$, and NaOH under microwave-hydrothermal conditions at 150 °C for 25 min.

Fe_3O_4 is an important magnetic functional material and has wide applications in many fields. Fe_3O_4 nanostructures are usually obtained using water-soluble iron(III) salt or salts of iron(III) and iron(II) and a reductant in aqueous solution under microwave irradiation. In some methods, an additive or a surfactant is used. Miao et al.[173] prepared Fe_3O_4 nanoparticles using a rusty iron foil (Fe and Fe_2O_3) in deionized water in the absence of any alkali, acid, or surfactant in a household microwave oven at 700 W for 30 min. The as-prepared Fe_3O_4 nanoparticles with sizes ranging from 20 to 60 nm attached to the iron surface, which were separated by ultrasonic and magnet. The as-synthesized Fe_3O_4 nanoparticles exhibited a saturation magnetization value of 51.3 emu g^{-1}. Fe_3O_4 nanoparticles were prepared using an aqueous solution containing $FeCl_3$, $FeSO_4$, and ammonia by the microwave-assisted method.[172] In another work, Fe_3O_4 nanoparticles were prepared using $FeCl_3$, $N_2H_4{\cdot}H_2O$, and PEG in aqueous solution by microwave heating at 100 °C for 10 min.[163] Zhou et al.[174] synthesized Fe_3O_4 hexagonal nanoplates with an average edge length of 80 nm using $FeSO_4{\cdot}7H_2O$, $CH_3COONa{\cdot}3H_2O$, citric acid, NaOH, and NaH_2PO_2 in aqueous solution via a facile microwave-assisted route. The morphology and size of the product could be varied by adjusting the reaction time, microwave power, and concentrations of reactants, and citric acid was found to play a key role in the formation of Fe_3O_4 nanoplates. Muraliganth et al.[175] adopted a microwave-hydrothermal approach to synthesize single-crystalline Fe_3O_4 nanowires in the presence of PEG as a soft template in aqueous solution at 150 °C within 15 min. Milosevic et al.[293] obtained magnetic nanorods of a mixture of Fe_3O_4, γ-Fe_2O_3, and β-FeOOH by microwave-assisted hydrothermal reduction at 100 °C using β-FeOOH nanorods as the iron source and template and hydrazine as a reductant, and the size and shape of the product could be controlled through adjusting experimental parameters. Wu et al.[294] reported the fast microwave-assisted synthesis of lamellar sodium/potassium iron oxide nanosheets consisting of two-dimensional iron oxide building blocks separated by the intercalated sodium/potassium ions using $FeSO_4{\cdot}7H_2O$, $Na_2S_2O_3{\cdot}5H_2O$, NaOH, and KOH in aqueous solution at 180 °C for 5 min.

The microwave-assisted method has also been applied in the rapid synthesis of cobalt oxide nanostructures. For example, Ma et al.[176] prepared Co_3O_4 nanocrystals using an aqueous solution containing $C_4H_6CoO_4{\cdot}4H_2O$ and NaOH by the microwave-hydrothermal method at 200 °C for 1 h. Li et al.[177] prepared spherical or cubic Co_3O_4 nanoparticles (10−20 nm) using cobalt salt, 3-mercaptopropionic acid, and NaOH in aqueous solution by microwave heating at 100−140 °C within 10 min. Spherical nanoparticles were obtained at a lower temperature; however, cubic nanoparticles formed at a higher temperature. Lai et al.[178] prepared Co_3O_4 nanorods by the microwave-assisted synthesis of cobalt hydroxide carbonate nanorods from a solution containing $Co(NO_3)_2{\cdot}6H_2O$ and urea under 500 W microwave irradiation for 3 min, followed by calcination at 400 °C. Al-Tuwirqi et al.[180] synthesized Co_3O_4 nanostructures using $Co(CH_3COO)_2$, NaOH, and citric acid through the microwave-assisted hydrothermal method at 200 °C for 30 min. Wang et al.[181] prepared Co_3O_4 nanowires with a porous structure constructed by self-assembly of nanocrystals by a microwave-assisted process (110 °C, 1 h) combined with a thermal transformation process (350 °C, 2 h, air). Meher et al.[179] investigated the effect of microwave heating on the morphology, optical, magnetic, and pseudocapacitance behavior of Co_3O_4. They found the difference in dimensionality of Co_3O_4 nanowires by employing the microwave-assisted reflux (120 °C, 15 min) and conventional reflux (120 °C, 12 h) using $Co(NO_3)_2{\cdot}6H_2O$, P123, and urea in aqueous solution. The Co_3O_4 sample obtained by the conventional reflux consisted of randomly distributed thin nanowires, while the microwave reflux method generated higher-dimensional and arranged Co_3O_4 nanowires.

Nanostructures of other metal oxides have also been rapidly synthesized by the microwave-assisted method. Qiu et al.[187] prepared CuO nanostructures in aqueous solution of $Cu(CH_3COO)_2$/urea or $Cu(NO_3)_2$/urea at 150 °C for 30 min via a microwave-assisted hydrothermal process. In the $Cu(CH_3COO)_2$/urea reaction system, CuO nanoparticles formed and assembled into spheroidal microspheres. However, CuO nanorods formed and assembled into flower-like structures in the $Cu(NO_3)_2$/urea aqueous solution. This study shows that the anions in the reaction system have an influence on the morphology of the product. Liang et al.[182] synthesized single-crystalline CuO nanosheets with a monoclinic structure from a layered precursor, copper(II) acetate hydroxide, in 0.1 M

dx.doi.org/10.1021/cr400366s | Chem. Rev. 2014, 114, 6462−6555

NaOH aqueous solution by microwave heating at 100 °C for 5−45 min, and the layered precursor was synthesized using $Cu(CH_3COO)_2·H_2O$ and NaOH in EG by microwave heating at 140 °C for 5 min. Moura et al.[188] prepared CuO nanoplates using $CuCl_2·2H_2O$ and NaOH in aqueous solution without any surfactant by a microwave-hydrothermal process at 130 °C for 30 min. Single-crystalline CuO nanoleaves with an average thickness of ∼10 nm were synthesized by microwave heating an aqueous solution containing copper salt and NaOH at 80 °C for 10 min or 100 °C for 20 min.[189] CuO hierarchical hollow nanostructures constructed by self-assembly of nanorods were synthesized using an aqueous solution containing $Cu(CH_3COO)_2·H_2O$ and $CO(NH_2)_2$ by microwave heating at 80 °C for 30 min.[184] Urchin-like CuO structures composed of spiny leaves were synthesized using $CuCl_2·2H_2O$ and Na_2CO_3 in aqueous solution by microwave heating at 30% of maximum power (800 W) for 20 min.[185] Volanti et al.[186] reported the rapid microwave-assisted hydrothermal synthesis of sea urchin-like CuO architectures, and they proposed a growth mechanism that involved a mesoscale self-assembly followed by fusing the adjacent crystallites.

Polshettiwar et al.[295] fabricated nanostructured metal (Fe, Co, Mn, Cr, Mo) oxides from the precursor $K_4Fe(CN)_6$, $K_3Co(CN)_6$, $K_3Mn(CN)_6$, $K_3Cr(CN)_6$, or $K_3Mo(CN)_8$ in aqueous solution under microwave-hydrothermal conditions at 180 °C for 3 h without using any reducing or capping reagent. The size and shape of the final product could be tailored by varying the experimental conditions. Different morphologies including octahedra, spheres, triangular rods, pines, and hexagonal snowflakes were obtained. α-Fe_2O_3 structures self-assembled into pine and hexagonal snowflake-like morphologies.

Mn_3O_4 polyhedral nanocrystals were prepared using an aqueous solution containing $Mn(CH_3COO)_2$ and $(CH_2)_6N_4$ by microwave heating. Cubic and rhombohedral shapes of Mn_3O_4 with edge lengths in the range of 15−40 nm were obtained at 80 °C for 1 h. Mn_3O_4 nanocrystals grew following the Ostwald ripening mechanism with increasing reaction time.[190] γ-MnO_2 nanoplates were synthesized using $KMnO_4$ and $Mn(NO_3)_2$ in aqueous solution under microwave irradiation at 160 °C for 30 min.[191] A rapid microwave-assisted hydrothermal process was reported for the preparation of cryptomelane-type manganese oxide octahedral molecular sieve (OMS-2) nanostructures using an aqueous solution containing K_2SO_4, $K_2S_2O_8$, and $MnSO_4·H_2O$ at temperatures of 80−200 °C with a hold time of 10 s to 30 min. In contrast, up to 4 days was required in a conventional hydrothermal reaction. The OMS-2 nanowires were produced from thin nanoflakes with increasing reaction temperature.[195] Birnessite-type MnO_2 nanospheres with 70−90 nm in diameter were synthesized using $KMnO_4$, $MnSO_4·H_2O$ in deionized water by the microwave-hydrothermal method at 75 °C for 30 min at a low pressure.[196] Du et al.[192] synthesized δ-MnO_2 with a layered structure using an aqueous solution containing $KMnO_4$ and HCl by the microwave-assisted hydrothermal method at 110 °C for 1 h, the product consisted of flower-like microspheres, and they were formed by self-assembly of nanosheets as the building blocks with thicknesses ranging from 5 to 10 nm. Li et al.[193] synthesized birnessite flower-like and α-type tubular MnO_2 nanostructures from an aqueous solution containing $KMnO_4$ and HCl by the microwave-assisted hydrothermal method for 25 min, and the crystal phase and morphology could be controlled by adjusting the reaction temperature. Truong et al.[194] synthesized δ-MnO_2 microflowers consisting of assemblies of nanosheets, α-MnO_2 nanowires, and α-MnO_2 nanotubes through a microwave-assisted hydrothermal reduction of $KMnO_4$ in the presence of HCl in aqueous solution.

TiO_2 nanostructured materials are very important due to their technological importance and wide applications in many fields such as photocatalysis. Baldassari et al.[197] prepared anatase TiO_2 nanoparticles by microwave-assisted hydrolysis of $TiCl_4$ in a diluted acidic aqueous solution. The product was almost completely crystallized in a short reaction time of 30 min under microwave-hydrothermal conditions. The presence of a small amount of sulfuric acid was necessary to obtain a pure anatase phase because sulfate prevented the crystallization of a trace amount of brookite. TiO_2 nanoparticles were arranged in spherical aggregates in the presence of 1% sulfuric acid, while less aggregated nanoparticles were obtained with 0.1% sulfuric acid. They also prepared rutile TiO_2 nanoparticles from an aqueous solution of $TiCl_4$ by a microwave-hydrothermal process at different temperatures (100−160 °C) for 5−120 min, and the addition of PVP to the reaction system produced needle-shaped crystals.[198] Similarly, TiO_2 nanoparticles were also obtained from an aqueous solution containing $TiCl_4$/HCl,[199] $TiOCl_2$,[200] $TiOCl_2$/urea,[201] or $(NH_4)_2TiF_6/H_3BO_3$[202] by microwave heating in a short period of time. The microwave-assisted hydrothermal method was employed to prepare TiO_2 nanoparticles with sizes of ∼5 nm from commercial $K_2Ti_4O_9$ particles without using any organic species at 190 °C for 10 min.[203]

Rutile TiO_2 mesocrystals assembled with ultralong nanowires were prepared by the microwave-assisted hydrothermal approach using $TiCl_3$ as the only reactant in aqueous solution at 200 °C for only 1 min.[208] Suprabha et al.[205] prepared TiO_2 nanostructures with different morphologies, particle sizes, and surface areas using $TiCl_3$ as the titanium source and different precipitating agents at different pH values under microwave irradiation. The morphology of the product could be controlled by changing the pH value of the solution, and various morphologies were obtained including cubical, spherical, and rod shapes. Zheng et al.[204] reported the microwave-assisted hydrothermal synthesis of anatase TiO_2 nanocrystals with tunable percentage of the reactive (001) facet from an aqueous solution of tetrabutyl titanate and HF at 200 °C for 30 min. They found that the shapes of TiO_2 nanocrystals evolved from nanosheets to truncated octahedral bipyramids, resulting in a decrease in the percentage of the exposed (001) facet from 71% to 23% with increasing amount of water. Commercial TiO_2 nanoparticles (P25) were also adopted for the synthesis of anatase TiO_2 nanowires with diameters of 5−10 nm in KOH aqueous solution by microwave heating combined with calcination.[207] TiO_2 nanotubes with diameters of 8−12 nm were synthesized using TiO_2 of either anatase or rutile or mixed phases and NaOH in aqueous solution by microwave heating at 195 W for 90 min.[209] Titanate nanotubes with inner diameters of ∼5−9 nm were prepared in a high yield (>90%) using an aqueous solution containing anatase TiO_2 and 40% (w/w) NaOH by pulsed microwave heating for 6 h.[296] Sitthisang et al.[210] prepared undoped and C-doped anatase TiO_2 nanoparticles from a Ti precursor, such as Ti ethoxide, Ti isopropoxide, or Ti oxysulfate, and a carbon source (glucose, sucrose, or cyclodextrin) in deionized water by a microwave-hydrothermal process in the temperature range of 140−180 °C for 1 or 2 h. Anatase nanoparticles with sizes of 4−17 nm were obtained in all cases with specific surface areas in the range of

dx.doi.org/10.1021/cr400366s | Chem. Rev. 2014, 114, 6462−6555

151−267 m^2/g. Yin et al.[211] prepared nitrogen-doped titania ($TiO_{2-x}N_y$) nanoparticles by a microwave-assisted hydrothermal process. Glaspell et al.[212] synthesized TiO_2 nanoparticles doped with 1%, 5%, or 10% transition metal (Co, Fe, and Ni) using metal salts in aqueous solution by microwave heating.

SnO nanoparticles with sizes less than 30 nm were synthesized by a microwave-assisted solution process, in which amorphous oxy-hydroxy precipitate of Sn^{2+} was crystallized by microwave heating. It was found that microwave heating selectively accelerated SnO crystallization but not the concurrent Sn^{2+} oxidation, which otherwise prevailed in the conventional thermal heating process.[155] Pires et al.[156] prepared SnO powders with different morphologies using $SnCl_2·2H_2O$ as the tin source by a microwave-assisted hydrothermal process. By changing the hydrothermal processing time, temperature, type of mineralizing agent (NaOH, KOH, or ammonia), and its concentration, SnO crystals with a plate-like shape and thicknesses varying from 30 nm to 2 μm could be obtained. Yoshinaga et al.[158] prepared SnO_2 nanoparticles with sizes of ∼5 nm using $SnCl_4·5H_2O$ as the only starting reagent in aqueous solution by microwave heating at 100 °C for 5 min. The specific surface area of microwave-synthesized SnO_2 nanoparticles was about 10 times larger than that of the SnO_2 specimen synthesized by the conventional heating method. SnO_2 nanoparticles were investigated as a rechargeable electrode material, and the initial lithium insertion capacity was significantly higher than that of a specimen synthesized by the conventional heating method. SnO_2 nanoparticles with sizes of several nanometers were prepared from $SnCl_4$/urea or $SnCl_4$/HCl or $SnCl_4$/HCl/alkali (urea or ammonia) in aqueous solution by microwave heating.[157,159,160] Porous SnO_2 nanotubes were synthesized using $SnCl_4$ and glucose in aqueous solution by a rapid microwave-assisted hydrothermal process at 150 °C for 30 min followed by annealing in air, and SnO_2 nanotubes were formed by interconnected nanocrystals with sizes of ∼8 nm.[161] Solid solutions of $Ti_xSn_{1-x}O_2$ were prepared from a solution containing $TiCl_3$ and $SnCl_4$ by a microwave-assisted hydrothermal process at 200 °C for 10 min, and the difference in the formation rate of TiO_2 and SnO_2 could be effectively reduced by microwave heating under the constant power mode, resulting in the precise control of the solid solution composition.[162]

Rizzuti et al.[216] prepared ZrO_2 nanoparticles with sizes of ∼8 nm from an aqueous solution of $ZrOCl_2·8H_2O$ by the microwave-hydrothermal method, and the as-prepared ZrO_2 nanoparticles aggregated to form big aggregates of ∼50 nm. Bondioli et al.[215] prepared ZrO_2 nanoparticles with sizes of 10−20 nm using $ZrOCl_2·8H_2O$ and NaOH in aqueous solution under microwave-hydrothermal conditions at 194 °C for 2 h, and it was found that the tetragonal polymorph increased with increasing NaOH concentration and reached the maximum value by using 1 M $ZrOCl_2·8H_2O$. Bellon et al.[217] reported the microwave-forced hydrolysis preparation of ZrO_2 consisted of aggregates of small primary nanoparticles using $ZrCl_4$ solution at 180 °C, and the obtained solution was colloidally stable for more than 6 months without sedimentation. Bondioli et al.[218] used the microwave-assisted hydrothermal method for the synthesis of Pr-doped ZrO_2 nanoparticles with an average size of 7.9 nm using $ZrOCl_2·8H_2O$, $Pr(NO_3)_3$, and NaOH in aqueous solution (pH 9) at 14 atm for 2 h. Rizzuti et al.[219] reported that NaOH-based hydrolysis of zirconyl chloride in a solution containing $Ca(NO_3)_2$ followed by a microwave-hydrothermal process at 220 °C for 30 min resulted in calcia-stabilized tetragonal ZrO_2 nanoparticles with sizes of about 7 nm.

Hariharan et al.[220] reported the synthesis of WO_3 nanoparticles using H_2WO_4, NaOH, PEG, and HCl (pH 1) by microwave heating at 180 W for 10 min. Both samples prepared with and without the surfactant crystallized in the orthorhombic structure corresponding to $WO_3·H_2O$. However, subsequent annealing under identical conditions (600 °C/air/6 h) led to significantly different products, that is, monoclinic $W_{17}O_{47}$ from the surfactant-free sample and orthorhombic WO_3 from the PEG-assisted sample. Sun et al.[221] prepared $WO_3·2H_2O$ nanospheres using $Na_2WO_4·2H_2O$ and L-(+)-tartaric acid by a microwave-hydrothermal process at 320 W for 20 min, and the morphology of $WO_3·2H_2O$ nanostructures was dependent on the concentration of L-(+)-tartaric acid, which played an important role in the formation of $WO_3·2H_2O$ nanospheres. Phuruangrat et al.[222] prepared hexagonal WO_3 nanowires with diameters of 5−10 nm in an aqueous solution containing $(NH_4)_2SO_4$ and Na_2WO_4 by the microwave-assisted hydrothermal method at 150 °C for 3 h. Sungpanich et al.[223] synthesized WO_3 nanoplates using $Na_2WO_4·2H_2O$ and citric acid in deionized water by a microwave-hydrothermal process at 270 W for 0.5−3 h. Wei et al.[224] prepared MoO_3 nanoflowers with an orthorhombic structure directly grown on a Si substrate by a microwave-hydrothermal process at 90 °C for 2 min. The nanoflowers consisted of nanobelts with tens of nanometers in thickness, tens to several hundreds of nanometers in width, and up to ten micrometers in length.

Corradi et al.[225] prepared CeO_2 nanoparticles with diameters of 4−5.8 nm from the reaction between $(NH_4)_2Ce(NO_3)_6$ and NaOH in aqueous solution under microwave-hydrothermal conditions at 13.4 atm for 5 min. Araújo et al.[229] synthesized CeO_2 nanoparticles using an aqueous solution containing $Ce(NO_3)_2·6H_2O$ and NaOH by the microwave-assisted hydrothermal method at different temperatures for 16 min, and the morphology of the product could be varied by adjusting the hydrothermal temperature. The product synthesized at 80 °C consisted of spherical nanoparticles with sizes of ∼5 nm, while a mixture of spherical and rod-like nanostructures were obtained at 120 °C, and nanorods with an average diameter of 10 nm formed at 160 °C. CeO_2 nanoparticles were prepared using an aqueous solution containing $(NH_4)_2Ce(NO_3)_6$, a weak alkali (CH_3COONa or HMTA or ammonia), and PEG under microwave irradiation.[226−228] Natile et al.[230] prepared CeO_2 nanostructured powders by two different synthetic routes: two samples were obtained by precipitation from a basic solution of cerium nitrate at 250 and 650 °C, respectively, and the third one was prepared by microwave-assisted hydrolysis in aqueous solution using $[(NH_4)_2Ce(NO_3)_6]$, CH_3COONa, and PEG at 90 °C (350 W) for 10 min. A broad particle size distribution was observed for CeO_2 nanoparticles obtained by precipitation (8.0−15.0 nm), and smaller nanoparticles (around 3.3−4.0 nm) with a narrow particle size distribution were obtained by microwave heating.[230] Gao et al.[231] adopted the microwave-hydrothermal method for the fast synthesis of CeO_2 nanostructures, and the average sizes of CeO_2 nanoparticles could be adjusted from ∼1.6 to 20 nm. By changing the cerium source and amount of aqueous ammonia, CeO_2 nanorods could be obtained.

Microwave-assisted methods are also capable for the preparation of rare earth doped CeO_2 nanostructures in aqueous solution in a short period of time. Godinho et al.[53]

prepared Gd-doped CeO_2 nanoparticles using $Ce(NO_3)_3 \cdot 6H_2O$, Gd_2O_3, a small amount of HNO_3, and ammonia in aqueous solution by microwave-hydrothermal treatment at 130 °C for 30 min. Bondioli et al.[232] synthesized Pr-doped CeO_2 nanoparticles with sizes of ~25−30 nm using $(NH_4)_2Ce(NO_3)_2$, $Pr(NO_3)_3 \cdot 6H_2O$, and ammonia in aqueous solution by a microwave-assisted hydrothermal route for 1 h. Prado-Gonjal et al.[233] obtained Sm- and Gd-doped and undoped CeO_2 nanoparticles from aqueous solutions containing corresponding metal nitrates and KOH under microwave-hydrothermal conditions at 200 °C for 30 min.

de Moura et al.[235] reported the microwave-assisted synthesis of Y_2O_3:Eu^{3+} nanorods and nanoplates through thermal decomposition of $Y(OH)_3$ precursors. The precursors were prepared using $Y(NO_3)_3 \cdot 8H_2O$, Eu_2O_3, and HNO_3 (the final pH value of 12.5 was adjusted using a NaOH solution) under microwave-hydrothermal conditions at 140 °C for 10, 20, and 40 min. Y_2O_3 and Y_2O_3:Eu^{3+} powders were obtained from the decomposition of the precursors by solid-state microwave heating at 500 °C for 20 min. Dai et al.[236] prepared $(Y,Gd)_2O_3$ and $(Y,Gd)_2O_3$:Eu flower-like structures through two steps: $(Y,Gd)_2(CO_3)_3 \cdot nH_2O$ flower-like precursors were first synthesized by the urea-based microwave-hydrothermal method, then followed by heat treatment. The flower petals were composed of nanoparticles with diameters of 50−100 nm.

Nanostructures of other metal oxides synthesized by microwave heating have been less reported. For example, Al-Hazmi et al.[139] synthesized MgO nanowires with a diameter of 6 nm using $Mg(CH_3COO)_2$ and urea in aqueous solution by a microwave-assisted hydrothermal process at 180 °C for 30 min, followed by calcination at 600 °C for 1 h. Wang et al.[140] prepared polymer-stabilized PdO nanoparticles through hydrolytic decomposition of H_2PdCl_4 in aqueous solution in the presence of PVP and NaOH (or CH_3COONa or sodium benzoate) under microwave irradiation. Pan et al.[141] prepared PtO_2 nanoparticles using $H_2PtCl_6 \cdot 6H_2O$, NaOH, CH_3COONa, and PVP in aqueous solution by the microwave and conventional heating, respectively. PtO_2 nanoparticles obtained by microwave heating were smaller (1.68 nm) and more narrowly distributed in size than those obtained by the conventional heating (2.1 nm). PtO_2 nanoparticles obtained by microwave heating showed a higher catalytic activity than those obtained by the conventional heating for hydrogenation of cyclohexene. Qiu et al.[237] prepared bundles of $V_2O_5 \cdot xH_2O$ nanobelts with high flexibility from the microwave-assisted refluxing reaction between $VOSO_4$ and $(NH_4)_2S_2O_8$ in aqueous solution at 100 °C for 1 h.

Siqueira et al.[238] reported the microwave-assisted synthesis of nanoparticles of $NiWO_4$, $CoWO_4$, and $MnWO_4$ using the corresponding metal nitrate and $Na_2WO_4 \cdot 2H_2O$ in deionized water at 110 or 150 °C for 10 or 20 min. Almeida et al.[239] synthesized $FeWO_4$ nanocrystals using an aqueous solution containing $(NH_4)_2Fe(SO_4)_2 \cdot 6H_2O$ and $Na_2WO_4 \cdot 2H_2O$ by the microwave-hydrothermal approach at 170 °C for 45 min. $BaWO_4$ nanoparticles were synthesized using $BaCl_2$ and $Na_2WO_4 \cdot 2H_2O$ without any surfactant in aqueous solution under microwave irradiation at 180 °C for 10 min.[240] However, $BaWO_4$ nanosheets and nanobelts were obtained in the presence of PVP under microwave irradiation at 100 °C for 5 min. It was found that the PVP concentration played an important role in the formation of $BaWO_4$ nanostructures with different morphologies.[241] Thongtem et al.[242] prepared AWO_4 (A = Ca, Sr) nanostructured materials with different morphologies such as spheres, peaches with notches, dumbbells and bundles from metal salts, $Na_2WO_4 \cdot 2H_2O$, and CTAB in aqueous solution under cyclic microwave irradiation at 300 W for 10 min. $AgIn(WO_4)_2$ mesocrystals were prepared from an aqueous solution containing $AgNO_3$, $In(NO_3)_3 \cdot 4.5H_2O$, and $Na_2WO_4 \cdot 2H_2O$ by microwave heating at 180 °C for 20 min, and the pH value played an important role in the phase formation and shape evolution process. The oriented attachment process was responsible for the formation of the hierarchical structures.[243] Sn^{2+}-doped $ZnWO_4$ nanocrystals with sizes of ~3.2−20.6 nm were prepared using $ZnCl_2$, $SnCl_2 \cdot 2H_2O$, Na_2WO_4, and NaOH in aqueous solution (pH 7) through the rapid microwave-assisted hydrothermal approach at 180 °C for 10 min.[244]

Bi_2WO_6 nanoplates were synthesized using $Bi(NO_3)_3$, H_2WO_4, and ammonia as the starting reagents by the microwave-hydrothermal approach.[245] Bi_2WO_6 flower-like nanostructures constructed by nanosheets with thicknesses of ~15 nm were obtained using $Bi(NO_3)_3 \cdot 5H_2O$, Na_2WO_4, HMTA, and HNO_3 in aqueous solution via a rapid microwave-assisted process at 180 °C for 5 min, the experiments showed that HMTA and HNO_3 played important roles in the formation of flower-like nanostructures, and the Ostwald ripening process was proposed for the formation of Bi_2WO_6 flower-like nanostructures.[246] Flower-like aggregates of Bi_2WO_6 nanoflakes were obtained in acid precursor suspension by the microwave-hydrothermal method, and the octahedral nanocrystals of $Bi_{3.84}W_{0.16}O_{6.24}$ were synthesized in the alkalescent precursor system.[247] $NaY(WO_4)_2$ hierarchical dumbbells constructed by self-assembly of nanosheets were synthesized using an aqueous solution containing $Y(NO_3)_3 \cdot 6H_2O$, trisodium citrate, and Na_2WO_4 by the microwave-assisted hydrothermal approach at 180 °C for 10 min, followed by heat treatment at 600 °C in air for 1 h. It was found that the amount of trisodium citrate played a crucial role in the self-assembly process of the precursor.[248]

Lehnen et al.[252] prepared Zn_2SnO_4 quantum dots with a narrow size distribution using $ZnCl_2$, $SnCl_4 \cdot 5H_2O$, NaOH, and SDS in aqueous solution under microwave-hydrothermal conditions at 190 °C for different reaction times (5−60 min). The experiments revealed a significantly shortened reaction time in comparison with the conventional hydrothermal synthesis. The stable aqueous suspension of Zn_2SnO_4 quantum dots was further exploited for inkjet printing of functional devices, which could be applied for humidity sensing. Zhang et al.[284] prepared $Cd_2Ge_2O_6$ hierarchical nanostructures formed by self-assembly of nanoneedles employing an aqueous solution containing $Cd(CH_3COO)_2 \cdot 2H_2O$, GeO_2, and $N_2H_4 \cdot H_2O$ via the microwave-assisted approach at 180 °C for 10 min. It was found that the reaction time, reaction temperature, volume of $N_2H_4 \cdot H_2O$, and cadmium source played important roles in the formation of $Cd_2Ge_2O_6$ hierarchical nanostructures. Sun et al.[253] synthesized $ZnGa_2O_4$ nanoparticles with an average diameter of 10 nm from an aqueous solution containing $Ga(NO_3)_3 \cdot 9H_2O$, $ZnCl_2$, and ammonia via the microwave-assisted hydrothermal method at 160 °C for 20 min.

Komarneni et al.[256] reported the rapid microwave-hydrothermal synthesis of ~5−20 nm ferrite nanoparticles such as $ZnFe_2O_4$, $NiFe_2O_4$, $MnFe_2O_4$, and $CoFe_2O_4$ using nitrates of zinc, nickel, manganese, cobalt, and iron at ~164 °C for 4 min, and their specific surface areas ranged from 72 to 247 $m^2\ g^{-1}$. Verma et al.[255] synthesized $MgFe_2O_4$ nanoparticles with an average particle size of ~3 nm from an aqueous solution of

dx.doi.org/10.1021/cr400366s | Chem. Rev. 2014, 114, 6462−6555

$Mg(NO_3)_2·6H_2O$, $Fe(NO_3)_3·9H_2O$, and KOH under microwave-hydrothermal conditions at 150 °C for 25 min. Nyutu et al.[257] preapred $NiFe_2O_4$ (6−20 nm) and $ZnAl_2O_4$ (∼9 nm) nanoparticles by the continuous flow method that combined microwave heating and in situ ultrasonic nozzle spray mixing; the experimental results showed that the ultrasonic nozzle and microwave irradiation complemented each other, with respect to the purity of the products. Kim et al.[258] prepared $Co_{1-x}Zn_xFe_2O_4$ and $Ni_{1-x}Zn_xFe_2O_4$ nanoparticles with an average particle size of ∼10 nm using $FeCl_3·6H_2O$, $NiCl_2·6H_2O$, $CoCl_2·6H_2O$, and $ZnCl_2$ in aqueous solution by the microwave-hydrothermal method. Lai et al.[259] prepared $Mn_{0.5}Zn_{0.5}Fe_2O_4$ nanoparticles with an average size of about 10 nm by microwave-assisted coprecipitation at 100 °C, and it was found that the particle size of the product increased with microwave heating time.

$BiFeO_3$ nanoparticles with sizes of 30−50 nm were prepared using an aqueous solution containing $Bi(NO_3)_3·5H_2O$, $Fe(NO_3)_3·9H_2O$, HNO_3, ammonia, and CTAB by microwave heating at 100 °C for 20 min, followed by annealing at different temperatures of 400−600 °C for 3 h in air.[264] $BiFeO_3$ nanostructures with spherical (15−55 nm) and rectangle-like morphologies and $Bi_2Fe_4O_9$ nanowires with a diameter of 40 nm were obtained using bismuth nitrate/iron nitrate alkaline solutions under microwave-hydrothermal conditions.[265] Perovskite-type $BiFeO_3$ spherical nanocrystals with diameters of 10−50 nm and sillenite-type $Bi_{12}Fe_{0.63}O_{18.945}$ hexagonal-shaped nanocrystals with sizes of 18−33 nm were synthesized using $Bi(NO_3)_3·5H_2O$, $Fe(NO)_3·9H_2O$, KOH, and Na_2CO_3 (Na_2CO_3 was not used for the synthesis of sillenite-type $Bi_{12}Fe_{0.63}O_{18.945}$) by the microwave-hydrothermal method at 180 °C for 1 h.[266]

Zawadzki et al.[261] reported the microwave-assisted hydrothermal synthesis of $ZnAl_2O_4$ nanoparticles with a mean particle size of 2.4 nm at 200 °C for 5 min. Conrad et al. reported the microwave-assisted hydrothermal synthesis of Cu-substituted $ZnAl_2O_4$ nanoparticles[262] and Cu^{2+}-containing $ZnGa_2O_4$ solid solutions.[254] In contrast, the analogous conventional hydrothermal approach failed to generate phase-pure products with homogeneously distributed morphologies, indicating the advantages of the microwave-hydrothermal synthesis over the conventional hydrothermal technique in terms of shorter reaction time and homogeneous products. Obata et al.[263] prepared $CoAl_2O_4$ octahedral nanocrystals with sizes of ∼70 nm by a microwave-hydrothermal process at 240 °C for 2 h, and inkjet printing with as-prepared aqueous pigment ink was performed to decorate porcelain. The nanoparticles were well dispersed in the aqueous suspension with a high stability. The precursor concentration of the suspension greatly affected the color tone of the resulting particles, the printing system experienced no clogging, and the printed image was of good quality.

Komarneni and Katsuki[45,269] used commercial TiO_2 as the titanium source to prepare $BaTiO_3$ nanoparticles with an average particle size of ∼30 nm in an aqueous solution of $Ba(OH)_2$ by microwave heating at 90 or 180 °C. Jhung et al.[270] prepared $BaTiO_3$ nanoparticles with sizes less than 30 nm from an aqueous solution containing $TiCl_4$, $BaCl_2·2H_2O$, and KOH by microwave heating at 180 °C for 30 min, and it was found that the particle size decreased with increasing concentrations of KOH and $BaCl_2$. Similarly, $Ti(OC_4H_9)_4$ was adopted as the titanium source for the microwave-hydrothermal synthesis of $BaTiO_3$ nanoparticles with a nearly uniform size of 50 nm at 150 °C for 50 min.[271] Pazik et al.[272] and Simões et al.[273] reported the microwave-hydrothermal synthesis of $Ba_{1-x}Sr_xTiO_3$ (x = 0.1−0.4) nanoparticles using $Ba(CH_3COO)_2$, $Ti(OC_4H_9)_4$ or $TiCl_4$, $Sr(NO_3)_2$ or $SrCl_2·6H_2O$, and NaOH in aqueous solution. Pazik et al.[272] found that the average particle sizes of the products were in the range of 20−50 nm depending on the hydrothermal time (10−90 min). Nanoparticles (30−60 nm) of Eu^{3+}-doped $BaTiO_3$ were obtained using $Ba(CH_3COO)_2$, titanium butoxide, Eu_2O_3 in nitric acid, and NaOH in aqueous solution by the microwave-hydrothermal method at 300 °C followed by calcination at 600−1000 °C for 1 h.[274] Sulaeman et al.[275] reported the microwave-assisted hydrothermal synthesis of $SrTiO_3$ nanoparticles with particle sizes of 30−40 nm and with various Sr/Ti atomic ratios using $SrCl_2$, $Ti(OC_3H_7)_4$, and KOH in aqueous solution. Moreira et al.[276] conducted a detailed investigation of microwave-assisted hydrothermal synthesis of $SrTiO_3$ nanospheres to gain a better insight into thermodynamic, kinetic, and reaction phenomena involved in $SrTiO_3$ nucleation and crystal growth processes. A possible formation mechanism was proposed, based on dehydration of titanium and strontium clusters followed by mesoscale transformation and self-assembly by the oriented attachment mechanism, resulting in a spherical-like shape. $PbTiO_3$ nanowires with diameters of 20−80 nm were synthesized using $PbCl_2$, $Ti(OC_4H_9)_4$, and KOH as starting reactants by a microwave-hydrothermal process at 200 °C for 1.5 h.[277]

Nosheen et al.[297] reported a phase transition from TiO_2 particles to titanate nanotubes by the breakage of the Ti−O bond. 1-D nanostructures of titanates ($H_2Ti_4O_9·nH_2O$) were obtained using precursors of anatase and P-25 at a low concentration of alkaline solution (1 M NaOH) by a microwave-assisted soft chemical process at 100−110 °C for 12 h. Chou et al.[279] synthesized $Li_4Ti_5O_{12}$ microspheres composed of nanoflakes as the building blocks by a combination of the microwave-assisted hydrothermal method and microwave post annealing. The synthesis was performed using LiOH, H_2O_2, and titanium isopropoxide in aqueous solution by microwave-assisted hydrothermal treatment at 150 °C for 15 min to yield the lithium titanium oxide precursor, which was subsequently annealed by microwave heating in air for 20 min to obtain $Li_4Ti_5O_{12}$ microspheres. Zhang et al.[280] prepared $K_2Ti_6O_{13}$ nanowires with an average diameter of ∼10 nm and lengths ranging from hundreds of nanometers to tens of micrometers using commercial TiO_2 powder (anatase, ∼20 nm) and concentrated KOH aqueous solution under microwave irradiation for 6 h at normal pressure.

$BaMoO_4$ microspheres consisting of nanosheets were synthesized through microwave reflux using $BaCl_2·2H_2O$, $(NH_4)_6Mo_7O_{24}·4H_2O$, and PVP in aqueous solution.[281] $CaMoO_4$ with a persimmon-like shape, which was made up of nanosheets with thicknesses of 10−25 nm, was prepared using $Ca(NO_3)_2$ and $(NH_4)_6Mo_7O_{24}·4H_2O$ in aqueous solution by microwave heating for 1−15 min.[282] γ-Bi_2MoO_6 nanoplates were synthesized using $Bi(NO_3)_3·5H_2O$ and $(NH_4)_2MoO_4$ in aqueous solution by the microwave-hydrothermal approach at 140 °C for 1 h.[283]

Shi et al.[285] reported a fast microwave-assisted hydrothermal process for the preparation of perovskite $NaTaO_3$ nanocrystals using Ta_2O_5 and NaOH as starting materials. The reaction mixture was heated to 100−220 °C in 20 min and maintained at the designated temperature for 5 min to 6 h. By pretreating the Ta_2O_5 powder with ball milling, pure phase $NaTaO_3$ could

be synthesized under mild conditions through the formation of an intermediate pyrochlore $Na_2Ta_2O_6$ phase, while much longer times were required in a conventional hydrothermal process. That is, pretreatment of the raw material Ta_2O_5 by ball milling is a crucial step in obtaining a pure perovskite $NaTaO_3$ phase. The mechanism for the fast growth of pure $NaTaO_3$ nanocrystals was proposed according to the phase evolution during the reactions. An indirect formation route of $Ta_2O_5 \rightarrow Na_2Ta_2O_6 \rightarrow NaTaO_3$ was suggested when using the ball milled Ta_2O_5 as the starting material, while a direct conversion from Ta_2O_5 to $NaTaO_3$ was put forward for the reaction starting from Ta_2O_5 without ball milling. They proposed that the indirect path is a process with a lower thermodynamic energy barrier in comparison with the direct one, so that it can drive a complete reaction to produce the pure perovskite $NaTaO_3$ under mild conditions. $SnNb_2O_6$ nanosheets with thicknesses of 1−4 nm were prepared using $Nb_2O_5{\cdot}nH_2O$ (n = 5−8) and $SnCl_2$ in aqueous solution by the microwave-assisted hydrothermal method without exfoliation at 200 °C for various times.[286]

$BiVO_4$ nanostructures with the tetragonal and monoclinic phases were prepared from aqueous solutions containing $Bi(NO_3)_3$ and $NaVO_3$ by the rapid microwave-assisted method, and the highly crystalline phase converted irreversibly from tetragonal to monoclinic $BiVO_4$ with prolonged microwave irradiation time.[287] $BiVO_4$ hollow microspheres constructed by nanorods were synthesized using an aqueous solution containing $Bi(NO_3)_3{\cdot}5H_2O$ and NH_4VO_3 in the presence of ethylenediaminetetraacetic acid (EDTA) by the microwave-hydrothermal method at 180 °C for 3 h, and it was found that the amount of EDTA played a crucial role in determining the morphology of the product.[288] $CeVO_4$ nanoparticles were synthesized using $Ce(NO_3)_3$ and $NaVO_3$ under microwave irradiation for 10 min, and the sizes of $CeVO_4$ nanoparticles were in the range of 6−18 nm and were dependent on the pH value.[289] YVO_4 nanoparticles were obtained by a similar method.[290] $LaVO_4$:Ln^{3+} (Ln^{3+} = Eu^{3+}, Tb^{3+}, Sm^{3+}, and Dy^{3+}) nanorods with diameters of 10−20 nm and lengths up to 200 nm were prepared using $Tb(NO_3)_3$, $La(NO_3)_2$, and NH_4VO_3 in aqueous solution (pH between 8 and 9) by simultaneous supersonic and microwave irradiation at a low temperature (70 °C) for 45 min, and red, green, orange-red, and blue-yellow emission colors were obtained using different lanthanide ions.[291]

2.3. Metal Sulfides

Nanostructured metal sulfides are important functional materials and widely used in many areas. Microwave-assisted rapid synthesis of metal sulfide nanostructures has aroused much interest due to its advantages especially in terms of very short processing time. In the microwave-assisted synthesis of metal sulfide nanostructures in aqueous solution, a water-soluble metal salt is usually used as the metal source, a sulfur source is used to provide S^{2-} ions, and an additive or surfactant is sometimes adopted to control the morphology and size of the product. A variety of metal sulfide nanostructures with various morphologies have been reported by the rapid microwave-assisted method in aqueous solution, including PbS,[298−300] CuS,[301] Cu_9S_8,[302] CdS,[303−309] ZnS,[303,310−313] Ag_2S,[314] Bi_2S_3,[315,316] HgS,[317] $AgInS_2$,[318] $AgIn_5S_8$,[319] $CuInS_2$,[320] $CuInSe_2$,[320] $CdIn_2S_4$,[321] and Cu_2ZnSnS_4.[322] The sulfur sources commonly adopted in microwave-assisted synthesis of metal sulfide nanostructures in aqueous solution include Na_2S,[305,307,311,317] CS_2,[304] $Na_2S_2O_3$,[309] NH_2CSNH_2,[298,301,308,316,321] $NH_2NHCSNH_2$,[299] CH_3CSNH_2,[302,303,306,310,312,314,318,319,322] and 3-mercaptopropanoic acid.[300]

A micelle-assisted solution route was adopted to synthesize pure and Zn-doped PbS nanocrystals using $PbCl_2ZnCl_2$, 3-mercaptopropanoic acid, thioacetamide, and NaOH under microwave irradiation for 40 s, and the micelle structure played an important role in the formation of PbS nanocrystals.[300] PbS nanostructures with different sizes and morphologies were prepared using $Pb(CH_3COO)_2{\cdot}3H_2O$ and thiourea in the solvent of distilled water, ethanol, ethylene glycol, or PEG-200 by microwave heating.[298] Nanoparticle-assembled PbS nanotubes with diameters of 20−40 nm were prepared from an aqueous solution containing $Pb(NO_3)_2$, $NH_2NHCSNH_2$, and NaOH through a microwave-assisted route without using any surfactant.[299] Bi_2S_3 nanorods with diameters of ∼10 nm were prepared from a formaldehyde aqueous solution containing $Bi(NO_3)_3{\cdot}5H_2O$ and thiourea under microwave irradiation.[315] Bi_2S_3 nanorods in flower-shaped bundles were synthesized using thiourea as the sulfur source and PVP as a surfactant by a microwave-assisted hydrothermal process at 200 °C for 1 h.[316]

Cu_9S_8 nanorods with diameters of 5−10 nm and lengths of 30−60 nm were prepared from an aqueous solution containing $Cu(NO_3)_2{\cdot}3H_2O$, thioacetamide, and SDS under pulsed microwave irradiation for 20 min.[302] CuS hierarchical flower-like spheres and self-assembled chains were synthesized using $CuCl_2{\cdot}2H_2O$, thiourea, NaOH, and EDTA in aqueous solution under pulsed microwave irradiation for 20 min. The as-prepared CuS flower-like spheres were constructed by nanosheets as primary building units, whereas the hierarchical chains were formed by the oriented attachment of the flower-like spheres.[301]

ZnS and CdS nanoparticles were prepared by a fast microwave-assisted reaction between $CdCl_2$ or $Zn(CH_3COO)_2$ and thioacetamide in aqueous solution, and the particle size was ∼9 and 3 nm for CdS and ZnS, respectively.[303] ZnS nanoparticles (∼6.5 nm) and doped ZnS nanoparticles were synthesized using corresponding metal salts and Na_2S via microwave irradiation for 10 min, and it was found that the luminescent properties of ZnS nanoparticles were greatly affected by either the microwave irradiation time or the dopants of various metallic ions (Ag^+, Cu^{2+}, Ce^{3+}, and Sn^{4+}).[311] ZnS nanoballs formed by self-assembly with nanoparticles were prepared using $Zn(CH_3COO)_2$ and thioacetamide in aqueous solution via a microwave-assisted route, and $ZnSO_4$ and $Zn(NO_3)_2$ were also used as the zinc source to prepare ZnS nanoparticles instead of nanoballs.[310] Mehta et al.[312] prepared monodisperse PEG-coated ZnS nanoparticles with a cubic zinc blend structure and diameters of ∼11 ± 3 nm using $Zn(CH_3COO)_2{\cdot}2H_2O$, CH_3CSNH_2, and PEG in aqueous solution by microwave heating (Figure 9). It can be seen from the TEM micrographs in Figure 9 that a thin layer of PEG was uniformly coated on the surface of the as-synthesized ZnS nanoparticles. The fast microwave heating accelerated the decomposition of thioacetamide to provide S^{2-} ions:[312]

$$CH_3CSNH_2 + H_2O \rightarrow CH_3CONH_2 + H_2S$$

$$H_2S \rightarrow 2H^+ + S^{2-}$$

The nucleation of ZnS occurred due to the reaction between Zn^{2+} and S^{2-} ions:

dx.doi.org/10.1021/cr400366s | Chem. Rev. 2014, 114, 6462−6555

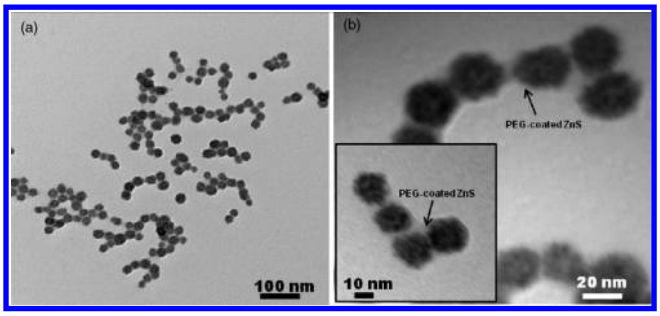

Figure 9. Typical TEM micrographs of PEG-coated ZnS nanoparticles prepared by a microwave-assisted process. Reproduced with permission from ref 312. Copyright 2011 Elsevier B.V.

$$Zn^{2+} + S^{2-} \rightarrow ZnS$$

A similar method was reported for the preparation of $Zn_{1-x}Cd_xS$ particles using $Zn(CH_3COO)_2{\cdot}2H_2O$, $Cd(CH_3COO)_2{\cdot}2H_2O$, and CH_3CSNH_2 in aqueous solution by household microwave oven heating for 6 min,[313] in which no PEG was used as a surfactant, and the sizes of $Zn_{1-x}Cd_xS$ particles were much larger (100−300 nm) than those synthesized using PEG (~11 nm).[312]

CdS nanoparticles were produced from the reactions between $CdCl_2$ and various sulfur sources in aqueous suspension of laponite, which was used for good dispersion of CdS nanoparticles and for facilitating the formation of the product by providing a basic environment when CS_2 was used as a sulfur source; CdS structures with different shapes and sizes were obtained by adjusting reaction conditions.[304] CdS hollow nanospheres packed with square subunits were fabricated using $CdSO_4{\cdot}(8/3)H_2O$, $Na_2S{\cdot}6H_2O$, and pentaerythritol in aqueous solution via microwave irradiation in a rectangular waveguide at room temperature (25 °C).[305] CdS nanowires on DNA scaffolds were synthesized using $Cd(ClO_4)_2$, thioacetamide, and DNA in aqueous solution under pulsed microwave irradiation for 1 min. Highly selective deposition on DNA was obtained by specific complexation between Cd^{2+} ions and DNA molecules, followed by decomposition of thioacetamide to S^{2-} to form CdS. This one-step process did not perturb the overall conformation of the DNA chain.[306] CdS nanotubes were synthesized using $CdSO_4$ and Na_2S in aqueous solution via microwave irradiation, the solutions were maintained in a circular waveguide at room temperature (25 °C) and under ambient pressure for 20 days, and the waveguide was made of copper with a diameter of 95 mm in cross-section, which propagated 10 W of microwave irradiation (2.45 GHz).[307] Arrays of noncrystalline CdS nanotubes were prepared by employing an aqueous solution containing $CdCl_2$ and thiourea in the presence of anodic porous alumina membrane under microwave refluxing for 10 min.[308] Hu et al.[309] demonstrated a two-step microwave-assisted coating of CdS nanoparticles on the surface of carbon spheres. First, cadmium ions were adsorbed on the hydrophilic shell of carbon spheres. Second, the above carbon spheres were dispersed in distilled water, and then $Na_2S_2O_3{\cdot}5H_2O$ as the sulfur source was added. The mixture was heated under microwave refluxing at 280 W for different times, resulting in C@CdS hybrid spheres. The thickness of the CdS nanoparticle shell could be varied by the microwave heating time. In addition, CdS nanospheres were prepared using $CdCl_2{\cdot}2.5H_2O$, $Na_2S_2O_3{\cdot}5H_2O$, and PVP in aqueous solution via microwave refluxing at 28 W for different times.

Ag_2S nanoworms with diameters of ~50 nm were prepared by reacting $AgNO_3$ with thioacetamide in the presence of BSA in aqueous solution via the rapid microwave-assisted hydrothermal method. The as-prepared Ag_2S nanoworms were formed by assembly of Ag_2S nanoparticles and stabilized by a layer of BSA.[314] HgS nanotubes were prepared using $HgCl_2$ and Na_2S in aqueous solution by microwave heating under ambient conditions, and the reaction solution was maintained in a circular waveguide at room temperature (25 °C) and under ambient pressure for 20 days. The waveguide was made of copper with a diameter of 95 mm in cross section, which propagated 10 W microwaves (2.45 GHz).[317]

$AgInS_2$ and $AgIn_5S_8$ nanoparticles were synthesized using thioacetamide as the sulfur source by the microwave-hydrothermal method.[318,319] Bensebaa et al.[320] reported the microwave-assisted preparation of $CuInS_2$ and $CuInSe_2$ nanoparticles using Cu, In, and S/Se precursors in the presence of mercaptoacetic acid in aqueous solution for 30 min. Apte et al.[321] synthesized $CdIn_2S_4$ hierarchical nanostructures using $Cd(NO_3)_2{\cdot}4H_2O$, $In_2(NO_3)_2$, and thiourea by microwave-assisted reactions, and different capping agents such as Titron X, SDS, and sodium lauryl sulfate were also used. Shin et al.[322] synthesized Cu_2ZnSnS_4 nanocrystals by a two-step process. In the first step, the precursor powder was obtained from an aqueous solution containing $Cu(CH_3COO)_2$, $Zn(CH_3COO)_2$, $SnCl_2$, and thioacetamide under microwave irradiation at 700 W for 10 min. In the second step, the precursor powder was sulfurized by annealing in H_2S (5%)/N_2 (95%) at 550 °C for 1 h in a commercial furnace.

2.4. Metal Selenides

As compared to the microwave-assisted synthesis of nanostructured metal oxides and sulfides, the microwave-assisted synthesis of metal selenide nanostructures has been less reported, possibly due to relatively high-cost, less available selenide sources and challenges in the preparation. The rapidness of microwave-assisted synthesis is more remarkable for nanostructures of metal selenides, with significantly reduced reaction time to minutes. Zhu et al.[323] synthesized nanoparticles of CdSe, PbSe, and $Cu_{2-x}Se$ by fast microwave refluxing reactions between acetates or sulfates of Cd, Pb, Cu, and Na_2SeSO_3 in the presence of the complexing agent in aqueous solution. It was found that the crystal phase of CdSe was dependent on microwave reaction time. CdSe with a cubic structure was obtained by microwave heating for 10 min; however, longer reaction time led to a crystal phase transition. When the reaction time was prolonged to 30 min, CdSe with a hexagonal structure was obtained. Gallagher et al.[324] reported the microwave-assisted synthesis of chiral CdSe quantum dots by using chiral stabilizers dextrorotatory (D-) and levorotatory (L-) enantiomers as well as the racemate (*rac*-) of the amino acid in aqueous solution at 1500 W for 40 s. CdSe quantum dots were prepared in aqueous solution under microwave-assisted hydrothermal conditions at temperatures between 120−210 °C for minutes.[325] CdSe nanoparticles with a cubic phase and narrow photoluminescent emission were synthesized in aqueous solution in the presence of citric acid under microwave irradiation.[326]

ZnSe nanocrystals were synthesized using $ZnCl_2$ and NaHSe in the presence of 3-mercaptopropionic acid as a stabilizer in aqueous solution (pH 6.5) by microwave heating at 140 °C.[327] Glutathione-capped ZnSe quantum dots with sizes of 2−3 nm were prepared using Na_2SeO_3 as a selenium source to replace

dx.doi.org/10.1021/cr400366s | *Chem. Rev.* 2014, 114, 6462−6555

commonly adopted NaHSe or H_2Se in aqueous solution by microwave refluxing under air atmosphere for 1 h. In this method, Na_2SeO_3 was reduced by $NaBH_4$ under ambient conditions to generate Se^{2-} ions.[328] ZnSe:Cu and ZnSe:Mn quantum dots with a passivated surface were synthesized using $Zn(NO_3)_2·6H_2O$, $CuCl_2·2H_2O$ or $MnCl_2·4H_2O$, NaHSe, 3-mercaptopropionic acid, and NaOH in aqueous solution by microwave refluxing two times for a total heating time of 20 min.[329]

Bensebaa et al.[320] prepared $CuInSe_2$ nanoparticles in an aqueous solution containing Cu, In, and S/Se precursors in the presence of mercapto-acetic acid by microwave heating for 30 min. A green microwave synthetic route to $CuIn_{1-x}Ga_xSe_2$ nanoparticles with $x = 0$, 0.25, and 0.5 and with sizes of several nanometers in aqueous solution at 95 °C for 30 min was described by Al Juhaiman et al.[330] In this method, appropriate amounts of $Cu(CH_3COO)_2·2H_2O$, $InCl_3$, $GaCl_3$, Na_2Se, and mercapto-acetic acid were used as the starting reagents. The as-prepared nanoparticles were stable in aqueous solution for several weeks.

2.5. Metal Tellurides

The preparation of nanostructured metal tellurides is even more challenging as compared to the synthesis of metal selenides. The reported work has focused on the microwave-assisted synthesis of CdTe nanostructures, which is a very important semiconductor and has wide applications in various fields. CdTe is used as an infrared optical window and a solar cell material. It is usually sandwiched with CdS to form a p−n junction photovoltaic solar cell.

The traditional aqueous solution route to the preparation of CdTe nanocrystals is usually time-consuming. NaHTe has been commonly used as the tellurium source. Li et al.[331] reported the microwave-assisted synthesis of high-quality CdTe nanocrystals using $CdCl_2$, NaHTe, 3-mercaptopropionic acid, and NaOH in aqueous solution. At a relatively low temperature (below or equal to 160 °C), CdTe nanocrystals with various sizes and with high quantum yield were synthesized by simply varying the reaction temperature and reaction time. This method allows the rapid preparation of a series of CdTe nanocrystals emitting at the green to near-infrared spectral window (505−733 nm) at moderate temperatures. Similarly, highly luminescent CdTe nanocrystals with diameters of ∼2−4 nm were rapidly prepared (1−30 min) using $CdCl_2$ and NaHTe in the presence of 3-mercaptopropionic acid in aqueous solution through microwave irradiation.[332] CdTe nanocrystals were prepared using $CdCl_2$ and NaHTe at pH 11.4 in the presence of thioglycolic acid in aqueous solution by microwave heating at 90 °C for 15 min. When 3-mercaptopropionic acid was substituted for thioglycolic acid, the pH value of precursors was adjusted to 8.4, and the reaction temperature was raised to 100 °C.[333] Guo et al.[334] synthesized *N*-acetyl-L-cysteine-capped CdTe nanocrystals with the average particle sizes ranging from 2.5 to 3.6 nm using $CdCl_2$ and NaHTe in the presence of *N*-acetyl-L-cysteine via microwave heating at 95 °C. A series of CdTe samples were prepared by controlling the microwave heating time. Fluorescent CdTe quantum nanospheres with sizes of ∼35 nm consisting of quantum dots were synthesized using NaHTe as the tellurium source in the presence of poly(allylamine) in aqueous solution under microwave irradiation at 100 °C for 15 min. He et al.[335] prepared multicolor CdTe nanospheres with maximum emission wavelengths ranging from 525 to 610 nm; they found that only irregularly shaped quantum dots−polymer complexes were obtained when the conventional heating was used, indicating the important role of microwave heating in the formation of CdTe nanospheres.

Na_2TeO_3 has also been adopted as a tellurium source. A one-pot microwave-assisted reduction route was reported for the synthesis of highly luminescent CdTe quantum dots using Na_2TeO_3 as the tellurium source in an aqueous environment. It was found that the experimental parameters including the reaction temperature and time, pH value of solution, and molar ratio of 3-mercaptopropionic acid to Cd^{2+} had considerable effects on the particle size and photoluminescence quantum yield of CdTe quantum dots.[336] Glutathione-capped $Zn_{1-x}Cd_xTe$ quantum dots were obtained using $CdCl_2·2.5H_2O$, $ZnCl_2$, Na_2TeO_3, KBH_4, and glutathione under microwave refluxing.[337] $CdSe_xTe_{1-x}$ ($0 \le x \le 1$) nanocrystals were synthesized by coreduction of Na_2SeO_3 and Na_2TeO_3 in aqueous solution under microwave irradiation at 120 °C for 10−30 min.[338]

2.6. Inorganic Biomaterials − Hydroxyapatite and Calcium Phosphates

Hydroxyapatite (HAP) and calcium phosphates are important inorganic biomaterials and have wide applications in the biomedical fields. In recent years, the microwave-assisted synthesis of nanostructured biomaterials has aroused much interest. Lee et al.[339] prepared HAP and biphasic tricalcium phosphate nanopowders using $Ca(OH)_2$ as the calcium source, H_3PO_4 as the phosphorus source, and ammonia in aqueous solution by microwave heating at 700 W for 25 min. Finally, the calcination was carried out at 750 °C in air. The synthesized powders consisted of spherical nanoparticles with the average sizes in the range of 50−90 nm. In the pH range of 6−12, two phases of HAP and β-tricalcium phosphate coexisted. The average particle size of the synthesized powders decreased as the pH of the solution increased, and the particle sizes at pH 6 and 12 were about 80−90 and 50−70 nm, respectively. The yield of HAP increased as the pH value of solution increased, while the yields of α-tricalcium phosphate and β-tricalcium phosphate decreased. At pH 12, HAP nanoparticles were obtained.

Vani et al.[340] prepared mesoporous HAP nanorods with lengths of 40−75 nm and a diameter of 25 nm using a solution (pH 10) containing $Ca(NO_3)_2·4H_2O$, $(NH_4)_2HPO_4$, and ammonia under microwave irradiation at 900 W for 30 min. Lak et al.[341] obtained single-crystalline HAP nanorods with diameters of ∼25 nm and lengths of ∼100 nm using $Ca(NO_3)_2·4H_2O$, Na_2HPO_4, NaOH, and EDTA under microwave irradiation at 900 W for 2.5 min. The microwave-assisted reactions with the same reactants for 30 min produced HAP nanorods, and bow-knot-like and flower-like nanostructures. It was found that the pH value and the complex reagent EDTA played important roles in the formation of HAP nanostructures.[342]

The combination of sonochemistry and microwave irradiation provides a new unique route for the preparation of inorganic nanostructures in liquid phase. Liang et al.[343] reported the template-free sonochemistry-assisted microwave method for the synthesis of mesoporous HAP nanostructures using $Ca(NO_3)_2·4H_2O$ and $(NH_4)_2HPO_4$ in aqueous solution (pH 10.5) for 10 min. The product consisted of HAP nanorods with lengths of 50−100 nm and widths of about 20 nm. N_2 adsorption−desorption isotherms revealed an irregular mesoporous structure. It was found that microwave radiation played

dx.doi.org/10.1021/cr400366s | *Chem. Rev.* 2014, 114, 6462−6555

a dominant role in the formation of mesoporous structure, while ultrasound irradiation acted as a supporting role.

Chen et al.[344] reported the microwave-assisted hydrothermal synthesis of multifunctional Eu^{3+}/Gd^{3+} dual-doped HAP nanorods using $CaCl_2$, $Na_2HPO_4{\cdot}12H_2O$, europium nitrate, gadolinium nitrate, NaOH, and polylactide-*block*-monomethoxy(poly(ethylene glycol)) (PLA-mPEG) in deionized water at 200 °C. Figure 10 shows both undoped and

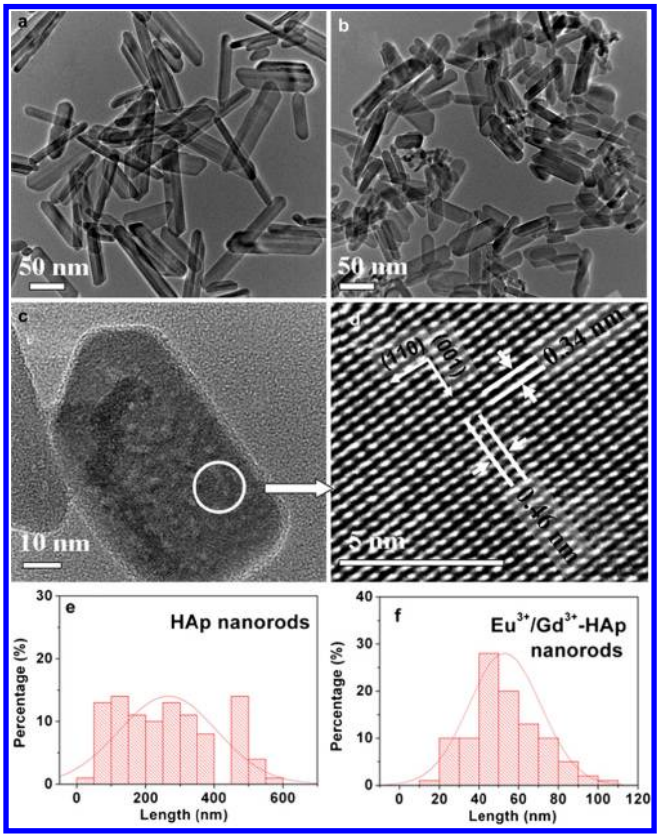

Figure 10. (a–d) TEM micrographs of the samples prepared by the microwave-assisted hydrothermal method at 200 °C for 30 min: (a) undoped HAP nanorods; (b–d) Eu^{3+}/Gd^{3+}-HAP nanorods (Eu^{3+}/Gd^{3+} molar ratio = 1:1). (e,f) Length distributions of HAP nanorods measured from TEM micrographs: (e) undoped HAp nanorods; (f) Eu^{3+}/Gd^{3+}-HAP nanorods. Reproduced with permission from ref 344. Copyright 2011 Elsevier Ltd.

doped HAP samples consisted of nanorods with diameters in the range of 10–50 nm. Figure 10d shows a high-resolution TEM (HRTEM) image of a single Eu^{3+}/Gd^{3+}-HAP nanorod; the fringe spacings measured in the HRTEM image were 0.46 and 0.34 nm, corresponding to the crystal planes of (110) and (002), respectively. The preferential growth direction of the nanorod was along the [001] direction of hexagonal HAP. As compared to undoped HAP nanorods, the sizes of Eu^{3+}/Gd^{3+}-HAP nanorods became smaller. The average lengths of undoped HAP and Eu^{3+}/Gd^{3+}-HAP nanorods were measured to be 265.4 ± 143.5 and 53.0 ± 18.2 nm, respectively. The doping of Eu^{3+} and Gd^{3+} led to smaller size and narrower size distribution of nanorods (Figure 10e and f). The photoluminescence, drug delivery, and in vivo imaging of the products were also investigated. The photoluminescent and magnetic multifunctions of HAP nanorods were realized by the dual-doping with Eu^{3+} and Gd^{3+}. The as-prepared Eu^{3+}/Gd^{3+} dual-doped HAP nanorods exhibited little toxicity to the cells in vitro, a high drug adsorption capacity, and sustained drug release, and they are promising for bioimaging applications.

Han et al.[345] synthesized HAP nanostructures using H_3PO_4 and $Ca(OH)_2$ as starting reagents by the microwave-hydrothermal method. HAP nanostructures consisted of needles with widths of ~4–15 nm and lengths of 20–50 nm and spherical nanoparticles with diameters of ~10–30 nm. The applied microwave power and molar ratio of Ca/P had significant effects on the product. Meejoo et al.[346] reported rapid synthesis of HAP needle-shaped nanocrystals with a diameter of ~50 nm and length of 200 nm using $Ca(OH)_2$ and $(NH_4)_2HPO_4$ in aqueous solution by microwave heating at 850 W for 20 min. Siddharthan et al.[347] obtained calcium-deficient HAP nanoneedles with lengths of 16–39 nm and widths of 7–16 nm and with a Ca/P ratio of 1.5 using $Ca(NO_3)_2{\cdot}4H_2O$, H_3PO_4, and ammonia under microwave irradiation in a household microwave oven for 15 min.

The surfactant-free rapid microwave-assisted hydrothermal synthesis of HAP nanosheet-assembled flower-like hierarchical nanostructures was reported using an aqueous solution containing $Ca(CH_3COO)_2{\cdot}H_2O$ and $NaH_2PO_4{\cdot}2H_2O$ (pH 4.5) at 100 °C for 5 min.[348] The morphology of the product was dependent on the experimental conditions such as the microwave heating temperature and heating time. HAP flower-like hierarchical nanostructures were obtained at a lower temperature (100 °C), and polyhedra were obtained at a higher temperature (200 °C). The loading capacities of the as-prepared HAP flower-like hierarchical nanostructures for BSA, hemoglobin, and fish sperm DNA were determined to be 165, 164, and 112 mg g^{-1}, respectively. The protein release was conducted at different pH values (pH 7.2, 5.5, and 4.8) in phosphate buffered saline, and the pH-sensitive protein release behavior was found.[348]

Wang et al.[349] reported a rapid microwave-assisted hydrothermal route to flower-like nanostructured HAP hollow microspheres assembled with nanosheets with a hierarchical morphology using $Ca(CH_3COO)_2$, NaH_2PO_4, and Na_2HPO_4 at 120 °C for 5 min. The presence and concentration of block copolymer PLA–PEG played an important role in the formation of HAP hollow microspheres. The possible formation mechanism of HAP hollow microspheres was proposed. The as-prepared HAP hollow microspheres were explored as the anticancer drug (mitoxantrone (MIT)) carriers for cellular delivery. The MIT-loaded HAP hollow microspheres exhibited a sustained drug release behavior in vitro. The MIT intracellular accumulation was observed in both MIT-sensitive human breast cancer (MCF-7) cells and MIT-resistant human breast cancer (MCF-7/MIT) cells for MIT-loaded HAP hollow microspheres, suggesting that the MIT could be successfully delivered into the MCF-7 and MCF-7/MIT cells with the help of nanocarriers. They also demonstrated the template-free microwave-assisted hydrothermal synthesis of HAP hollow microspheres constructed by the self-assembly of nanosheets using $Ca(CH_3COO)_2$, Na_2HPO_4, NaH_2PO_4, and sodium citrate in aqueous solution. The effects of experimental parameters on the product were investigated, and a possible formation mechanism was proposed. The HAP hollow microspheres exhibited 3-D nanoporous network structure. The use of cheap reagents, relatively low and flexible temperature (80–140 °C), and short reaction time (30 min) makes this approach rapid and economical.[350]

Escudero et al.[351] reported the microwave-assisted hydrothermal synthesis of europium-doped HAP and fluoroapatite

dx.doi.org/10.1021/cr400366s | *Chem. Rev.* 2014, 114, 6462–6555

nanostructures functionalized with poly(acrylic acid) from aqueous basic solutions containing $Ca(NO_3)_2{\cdot}4H_2O$, $Eu(NO_3)_3{\cdot}5H_2O$, NaH_2PO_4, and poly(acrylic acid) as well as NaF in the case of the fluoroapatite at 180 °C for 1 h with a heating rate of 14 °C min^{-1}. In both cases, a spindle-like morphology was obtained, resulting from an aggregation process of smaller subunits, as shown in Figure 11. The sizes

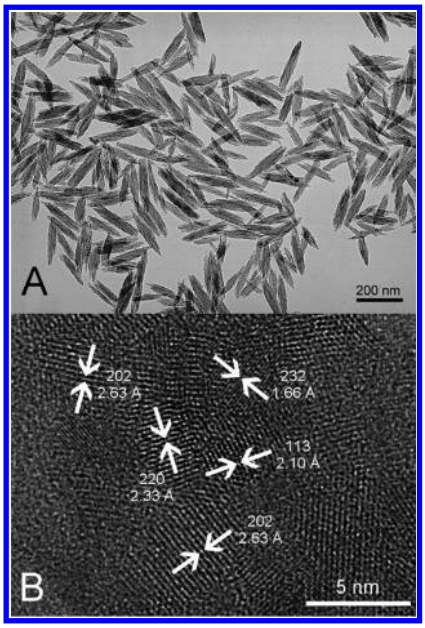

Figure 11. (A) TEM micrograph of Eu-doped HAP spindle-like nanostructures functionalized with poly(acrylic acid). (B) HRTEM image of a single spindle-like nanostructure in which several planes compatible with the HAP structure, as well as the *d* spacings, are shown. Reproduced with permission from ref 351. Copyright 2013 American Chemical Society.

of the spindles were 191 × 40 nm for HAP and 152 × 38 nm for fluoroapatite. The as-prepared samples showed negligible toxicity for Vero cells and high colloidal stability (up to at least 1 week) in 2-(*N*-morpholino)ethanesulfonic acid at pH 6.5, which is a commonly used buffer for physiological pH. All of these features make both kinds of apatite-based nanostructures promising for biomedical applications.

Carbonated HAP nanostructures were synthesized using an aqueous solution containing $Ca(NO_3)_2$, $(NH_4)_2HPO_4$, and ammonia (pH 10.8) via an ultrasound-assisted microwave irradiation process. Rod-like nanocrystals with diameters of ∼8 nm and lengths of ∼30 nm were obtained at a high yield of 98.8% in a short period of time (5 min). In addition, the crystallization process was promoted with the increase of ultrasonic and microwave power and irradiation time.[352] Rameshbabu et al.[353] prepared Ag (0.5−3 at. %) substituted needle-like HAP (AgHAP) nanostructures with lengths of 60−70 nm and widths of 15−20 nm using $Ca(OH)_2$, $AgNO_3$, and $(NH_4)_2HPO_4$ by microwave heating for 30 min. The antibacterial effect of AgHAP against *Escherichia coli* and *Staphylococcus aureus* was observed even for a low concentration of Ag^+ ions (0.5%). André et al.[354] adopted the microwave-hydrothermal method to prepare Eu-doped HAP nanorods with diameters from 9 to 26 nm using an aqueous solution containing $Ca(NO_3)_2{\cdot}4H_2O$, Eu_2O_3, $(NH_4)_3PO_4$, and HNO_3 at 140 °C for different times (1, 20, or 40 min).

Very recently, exciting progress has been made by Zhu's research group in the use of biocompatible phosphorus-containing biomolecules as organic phosphorus sources for the microwave-assisted environmentally friendly synthesis of nanostructured calcium phosphates and HAP.[355−360] Inorganic phosphate ions have mostly been used as the phosphorus source in the synthesis of calcium phosphate nanostructures. However, in the case of supersaturation of Ca^{2+} ions and PO_4^{3-} ions in the precursor solution, rapid nucleation and a disordered growth of calcium phosphates may occur, and the morphology and size of the products are difficult to control. As compared to the inorganic phosphorus sources, the use of phosphorus-containing biomolecules as organic phosphorus sources has several advantages.[359] First, the phosphorus source exists in the form of phosphate groups in an organic biomolecule and no PO_4^{3-} ions exist in the precursor solution, thereby avoiding the fast nucleation and disordered growth of the calcium phosphates. Second, organic biomolecules generally require certain conditions such as heating in aqueous solution to hydrolyze to form PO_4^{3-} ions. The hydrolysis conditions can be used to control the hydrolysis rate of organic biomolecules, which determines the morphology, size, and structure of the calcium phosphate product. Third, organic biomolecules hydrolyze to form PO_4^{3-} ions in a progressive manner, thereby avoiding the fast nucleation and disordered growth of calcium phosphates. Fourth, organic biomolecules can regulate the crystal growth of calcium phosphates, for example, by stabilizing the initially formed amorphous calcium phosphate (ACP) phase in aqueous solution and inhibiting the transformation of ACP into HAP. Fifth, biomolecules are biocompatible and exist in vivo. Thus, they are essentially nontoxic with high biocompatibility. On the basis of these points, biocompatible phosphorus-containing biomolecules as organic phosphorus sources are considered to be very promising for the "green" synthesis of calcium phosphate nanostructures. The reported organic phosphorus sources adopted for microwave-assisted synthesis of nanostructured calcium phosphates and HAP include adenosine 5′-triphosphate (ATP), fructose 1,6-bisphosphate, creatine phosphate, and pyridoxal-5′-phosphate.[355−360]

Adenosine 5′-triphosphate (ATP) is the most common cell's energy carrier in the biological systems. It can be used as a promising biocompatible organic phosphorus source for the rapid synthesis of nanostructured calcium phosphates and HAP by microwave heating.[355,356,360] Qi et al.[355] reported the microwave-assisted hydrothermal synthesis of HAP nanowires using $CaCl_2{\cdot}2H_2O$ and ATP in aqueous solution without any surfactant. HAP nanowires with diameters of ∼30 nm could be obtained by this rapid method at 160 °C for a short period of time (30 min). The effects of the reaction temperature and time on the morphology of the product were investigated. This method does not need any hard template or surfactant, avoiding the procedures and cost for their removal in the product. The advantages of this method are simple, rapid, surfactant-free, and environment-friendly. Another work has been reported on the synthesis of highly stable ACP porous nanospheres with a relatively uniform size and an average pore diameter of ∼10 nm by using $CaCl_2{\cdot}2H_2O$ as the calcium source and ATP as both the phosphorus source and the stabilizer in the microwave-assisted hydrothermal process at 120 °C for 10 min (Figure 12).[356] In this method, ATP biomolecules are used as the organic phosphorus source for the formation of ACP porous nanospheres with a relatively uniform

dx.doi.org/10.1021/cr400366s | *Chem. Rev.* 2014, 114, 6462−6555

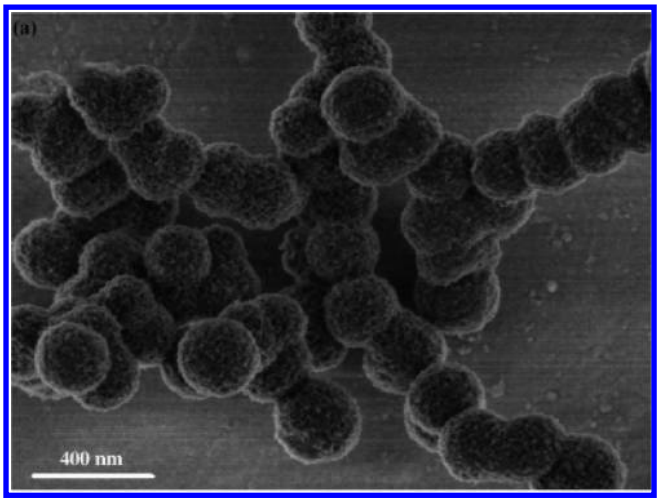

Figure 12. SEM image of ACP porous nanospheres synthesized by using $CaCl_2 \cdot 2H_2O$ as the calcium source and ATP as both the phosphorus source and the stabilizer by the microwave-assisted hydrothermal method at 120 °C for 10 min. Reproduced with permission from ref 356. Copyright 2012 Wiley-VCH.

morphology and size, and the residual ATP molecules can be used as the stabilizer for ACP porous nanospheres, leading to high stability of ACP porous nanospheres in aqueous solution. The as-prepared ACP porous nanospheres were efficient as the drug nanocarrier for anticancer drug loading and sustained drug release. The ACP porous nanosphere drug-delivery system exhibited a high ability to damage tumor cells after loading docetaxel, and thus is promising for the application in anticancer treatment.[356] The experimental results show that by adjusting the experimental parameters (temperature and time), the crystal phase and morphology of the product can be controlled.

Zinc-doped amorphous calcium phosphate (Zn/ACP) mesoporous microspheres were prepared using $CaCl_2$, $ZnCl_2$, and ATP as a biocompatible organic phosphorus source by the microwave-assisted hydrothermal method at 110 °C for 10 min. It was found that ATP was the main factor for stabilizing ACP in aqueous solution and Zn^{2+} ions were doped in ACP for the antibacterial benefit. The experimental results revealed that some residual ATP molecules were adsorbed on the surface of the Zn/ACP mesoporous microspheres. The Zn/ACP mesosporous microspheres exhibited pH-sensitive Zn^{2+} ion release behavior and good antibacterial activity against bacteria *Staphylococcus aureus* and *Escherichia coli*, indicating they are promising for the applications in the biomedical fields.[360]

Fructose 1,6-bisphosphate trisodium salt (FBP) has also been used as a biocompatible organic phosphorus source for rapid synthesis of a variety of calcium phosphate nanostructures, including porous ACP microspheres, HAP nanorods, and ACP/HAP composite microspheres, by the rapid microwave-assisted hydrothermal method.[357] The important role of FBP and the effect of the experimental conditions on the formation and evolution of calcium phosphate nanostructures were investigated. This method combines the advantages of FBP as an organic phosphorus source with rapid microwave volumetric heating; it is facile, rapid, surfactant-free, and environmentally friendly. Moreover, the as-prepared porous ACP microspheres exhibited a relatively high drug loading capacity and good sustained drug release behavior; thus, they are promising for the application in drug delivery.[357]

Qi et al.[358] reported the rapid and environmentally friendly synthesis of HAP hierarchically nanostructured porous hollow microspheres by the microwave-assisted hydrothermal method at 120 °C for 10 min. In this method, biocompatible phosphorus-containing creatine phosphate is used as an organic phosphorus source instead of the inorganic phosphorus source that is typically employed in the literature. Creatine phosphate is a biomolecule that provides energy to cells by synthesizing ATP. This method combines the advantages of creatine phosphate as an organic phosphorus source with rapid microwave volumetric heating for the controlled synthesis of HAP nanostructured materials. The as-prepared product consisted of HAP nanosheets/nanorods as the building blocks with a nanoporous structure with an average pore size of ~20.6 nm. The important role of creatine phosphate and the influence of the experimental conditions on the morphology and size of the product were systematically investigated. The as-prepared HAP product was explored for potential applications in drug delivery and protein adsorption and release, which exhibited a relatively high drug loading capacity and high protein adsorption ability, by using ibuprofen as a model drug and hemoglobin as a model protein.

Zhao et al.[359] reported the biomolecule-assisted microwave-hydrothermal rapid synthesis of HAP hierarchical nanostructures with different morphologies by using pyridoxal-5′-phosphate as a new biocompatible organic phosphorus source, and various HAP hierarchical nanostructures have been obtained including HAP nanorod-assembled hierarchical hollow microspheres, HAP nanorod-assembled hierarchical microspheres, and HAP nanosheet-assembled hierarchical microspheres. This preparation method is time-saving, with the microwave heating time as short as 5 min. The effects of the experimental conditions on the morphology and crystal phase of the product were investigated, and a possible formation mechanism was proposed. The products were explored for potential applications in protein adsorption and drug delivery. The experimental results showed that the HAP nanorod-assembled hierarchical hollow microspheres had a high drug/protein loading capacity and sustained drug/protein release behavior.

2.7. Other Compounds

In addition to nanostructures of various metals and metal compounds discussed above, many other nanostructured materials have also been prepared by the microwave-assisted method in aqueous solution. For the microwave-assisted synthesis of nanostructured metal hydroxides, a water-soluble metal salt, an alkali as a precipitator, and sometimes an additive are used in aqueous solution under microwave irradiation. Umar et al.[361] adopted a microwave-assisted hydrothermal process for the preparation of $Mg(OH)_2$ hexagonal nanodisks using $Mg(CH_3COO)_2$, HMTA, and NaOH (pH 8.5) in aqueous solution at 160 °C for 15 min. By using as-synthesized $Mg(OH)_2$ hexagonal nanodisks, an efficient ethanol chemical sensor with a high sensitivity was fabricated. Al-Hazmi et al.[362] reported the microwave-assisted hydrothermal synthesis of $Mg(OH)_2$ nanosheet-assembled spherical networks and their utilization for the fabrication of efficient ethanol chemical sensor, using $MgCl_2 \cdot 6H_2O$, urea, and NaOH as starting reagents in distilled water (pH 10) at 220 °C for 30 min. The as-synthesized $Mg(OH)_2$ nanosheet-assembled spherical networks were composed of the accumulation of hundreds of nanosheets with thicknesses of ~95 ± 10 nm. Patra et al.[363]

synthesized $In(OH)_3$ nanoparticles in high yields (>95%) using an aqueous solution containing $InCl_3$ and ammonia under microwave irradiation in a household microwave oven. α-GaOOH nanorods were synthesized using $Ga(NO_3)_3$, urea, and L-cysteine (or EDTA disodium salt) in aqueous solution by microwave heating at 80 °C for 45 min.[364]

$Ni(OH)_2$ nanoparticles were prepared from an aqueous solution containing $Ni(NO_3)_2{\cdot}6H_2O$ and NaOH by microwave heating at 100 W for 10 min.[365] Coralloid nanostructured nickel hydroxide hydrate was synthesized using $NiSO_4{\cdot}6H_2O$ and urea by a microwave-assisted hydrothermal process at 500 W for 3 min.[366] Flower-like α-$Ni(OH)_2$ and β-$Ni(OH)_2$ architectures constructed with nanosheets were synthesized via the microwave-assisted hydrothermal method. It was found that the reaction temperature played a critical role in the formation of the products. Flower-like β-$Ni(OH)_2$ with monolayer petals and α-$Ni(OH)_2$ with bilayer petals were prepared at 120 and 150 °C, respectively.[367] The microwave-assisted hydrothermal method was reported for the production of layered cobalt hydroxide nanocones intercalated with dodecyl sulfate ions by using HMTA as an alkaline reagent and SDS as both a surfactant and a structure-directing agent in aqueous solution at 100 °C for 1 h. A rolling process of lamellar hydroxide was proposed for the formation of conical structures with hollow interiors.[368] Single-crystalline β-$Co(OH)_2$ nanosheets with an average thickness of ∼10 nm were synthesized from a layered precursor cobalt(II) acetate hydroxide in aqueous solution by microwave heating at 100 °C for 20 min. The layered precursor was prepared using $Co(CH_3COO)_2{\cdot}4H_2O$ in mixed solvents of EG and water by microwave heating at 170 °C for 5 min. Co_3O_4 nanosheets were obtained by hydrothermal oxidation of the layered precursor cobalt(II) acetate hydroxide using H_2O_2 in aqueous solution.[369]

Morales et al.[370] prepared amorphous chromium hydroxide particles by forced hydrolysis combined with microwave heating by aging both solutions of $KCr(SO_4)_2{\cdot}12H_2O$ and $Cr(NO_3)_3{\cdot}9H_2O/K_2SO_4$ with different initial ratios of $[Cr^{3+}]/[SO_4^{2-}]$ at the boiling temperature. In the first case, the particles with sizes in the submicrometer range were obtained. In the second case, the mean size of particles decreased drastically from the submicrometer range for $[Cr^{3+}]/[SO_4^{2-}]$ ratios of 0.5, 0.8, and 1.0 to the nanometer range for ratios of 1.6 and 2.0. Phuruangrat et al.[371] prepared $Nd(OH)_3$ nanorods with diameters of 20−40 nm and lengths of 200−400 nm using an aqueous solution containing $Nd(NO_3)_3$ and ammonia (pH 10) under microwave-hydrothermal conditions at 150 °C for 1 h. $Pr(OH)_3$ nanorods with a diameter of 12 nm and different lengths ranging from 50 to 220 nm were prepared using praseodymium oxide, HNO_3, and KOH in aqueous solution via the rapid microwave-assisted method at 520 W for 1 h.[372]

The microwave-assisted method has also been adopted for the rapid synthesis of nanostructured metal fluorides in aqueous solution. Some examples are discussed below. PrF_3 hollow nanostructures with the mean particle size of ∼31 nm were synthesized using praseodymium oxide, HNO_3, NaF, and ammonia in aqueous solution under microwave refluxing for 20 min.[373] Flower-like CeF_3 nanostructures assembled with nanodisks were synthesized using EDTA disodium salt as the complexing reagent in aqueous solution via microwave heating for 26 min.[374] Lanthanide-doped GdF_3 nanostructures were synthesized using $Gd(NO_3)_3$ and $NaBF_4$ in aqueous solution by a rapid microwave-assisted process for 10 min, and raisin-like hierarchical nanostructures constructed from densely packed nanosheets with an average thickness of ∼20 nm were obtained.[375] Parhi et al.[376] reported the microwave-assisted hydrothermal synthesis of nanostructures of KMF_3 (M = Zn, Mn, Co, Fe) with a cubic morphology. Schäfer et al.[377] reported the microwave-assisted hydrothermal synthesis of lanthanide-doped RbY_2F_7 nanocrystals with a mean diameter of ∼60 nm in aqueous solution at 185 °C for 2 h.

A variety of nanostructured metal phosphates have been successfully synthesized in aqueous solution by the microwave-assisted method. Zhou et al.[378] prepared amorphous magnesium phosphate nanospheres from an aqueous solution containing $MgCl_2{\cdot}6H_2O$, KH_2PO_4, and $NaHCO_3$ in a household microwave oven at 100 W for 5 min, and some experimental parameters such as the pH value, Mg/P ratio, and solution composition were investigated. BPO_4 nanoparticles were synthesized using H_3BO_3 and H_3PO_4 (85%) under microwave irradiation at powers lower than 640 W and irradiation time ranging from 2.5 to 5 min, and the particle sizes of BPO_4 nanoparticles obtained under microwave irradiation at 640 and 400 W were 40−90 and 30−60 nm, respectively.[379] $BiPO_4$ nanoneedles were synthesized using an aqueous solution containing $Bi(NO_3)_3{\cdot}5H_2O$ and $NaH_2PO_4{\cdot}2H_2O$ by microwave heating (80% of 800 W) for 15 min.[380] TiP_2O_7 nanoparticles were synthesized by the microwave-assisted reaction between $TiO(OH)_2{\cdot}0.6H_2O$ and H_3PO_4 (85%) at 800 W for 5 min, and it was found that the particle sizes of TiP_2O_7 nanoparticles ranged from 20 to 100 nm and varied with the microwave heating time.[381] By using the microwave-assisted hydrothermal approach, single-phase $LiFePO_4$ could be rapidly synthesized in aqueous solution for 5 min, and the particle sizes of $LiFePO_4$ were dependent on the microwave-hydrothermal conditions.[382] Ekthammathat et al.[383] prepared $LaPO_4$ nanorods from $LaCl_3{\cdot}7H_2O$, $Na_3PO_4{\cdot}12H_2O$, and HNO_3 in aqueous solution at pH 1 under microwave irradiation at 180 W for 1 h. Monoclinic $CePO_4$ nanorods with 50 nm in diameter were also synthesized by a similar experimental procedure.[384] Patra et al.[385] synthesized hexagonal $LnPO_4{\cdot}nH_2O$ (Ln = La, Ce, Nd, Sm, Eu, Gd, Tb) nanorods/nanowires and body-centered tetragonal $ErPO_4{\cdot}nH_2O$ nanoparticles using aqueous solutions of Ln(III) nitrate and $NH_4H_2PO_4$ under microwave-solvothermal conditions at the pH values ranging from 1.8 to 2.2 in a household microwave oven, and the diameters of the resulting lanthanide orthophosphate nanowires/nanorods were in the range of 6−130 nm. $LaPO_4$:Ln (Ln = Ce^{3+}, Eu^{3+}, and Tb^{3+}) nanorods with diameters from 6 to 30 nm were synthesized using $NH_4H_2PO_4$ as the phosphorus source in aqueous solution by microwave refluxing for 20 min.[386] $YP_{0.8}V_{0.2}O_4$:Ln^{3+} (Ln = Eu, Sm, Dy) nanoparticles were synthesized using Na_3VO_4, Na_3PO_4, $LnCl_3$, and PVP by the microwave-assisted hydrothermal method at 150 °C for 30 min.[387]

Du et al.[388] reported the microwave-assisted hydrothermal synthesis of molecular sieve $AlPO_4$-5 using $Al(OH)_3$, H_3PO_4, and tetraethylammonium hydroxide at temperatures of 150−160 °C for 7−25 min. The sizes of the microwave hydrothermally synthesized $AlPO_4$-5 nanoparticles were usually smaller than those synthesized by the conventional hydrothermal method with a long processing time (typically 7 h). Ng et al.[389] addressed the efficient utilization of reactants for enhanced synthesis of nanosized aluminophosphate molecular sieve by microwave heating, decreasing or almost eliminating the related waste. AlPO-18 nanosheets were prepared by a multicycle synthesis approach via reusing nonreacted com-

dx.doi.org/10.1021/cr400366s | Chem. Rev. 2014, 114, 6462−6555

pounds from precursor suspensions with minimal requirement of chemical compensation after recovering of crystalline nanoparticles from each step. This approach is environmentally benign, and the organic templates and phosphorous acid can be almost completely consumed without disposing these harmful reagents to the environment. Also, the use of microwave irradiation leads to the preparation of the product within 5 min, instead of 3 days by the conventional heating.

Square-brick-like CuC_2O_4 was synthesized using $CuCl_2$ and $K_2C_2O_4$ in the presence of sodium dodecyl benzenesulfonate by a microwave-assisted aqueous solution route at 160 W for 30 min. The CuC_2O_4 square brick consisted of a large number of nanoparticles in the middle and a thin nanosheet layer at the outside surface.[390] $BaCO_3$ superstructures formed by the self-assembly of nanoflakes were synthesized employing $BaCl_2 \cdot 2H_2O$ and $NaHCO_3$ in the presence of SDS in aqueous system via rapid microwave refluxing for 15 min.[391] $SrCO_3$ with a flower-like or bundle-like morphology was synthesized using $Sr(NO_3)_2$ and $(NH_4)_2CO_3$ in aqueous solution by the microwave-assisted method at 90 °C.[392] $Pb_3(CO_3)_2(OH)_2$ nanoparticles were prepared using $Pb(NO_3)_2$ and urea in aqueous solution under microwave irradiation, and the reaction time was drastically shortened to 17 min from 4 h of the conventional water bath heating method.[393]

Mahapatra et al.[394] prepared nanoparticles of lanthanide orthovanadates $CeVO_4$, $PrVO_4$, and $NdVO_4$ with sizes in the range of 25−30 nm by microwave heating. The degradation rates of dyes and organics in the presence of microwave-synthesized orthovanadates under UV irradiation were higher as compared to those synthesized by the solid-state technique. $Fe_2(MoO_4)_3$ nanosheet (~40 nm thick) stacked nanostructures were fabricated adopting $Fe(NO_3)_3 \cdot 9H_2O$ as the iron source and $(NH_4)_6Mo_7O_4 \cdot 4H_2O$ as the molybdenum source in aqueous solution by a microwave-assisted process at 150 °C for 1 min.[395]

$Ca_6Si_6O_{17}(OH)_2$ nanobelts were synthesized by the microwave-assisted hydrothermal method at 180 °C for 90 min independent of the feeding molar ratio of $Ca(NO_3)_2 \cdot 4H_2O$ to $Na_2SiO_3 \cdot 9H_2O$ in the range of 0.8−3.0. β-$CaSiO_3$ nanobelts were obtained by microwave heating the powder of $Ca_6Si_6O_{17}(OH)_2$ nanobelts as the precursor and template at 800 °C for 2 h. The morphology and size of $Ca_6Si_6O_{17}(OH)_2$ nanobelts could be well preserved during the microwave thermal transformation process.[396] $Bi_6O_6(OH)_3(NO_3)_3 \cdot 1.5H_2O$ nanosheets with thicknesses of 50−60 nm were synthesized using an aqueous solution containing $Bi(NO_3)_3 \cdot 5H_2O$ and NaOH (pH 7) via the microwave-assisted hydrothermal method at 160 °C for 1 h.[397] $CaSb_2O_5(OH)_2$ nanocrystals with sizes of 5−10 nm were synthesized using $CaCl_2$ and $K_2H_2Sb_2O_7$ via the microwave-hydrothermal method at 120−180 °C for 20 min. The as-prepared sample had a higher photocatalytic activity than that of P25.[398] A microwave-assisted two-step hydrothermal procedure was reported for the preparation of a variety of zeolite nanostructures. The reaction solution was first treated at 80 °C for 1.5 h under microwave irradiation, and then the temperature was increased to facilitate the crystal growth.[399] Zeolite nanospheres with various organosilanized surfaces were synthesized in situ by the microwave-assisted method, and the as-prepared zeolite nanospheres were aggregates of primary nanoparticles with sizes of ~10 nm.[400]

2.8. Inorganic/Inorganic Nanocomposites

A nanocomposite is a multiphase solid material where at least one of the constituent phases has one, two, or three dimensions of less than 100 nm.[401] It is usually the solid combination of a bulk matrix and nanodimensional phase(s) differing in properties due to differences in structure and chemistry. The properties of the nanocomposite will differ markedly from those of the component materials. The promise of nanocomposites lies in their multifunctionality, the possibility of realizing a unique combination of properties that is not achievable with traditional materials. The challenges in realizing this promise are tremendous, which include the control over the distribution in size and dispersion of the nanosized constituents, tailoring, and understanding the role of interfaces between structurally or chemically different phases on bulk properties.[401] The field of nanocomposite materials has received much attention, imagination, and investigation of researchers in recent years, which results from the simple premise of using building blocks with dimensions in the nanosize range to design and create new materials with unprecedented flexibility and improvement in the properties. Because the constituents of a nanocomposite have different structures and chemical compositions and hence properties, they serve various functions; thus, the nanocomposite is multifunctional. Taking some clues from nature and based on the demands of emerging technologies, which require new materials for satisfying several functions at the same time in many applications, scientists have been devising synthetic strategies for the synthesis of various nanocomposites.[401] Microwave-assisted methods are especially advantageous for producing nanocomposites in terms of simplicity, rapidness, low cost, and energy saving.

Much effort has been devoted to the microwave-assisted rapid synthesis of inorganic/inorganic nanocomposites in aqueous solution. A variety of inorganic/inorganic nanocomposites have been reported, including Pd/Au,[402] Pt/Au,[402] Pt/C,[403−405] Ag/C,[406,407] PtNi/C,[408] PtCo/C,[409] Se/C,[410] Pt/carbon nanotubes,[411] metal/graphene,[412−416] Au/graphene oxide,[417] carbon nanotubes/graphene oxide,[418] Au/SiO_2,[419,420] Au/ZnO,[421,422] Ag/SnO_2,[423] Ag/TiO_2,[424,425] Cu/iron oxide,[426] C/SnO_2,[427] C/ZnO,[428] C/Fe_3O_4,[429] C/$LiMPO_4$ (M = Mn, Fe, and Co),[430] carbon nanotubes/ZnO,[431] carbon nanotubes/MnO_2,[432,433] carbon nanotubes/RuO_2,[434] graphene/SnO_2,[435] graphene/ZnO,[436] graphene/iron oxide,[437] graphene/Co_3O_4,[438] graphene/carbon nanotubes/SnO_2,[439] carbon nanotubes/ZnS,[440] carbon nanotubes/$Zn_xCd_{1-x}S$,[441] graphene/ZnS,[442] graphene/CdS,[443] graphene/TiO_2,[444] LiFePO$_4$/C/graphene,[445] α-Fe_2O_3/ZnO,[446] Co_3O_4/CoO,[447] ZrO_2/Al_2O_3,[448] $RuO_2 \cdot xH_2O$/TiO_2,[449] Bi_2O_3/Bi_2CrO_6,[450] ZnO/zinc aluminum hydroxide,[451] ZnO/CdS,[452] ZnO/ZnS,[453,454] Pb_3O_4/CdS,[452] CdO/CdS,[455] SiO_2/CdS,[456] ZnO/ZnSe,[457] $Cd(OH)_x$/CdSe,[458] ZnS/ZnS:Ag,[459] CdS/CdSe,[325,460] ZnS/CdSe,[461] CdS/CdTe,[462] CdSe/CdTe,[463] CdSeS/ZnS,[464] CdSeTe/ZnS/SiO_2,[465] Mn:ZnSe/ZnS,[466] CdSe/CdS/ZnS,[325] CdTe/CdS/ZnS.[467] Ag/AgCl,[468] and nickel boride/MgO.[469]

Metal/metal alloy or core/shell nanostructures have been prepared by the rapid microwave-assisted methods in aqueous solution. Belousov et al.[402] reported the reduction of chlorocomplexes of Au(III) from muriatic solutions by nanopowders of Pd and Pt at 110 and 130 °C under hydrothermal conditions and microwave irradiation, and bimetallic nanoparticles with a core/shell structure were obtained. The as-prepared core/shell nanostructures had a

dx.doi.org/10.1021/cr400366s | Chem. Rev. 2014, 114, 6462−6555

core of the metal reductant covered with a substitutional solid (Au, Pd) solution in the case of Pd, and isolated by a Au layer in the case of Pt. An example of the Au/Pd system was demonstrated that the use of microwave irradiation not only accelerated the preparation of nanoparticles but also obtained more homogeneous materials in comparison with the conventional heating.

It has been demonstrated that the microwave-assisted method is suitable for the preparation of carbon-supported nanostructures in aqueous solution, and a considerable work has been devoted to this topic. Zeng et al.[403] prepared carbon-supported Pt nanoparticles with an average particle size of 2.2 nm in aqueous solution by microwave-assisted reduction of H_2PtCl_6 using sodium citrate as the reducing agent and stabilizer in the presence of the commercial carbon at boiling temperature for 1 h. It was found that the presence of citrate was generally beneficial to the formation of smaller and more uniform Pt nanoparticles. Liu et al.[404] prepared Pt nanoparticles with a narrow size distribution using $Pt(phen)_2^{2+}$ complex (phen = 1,10-phenanthroline) in aqueous solution by microwave heating at 700 W for 6 min, and Pt nanoparticles/carbon nanocomposite was obtained using commercial carbon powder. It was found that the chelating agent improved the Pt particle size as well as the dispersion of Pt nanoparticles. Hollow carbon spheres were prepared by combining the hydrothermal method with intermittent microwave heating, and then Pt nanoparticles supported on hollow carbon spheres were prepared by the reduction of H_2PtCl_6 with formic acid in aqueous solution by microwave heating.[405] Deivaraj et al.[408] prepared carbon-supported PtNi nanoparticles by the reduction of K_2PtCl_4 and $NiCl_2{\cdot}6H_2O$ with hydrazine using PVP as a stabilizer and in the presence of carbon by microwave heating at 100 W for 10 min. Hwang et al.[409] prepared carbon-supported PtCo alloy nanoparticles with different alloying extents by employing microwave heating at 100 °C for 1 h. The as-prepared PtCo alloy nanoparticles were well dispersed on the surface of the commercial carbon support with a narrow particle size distribution.

A microwave-assisted hydrothermal reduction/carbonization solution route was developed for the rapid synthesis of coaxial Ag/C nanocables using $AgNO_3$ and sucrose in deionized water at 200 °C for 20 min, and the nanocables could self-assemble in situ in an end-to-end fashion into interconnected chains.[407] The nanocomposite of carbon spheres with Ag nanoparticles was prepared from an aqueous solution containing nanoporous carbon spheres, $Ag(NH_3)_2^+$ and PVP, the nanocomposite was synthesized in high yield within a short reaction time, and the size, number density, and to some extent even the locations of Ag nanoparticles in/on carbon spheres could be controlled by adjusting experimental parameters.[406] The Se/C nanocomposite with a core−shell structure was prepared using starch and H_2SeO_3 in deionized water through a microwave-hydrothermal process at 200 °C for 30 min; the product consisted of Se nanorod assemblies as the core and an amorphous carbon as the shell.[410]

The graphite/SnO_2 nanocomposite was prepared by microwave-assisted urea-mediated homogeneous hydrolysis of $SnCl_4$ in aqueous solution at 85 °C for 3 min, and the as-prepared SnO_2 nanoparticles had a narrow size distribution (1−3 nm, mean: 2.1 nm).[427] The carbonaceous species/ZnO nanocomposite was synthesized using an aqueous solution containing 0.01 M $Zn(NO_3)_2{\cdot}6H_2O$, 0.01 M HMTA, and 0.002 M L-(+)-ascorbic acid by a microwave-assisted hydrothermal reaction at 180 °C for 30 min. The nanocomposite consisted of quasi-single crystalline ZnO regions and amorphous carbonaceous regions.[428] Murugan et al.[430] reported the microwave-hydrothermal synthesis of carbon-coated $LiMPO_4$ (M = Mn, Fe, and Co) nanocomposite involving in situ carbonization of glucose. An aqueous solution containing LiOH, H_3PO_4, glucose, and the sulfate of Mn^{2+}, Fe^{2+}, or Co^{2+} was adopted. With a significantly shortened reaction time as compared to the reported synthetic methods, the microwave-assisted hydrothermal method offers advantages of being rapid, cost-effective, and energy-saving.

Carbon nanotubes have been a hot research topic in recent years due to their excellent properties and promising applications in various fields. Carbon nanotubes have also been adopted as the matrix for a variety of nanostructures prepared by rapid microwave-assisted approaches in aqueous solution. Wu et al.[411] prepared Pt nanoparticles dispersed on multiwalled carbon nanotubes by microwave heating at 1000 W with a mode of on for 20 s and off for 60 s for six times. Sun et al.[418] reported a unique microwave-assisted unzipping process of multiwalled carbon nanotubes in the solution of H_2SO_4/H_3PO_4/$KMnO_4$ for the synthesis of graphene oxide nanoribbons, forming core/shell heterostructures. This process was rapid with a total microwave heating time of 6 min. Potirak et al.[431] synthesized the nanocomposite of carbon nanotubes/ZnO via a microwave-assisted process using $Zn(CH_3COO)_2{\cdot}2H_2O$ and preformed multiwalled carbon nanotubes. ZnO nanoparticles with sizes of ∼15 nm were dispersively coated on the surface of carbon nanotubes. The nanocomposite prepared by microwave heating was much better than that obtained by the conventional annealing. The nanocomposite of MnO_2 nanoplates/multiwalled carbon nanotubes was prepared using preformed carbon nanotubes, $MnSO_4{\cdot}H_2O$, $(NH_4)_2S_2O_8$, and $(NH_4)_2S_2O_4$ in aqueous solution under microwave irradiation at 700 W for 16 min.[433] The nanocomposite of aligned carbon nanotubes/MnO_2 was fabricated using $KMnO_4$ and aligned carbon nanotubes in aqueous solution under microwave irradiation using a household microwave oven at 700 W for 5 min.[432] The nanocomposite of multiwalled carbon nanotubes/RuO_2 was prepared using $RuCl_3$ as the Ru source and $NH_3{\cdot}H_2O$ as a precipitator in the presence of commercial carbon nanotubes in aqueous solution by microwave heating at 700 W for a short period of time (30 s). RuO_2 nanoparticles were located both inside and outside of the carbon nanotubes.[434] The multiwalled carbon nanotubes wrapped with face-centered cubic ZnS nanoparticles were prepared using $Zn(CH_3COO)_2$ and thioacetamide in aqueous solution under microwave irradiation at 280 W for 15 min. The dispersion, morphology, ratio of loading, and size of ZnS nanoparticles in the range of 11.7−24.5 nm could be controlled by adjusting the microwave power, initial concentration of $Zn(CH_3COO)_2$, and molar ratios of $Zn(CH_3COO)_2$/thioacetamide and $Zn(CH_3COO)_2$/carbon nanotubes.[440]

Graphene has aroused much interest in recent years due to its excellent properties and promising applications in various fields. Graphene has also been adopted as the matrix for a variety of nanostructures. Jasuja et al.[417] prepared the nanocomposite of Au nanostructures on graphene oxide sheets, which was synthesized by microwave exposure (1.05 kW) on an aqueous solution of graphene oxide and $HAuCl_4{\cdot}3H_2O$ for a time interval between 1 and 5 min with intermittent cooling after every 10 s, resulting in the formation of Au nanostructures with triangular, hexagonal, and dendritic morphologies, which

dx.doi.org/10.1021/cr400366s | Chem. Rev. 2014, 114, 6462−6555

either assembled on or were wrapped with graphene oxide sheets, depending on the microwave exposure time. Zhang et al.[415] prepared the nanocomposite of Pd nanoparticles/graphene using tannic acid as a reducing agent in aqueous solution by the microwave-assisted method. The preformed graphene oxide, H_2PdCl_4, and tannic acid were adopted as the starting reactants. The reaction system was heated by microwaves at 750 W for 1 or 2 min. The loading amount and size of Pd nanoparticles on graphene sheets could be controlled by the ratio of raw materials and microwave irradiation time. It was found that the electrocatalytic activity and stability of the Pd/graphene nanocomposite were much better than those of commercial Pd/C catalysts toward methanol electrooxidation in alkaline media. Siamaki et al.[414] prepared Pd nanoparticles with small particle sizes of 7−9 nm supported on graphene by microwave-assisted chemical reduction of the corresponding aqueous mixture of palladium nitrate, hydrazine hydrate, and dispersed graphite oxide sheets (Figure 13). The reaction mixture was microwave-heated at a

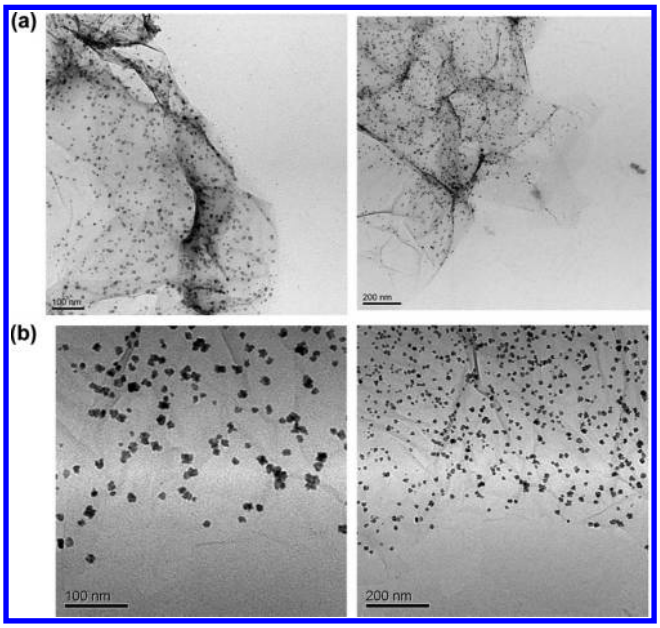

Figure 13. TEM micrographs of (a) 7.9 wt % Pd/graphene and (b) 6.4 wt % Pd/graphite oxide prepared by microwave heating a mixture of graphite oxide and palladium nitrate in the presence and absence of hydrazine hydrate, respectively. Reproduced with permission from ref 414. Copyright 2010 Elsevier Inc.

full power (1000 W) in 30 s cycles for a total reaction time of 1 min. The TEM micrographs in Figure 13 show the presence of well-dispersed uniform Pd nanoparticles on both graphene and graphite oxide sheets over large areas of several micrometers. However, Pd nanoparticles supported on graphene were smaller than those supported on the graphite oxide sheets. The average particle sizes of Pd nanoparticles supported on graphene and graphite oxide were determined to be 7−9 and 12−15 nm, respectively. The mean size of Pd nanoparticles dispersed on graphene and graphite oxide was 8 and 14 nm, respectively. There was more agglomeration of Pd nanoparticles on graphite oxide than on graphene.

Hassan et al.[412] reported the microwave-assisted chemical reduction preparation of metal nanoparticles (Pd, Cu, Cu/Pd) dispersed on graphene sheets. This method allows rapid chemical reduction of exfoliated graphite oxide using a variety of reducing agents such as hydrazine hydrate in either aqueous or organic media. It also allows the simultaneous reduction of graphite oxide and a variety of metal salts, thus resulting in the dispersion of metallic and bimetallic nanoparticles supported on graphene sheets. The Sn/graphene nanocomposite was prepared using $SnCl_4{\cdot}5H_2O$, urea, and graphite oxide in aqueous solution by the combination of the microwave-hydrothermal process at 120 °C for 20 min and one-step hydrogen gas reduction at 300 °C for 2 h.[416] Graphene-supported $PdPt_3$ nanoparticles were prepared using graphene oxide sheets, $PdCl_2$, K_2PtCl_4, CTAB, NaOH, and ascorbic acid as a reducing agent at pH 9 via microwave heating at 200 W for 4 min.[413]

The nanocomposite consisting of graphene sheets with only a few layers and embedded SnO_2 nanoparticles with sizes of 4−5 nm was prepared using $SnCl_2{\cdot}2H_2O$, HCl, and graphite oxide in aqueous solution by the microwave-assisted hydrothermal method at 120 °C for 5 min; and subsequently the obtained SnO_2/graphite oxide was reduced by $H_4N_2{\cdot}H_2O$ in NaOH aqueous solution by microwave heating at 120 °C for 15 min.[435] The nanocomposite of SnO_2/reduced graphene oxide/carbon nanotubes was obtained using graphene oxide, carbon nanotubes, and $SnCl_4{\cdot}5H_2O$ in aqueous solution by the microwave-assisted hydrothermal method at 150 °C for 10 min.[439] The graphene/ZnO nanocomposite was prepared using $ZnSO_4{\cdot}7H_2O$ and NaOH in aqueous solution (pH 9) via microwave-assisted reduction in the presence of graphite oxide, and the reaction mixture was microwave-heated at 150 °C for 30 min. The as-prepared product consisted of graphene sheets decorated densely with ZnO nanoparticles with diameters of 5−10 nm.[436] The nanocomposite of reduced graphene oxide/Fe_2O_3 was prepared by a two-step process using an aqueous suspension containing $FeCl_3$, urea, graphene oxide, and hydrazine by homogeneous precipitation and subsequent reduction of graphene oxide with hydrazine under microwave irradiation to yield reduced graphene oxide platelets decorated with Fe_2O_3 nanoparticles.[437] The graphene/Co_3O_4 nanocomposite with a homogeneous distribution of Co_3O_4 nanoparticles (3−5 nm) on graphene sheets was synthesized using cobalt nitrate hexahydrate and urea in aqueous solution by microwave heating at 700 W for 10 min.[438]

The graphene/ZnS nanocomposite was prepared in aqueous medium under microwave irradiation at 85 °C for 20 min. This process involved the reactions of graphene oxide nanosheets, $Zn(CH_3COO)_2$, and thioacetamide as well as a reducing agent, resulting in the formation of ZnS nanoballs with an average diameter of 41.9 nm supported on graphene nanosheets, and ZnS nanoballs were composed of many self-assembled ZnS nanocrystals with an average size of 3 nm.[442] The reduced graphene oxide/CdS nanocomposite was prepared via microwave-assisted reduction of graphite oxide at 150 °C for 10 min in a solution containing $Cd(NO_3)_2$, CH_4N_2S, graphite oxide, and NaOH (pH 9).[443] A similar microwave-assisted synthesis was reported for the reduced graphene oxide/TiO_2 nanocomposite.[444]

Various nanocomposites of metal/metal oxide and metal oxide/metal oxide have been synthesized by rapid microwave-assisted approaches in aqueous solution. Gu et al.[419] prepared highly dispersed Au nanoparticles with diameters of 5−10 nm incorporated into pore channels of mesoporous silica SBA-15 in an aqueous solution of $HAuCl_4$ under microwave irradiation at 700 W for 1 min. Au/SnO_2 core−shell nanoparticles were synthesized using the microwave-hydrothermal method, and

dx.doi.org/10.1021/cr400366s | Chem. Rev. 2014, 114, 6462−6555

the formation of the SnO_2 shell on the surface of Au nanoparticles was faster (~5 min) than that with the conventional hydrothermal method.[420] Kundu et al.[421] reported the microwave-assisted synthesis of the Au/ZnO nanocomposite. The preformed ZnO nanorods grown by the hydrothermal method exhibited a hexagonal prismatic morphology. Microwave irradiation (800 W, 3 min, ~100 °C) of an aqueous solution containing ZnO nanorods and $HAuCl_4$ resulted in the formation of Au nanoparticles dispersed on the surface of ZnO nanorods. Geng et al.[422] synthesized the hollow doughnut-like Au/ZnO nanocomposite using $Zn(NO_3)_2{\cdot}6H_2O$, $HAuCl_4$, HMTA, and trisodium citrate through a microwave-assisted hydrothermal route at 100 °C for 30 min, and other different nanocomposites such as ZnO nanorods/Au nanoparticles, ZnO nanodisks/Au nanoparticles, and ZnO nanospheres/Au nanoparticles were also obtained by adjusting experimental conditions. The hollow spheres of Ag/TiO_2 nanocomposite were prepared by a template-free microwave-hydrothermal process, followed by a photochemical reduction process under the xenon lamp irradiation.[424] Li et al.[425] prepared the Ag/TiO_2 nanocomposite consisting of Ag nanoparticles (~5 nm) and TiO_2 with various Ag/Ti molar ratios using preformed TiO_2 by the microwave-assisted method. As compared to the hydrothermal method, the Ag/TiO_2 nanocomposite with smaller crystallite size and higher crystallinity could be obtained by the microwave-assisted method. Wong et al.[426] reported the microwave-assisted synthesis of copper-doped and ^{64}Cu-doped iron oxide core/shell nanoparticles with a dextran coating and with diameters between 20 and 100 nm; $FeCl_3{\cdot}6H_2O$, reduced dextran, $FeCl_2{\cdot}4H_2O$, $CuCl_2$, and $NH_3{\cdot}H_2O$ were used as the starting reagents in aqueous solution. Reaction times were significantly shortened while yielding similar sized particles by microwave heating, and the size of nanoparticles could be controlled simply by the microwave heating time or by the maximum power. Al-Tuwirqi et al.[447] reported the microwave-hydrothermal synthesis of Co_3O_4/CoO nanorods with an average length of around 80 nm and an average diameter of 42 nm using cobalt acetate dehydrate and NaOH in aqueous solution at 200 °C for 10 min. Prete et al.[448] prepared ZrO_2-doped (5 mol %) Al_2O_3 nanopowder using $AlCl_3{\cdot}6H_2O$, $ZrOCl_2{\cdot}8H_2O$, and NaOH in aqueous solution by the microwave-hydrothermal method. Hu et al.[449] synthesized the $RuO_2{\cdot}xH_2O/TiO_2$ nanocomposite from a solution containing $TiCl_3$, $RuCl_3{\cdot}xH_2O$, and $NaNO_3$ through a microwave-assisted hydrothermal process at 150 °C for 10 min. Zhang et al.[450] fabricated Bi_2O_3/Bi_2CrO_6 composite nanowires using $Bi(NO_3)_3$, Na_2CrO_4, and HCl (pH 1−5) by the microwave-assisted hydrothermal method at 180 °C for 1 h, and the diameters of the composite nanowires varied from 30 to 100 nm.

The nanocomposites of metal chalcogenide/metal oxide have also been prepared by the rapid microwave-assisted method in aqueous solution. Hu et al.[453] demonstrated the microwave-assisted refluxing synthesis of ZnO/ZnS core−shell nanorods via in situ surface sulfidation of ZnO nanorods. ZnO nanorods were prepared by the conventional heating method and used as the template. By using this method, a layer of ZnS nanoparticles was deposited onto ZnO nanorods, while retaining the shape of the original ZnO nanorods, and the thickness and particle size of the ZnS shell could be adjusted by the concentration of thioacetamide as the sulfur source. Chen et al.[454] used the microwave-hydrothermal method to synthesize hollow ZnO core/ZnS shell nanostructures using $Zn(NO_3)_2{\cdot}6H_2O$, thiourea, and dodecylamine at 130 °C for a designated period of time (1−50 min) with an initial microwave power of 150 W. The morphological evolution first underwent a process from precursor flakes to ZnO truncated hexagonal pyramids, and then toward ZnO hexagonal twin crystals, and the bipods immediately grew up into solid peanuts, followed by inner dissolving to form hollow ZnO core/ZnS shell nanostructures. Cho et al.[457] prepared the ZnO/ZnSe porous nanocomposite by a two-step microwave-assisted hydrothermal process. Porous ZnO nanostructures were synthesized using $Zn(NO_3)_2{\cdot}6H_2O$, HMTA, and L-(+)-ascorbic acid in aqueous solution via a microwave-assisted hydrothermal process at 120 °C for 2 h, and then porous ZnO nanostructures were converted into porous ZnO/ZnSe nanocomposite by a microwave-assisted dissolution−recrystallization process using an aqueous solution containing Na_2SeO_3 and $N_2H_4{\cdot}H_2O$ at 160 °C for 2 min. ZnO and ZnSe were well-mixed (rather than forming core−shell structures) in the nanocomposite, particularly in the outer regions. Yang et al.[455] prepared CdO/CdS porous core−shell nanoboxes by microwave-assisted in situ surface sulfidation of $CdCO_3$ nanocubes using thioacetamide as the sulfur source in aqueous solution followed by annealing treatment.

Metal chalcogenide/metal chalcogenide nanocomposites have also been prepared by the microwave-assisted method in aqueous solution. Jian et al.[459] deposited the ZnS shell on the surface of preformed ZnS:Ag nanocrystals using $Zn(CH_3COO)_2{\cdot}2H_2O$, NaOH, and 3-mercaptopropionic acid (MPA) by the microwave-assisted epitaxy growth at 600 W for 3 min. Growth of the ZnS shell was induced by thermal decomposition of the Zn−MPA complex under microwave irradiation. The quantum yield of nanocrystals was significantly enhanced after the shell growth. Qian et al.[460] reported the seed-mediated microwave-assisted synthesis of alloyed CdSe/CdS quantum dots in aqueous phase at 140 °C for 5−60 min. CdSe seeds were first obtained by the reaction between NaHSe and Cd^{2+} ions, and then CdSe/CdS quantum dots were rapidly produced under microwave irradiation in the presence of 3-mercaptopropionic acid as a sulfide source. Schumacher et al.[461] reported the microwave-assisted aqueous synthesis of CdSe/ZnS core−shell quantum dots using Cd−MPA, $Zn(NH_3)_4^{2+}$ as the zinc source in the presence of 3-mercaptopropionic acid at 140−170 °C for 45−120 min. He et al.[462] synthesized water-dispersed and highly luminescent CdTe/CdS core−shell nanocrystals by the microwave-assisted method in aqueous phase. A short period (5 min) was required to form an optimum thickness of the CdS shell using the microwave-assisted synthesis as compared to several days by the illumination method. Sai and Kong[463] reported the microwave-assisted synthesis of mercaptanacid-capped CdTe/CdSe core/shell quantum dots using CdTe quantum dots, $CdCl_2$, NaHSe, and 3-mercaptopropionic acid at pH 11.2 in aqueous solution. They first prepared CdTe core quantum dots by using $CdCl_2$ and NaHTe in the presence of 3-mercaptopropionic acid under microwave irradiation at 100 °C for ~2 min. Zhan et al.[464] reported the microwave-assisted aqueous-phase synthesis of CdSeS/ZnS core−shell quantum dots. First, CdSeS core quantum dots were produced by heating a precursor solution containing $CdCl_2{\cdot}2.5H_2O$, 3-mercaptopropionic acid, and Na_2SeSO_3 at 130 °C for 30 min. After purification through centrifugation, CdSeS core quantum dots were successfully capped with a ZnS shell through heating a solution containing $Zn(CH_3COO)_2{\cdot}2H_2O$, Na_2S, 3-mercaptopropionic acid, and NaOH at 100 °C for 1 h. Zhu et al.[466] prepared Mn:ZnSe core

dx.doi.org/10.1021/cr400366s | Chem. Rev. 2014, 114, 6462−6555

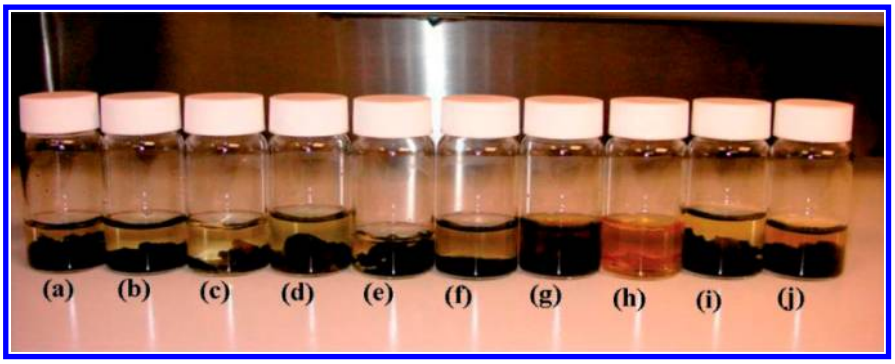

Figure 14. Photographic image of cross-linked PVA with various metallic and bimetallic systems: (a) Pt, (b) Pt−In, (c) Ag−Pt, (d) Cu, (e) Pt−Fe, (f) Pt with higher concentration ratio, (g) Cu−Pd, (h) In, (i) Pt−Pd, and (j) Pd−Fe. Reproduced with permission from ref 473. Copyright 2007 Wiley VCH.

nanocrystals with oleate capping ligand via a microwave-assisted hydrothermal process at 170 °C for 40 min, and then the core nanocrystals reacted with mercaptopropionic acid. An additional ZnS shell was deposited on the outer layer of Mn:ZnSe to form Mn:ZnSe/ZnS core−shell nanostructures. In a traditional aqueous synthesis, the growth rate of ZnSe quantum dots with mercaptopropionic acid capping ligand was slow by refluxing. The as-prepared Mn:ZnSe/ZnS core/shell nanocrystals were investigated to label antibodies for selective detection of human immunoglobulin G (IgG) based on fluorescence resonance energy transfer between Mn:ZnSe/ZnS and Au nanoparticles.

A green and fast approach (5 min) was reported for the fabrication of Ag/AgCl hybrid nanoparticles with sizes of about 100 nm using $AgNO_3$, NaCl, and beet juice in aqueous solution by the microwave-hydrothermal approach at 100 °C and a maximum pressure of 1930 kPa. In this method, beet juice was adopted as an environmentally friendly reducing reagent, which is an abundant sugar-rich agricultural produce.[468]

2.9. Inorganic/Organic Nanocomposites

In recent years, inorganic nanostructure/organic polymer nanocomposites have received much attention due to their interesting properties and promising applications in various fields. In these nanocomposites, inorganic nanoparticles with high specific surface areas and unsaturated atoms may interact with the organic polymer, leading to the enhanced properties of the nanocomposite. These nanocomposites are considered to be interesting functional materials with many applications in various fields. Bogdal et al.[19] have published a review article on the synthesis of polymer−inorganic hybrid nanocomposites under microwave irradiation, a research area that has made rapid progress in recent years. They reviewed and discussed the microwave-assisted preparation and characterization of polymer nanocomposites composed of layer materials like clays and layered double hydroxides, metal nanoparticles, and nanowires as well as carbon-based materials (i.e., fullerenes and nanotubes).

It is desirable to develop simple, fast, and low-cost methods for the synthesis of inorganic/organic nanocomposites from the technological point of view. The control over the particle size, size distribution, and dispersity is very important for the synthesis and application of high-performance nanocomposites. Conventionally, the polymerization of the organic monomer and formation of inorganic particles were conducted separately, and then the polymer and inorganic particles were physically mixed together, thus the organic polymer and inorganic particles were not homogeneously mixed, leading to severe aggregation of inorganic particles and uneven properties in the composites. In some cases, relatively high temperatures or pressures were needed, which made the preparation complex, difficult, and of high-cost. There have been only a few reports on the one-step simultaneous formation of inorganic nanoparticles and polymerization of the organic monomer in the same reaction system for producing high-quality inorganic/organic nanocomposites.[470,471]

Kundu et al.[472] reported the one-step synthesis of electrically conductive Au nanowires on DNA in solution and immobilized on a solid substrate under microwave irradiation for 2−3 min. DNA served as a reducing and nonspecific capping agent for the growth of Au nanowires. The as-prepared nanowires were micrometers long with diameters of 10−15 nm in solution and of 20−30 nm in immobilized DNA. The nanowires exhibited ohmic behavior with a low resistance, indicative of continuous metallic structure.

A variety of metal/polymer nanocomposites were rapidly prepared in aqueous solution by the microwave-assisted method. Nadagouda et al.[473] reported a microwave-assisted cross-linking reaction of PVA with metallic and bimetallic systems in aqueous solution at 100 °C for 1 h. The nanocomposites of PVA cross-linked metallic systems such as Pt, Cu, and In and bimetallic systems such as Pt−In, Ag−Pt, Pt−Fe, Cu−Pd, Pt−Pd, and Pd−Fe were obtained by reacting the respective metal salt with 3 wt % PVA. Metallic and bimetallic nanocomposites with various shapes, such as nanospheres, nanodendrites, and nanocubes, were obtained. A photographic image of the metallic- and bimetallic-cross-linked PVA nanocomposites is shown in Figure 14. The cross-linking and precipitation of PVA occurred for all of the bimetallic systems: Pt−In, Ag−Pt, Pt−Fe, Cu−Pd, Pt−Pd, and Pd−Fe. However, except for Pt, In, and Cu, the other metallic systems such as Ag−, Pd−, and Fe−PVA did not precipitate.

El-Shall et al.[474] have developed a facile approach based on microwave-assisted incorporation of a variety of metallic and bimetallic nanoparticles within the porous coordination polymer MIL-101, a chromium-based metal−organic framework with the molecular formula $Cr_3F(H_2O)_2O[(O_2C)-C_6H_4-(CO_2)]_3{\cdot}nH_2O$ (where n is ∼25). Metal precursors and the reducing agent diffused within the pores of the MIL and adsorbed on the internal and external surfaces of the MIL. Microwave-assisted reduction for a short period of only 1−2 min resulted in the formation of high concentrations of metal atoms, which immediately nucleated to form metal nanocrystals. The growth of nanocrystals inside the pores was limited by

dx.doi.org/10.1021/cr400366s | Chem. Rev. 2014, 114, 6462−6555

the size of the pores, thus resulting in the incorporation of small nanoparticles with 2−3 nm diameters within the pores. On the other hand, nanocrystals nucleated on the external surfaces of the MIL crystals grew larger in size (4−6 nm). The observed catalytic activities toward CO oxidation of Pd nanoparticles supported on the highly porous MIL-101 polymer were significantly higher than those of other reported metal clusters supported on metal−organic frameworks. Khan et al.[475] prepared microgel particles based on poly(*N*-isopropylacrylamide-*co*-acrylic acid) by emulsion polymerization in the presence of *N*,*N*′-methylenebis(acrylamide). The microwave heating was adopted for the rapid preparation of highly stable and monodisperse Ag nanoparticles with an average diameter of 8.5 nm using the microgel as the template via in situ reduction of $AgNO_3$ in the presence of glucose as a mild reducing agent. The mixture was heated with a household microwave oven at a power up to 1.25 kW for only 15 s. The as-prepared Ag nanoparticles were stable for more than 8 months at room temperature. Nguyen et al.[476] fabricated the nanocomposite consisting of Ag nanoparticles/PVA nanowires by conjugation of electrospinning and microwave heating. The 12 wt % aqueous PVA solutions with and without 2 wt % $AgNO_3$ solution were irradiated for 1 or 1.5 min in a microwave oven. PVA was used not only as a carrier for loading of Ag nanoparticles but also as a reducing agent with which the Ag^+ ions were reduced to form Ag nanoparticles under microwave irradiation. Nadagouda and Varma[477] reported an environmentally friendly approach for the synthesis of bulk quantities of the nanocomposites containing transition metals using a biodegradable polymer, CMC, by reacting respective metal salts with the sodium salt of CMC in aqueous media. The spontaneous reduction of noble metals such as Au, Pt, and Pd could be accomplished using CMC under microwave irradiation at 100 °C within 5 min in the absence of any reducing or surfactant agent.

The microwave-assisted preparation method has also been proved to be effective for a variety of metal oxide/polymer nanocomposites in aqueous solution. You et al.[478] reported the microwave-hydrothermal synthesis of magnetic Fe_3O_4/phenol formaldehyde (PF) core−shell microspheres at 160 °C for 20 min. The structure of the Fe_3O_4/PF core−shell microspheres could be well controlled by in situ polycondensation of phenol and formaldehyde with magnetic Fe_3O_4 nanospheres as the seeds in an aqueous solution without any surfactant, and the shell thickness could be controlled in the range of 10−200 nm. The as-prepared Fe_3O_4/PF microspheres were monodisperse and highly dispersible in water, ethanol, *N*,*N*-dimethylformamide, and acetone. Density-controlled ZnO nanoneedle arrays on a flexible substrate (Teflon) were prepared using $Zn(CH_3COO)_2{\cdot}2H_2O$, $AlCl_3$, and ammonia in aqueous solution in the presence of the substrate under microwave irradiation at 95 °C for 30 min, and the density of ZnO nanoneedles on the substrate could be controlled by adjusting the concentration of $AlCl_3$.[479] The nanocomposite of $RuO_2{\cdot}xH_2O$/poly(3,4-ethylenedioxythiophene) (∼1 wt % RuO_2) was prepared via in situ chemical polymerization of 3,4-ethylenedioxythiophene under microwave irradiation with a power 900 W within 5 min followed by thermal treatment in air for 3 h at different temperatures ranging from 100 to 200 °C.[480] Murugan et al.[481] reported the rapid synthesis of poly(3,4-ethylenedioxythiophene) nanoribbons interleaved between the layers of crystalline V_2O_5 under microwave irradiation via a redox intercalative polymerization reaction of 3,4-ethylenedioxythiophene monomer and commercial crystalline V_2O_5 in aqueous solution at different time intervals. As compared to the conventional refluxing (12 h) for intercalative polymerization, the microwave-assisted redox polymerization process proceeded rapidly, enabling the expansion of the interlayer spacing of crystalline V_2O_5 from 0.43 to 1.41 nm within 8 min. Jagtap et al.[482] synthesized polyaniline/V_2O_5 composite nanosheets with thicknesses of 15−20 nm and with a tremella-like morphology by in situ intercalation of V_2O_5 powder and aniline and subsequent in situ polymerization of aniline in aqueous solution by the microwave-hydrothermal method at 500 W for 15 min.

Hussein et al.[483] reported the microwave-assisted synthesis of the nanocomposite of Zn−Al-layered double hydroxide/sodium dodecyl sulfate. They investigated the microwave-assisted intercalation of anionic surfactant SDS into Zn−Al-layered double hydroxide to form the nanocomposite. Spontaneous self-assembly of organic and inorganic component molecules by the microwave-assisted method was realized in this study. The effect of the microwave heating time on the crystallinity and composition of the resulting nanocomposite was investigated. It was found that the nanocomposites could be synthesized by microwave heating much faster (0.5−2 h) as compared to the conventional heating method (3 days).

The microwave-assisted method has been successfully demonstrated in the rapid synthesis of nanocomposites consisting of inorganic biomaterials and organic polymers in aqueous solution. Guha et al.[484] reported the post processing of in situ synthesized HAP/PVA nanocomposite by microwave heating. They found that the aging time of 1 week required for the normal biomimetic process was reduced to 1 h under microwave irradiation. The microwave energy seems to provide a directional pull to the polymer chains, which leads to an enhancement of the kinetics of phase formation. Tang et al.[485] synthesized the calcium phosphate/polyacrylamide nanocomposites with calcium phosphate nanostructures homogeneously dispersed in the polymer matrix using calcium salt, phosphate, and acrylamide monomer in aqueous solution by the single-step microwave-assisted method. The calcium phosphate phase obtained in a basic medium consisted of hexagonal HAP nanorods, and HAP nanorods were homogeneously dispersed in polyacrylamide matrix, while the amorphous calcium phosphate nanoparticles were formed in a weak acidic medium.

3. MICROWAVE-ASSISTED PREPARATION OF NANOSTRUCTURES IN POLYOLS

Polyalcohols, such as ethylene glycol (EG), 1,3-propanediol, 1,4-butanediol, and glycerol, have high loss tangents (for example, EG has a very high loss tangent of 1.350 at 2.45 GHz and 20 °C); therefore, they belong to the family of strongly microwave absorbing solvents, and thus are excellent solvents for microwave-assisted synthesis of inorganic nanostructures. Polyalcohols are able to form hydrogen bonds extensively, leading to high viscosities, which in turn correlate with a long relaxation time.[25] The most commonly used polyalcohol is ethylene glycol due to its much higher dielectric loss and much higher boiling point as compared to water, and the heating rate and temperature that can be reached in an open reaction system are even higher than those in some hydrothermal processes. Soltani et al.[486] reported that ZnS nanocrystals synthesized with the microwave-polyol method had a higher degree of crystallinity as compared to that synthesized in water using the microwave-hydrothermal method.

dx.doi.org/10.1021/cr400366s | *Chem. Rev.* 2014, 114, 6462−6555

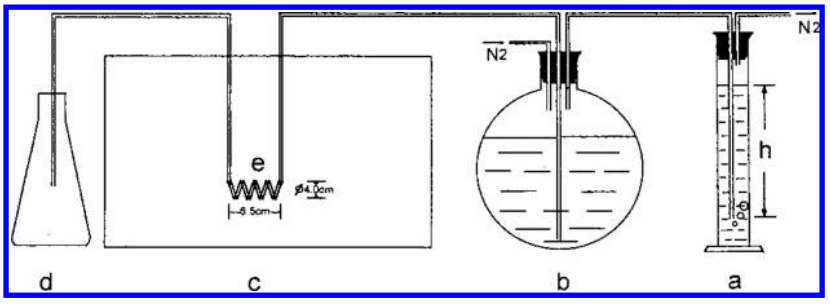

Figure 15. Reaction equipment system for the continuous preparation of colloidal metallic nanoparticles by microwave heating: (a) the liquid column as a pressure regulator, (b) reaction solution container, (c) microwave oven cavity, (d) product suspension receiver, and (e) spiral tube reactor. For more details, refer to ref 488. Reprinted with permission from ref 488. Copyright 2000 American Chemical Society.

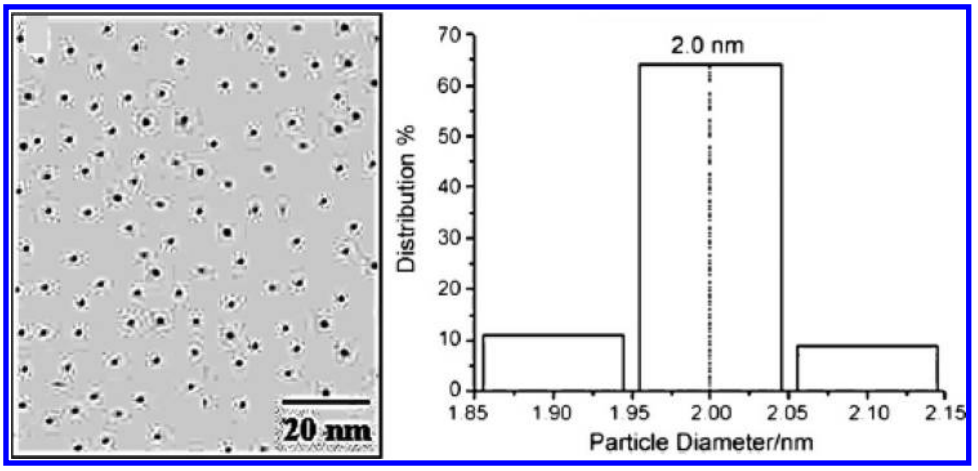

Figure 16. TEM image of the PVP-protected Pt nanoparticles obtained by the microwave-assisted polyol method and the corresponding histogram of the size distribution of Pt nanoparticles. Reprinted with permission from ref 490. Copyright 2007 Elsevier B.V.

3.1. Metals, Semimetals, Nonmetals, and Alloys

In the polyol process, the polyol can be used as both the solvent and the reductant; therefore, in many cases, no additional reducing reagent is needed in the reaction system. In contrast, a reductant is usually necessary for the preparation of metal nanostructures in aqueous solution. When EG is used as the solvent and reductant, metallic nanostructures (M) are produced by the following chemical reactions according to the reduction mechanism proposed by Fievet et al.:[487]

$$CH_2OH{-}CH_2OH \rightarrow CH_3CHO + H_2O$$

$$CH_3CHO + M^{n+} \rightarrow M + CH_3COCOCH_3 + H_2O$$

By using the microwave-assisted polyol method, many nanostructures of metals, semimetals, nonmetals, and alloys have been prepared, including Pt,[488−493] Pd,[488,490,493−496] Au,[497−502] Ag,[35,490,503−514] Ru,[490,491,515−517] Rh,[491] Cu,[518−521] Fe,[522] Co,[523] Ni,[524−530] Bi,[531] Pt−Ag,[493] Au−Pt,[502] Au−Pd,[502] Au−Ag,[502] Au−Rh,[532] Pd−Ag,[493] Ag−Cu,[533] Fe−Ru,[534,535] Fe−Pt,[534,536,537] Bi−Rh,[538] $FeNi_3$,[539] $Co_{0.8}Ni_{0.2}$,[540] Se,[541] and Te.[542,543]

Exciting progress has been made in the microwave-assisted continuous production of metal nanostructures in liquid phase. This novel method is promising for large-scale production of nanostructured materials and their industrial applications. Tu et al.[488] reported the microwave-assisted polyol continuous production of Pt and Pd colloidal nanoparticles using $H_2PtCl_6{\cdot}6H_2O$ or palladium compound, NaOH, and PVP in the solvent of EG. They designed a microwave-assisted continuous production reactor, as shown in Figure 15. The microwave reactor consists of a glass tubing coil with an inner diameter of 2.8 mm (e) located inside the cavity of a household microwave oven and a 3.0 L round-bottomed flask containing the reaction system (b), and nitrogen gas flows to the reaction system (b); thereby, an adequate pressure is exerted in the round-bottomed flask. As a result, the reaction solution flows steadily through the spiral tube (e). The flowing rate of the solution and thus the microwave heating time of the solution in the microwave oven cavity can be regulated by changing the height of the liquid column *h* (a). After microwave heating, the resulting colloidal solution flows out of the coil and is collected by the receiver (d).

In recent years, the microwave-assisted continuous flow-type preparation of nanostructured materials has been investigated by several research groups. For example, Nishioka et al.[503] reported the continuous preparation of Ag nanoparticles using a flow-type microwave heating tubular reactor installed in a cylindrical single-mode microwave cavity using $AgNO_3$, PVP, and EG based on a polyol process. Ag nanoparticles with narrow size distributions were synthesized steadily for 5 h, maintaining almost constant yield (>93%). The microwave reaction occurred within 2.8 s of residence time, although Ag nanoparticles were not formed at this flow rate by the conventional heating. A narrower particle size distribution was realized by increasing the flow rate of the reaction solution. Ag nanoparticles with an average size of 9.8 nm and a standard deviation of 0.9 nm were obtained at a flow rate of 100 mL h^{-1}. The microwave-assisted polyol continuous flow process was also reported by other researchers for the preparation of nanoparticles of noble metals with a narrow size distribution.[544]

Rapid and continuous fabrication of Pt nanoparticles was achieved using a single-mode microwave flow reactor controlled with a temperature feedback module, and Pt nanoparticles were obtained under microwave irradiation within 2.8 s of residence time in glycerol and 1,3-propanediol.[489] Groisman and Gedanken[504] developed a continuous circulating flow microwave system that combined reactions in a household microwave oven with a circulating pump. This system allows the reagents and products to circulate in and out of the microwave reactor until the end of the synthesis. The continuous microwave oven system has several advantages over the batch microwave oven, such as its ability to work with large quantity of reagents, the possibility to withdraw the product without stopping the process, and the constant stirring of the reagents during the reaction. Various Ag nanoparticles with different particle sizes were prepared by using this continuous circulating flow microwave reactor.

As compared to the microwave-assisted continuous flow-type preparation of nanostructured materials, much more research has been carried out for the nonflow-type microwave-assisted preparation. Yu et al.[492] reported the rapid microwave-assisted preparation of polymer-stabilized Pt colloids with a narrow size distribution in a domestic microwave oven at 750 W for 30 s. The average diameters of as-prepared Pt colloids varied ranging from 2 to 4 nm by adjusting the preparation conditions. The relative standard deviation in diameter of the Pt colloids synthesized via microwave heating (~0.17) was much smaller than that synthesized via the oil bath heating (~0.3), indicating that the microwave heating is favorable for the preparation of narrow size-distributed nanoparticles. Grace et al.[490] prepared uniform and stable polymer-protected spherical Pt, Pd, Ag, and Ru nanoparticles using glycerol as the solvent and reducing agent at 290 °C for 2 min in a domestic microwave oven operated in a cyclic mode. Figure 16 shows a TEM image of the as-prepared PVP-protected Pt nanoparticles obtained by the microwave-assisted polyol method and the corresponding histogram of the size distribution of Pt nanoparticles. The as-prepared PVP-protected Pt nanoparticles had a narrow size distribution with a mean particle size of 2.0 nm. A comparative study was done on the size and morphology of nanoparticles using different heating modes via the conventional refluxing and microwave irradiation. The average size of Pt nanoparticles was 6 nm when the reaction was carried out by the conventional reflux heating mode (1 h), whereas when the reaction was carried out by microwave heating mode (2 min), a decrease in particle size (2 nm) was observed. Similar results were observed for Pd, Ag, and Ru nanoparticles when these were synthesized by microwave heating. In addition, in the case of Pd nanoparticles, triangular nanoprisms were produced in addition to spherical nanoparticles by microwave heating. A similar phenomenon was observed for PVP-protected Au nanostructures prepared using $HAuCl_4 \cdot 3H_2O$ and PVP in glycerol at 290 °C.[497]

Tsuji et al.[498] used the cationic surfactant alkyltrimethylammonium bromide (C_nTAB: n = 10−16, even numbers) or cetylpryridinium chloride ($C_{16}PC$) to modulate the morphology of Au nanostructures using $HAuCl_4 \cdot 4H_2O$ in the solvent of EG by a microwave-polyol process for 2 min. They found that the morphology of Au nanostructures was dependent both on the chain length of hydrophobic alkyl group and on the hydrophilic headgroup. Major products were Au spherical aggregates for C_nTAB (n = 10, 12, 14), while triangular, pentagonal, and hexagonal nanoplates were preferentially formed in the presence of $C_{16}TAB$. Spherical spike-ball structures were obtained in the presence of $C_{16}PC$. Au nanocrystals were obtained in the $HAuCl_4 \cdot 4H_2O$/PVP/EG and $HAuCl_4 \cdot 4H_2O$/MCl (M = Na, K, H)/PVP/EG reaction systems by the microwave-polyol method. When $HAuCl_4 \cdot 4H_2O$ was reduced in EG in the presence of PVP at a low $HAuCl_4$ concentration, mixtures of spherical, triangular, octahedral, and decahedral Au nanocrystals were obtained in several minutes. They found that the shape-selective oxidative etching by $AuCl_4^-$ + Cl^- anions and crystal growth occurred simultaneously at high $HAuCl_4$ concentrations. The addition of MCl (M = Na, K, H) was effective to enhance the shape-selective oxidative etching by $AuCl_4^-$ + Cl^- anions.[499] When di-, tetra-, and poly(ethylene glycol) were heated to 240 °C at a heating rate of 160 °C/min and held for 5 min, Au icosahedral nanocrystals with average sizes of 55−85 nm were obtained from the reaction system of $HAuCl_4$ and PVP in di-, tetra-, and PEG at high yields (>91%). Plate-like and decahedral particles were obtained at high yields from the reaction system of $HAuCl_4$/PVP/NaCl.[500] Single-crystalline Au nanorods and nanowires as well as Au nanostructures with other morphologies were prepared using $HAuCl_4 \cdot 4H_2O$ and surfactants (PVP and SDS) in EG by the microwave-polyol method at 160 °C.[501]

Considerable effort has been devoted to the microwave-assisted preparation of Ag nanostructures in polyols. Li et al.[505] adopted the microwave-assisted polyol method for the preparation of Ag nanoparticles and nanowries in EG at 100 or 150 °C. Ag nanoparticles of ~10−36 nm and nanowires with a diameter of 40 nm were obtained. The particle size and shape of the product could be varied by adjusting the concentration of the Ag source, PVP molecular weight, and $NH_4F \cdot HF$ as a ligand. By binding Ag^+ ions with the ligand, Ag nanoparticles with larger particle sizes were obtained, and Ag nanowires were obtained at 100 °C by using F^- as a ligand but with relatively high ratios of ligand/Ag^+ and ligand/PVP. Navaladian et al.[506] prepared anisotropic Ag nanostructures by decomposition of silver oxalate in a glycol medium using PVP as a capping agent under microwave irradiation. It was found that EG was a more suitable medium than diethylene glycol. Anisotropic Ag nanostructures were obtained under microwave irradiation for 75 s, whereas spherical nanoparticles with sizes of ~5−6 nm formed for 1 min of microwave irradiation. Chen et al.[507] prepared Ag nanocubes and nanowires by reducing $AgNO_3$ with EG in the presence of Na_2S and PVP. Ag nanocubes could be obtained by changing the concentration of Na_2S and the heating power. The presence of Na_2S had an important effect on the morphology of Ag nanostructures. When a low concentration of Na_2S solution was used, Ag nanocubes were produced under different heating powers (300 and 400 W), and Ag nanowires were obtained at 400 W when a high concentration of Na_2S solution was used. Gou et al.[508] reported the rapid microwave-assisted aerobic polyol preparation of Ag nanowires with a diameter of 45 nm using $AgNO_3$, NaCl, and PVP in EG, and the yield of Ag nanowires was 80% in 3.5 min. Wire formation was highly dependent upon the microwave heating power, time, and $NaCl/AgNO_3$ ratio. Extended microwave heating caused the wires to fuse or degrade to shorter wires presumably via the etching reaction. Kou et al.[514] fabricated Ag nanowires using glycerol as both a reductant and a solvent by a nonstirred microwave-assisted polyol process for 1 min, where SDS was used to prevent the growth of Ag nanowires. In contrast, no Ag particles were formed at the same temperature using the conventional heating method. The

dx.doi.org/10.1021/cr400366s | Chem. Rev. 2014, 114, 6462−6555

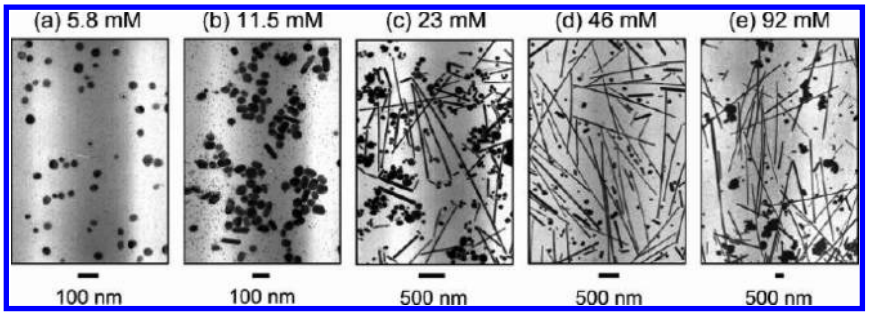

Figure 17. TEM micrographs of Ag nanostructures prepared from $AgNO_3/H_2PtCl_6{\cdot}6H_2O$ (57.5 μM)/PVP (132 mM)/EG at various $AgNO_3$ concentrations at a constant $AgNO_3$/PVP molar ratio of 5.7. Reprinted with permission from ref 510. Copyright 2007 American Chemical Society.

diameter of Ag nanowires could be controlled by changing the amounts of $AgNO_3$, glycerol, and SDS. When the amount of SDS was low, the bundles of Ag nanowires were obtained, while dispersed Ag nanowires formed with a higher SDS amount.

Tsuji et al.[509] prepared Ag nanostructures in the presence of PVP with different molecular weights by the microwave-polyol method. Ag spherical nanoparticles, nanosheets, polygonal nanoplates, nanorods, and nanowires were obtained within 8 min. Ag nanosheets and nanoplates were dominantly formed in the presence of PVP with a shorter chain (10k), while Ag nanorods and nanowires were preferentially formed using PVP with a longer chain (40k, 360k). The number density of Ag nanostructures increased with increasing chain length of PVP. When $AgNO_3$ was reduced by EG in the presence of Pt seeds and PVP with a long chain length, Ag nanostructures with different morphologies were obtained within a few minutes. It was found that the size and shape of Ag nanostructures were dependent on experimental parameters such as concentrations of Pt, PVP, and $AgNO_3$ and heating time. For the preparation of long nanorods and nanowires at high yields, low Pt concentrations and high $AgNO_3$ concentrations were required (Figure 17).[510] Figure 17 shows TEM images of the products obtained in the $AgNO_3$ concentration range of 5.8−92 mM at constant $H_2PtCl_6{\cdot}6H_2O$ and PVP concentrations of 57.5 μM and 132 mM, respectively. At the lowest $AgNO_3$ concentration of 5.8 mM, only spherical Ag nanoparticles with average diameters of 42 ± 6 nm were obtained. 1-D Ag nanostructures were prepared in the 11.5−92 mM $AgNO_3$ concentration range. The average diameters were similar (~50 nm) in the low $AgNO_3$ concentration range of 5.8−46 mM and increased to ~110 nm at the highest $AgNO_3$ concentration of 92 mM. These experimental results indicate that 1-D Ag nanostructures with larger diameters can be prepared at a high $AgNO_3$ concentration. The average length of 1-D Ag nanostructures increased from ~120 nm to ~2.6 μm with increasing $AgNO_3$ concentration from 11.5 to 92 mM. The yield of 1-D Ag nanostructures increased from nearly zero to 34% when the $AgNO_3$ concentration was increased from 5.8 to 11.5 mM and reached ~60% in the higher $AgNO_3$ concentration range.

Tsuji et al.[511] prepared Ag nanorods and nanowires by the microwave-polyol method for 3 min. Various Pt compounds such as H_2PtCl_6 and platinum(II) bis-acetylacetonate were used to investigate the roles of Pt seeds and anions in the formation of Ag nanostructures. Furthermore, the effect of Cl^- anions on the morphology of Ag nanostructures was explored by adding the Cl^- additive such as NaCl or KCl in EG solutions containing $AgNO_3$ and PVP. It was found that the presence of Cl^- ions could accelerate redissolution of formed spherical Ag particles and was favorable for the growth of 1-D and other Ag nanostructures with well-defined crystal structures such as single-crystalline cubes and twinned bipyramids in the microwave-assisted polyol process. The difference in the adsorption ability of different species on Ag crystals in solution determined the shape, size, and yield of Ag nanostructures.[512]

The microwave-assisted polyol method has also been adopted for the preparation of Pd nanostructures. Zawadzki[494] prepared PVP-stabilized Pd nanoparticles with average sizes from 2.0 to 15.9 nm using $H_2PdCl_4{\cdot}nH_2O$ and PVP in various polyol solvents (EG, diethylene glycol, triethylene glycol) under microwave solvothermal conditions at 150 °C for 5 min. The morphology and size of Pd nanoparticles were greatly affected by the concentration of PVP and Pd salt. The nature of the reducing agent was of less significance under microwave solvothermal conditions at fixed parameters (temperature, pressure, and time); for example, the average size of Pd nanoparticles obtained using a PVP/Pd molar ratio of 50:1 in EG, diethylene glycol, and triethylene glycol was 2.0, 3.0, and 3.5 nm, respectively. Yu et al.[495] prepared Pd nanocubes and nanobars with a mean size of about 23.8 nm using H_2PdCl_4 as the Pd source, and tetraethylene glycol as both the solvent and the reducing agent in the presence of PVP and CTAB under microwave irradiation at 900 W for 80 s, and the effect of CTAB on the shape of Pd nanocrystals was also investigated. Pd icosahedra were prepared using H_2PdCl_4 as the Pd precursor and PVP as the stabilizer in the presence of an appropriate amount of KOH in tetraethylene glycol under microwave irradiation. Pd icosahedra with uniform sizes and well-defined shapes could be obtained with a yield of over 90% by microwave heating for 1 min. The sizes of Pd icosahedra could be controlled by adjusting the concentration of H_2PdCl_4.[496]

Cu nanoparticles with sizes of ~10 nm were prepared by reducing $CuSO_4{\cdot}5H_2O$ with $NaH_2PO_2{\cdot}H_2O$ in the presence of PVP in EG under microwave irradiation for 5 min.[518] Hydrazine was also adopted as a reductant for the microwave-polyol preparation of Cu nanoparticles with diameters of ~15 nm.[519] Kawasaki et al.[520] obtained Cu nanoparticles with sizes of ~2 nm using $CuCl_2$ and NaOH in EG via a microwave-assisted polyol process at 185 °C for a few minutes without using additional protective agents. Blosi et al.[521] used diethylene glycol in a microwave-assisted polyol process for the preparation of Cu nanoparticles. The preparation was carried out at 60−170 °C for 10 min using $Cu(CH_3COO)_2{\cdot}H_2O$ as the copper source in the presence of additives such as ascorbic acid (reducing agent) and PVP. In the optimum conditions, Cu nanoparticles with sizes of 46 ± 9 nm could be obtained. The as-prepared colloidal suspensions were stable for months despite the high metal concentration.

Wada et al.[524] prepared Ni nanoparticles with a narrow size distribution through the reduction of $Ni(OH)_2$ with EG under microwave irradiation, and the average particle size could be varied between 5 and 8 nm by adjusting the microwave heating time and power. Eluri et al.[525] prepared Ni nanoparticles using $Ni(CH_3COO)_2{\cdot}4H_2O$, $NaH_2PO_2{\cdot}H_2O$, and NaOH in propylene glycol under microwave irradiation for 35 s. By varying the molar ratio of the reactants, Ni nanoparticles with sizes of 3.9−7.2 nm were obtained. Increasing the concentration of NaOH resulted in a morphological change from isolated spherical particles to agglomerated nanoflowers (72 ± 14 nm). Addition of a small amount of PVP or CTAB resulted in a slight increase in particle size. Ni nanoparticles with sizes in the range of 30−100 nm were prepared using PVP and dodecylamine as protecting agents through a microwave-assisted polyol process in EG, and the morphology of Ni nanoparticles could be controlled by the amount of dodecylamine, and the particle size and size distribution could be adjusted by the concentration of the metal source and dodecylamine/PVP ratio.[526] Donegan et al.[529] prepared Ni nanocrystals with an icosahedral morphology in EG using the microwave-assisted polyol method. Nickel acetylacetonate was used as the nickel precursor, while sodium formate and *n*-trioctylphosphine oxide were employed as the reducing agent and capping ligand, respectively. Hu et al.[530] prepared Ni nanowires using $NiCl_2{\cdot}6H_2O$, trioctylphosphine oxide, and hydrazine monohydrate in EG by a rapid microwave-assisted process at 160 °C for 5 min. Ni nanospheres with sizes of 5−100 nm, formed by self-assembly of primary nanoparticles with an average dimension of ∼6.3 nm, were prepared using $NiCl_2$, Na_2CO_3, NaOH, hydrazine hydrate, and PVP in EG under microwave irradiation at 450 W for 1 min.[528] Liu et al.[527] prepared Ni nanospheres using $Ni(CH_3COO)_2{\cdot}4H_2O$ in triethylene glycol by a microwave-assisted polyol refluxing process.

Chefetz et al.[545] developed a combined procedure composed of adsorption of metallic ions on aquatic plants and conversion of adsorbed metal ions into metallic nanoparticles in EG by microwave heating. The combined process offers a promising approach for the removal of heavy metal ions from the wastewater and recycling of adsorbed metal ions into metallic nanoparticles. They used the aquatic plant *Azolla* as the sorbent for Ag^+, Pb^{2+}, and Ru^{3+} ions in aqueous solution.

The microwave-assisted polyol method has also been demonstrated for the rapid synthesis of metal alloy nanostructures. Du et al.[535] prepared Fe−Ru bimetallic nanoparticles using 1,2-propanediol to reduce the mixture of $FeCl_3$ and $RuCl_3$ in the presence of PVP as a protective agent by the microwave-assisted polyol method at 300 W for 3 min. Köhler et al.[538] prepared Bi−Rh pseudohexagonal nanoplates using bismuth acetate and rhodium acetate dimer in EG by a microwave-assisted polyol process at 240 °C for 1 h. $FeNi_3$ nanochains were prepared by reducing iron(III) acetylacetonate and nickel(II) acetylacetonate with hydrazine in EG under microwave irradiation at 160 °C for 5 min.[539] $Co_{0.8}Ni_{0.2}$ nanostructures were prepared in 1,2-propanediol by a microwave-assisted polyol process, and it was found that rapid heating led to the formation of nanowires while slow heating resulted in nanourchins, and the aspect ratio of $Co_{0.8}Ni_{0.2}$ nanowires decreased with increasing temperature.[540]

Zhu et al.[543] prepared Te nanorods and nanowires using TeO_2 in EG by a surfactant-free microwave-polyol process at 185 °C for 30 min. The aspect ratio of Te nanostructures could be controlled by adjusting the experimental parameters. The yield of Te powder was usually higher than 90%. They also prepared Se nanorods and nanowires by one-step surfactant-free microwave-polyol reduction of SeO_2 with EG at 195 °C for 30 min.[541]

In addition to polyols, the polythiol (1,2-ethanedithiol) was also adopted for the microwave-assisted preparation of nanostructures. Zhu et al.[546] developed a new microwave-polythiol method using a polythiol (1,2-ethanedithiol) as both a reducing reagent and a solvent. 1,2-Ethanedithiol has a boiling point of about 147 °C, much lower than that of its polyol counterpart (EG with a boiling point of ∼197 °C). By using the microwave-polythiol method, Te structures with various morphologies were obtained at relatively low temperatures (≤140 °C) for 30 min. The morphology of Te could be controlled by adjusting experimental parameters. In addition, Ag nanowires were obtained using Ag_2O as the silver source and 1,2-ethanedithiol as both a reducing reagent and a solvent through a solid−liquid reaction mechanism by the microwave-polythiol method at temperatures between 80 and 140 °C.[547]

3.2. Metal Oxides

Microwave-assisted synthesis of metal oxide nanostructures has aroused much interest due to interesting properties of different kinds of metal oxides and their wide applications. Usually, a metal salt is used as the metal source, and an alkali and/or an additive is adopted in a polyol solvent. Many kinds of nanostructured metal oxides prepared by the microwave-assisted polyol method have been reported, including MgO,[548] ZnO,[549−554] Fe_3O_4,[522,555−559] α-Fe_2O_3,[560] γ-Fe_2O_3,[556] CuO,[561] Cu_2O,[561] Co_3O_4,[562] NiO,[563] MnO,[564] $ZnAl_2O_4$,[565] $CoFe_2O_4$,[566,567] $NiFe_2O_4$,[567] $ZnFe_2O_4$,[567] $MnFe_2O_4$,[567] $Co_{1-x}Zn_xFe_2O_4$,[568] $Mn_{1-x}Zn_xFe_2O_4$,[569] $BaTiO_3$,[570] $PbTiO_3$,[570] $Ba_6Ti_{17}O_{40}$,[570] $BaZrO_3$,[570] $La_{0.67}Ca_{0.33}MnO_3$,[571] $SrWO_4$,[572,573] $BaWO_4$,[574] $CaMoO_4$,[575,576] $SrMoO_4$,[573,576] $BaMoO_4$,[574,576] $PbWO_4$,[577] $PbMoO_4$,[577] Bi_2WO_6,[578] and $Y_3Al_5O_{12}$.[579] Various polyols have been adopted as the solvent, including ethylene glycol,[522,548,553,554,556−563,566,568−575,577,578] propylene glycol,[576] 1,3-propanediol,[551] 1,4-butanediol,[550,565,579] diethylene glycol,[549,552,555] and triethylene glycol.[564,567]

Hu et al.[552] reported the rapid microwave-polyol synthesis of ZnO spheres composed of small primary nanocrystals in the solvent of diethylene glycol with a boiling point of ∼245 °C. The size of ZnO spheres could be tuned from ∼57 to 274 nm by simply varying the amount of the Zn complex precursor. In this method, the $Zn(CH_3COO)_2$/diethylene glycol stock solution (20 mL) was microwave-heated with magnetic stirring at 180 °C for 5 min to form a slightly turbid solution, which was used as a seeding solution for further reactions. When another aliquot of the $Zn(CH_3COO)_2$/diethylene glycol stock solution (20 mL) was microwave-heated to 120 °C within 1 min, the above resulting seeding solution (1.8 mL) was injected rapidly into this hot mixture, and the temperature was maintained at 120 °C for 1 min. The reaction temperature then was promptly elevated to 180 °C and further kept at this temperature for 5 min to yield ZnO spheres. The amount of the seeding solution determined the size of ZnO spheres. For example, the amounts of seeding solution of 2.2, 2.5, 3, 5, 8, and 10 mL produced ZnO spheres with average sizes of 210, 183, 162, 125, 86, and 57 nm, respectively. Liang et al.[553] synthesized ZnO nanosheets by decomposition of a layered precursor, which was synthesized using $Zn(CH_3COO)_2{\cdot}2H_2O$ in EG by microwave heating, and the thicknesses of ZnO

dx.doi.org/10.1021/cr400366s | *Chem. Rev.* 2014, 114, 6462−6555

nanosheets were in the range of 5−10 nm. Lojkowski et al.[554] prepared ZnO nanostructures doped with Mn^{2+}, Ni^{2+}, Co^{2+}, and Cr^{3+} ions by a microwave-solvothermal reaction from an EG solution containing zinc acetate and acetates of manganese-(II), nickel(II), cobalt(II), and chromium(III). The average grain size of the powder doped with 10 mol % Mn^{2+}, Ni^{2+}, Co^{2+}, and Cr^{3+} was about 20 nm, and the grain size of doped ZnO nanostructures decreased with increasing dopant content.

Fe_3O_4, γ-Fe_2O_3, or α-Fe_2O_3 hierarchically nanostructured hollow microspheres assembled by nanosheets were prepared by a novel precursor-templated thermal conversion method. The hierarchically nanostructured hollow microspheres organized by nanosheets of a layer-structured ferrous precursor were synthesized using $FeCl_3{\cdot}6H_2O$, NaOH, and sodium dodecyl benzenesulfonate (SDBS) in the solvent of EG by the microwave-assisted solvothermal method at 200 °C for 30 or 90 min.[556,560] EG acted as both a solvent and a reductant to reduce ferric salt to ferrous precursor in the presence of NaOH and SDBS. The hollow microspheres of the precursor were used as the iron source and morphological template for subsequent thermal transformation to prepare hierarchically nanostructured hollow microspheres assembled by Fe_3O_4, γ-Fe_2O_3, or α-Fe_2O_3 nanosheets. One of the advantages of this method is that Fe_3O_4, γ-Fe_2O_3, or α-Fe_2O_3 hierarchically nanostructured hollow microspheres consisting of organized nanosheets can be synthesized using the same single source precursor. Hierarchically nanostructured hollow microspheres assembled by Fe_3O_4 or γ-Fe_2O_3 nanosheets were surface modified with PEG. The hierarchically nanostructured magnetic hollow microspheres of Fe_3O_4 or γ-Fe_2O_3 had a high drug loading capacity and favorable drug release property for ibuprofen, with an ibuprofen uptake amount of 297 and 237 mg g^{-1} for PEG-coated Fe_3O_4 and PEG-coated γ-Fe_2O_3, respectively; thus, they are promising for the application in drug delivery.[556] The as-prepared α-Fe_2O_3 hierarchically nanostructured hollow microspheres exhibited a better photocatalytic property than that of ringlike nanoparticles and also showed a satisfactory removal capacity for methyl orange in wastewater treatment.[560]

Fe_3O_4 nanoporous spheres with an average size of ∼100 nm were synthesized using $FeCl_3{\cdot}6H_2O$, CH_3COONa, and PEG in EG by microwave heating at 200 °C for 5 min.[558] The microwave-assisted polyol approach was adopted for the synthesis of Fe_3O_4 nanoroses constructed by nanosheets using $FeCl_3{\cdot}6H_2O$, CH_3COONa, and PEO−PPO−PEO block copolymer (P123) in EG at 160 °C for 15−60 min.[559] Flower-like Fe_3O_4 structures formed by self-assembly of nanosheets were synthesized using the precursors that were prepared using $FeCl_3{\cdot}6H_2O$, tetrabutylammonium, and $CO(NH_2)_2$ in EG through a microwave-assisted reaction at 120−210 °C for 30 min, and, subsequently, the precursors were thermally treated in nitrogen at 400 °C for 2 h.[522]

Staszak et al.[565] prepared $ZnAl_2O_4$ nanoparticles with a spinel structure (average crystallite size was 3 nm) using $Zn(CH_3COO)_2$ and aluminum isopropoxide in 1,4-butanediol under microwave-assisted solvothermal conditions at 200 °C for 30 min. Ibrahim et al.[566] prepared $CoFe_2O_4$ nanoparticles using $Co(NO_3)_2{\cdot}6H_2O$ and $Fe(NO_3)_3{\cdot}9H_2O$ in the solvent of EG via the microwave-polyol method at 900 W for 2 min. Solano et al.[567] prepared MFe_2O_4 (M = Fe, Co, Mn, Ni, and Zn) nanoparticles with diameters smaller than 10 nm by microwave heating at 220 or 280 °C for 10 min under magnetic stirring, based on the decomposition of acetylacetonate metal precursors in triethylene glycol. Giri et al.[568] prepared $Co_{1-x}Zn_xFe_2O_4$ ($0 \le x \le 0.8$) nanoparticles (5−30 nm) using $Zn(CH_3COO)_2{\cdot}H_2O$, $Co(CH_3COO)_2{\cdot}4H_2O$, $FeCl_3$, and KOH in EG by microwave refluxing, followed by calcination at 500 °C for 2 h. The particle size of the product was dependent on experimental parameters such as the pH value, Zn content, EG volume, and refluxing time. The pH values of 9−10 were optimum for the formation of well-dispersed nanoparticles. In addition, $Mn_{1-x}Zn_xFe_2O_4$ nanoparticles were prepared using $MnCl_2{\cdot}4H_2O$, $FeCl_3$, $ZnCl_2$, and PEG in EG by microwave refluxing for 30 min to 3 h, and the morphology and size of the product were dependent on experimental parameters such as the pH value, refluxing time, and PEG.[569]

Palchik et al.[570] reported the microwave-assisted synthesis of nanoparticles of $BaTiO_3$, $Ba_6Ti_{17}O_{40}$, $BaZrO_3$, and $PbTiO_3$ using $Pb(CH_3COO)_2{\cdot}3H_2O$, $BaCl_2$, zirconium perchlorate octahydrate, and titanium isopropoxide as the reactants in the solvent of EG by microwave refluxing for a relatively long period of time (1−5 h). Nayak et al.[571] prepared $La_{0.67}Ca_{0.33}MnO_3$ nanoparticles with sizes of 30−70 nm from metal acetates in EG by microwave refluxing for 1 h followed by annealing at different temperatures. Thongtem et al.[572] prepared $SrWO_4$ nanoparticles using $SrCl_2$ and Na_2WO_4 in EG at different pH values, microwave powers (180−600 W), and heating times (20−80 min). Bi_2WO_6 nanosheets were synthesized using $Bi(NO_3)_3{\cdot}5H_2O$ and $(NH_4)_{10}W_{12}O_{41}{\cdot}5H_2O$ in EG by a microwave-solvothermal process at 160 °C for different times (2 or 4 h).[578] $BaMoO_4$ nanoparticles (30−75 nm) and $BaWO_4$ nanoparticles (20−75 nm) were synthesized from the reactions between $Ba(NO_3)_2$ and Na_2MeO_4 (Me = Mo and W) in EG under 300 W microwave irradiation for 20 min.[574] $SrMoO_4$ nanocrystals with sizes of 14−40 nm and $SrWO_4$ nanocrystals with sizes of 14−38 nm were synthesized using $Sr(NO_3)_2$ and Na_2MeO_4 (Me = Mo and W) in EG under microwave irradiation at 50% of 180 W for 20 min.[573] $CaMoO_4$ nanoparticles with particle sizes of 16−44 nm were synthesized from $Ca(NO_3)_2$ and Na_2MoO_4 in EG under pulsed microwave irradiation at 300 W for 20 min.[575] $MMoO_4$ (M = Ba, Sr, and Ca) nanostructures were prepared by the reactions of $M(NO_3)_2{\cdot}2H_2O$, $Na_2MoO_4{\cdot}2H_2O$, and NaOH in propylene glycol under pulsed microwave irradiation at 600 W for 20 min.[576] $PbMoO_4$ (15−50 nm) and $PbWO_4$ (12−32 nm) nanoparticles were synthesized using $Pb(NO_3)_2$ and Na_2MO_4 (M = Mo and W) in EG under microwave irradiation at 50% of 180 W for 20 min.[577]

3.3. Metal Chalcogenides

Microwave-assisted polyol synthesis of nanostructures of metal sulfides, metal selenides, and metal tellurides is very important for applications of these materials in various fields. In the microwave-assisted polyol synthesis of nanostructures of metal chalcogenides in the solvent of a polyol, a metal salt is usually used as the metal source, and a source of sulfur or selenium or tellurium and sometimes an additive are adopted. As compared to the synthesis with the conventional heating methods, the microwave-assisted synthesis of metal chalcogenide nanostructures has an obvious advantage of rapidness, with much reduced preparation time often by orders of magnitude. Many kinds of nanostructured metal chalcogenides prepared by the microwave-assisted polyol method have been reported, including SnS,[580,581] SnS_2,[580,581] PbS,[582,583] Sb_2S_3,[584,585] Bi_2S_3,[586,587] CdS,[588−592] ZnS,[591,593,594] CuS,[595−597] FeS_2,[598] CoS,[591] Cu_3BiS_3,[599] Cu_2ZnSnS_4,[600] CdSe,[601,602] β-FeSe,[603]

dx.doi.org/10.1021/cr400366s | Chem. Rev. 2014, 114, 6462−6555

Sb_2Se_3,[604,605] Bi_2Se_3,[606] $MoSe_2$,[607] $Cd_{1-x}Zn_xSe$,[608,609] $CuInSe_2$,[610] Sb_2Te_3,[611] Bi_2Te_3,[612] PbTe,[613] Ni_2Te_3,[613] Cu_7Te_5,[613] $Cu_{(2-x)}Te$,[614] and $CuInTe_2$.[610] EG has been commonly adopted as the solvent.[580,581,583,584,586−601,606−609,611−614] In addition, other polyols have also been used as the solvents, such as propylene glycol,[582,603] 1,2-propanediol,[585] triethylene glycol,[601,610] 1,5-pentanediol,[604] glycerol,[602,605,612] and tetraethylene glycol.[610]

Oliveira et al.[588] prepared CdS nanostructures with a hexagonal crystal structure using $CdCl_2·H_2O$ and NH_2CSNH_2 in the solvent of EG or ethylenediamine via the microwave-assisted solvothermal method at 180 °C for 32 min. It was found that the solvent had a significant effect on the morphology of the product. Flower-like CdS nanostructures constructed with nanosheets (25 nm in thickness) were obtained in the presence of EG; in contrast, aggregates of nanoplates (40 nm in thickness) were formed in the solvent of ethylenediamine.

Recently, some researchers adopted the combination of both microwave and sonochemical irradiation for the synthesis of nanostructures in liquid phase. Tai et al.[590] prepared CdS nanoparticles using $Cd(CH_3COO)_2·2H_2O$, CH_3CSNH_2, S powder, and NaCl in EG by an ultrasound−microwave combined process at 140 °C for 15 min. Zinc blende CdS nanoparticles were produced in the absence of NaCl, while mixed zinc blende and wurtzite CdS nanoparticles were obtained when NaCl/Cd^{2+} molar ratios were below 1, and pure wurtzite CdS nanoparticles were produced at a molar ratio of 1. Tai and Guo[589] prepared flower-like CdS nanostructures consisting of hexagonal nanopyramids and/or nanoplates depending on the sulfur source by applying ultrasound and microwave irradiation simultaneously, using the starting reactants of $CdCl_2$, NH_2CSNH_2 or C_2H_5NS, and S powder in the solvent of EG. The synergistic effect of microwave and sonochemical irradiation was proposed for the formation of CdS nanostructured flowers. Ma et al.[592] adopted the ultrasound−microwave combined method to prepare Ag-doped CdS nanoparticles in EG at 140 °C for 15 min. It was found that Ag doping of CdS nanoparticles could induce the evolution of crystal structure from cubic to hexagonal under the synergistic effect of ultrasound and microwaves.

Wang et al.[595] reported the microwave-biomolecule-assisted synthesis of CuS nanostructures with different morphologies using $CuCl_2·2H_2O$, thiourea, and histidine in EG at 130 or 150 °C for 3−15 min. It was found that histidine played an important role in the formation of CuS hierarchical architectures. The morphology and size of the product could be tuned by adjusting the molar ratio of Cu^{2+}/histidine and Cu^{2+}/thiourea. Thongtem et al.[596] synthesized assemblies of nanoflakes, nanoparticles, nanofibers, nanorods, and spongelike structures of CuS from copper and sulfur sources ($CuCl_2·2H_2O$, CuBr, $Cu(CH_3COO)_2·H_2O$, CH_3CSNH_2, $NH_2CSNHNH_2$, and NH_2CSNH_2) in EG under cyclic microwave irradiation at different microwave powers and times. Liu et al.[597] reported the microwave-assisted solvothermal synthesis of CuS nanotubes assembled with nanoparticles using $Cu(OH)_2$ nanowires and thiourea in the solvent of EG at 80 °C for 10 min to 2 h. ZnS nanoparticles with sizes of ∼3 nm were prepared using $Zn(CH_3COO)_2·2H_2O$ and $Na_2S·9H_2O$ in EG by microwave heating at 65 W for 10 min.[593] Hexagonal phase ZnS nanocrystals with sizes of ∼5 nm were synthesized by microwave thermolysis of a single-source molecular precursor of zinc diethyldithiocarbamate in EG at 110 °C for 5 min.[594] FeS_2 microspheres were synthesized using $FeSO_4·7H_2O$, PVP, and S powder in EG by microwave-assisted polyol refluxing for 1 h under nitrogen flow.[598] The formation of FeS_2 microspheres was proposed via a nanocrystal aggregation-based mechanism, in which primary FeS_2 nanocrystals were first formed, then they self-assembled into microspheres, and finally the Ostwald ripening led to the monodisperse microspheres.

Kavinchan et al.[584] synthesized orthorhombic Sb_2S_3 nanorod bundles with a dumbbell-like morphology using $SbCl_3$, $Na_2S_2O_3$, and PVP in the solvent of EG under cyclic microwave irradiation (600 W, 50 s on and 20 s off) for 15 cycles. Sb_2S_3 nanorods with diameters ranging from 30 to 50 nm were synthesized by the reaction between $SbCl_3$ and thiourea in the presence of PVP in the solvent of 1,2-propanediol via microwave irradiation for 15 min.[585] Nest-shaped Bi_2S_3 nanostructures were synthesized using CdS mother nanocrystals, $Bi(NO_3)_3·5H_2O$, and CTAB in EG via the dissolution−recrystallization process by microwave heating in a household microwave oven at 800 W for 50 s. During the dissolution−recrystallization process, the growth regime could be controlled from the thermodynamic control to the kinetic domination through adding more Bi^{3+} ions or changing the heating method from oil bath to microwave heating.[586] Bi_2S_3 flower-like superstructures consisting of nanorods with average diameters of 10−20 nm were prepared using $Bi(NO_3)_3·5H_2O$ and thiourea in EG under microwave irradiation for 3 min.[587]

Aup-Ngoen et al.[599] synthesized nanostructured Cu_3BiS_3 dendrites using CuCl, $BiCl_3$, and L-cysteine in EG under cyclic microwave irradiation with powers of 300−700 W, and the morphology evolution from nanoparticles to nanostructured dendrites was observed with increasing microwave power. Flynn et al.[600] synthesized Cu_2ZnSnS_4 nanoparticle inks using CuCl, $ZnCl_2$ $SnCl_4·5H_2O$, and thioacetamide in EG (pH 2) by the microwave-assisted method at 190 °C for 30 min. The diameters of Cu_2ZnSnS_4 nanoparticles were determined to be 7.6 ± 2.1 nm, and these nanoparticles were found to agglomerate into larger particles.

In addition to nanostructured metal sulfides, nanostructures of metal selenides have also been prepared by the microwave-assisted polyol method. Palchik et al.[601] reported the microwave-assisted polyol preparation of CdSe nanoballs composed of CdSe nanocrystals with sizes of a few nanometers using $Cd(CH_3COO)_2$ and Se powder in the solvent of a polyol. The crystal phase of the product depended on the polyol used; the hexagonal CdSe was obtained in EG, and the cubic CdSe formed in triethylene glycol. Cao et al.[602] prepared a variety of multipod-shaped CdSe nanostructures using $Cd(NO_3)_2$ and Se powder in glycerol via microwave irradiation at 150 °C for 10 min. By selectively introducing organic additives (CTAB, oleic acid, and PVP) into the system, the morphology of CdSe varied from tetrapods to hexapods, octapods, and more complex multipods. Harpeness et al.[606] used the microwave-polyol method to prepare nanostructured Bi_2Se_3 using $BiONO_3$, elemental Se, and NaOH in EG for 30 min under nitrogen environment. Zhao et al.[605] prepared Sb_2Se_3 nanorods with diameters of 40−70 nm through the reaction between Se powder and sodium antimony tartrate in glycerol by microwave heating at 120 °C for 30 min. Mehta et al.[604] reported the rapid and scalable (gram-a-minute) microwave-assisted synthesis of sulfurized Sb_2Se_3 nanowires and nanotubes that exhibited about 10^4−10^{10} times higher electrical conductivity than bulk or thin film forms of this material. They adopted a microwave-activated solvothermal reaction of tri*n*-octylphosphine (TOP)-ligated

dx.doi.org/10.1021/cr400366s | *Chem. Rev.* 2014, 114, 6462−6555

selenium and thioglycolic acid (TGA)-ligated antimony salts in 1,5-pentanediol using a domestic microwave oven (1250 W) or a variable power single-mode CEM microwave reactor (300 W). They prepared the antimony and selenium precursors by independently microwave heating the antimony salt in pentanediol with TGA and selenium with TOP. The sulfur content was varied by adjusting the TGA/TOP−Se^{2-} molar ratio. The two precursors were then mixed and microwave heated for different time intervals between ∼1−2 min. This synthetic process is easily scalable and yields gram quantities in a few minutes, for example, 2−3 g in 2 min. Li et al.[603] prepared flower-like tetragonal β-FeSe microstructures assembled from nanoplates with thicknesses of ∼60−70 nm using $FeCl_3·6H_2O$, Se powder, and NaOH in 1,2-propylene glycol under microwave irradiation for 1 h.

The nanostructures of doped metal selenides have also been prepared by the microwave-assisted polyol method. Grisaru et al.[608] prepared $Cd_{0.8}Zn_{0.2}Se$ nanoparticles with an average diameter of 6 ± 2 nm using $Zn(CH_3COO)_2$, $Cd(CH_3COO)_2$, Se powder, and NaOH in EG by a microwave-assisted polyol process for 1 h, followed by annealing under nitrogen at 550 °C for 12 h. By using a similar microwave-assisted polyol process, nanoparticles of $Cd_{1-x}Zn_xSe$ alloy ($x \approx 0.1, 0.2, 0.3$) with average diameters of 5−8 nm were prepared, and the nanoparticles formed spherical aggregates with a diameter of approximately 200 nm.[609]

The nanostructured metal tellurides have also been prepared by the microwave-assisted polyol method. Palchik et al.[613] prepared nanostructured binary metal tellurides, such as PbTe, Ni_2Te_3, and Cu_7Te_5, by the microwave-assisted polyol method. Binary tellurides were formed only in the case when EG was used as a reducing agent under microwave irradiation. No product was obtained when the reactions were performed by the conventional heating. A rapid microwave-assisted polyol route was adopted for the preparation of Sb_2Te_3 hexagonal single-crystalline nanoplates using $Na(SbO)C_4H_4O_6$, Te powder, and NaOH in EG at 280 W for 45 min.[611] A mixture of Bi_2Te_3 nanorods and nanoflakes was prepared using $Bi(NO_3)_2·5H_2O$, Te powder, and KOH in EG or glycerol via the microwave-assisted polyol method.[612] $Cu_{(2-x)}Te$ single-crystalline nanowires were prepared employing Te nanotubes as the reactive and self-sacrificial template in EG by a microwave-assisted solvothermal process at 200 °C for 1 h.[614] Grisaru et al.[610] prepared nanoparticles of $CuInTe_2$ (∼100 nm) and $CuInSe_2$ (∼85 nm) by the microwave-assisted polyol method. For the preparation of $CuInSe_2$, CuCl, In, and Se were used as the reactants, and triethylene glycol was used as the solvent. For the preparation of $CuInTe_2$, the preparation procedure was similar to that of $CuInSe_2$, and Te was used instead of Se, and tetraethylene glycol was used as the solvent.

3.4. Other Compounds

A small number of nanostructures of other compounds have also been prepared by the microwave-assisted polyol method, and some examples include fluoride,[615−617] bromide,[618,619] hydroxide,[620] sulfate,[621] carbonate,[392,622,623] phosphate,[616,624] silicate,[625] molybdenate,[626] and tungstate.[627]

Polyethylenimine (PEI)-doped LaF_3 nanoparticles were synthesized using corresponding metal nitrates (or chlorides) and NaF in EG via the microwave-assisted polyol method at 120 or 150 °C for 30 min. The as-prepared nanoparticles had a hexagonal structure with an average size of about 12 nm. When doped with different ions (Ce^{3+}/Tb^{3+} or Eu^{3+}), the morphology and structure of the nanoparticles did not change, whereas the optical properties varied with doped ions and their molar ratio, and as a result emissions of four different colors (green, yellow, orange, and red) were achieved by simply changing the types of doping ions (Eu^{3+} and Tb^{3+}) and the molar ratio of the two doping ions.[615] The combination of the rapid microwave heating and the microfluidic reactor is advantageous for continuous production of nanostructured materials with high yields. Zhu et al.[616] utilized a microfluidic reactor heated by microwaves to prepare LaF_3:Ce,Tb nanoparticles with a mean diameter of 4.5 nm and $LaPO_4$:Ce,Tb nanorods with diameters of 10−15 nm and lengths of 60−70 nm using EG as the solvent. BiOBr microspheres formed by self-assembly of nanosheets were obtained using $Bi(NO_3)_3·5H_2O$ and CTAB in the solvent of diethylene glycol via the microwave-assisted solvothermal method at 180 °C for 10 min.[618] Flower-like BiOBr nanostructures were prepared using $Bi(NO_3)_3·5H_2O$ and CTAB in mannitol through a microwave-assisted process at 110 °C for 27 min. CTAB acted as both the bromide source and the soft template. Different flower-like BiOBr nanostructures could be obtained by varying the CTAB concentration. The as-prepared flower-like BiOBr nanostructures exhibited a high removal capacity and fast adsorption rate for Cr^{6+} ions in a wide pH range.[619]

Li et al.[621] prepared $CaSO_4·0.5H_2O$ single-crystalline nanowires by thermal transformation of calcium dodecyl sulfate in EG or *N*,*N*-dimethylformamide (DMF) at 100 °C for 15 min. Two samples were prepared both in EG solution at 100 °C with different heating methods. When microwave heating was used, it took only 15 min for the formation of $CaSO_4·0.5H_2O$ nanowires. In comparison, much longer time (60 h) was needed for the formation of $CaSO_4·0.5H_2O$ nanowires using oil bath heating. These results indicate that the microwave heating could remarkably shorten the reaction time as compared to the conventional heating method. It was found that different types of organic solvents (EG or DMF) had no obvious influences on the crystal phase, morphology, and formation time of the product.

Tipcompor et al.[622] synthesized $SrCO_3$ and $BaCO_3$ nanoparticles using $Sr(NO_3)_2$ or $Ba(NO_3)_2$ and Na_2CO_3 in EG under cyclic microwave irradiation at 20% of 180 W for 20 min; the as-prepared orthorhombic $SrCO_3$ and $BaCO_3$ nanoparticles had particle sizes of 20−50 and 40−100 nm, respectively. Ma et al.[392] synthesized $SrCO_3$ with an olive-like morphology using $Sr(NO_3)_2$ and $(NH_4)_2CO_3$ in EG by a microwave-assisted process at 90 °C for 5 min. They also prepared $BaCO_3$ nanorods using $Ba(NO_3)_2$ and $(NH_4)_2CO_3$ in the presence of NaOH or HMTA in EG by the microwave-assisted method at 90 °C. The microwave heating time and type of alkali played important roles in the size and morphology of $BaCO_3$. $BaCO_3$ nanorods assembled from nanoparticles were obtained in the presence of a strong alkali NaOH in EG by microwave heating at 90 °C for 40 min; however, $BaCO_3$ nanorods with a hexagonal cross section formed in the presence of a weak alkalescent additive.[623]

Muraliganth et al.[625] reported the microwave-polyol synthesis of Li_2FeSiO_4 and Li_2MnSiO_4 nanoparticles using tetraethyl orthosilicate, LiOH, and $Fe(CH_3COO)_2$ or $Mn(CH_3COO)_2$ or $Mn(CH_3COO)_2·4H_2O$ in tetraethylene glycol at 300 °C for 5 min. Phuruangrat et al.[626] synthesized $CdMoO_4$ nanoparticles with sizes of 14−20 nm using $Cd(NO_3)_2·4H_2O$ and $Na_2MoO_4·2H_2O$ in propylene glycol by microwave heating at 20% microwave power of 180−600 W for 20−60 min;

dx.doi.org/10.1021/cr400366s | *Chem. Rev.* 2014, 114, 6462−6555

however, the product consisted of aggregated $CdMoO_4$ nanopartcles. $CaWO_4$ nanoparticles with an average particle size of 12 nm were synthesized using $Ca(NO_3)_2$ and Na_2WO_4 in EG via microwave irradiation.[627]

3.5. Nanocomposites

Microwave-based methods have been employed to synthesize inorganic nanostructures on various substrates. The effects of microwaves on heterogeneous systems have also been investigated both experimentally and theoretically. The proposed mechanism is the rapid heating of the high dielectric loss solvent leading to the formation of nanostructures on the substrate. However, the exact reason why the nanostructures form on the substrate and not homogeneously in the solution phase has not been fully understood. Anumol et al.[628] proposed a formation mechanism for metal nanoparticles on substrates. They discussed the thermodynamic and kinetic aspects of reduction of metal salts by EG under microwave heating conditions. They discussed the temperatures above which the reduction of the metal salt is thermodynamically favorable and temperatures above which the rates of homogeneous nucleation of the metal and the heterogeneous nucleation of the metal on supports are favored. They investigated different conditions that favor the heterogeneous nucleation of the metal on the supports over homogeneous nucleation in the solvent based on the dielectric loss parameters of the solvent and the support and the metal/solvent and metal/support interfacial energies. They showed that metal particles can be selectively formed on the substrate even under situations where the temperature of the substrate is lower than that of the surrounding medium.

Many kinds of nanocomposites have been prepared by the microwave-assisted polyol method, including Au/Ag,[629−631] Ag/Ni,[632] Pt/C,[633−640] Pt/graphene,[641,642] Pt/carbon nanotubes,[643−645] Pd/carbon nanotubes,[646] Ni/carbon nanotubes,[647,648] PtPd/C,[649] PtSn/C,[650] PtRu/C,[638,651] PtAuSn/C,[652] PtRuIr/C,[653] $Pt_{75}Co_{25}$/C,[654] $Pt_{70}Pd_{20}Co_{10}$/C,[654] $Pt_{50}Pd_{30}Co_{20}$/C,[654] PtRuNi/C,[655] PtRu/carbon nanotubes,[656,657] PtSn/carbon nanotubes,[658,659] PtFe/carbon nanotubes,[660] PtZn/carbon nanotubes,[661] CoNi/carbon nanotubes,[662] SnO_2/C,[663] MnO/C,[664] Fe_3O_4/graphene,[665] Fe_3O_4/carbon nanotubes,[666] Bi_2Te_3/carbon nanotubes,[667] Ru/MgO/carbon nanotubes,[668] Pt−S-SnO_2/carbon nanotubes,[669] Ru/γ-Al_2O_3,[670] Ag/TiO_2,[671] Bi/Bi_2O_3,[672] Ag/SiO_2,[673] C/ZnO,[674] C/MnO,[675] AgCl/Ag,[676] Sb-doped PbTe/Ag_2Te,[677] Ag/polycarbazole,[678] metal (Pt, Ag or Cu)/polyacrylamide,[470] metal (Pd or Ag)/polyacrylonitrile,[679] Fe_3O_4/polyacid,[680] Fe_3O_4/polypyrrole,[557] and metal sulfide (Ag_2S, Cu_2S, or HgS)/polyacrylamide.[471]

Tsuji et al.[629] investigated the role of Cl^- ions in the formation of Au/Ag core−shell nanostructures through a two-step microwave-polyol process in the solvent of EG. In the absence of Cl^- ions, the major product consisted of spherical Ag nanoparticles, and few Au/Ag nanoparticles could be produced. However, higher Cl^- ion concentration led to the formation of a significant amount of AgCl. A small amount of Cl^- anions (~0.3 mM) was found to be a key factor for the preferential formation of Au/Ag core−shell nanostructures with well-defined shapes. The role of Cl^- anions was discussed in terms of shape-selective oxidative etching of spherical Ag nanoparticles and the formation of AgCl, leading to slow face-selective crystal growth by decreasing the concentration of free Ag^+ ions. They also prepared shape-dependent Au/Ag core−shell nanostructures by using a two-step method. First, Au nanocrystal seeds with various shapes including single-crystal octahedron, single-twinned triangle or hexagon plate, and multiple-twinned decahedron were prepared by reducing $HAuCl_4$ in EG in the presence of PVP by microwave heating. Subsequently, Au seeds were added into DMF solution containing $AgNO_3$ for the growth of Ag shells by oil bath heating. The shape of Ag shells strongly depended on the shape of initiated Au seeds. These newly produced triangular or hexagonal platelike, octahedral, and multiple-twinned decahedral Au/Ag nanostructures were mainly dominated by Ag shells having the (111) facet. These studies indicate that it is possible to controll the core−shell nanostructures with desirable crystal planes by using the same seeds in the appropriate solvent.[630] They also prepared octahedral and decahedral Au/Ag core−shell nanocrystals in high yields using a two-step reduction method. In the first step, octahedral or decahedral Au core seeds were prepared by reducing $HAuCl_4{\cdot}4H_2O$ in tetraethylene glycol by microwave heating or in diethylene glycol by oil bath heating, respectively, in the presence of PVP. In the second step, Ag shells were grown on Au seeds in DMF in the presence of PVP by oil bath for 3 h or microwave heating for 10 min. Octahedral or decahedral Au/Ag nanocrystals nearly fully covered by uniform Ag shells were prepared by oil bath heating. In contrast, decahedral Au/Ag core−shell particles formed through stepwise growth of tetrahedral units after covering decahedral Au cores with thin Ag shells by fast microwave heating.[631]

Tsuji et al.[632] prepared Ag core/Ni shell nanoparticles in high yield by reduction of a mixture of $AgNO_3$ and $NiSO_4{\cdot}6H_2O$ or $NiCl_2{\cdot}6H_2O$ or $Ni(NO_3)_2{\cdot}6H_2O$ in EG in the presence of NaOH and PVP by microwave heating at 400 W for 10 min. Nanoparticles with average sizes of 36 ± 6, 22 ± 3, and 33 ± 4 nm were obtained from $NiSO_4{\cdot}6H_2O$, $NiCl_2{\cdot}6H_2O$, and $Ni(NO_3)_2{\cdot}6H_2O$, respectively. The Ag/Ni core−shell nanostructures were confirmed by the contrast of TEM−energy dispersed X-ray spectroscopy (EDS) measurements in Figure 18. The distributions of Ag and Ni components along the cross-section line of a typical nanoparticle shown in Figure 18c and similar line analysis indicated that Ni shells with different thicknesses were grown on spherical Ag cores. The

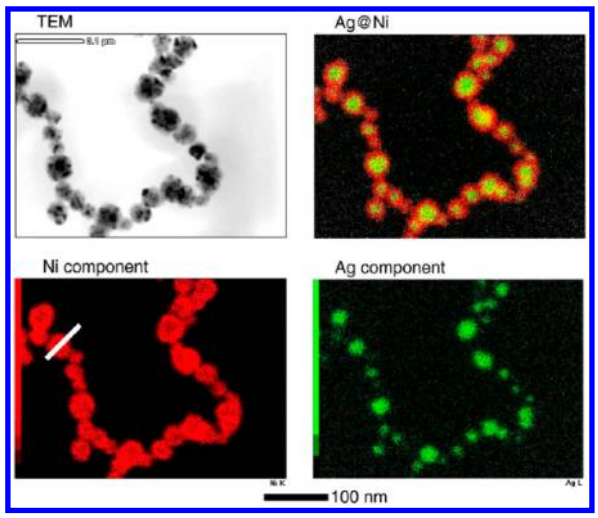

Figure 18. TEM image and EDS data of Ag core/Ni shell nanoparticles obtained from a mixture of $AgNO_3$ and $Ni(NO_3)_2{\cdot}6H_2O$ by microwave heating. Reprinted with permission from ref 632. Copyright 2010 Elsevier B.V.

dx.doi.org/10.1021/cr400366s | Chem. Rev. 2014, 114, 6462−6555

structure and Ag/Ni atomic ratio of the product were essentially independent of the nickel salt. Although Ag/Ni nanoparticles could be prepared by the oil bath heating, it took at least 40 min, and the average size of Ag/Ni nanoparticles and thicknesses of Ni shells were 57 ± 17 and 17 ± 2.3 nm, respectively, which were larger than those obtained by microwave heating. These results indicate that smaller nanoparticles with a narrower size distribution can be prepared in a shorter time under microwave irradiation as compared to those obtained by the conventional heating. The growth mechanism of Ag/Ni nanoparticles was also proposed.

Song et al.[634] prepared Pt/C nanocomposites with various Pt contents using H_2PtCl_6 and NaOH in EG (pH > 10) in the presence of commercial carbon black by the pulsed microwave-assisted polyol method. Pt nanoparticles were highly dispersed on the carbon support and had a narrow particle size distribution with a mean particle size of ~2.7 nm. Hu et al.[635] prepared Pt/C and Pt−Ir/C nanocomposites with different atomic ratios using commercial carbon black, $H_2PtCl_6{\cdot}6H_2O$, and $H_2IrCl_6{\cdot}6H_2O$ in EG in a closed vessel by a microwave-assisted polyol process at 190 °C for 30 min. The average Pt−Ir particle size only changed slightly, and the crystalline structure gradually became more amorphous with increasing Ir content. The particle size could be controlled by altering the pH value of solution and microwave heating rate. As compared to the microwave-polyol process in an open vessel, the microwave heating process in a closed vessel could attain a very fast heating rate, resulting in highly dispersed Pt/C and Pt−Ir/C nanoparticles. Highly dispersed Pt nanoparticles on mesoporous carbon nanofibers were prepared using H_2PtCl_6, NaOH, and preformed ordered mesoporous carbon nanofibers or ordered mesoporous carbon as the support in EG by the microwave-polyol method.[636,637] Guo et al.[639] prepared the Pt/carbon aerogel nanocomposite using $H_2PtCl_6{\cdot}6H_2O$ and KOH in the presence of carbon aerogel powder in EG by a microwave-assisted polyol process at 800 W for 3 min. Spherical Pt nanoparticles with a mean size of 2.7 nm were well dispersed on the carbon aerogel. The Pt/carbon aerogel catalyst showed higher electrochemical catalytic activity for methanol oxidation than that of a commercial Pt/C catalyst with the same Pt loading. Lebègue et al.[640] reported the microwave-polyol preparation of the Pt/C nanocomposite using $H_2PtCl_6{\cdot}6H_2O$ (pH value was adjusted to 11 by using 1 M NaOH solution) in EG. Pt/C nanocomposite prepared by the pulsed microwave polyol method displayed higher active surface areas and better kinetic parameters toward oxygen reduction reaction than those of a Pt/C catalyst prepared by the conventional polyol refluxing. The Pt/C nanocomposite synthesized by pulsed microwave heating had a mean particle size of ~2.5 nm against ~3.0 nm for that prepared by the conventional heating. Sarkar et al.[654] prepared carbon-supported $Pt_{75}Co_{25}$, $Pt_{70}Pd_{20}Co_{10}$, and $Pt_{50}Pd_{30}Co_{20}$ alloy nanoparticles with 20 wt % metal loading using $H_2PtCl_6{\cdot}6H_2O$, $(NH_4)_2PdCl_4$, $CoCl_2{\cdot}6H_2O$, and NaOH in tetraethylene glycol in the presence of carbon black by a microwave-assisted solvothermal process at 300 °C for 15 min.

Xu et al.[643] prepared the nanocomposite of Pt nanoparticles (15 ± 3 nm) dispersed on carbon nanotubes using $H_2PtCl_6{\cdot}6H_2O$, KOH, and commercial carbon nanotubes in EG under microwave irradiation at 800 W for 1 min. Sakthivel et al.[644] deposited Pt nanoparticles on multiwalled carbon nanotubes with a high loading using H_2PtCl_6, NaOH, a zwitterionic surfactant (3-(*N*,*N*-dimethyldodecylammonio) propanesulfonate), and multiwalled carbon nanotubes in EG by the microwave-assisted polyol method. The heating time and temperature were found to be the key factors for depositing Pt nanoparticles homogeneously on carbon nanotubes, and the smallest average particle diameter of 1.8 nm was obtained through microwave heating to 140 °C for 50 s. Pt nanoparticles with sizes less than 7 nm deposited on preformed carbon nanotubes were prepared using H_2PtCl_6 in EG in the presence of SDS by a microwave-polyol process at 150 °C for 20 min.[645] Hsieh et al.[646] deposited Pd nanoparticles on multiwalled carbon nanotubes by microwave heating an EG solution of $PdCl_2$ and KOH with a household microwave oven at a microwave power of 720 W for 3 min. Ni nanoparticles supported on carbon nanotubes were prepared using $NiCl_2$, NaOH, Na_2CO_3, $N_2H_4{\cdot}H_2O$, and preformed carbon nanotubes in EG by microwave heating for 1 min.[648] The microwave-assisted polyol method was adopted for the preparation of the Ru/MgO/carbon nanotube nanocomposite using $RuCl_3{\cdot}nH_2O$ (n = 1−3) and preformed MgO and carbon nanotubes in EG under microwave irradiation for 1 min, and Ru nanoparticles with sizes of 1.3−2.0 nm were uniformly dispersed on MgO and carbon nanotubes.[668]

The metal/metal oxide nanocomposites have also been prepared by the microwave-assisted polyol method. Okal et al.[670] prepared the Ru/γ-Al_2O_3 nanocomposite containing 1.1% Ru nanoparticles by reduction of $RuCl_3$ in EG using the microwave-assisted solvothermal method at 200 °C for 20 min. The microwave-assisted polyol synthesis of the Ag/TiO_2 nanocomposite was also reported.[671] Bi/Bi_2O_3 composite microspheres were synthesized via a microwave-assisted solvothermal route for 2.5 min, in which $BiCl_3$ was used as the bismuth source, glucose as a reductant, and EG as the solvent.[672]

The microwave-assisted polyol method has also been adopted for the rapid synthesis of nanocomposites containing metal alloy nanostructures. Wang et al.[656] prepared the nanocomposite of Pt−Ru nanoparticles/multiwalled carbon nanotubes using H_2PtCl_6, $RuCl_3$, and preformed 1-aminopyrene-functionalized multiwalled carbon nanotubes in EG by the microwave-polyol method for 2 min. Polyoxometallate-stabilized Pt−Ru alloy nanoparticles supported on multiwalled carbon nanotubes were synthesized by microwave heating an EG solution of $H_3PMo_{12}O_{40}$, $H_2PtCl_6{\cdot}6H_2O$, $RuCl_3{\cdot}xH_2O$, and KOH in the presence of multiwalled carbon nanotubes.[657] The microwave-assisted polyol method was also applied to the preparation of Pt−Sn alloy nanoparticles immobilized on carbon nanotubes and nitrogen-doped carbon nanotubes.[658,659] The nanocomposite of Pt−Fe nanoparticles/carbon nanotubes was prepared by the microwave-polyol method. By adjusting the experimental parameters, the ratio of Fe/Pt and the attached density of PtFe nanoparticles on the surface of carbon nanotubes could be varied.[660] Hsieh et al.[661] prepared Pt−Zn nanoparticles with sizes of ~3−5 nm dispersed on carbon nanotubes by the microwave-assisted polyol method. The reaction system was composed of $PtCl_4$, $Zn(NO_3)_2$, KOH, and EG in the presence of preformed carbon nanotubes, which was heated for a total time of 6 min in a household microwave oven with a power of 720 W. Wu et al.[662] prepared Co−Ni alloy nanoparticles with average diameters in the range of 15−48 nm deposited on the preformed multiwalled carbon nanotubes by the microwave-assisted method at 600 W for 2 min, and $Co(CH_3COO)_2{\cdot}4H_2O$, $Ni(CH_3COO)_2{\cdot}4H_2O$, a small

dx.doi.org/10.1021/cr400366s | Chem. Rev. 2014, 114, 6462−6555

amounts of NaOH and hydrazine hydrate were used as the reactants in EG.

The microwave-assisted polyol synthesis of nanocomposites containing metal oxide and carbon has also been reported. Chen et al.[666] prepared the nanocomposite of Fe_3O_4 nanoparticles (3−5 nm)/multiwalled carbon nanotubes by in situ decomposition of iron(III) acetylacetonate in polyol under microwave irradiation at 200 °C for 15 min. The resulting nanocomposite showed a superparamagnetic property at room temperature and was stable in aqueous dispersion for 2 months. Sulfated SnO_2 modified multiwalled carbon nanotube nanocomposite as the support for Pt nanoparticles (Pt−S−SnO_2/carbon nanotubes) was synthesized by a combination of the sol−gel and pulsed microwave polyol method.[669] Guo et al.[674] reported the deposition of carbon on the surface of ZnO nanorods by the microwave-assisted polyol method. The surface of the preformed ZnO nanorods was first modified by amino groups and then grafted by glucose, and finally irradiated by microwaves to induce the transformation of glucose into carbon in glycerol at 100 °C for 30 min. Courtel et al.[663] prepared SnO_2 nanoparticles (5−10 nm)/carbon nanocomposites using $SnCl_2{\cdot}2H_2O$ in the presence of a carbon matrix in the solvent of EG by the microwave-assisted polyol refluxing at 190−195 °C for 1 h. They also investigated the effect of the heating method and found that the use of microwaves was beneficial for not only shortening the reaction time but also producing smaller SnO_2 nanoparticles that were also better dispersed within the carbon matrix.

As compared to the preparation of the nanocomposites containing metal or metal oxide nanoparticles, the synthesis of the nanocomposites composed of nanostructured metal telluride is much more difficult and complex, and the related work has been less reported in the literature. Dong et al.[677] reported the microwave-assisted solvothermal preparation of Sb-doped PbTe/Ag_2Te core−shell composite nanocubes with the core of well-crystallized cubic Sb-doped PbTe and the shell of amorphous Ag_2Te. In this method, $SbCl_3$, $AgNO_3$, $Pb(CH_3COO)_2{\cdot}3H_2O$, Na_2TeO_3, NaOH, and $NaBH_4$ were used as the reactants, and EG was used as the solvent by microwave heating at 250 °C for 20 min. The TEM micrographs of Sb-doped PbTe/Ag_2Te core−shell composite nanocubes are shown in Figure 19. The product consisted of nanocubes with edge lengths of 25−55 nm, and the nanocube was composed of a well-crystallized inner nanocube as a core with edge lengths of 20−50 nm and an amorphous outer shell with thicknesses of 3−6 nm. The selected-area electron diffraction (SAED) pattern taken from the central site of a single nanocube revealed that the core of the nanocube was a well-crystallized single crystal, and the diffraction spots (Figure 19c) could be assigned to the Sb-doped PbTe crystal with a cubic structure. The high-resolution TEM image in Figure 19d provides further insight into the detail of the core/shell nanocube, which shows that the core was highly crystalline with a *d*-spacing of lattice fringes of 0.3220 nm; this value is in agreement with the calculated *d*(200) value of the cubic Sb-doped PbTe. The reaction mechanism of Sb-doped PbTe/Ag_2Te core/shell composite nanocubes was proposed.[677]

The control over the particle size, size distribution, and dispersity is very important for the synthesis and application of high-performance inorganic/organic nanocomposites. It is desirable to develop simple, fast, and low-cost methods for the synthesis of inorganic/organic nanocomposites. Zhu et al.[470] have developed a novel single-step microwave-assisted

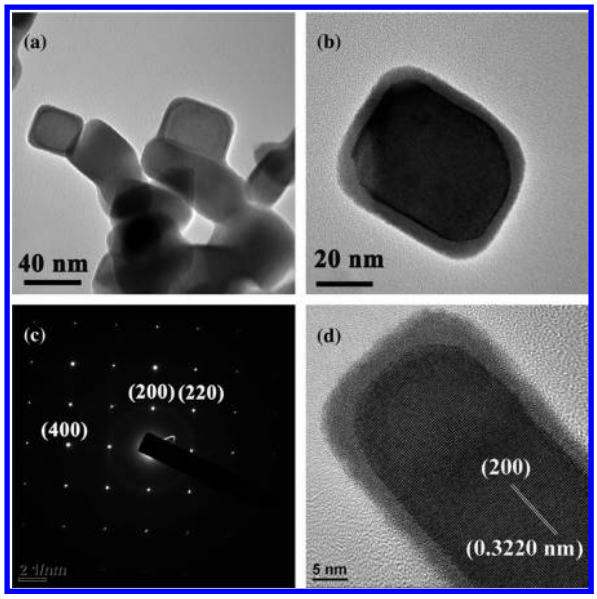

Figure 19. Characterization of Sb-doped PbTe/Ag_2Te core/shell composite nanocubes prepared by the microwave-assisted polyol solvothermal method at 250 °C for 20 min. (a and b) TEM micrographs; (c) SAED pattern taken from the core of a single nanocube; and (d) HRTEM image of a single nanocube. Reprinted with permission from ref 677. Copyright 2012 Elsevier B.V.

polyol method for the rapid synthesis of inorganic/organic nanocomposites. They prepared polyacrylamide (PAM)/metal (M = Pt, Ag, Cu) nanocomposites with metal nanoparticles homogeneously dispersed in the polymer matrix using the corresponding metal salt and acrylamide monomer in EG by the rapid microwave-assisted polyol method. This method is based on the single-step simultaneous formation of metal nanoparticles and polymerization of acrylamide monomer in solution, leading to the homogeneous distribution of metal nanoparticles in the polyacrylamide matrix. EG acts as a solvent, reducing reagent, and microwave absorber; thus no additional reductant is needed. Another advantage of this method is that no initiator for acrylamide polymerization and no surfactant for stabilization of metal nanoparticles are necessary. This makes it possible to avoid subsequent complicated work-up procedures for removal of the additives, leading to rapidity, simplicity, and low-cost for the preparation of polymer/metal nanocomposites. The diameters of Ag nanoparticles in the PAM/Ag nanocomposite were in the range of 6−18 nm with an average diameter of 11.3 ± 1.9 nm prepared by microwave heating an EG solution containing 0.01 M $AgNO_3$ and 3 M acrylamide at 125 °C for 15 min. As compared to pure PAM, the thermal stability of the PAM/Ag nanocomposite was improved. This novel single-step microwave-assisted polyol method can be extended to synthesize other inorganic/organic nanocomposites.

Zhu et al.[471] synthesized polyacrylamide/metal sulfide (Ag_2S, Cu_2S, HgS) nanocomposites with metal sulfide nanoparticles homogeneously dispersed in the polyacrylamide matrix using corresponding metal salt, S powder, and acrylamide monomer in EG by microwave heating at 125 or 190 °C for 15−60 min. This method is based on the simultaneous formation of metal sulfide nanoparticles and polymerization of the acrylamide in the same reaction system, leading to a homogeneous distribution of metal sulfide nanoparticles in the polyacrylamide matrix without aggregation. EG acts simultaneously as a

dx.doi.org/10.1021/cr400366s | *Chem. Rev.* 2014, 114, 6462−6555

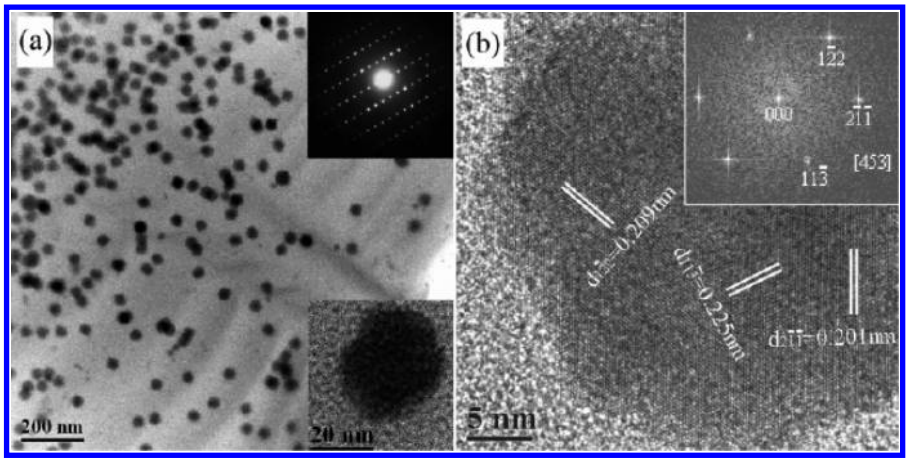

Figure 20. (a) TEM micrograph of the PAM/Ag_2S nanocomposite prepared by microwave heating an EG (50 mL) solution containing 2 mmol of $AgNO_3$, 2 mmol of S, and 0.15 mol of acrylamide at 125 °C for 15 min, the SAED pattern of an individual Ag_2S nanoparticle (upper inset), and magnified TEM micrograph of an individual nanoparticle (lower inset); (b) HRTEM image of the edge of an individual Ag_2S nanoparticle (inset: fast Fourier transform (FFT) pattern of the image). Reprinted with permission from ref 471. Copyright 2007 American Chemical Society.

solvent, microwave absorber, and reductant; thus no additional reductant is needed. Another advantage of this method is that no initiator for acrylamide polymerization and no surfactant for the stabilization of metal sulfide nanoparticles are necessary. Figure 20a shows the TEM micrograph of the PAM/Ag_2S nanocomposite prepared by the rapid microwave-assisted polyol method, from which one can see that spherical Ag_2S nanocrystals were homogeneously dispersed in the PAM matrix. The insets of Figure 20a and b show that each Ag_2S nanocrystal was single-crystalline in structure. The diameters of Ag_2S nanocrystals were in the range of 36−54 nm, and the average diameter of Ag_2S nanocrystals was 43.8 ± 1.7 nm. The PAM/Ag_2S nanocomposite with larger Ag_2S average size and broader size distribution was obtained by microwave heating at 125 °C for a longer reaction time (1 h) or at a higher temperature (190 °C) for 15 min. As compared to pure polyacrylamide, the thermal stability of Ag_2S/polyacrylamide and Cu_2S/polyacrylamide nanocomposites was improved.[471]

4. MICROWAVE-ASSISTED PREPARATION OF NANOSTRUCTURES USING IONIC LIQUIDS

4.1. Ionic Liquids and Microwave Heating Effects

Solvents are very important for microwave-assisted synthesis. The most commonly used solvents for chemical reactions and materials synthesis are water and organic solvents. Water is widely available, cheap, nonflammable, nontoxic, and environmentally benign. However, the liquid state temperature range of water is narrow (0−100 °C), and many organic compounds have low solubilities in water. These disadvantages limit the applications of water as a solvent for materials synthesis. Organic solvents have rich diversity in category and properties; however, many organic solvents have low boiling points and high vapor pressures, and the solubilities of inorganic reactants in organic solvents are usually low. Some organic solvents are highly toxic, flammable, and even explosive. In particular, the high vapor pressure and toxicity of some volatile organic solvents may cause significant environmental problems.[681]

The term "ionic liquid" is used loosely to describe organic salts that melt below about 100 °C and have an wide liquid temperature range. Ionic liquids define a class of fluids rather than a small group of individual examples. Ionic liquids have many applications, such as green solvents and electrically conducting fluids (electrolytes) and uses in electric battery. The most commonly studied systems contain ammonium, phosphonium, pyridinium, or imidazolium cations, with varying heteroatom functionality. Common anions that yield ionic liquids include hexafluorophosphate $[PF_6]^-$, tetrafluoroborate $[BF_4]^-$, and chloride CI^-. Ionic liquids are a new family of environmentally friendly solvents in terms of immeasurable vapor pressure, which are promising for green chemical reactions and materials synthesis. The detailed discussion on the properties and applications of ionic liquids has been provided in a book entitled "Ionic Liquids as Green Solvents".[682] The example of the industrial application of ionic liquids has been reported, and others may not be far behind.[683]

The chemical structures of some typical ionic liquids used in the microwave-assisted preparation of inorganic nanostructures are as follows:

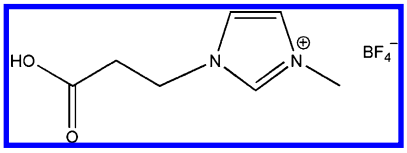

1-methyl-3-(3-carboxyethyl)-imidazolium tetrafluoroborate $[EmimCO_2H][BF_4]$

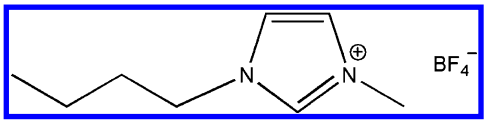

1-*n*-butyl-3-methylimidazolium tetrafluoroborate [BMIM]-$[BF_4]$

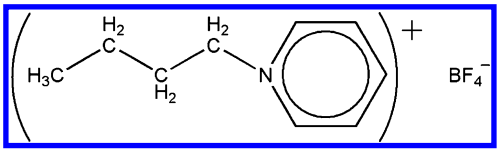

N-butylpyridinium tetrafluoroborate

In recent years, ionic liquids have been paid much attention as the novel green media for the synthesis of inorganic materials.[681,684,685] The importance of ionic liquids in the field of inorganic materials synthesis has been realized in terms of

dx.doi.org/10.1021/cr400366s | *Chem. Rev.* 2014, 114, 6462−6555

their excellent properties such as high thermal stability, immeasurable vapor pressure, wide temperature range for liquid state, low interfacial tension, and high ionic conductivity, while these properties are dependent on their structures and combination of ionic components. Ionic liquids are highly susceptible to microwave irradiation because of their ionic character and high polarizability; thus, they are excellent microwave adsorbers.

The combination of microwave heating and ionic liquids provides superior benefits for the rapid synthesis of materials over the conventional heating methods, especially in terms of rapidness and energy saving. With the help of ionic liquids, the microwave-assisted rapid synthesis of nanostructured materials can be realized even in the nonpolar solvent, which does not adsorb microwaves. Leadbeater et al.[57] investigated the use of an ionic liquid as an aid for microwave heating of nonpolar solvents. They found that the addition of a small quantity of an ionic liquid to a nonpolar solvent greatly increased the rate and yield of chemical reactions. By adding a small amount of 1,3-dialkylimidazolium iodide in hexane, the temperature reached 217 °C after microwave heating at 200 W for 10 s; in comparison, the temperature was only 46 °C after microwave heating at 200 W for 10 s in the absence of the ionic liquid.

In 2004, Zhu et al.[685] have reported their pioneering work on the microwave-assisted ionic liquid (MAIL) method for the rapid controlled preparation of Te nanorods and nanowires by combining the advantages of both the ionic liquid and microwave heating. The TEM characterization of the typical samples is shown in Figure 21. Figure 21a and b shows TEM

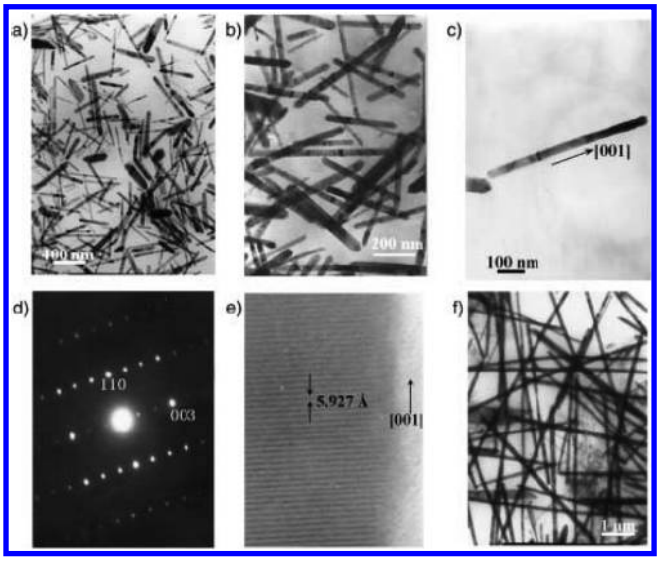

Figure 21. TEM micrographs of two typical samples prepared by the microwave-assisted ionic liquid method. (a)–(c) Te nanorods; (d) electron diffraction pattern of a single Te nanorod; (e) HRTEM image of a single Te nanorod; and (f) Te nanowires. Reprinted with permission from ref 685. Copyright 2004 Wiley-VCH.

micrographs of the as-prepared Te nanorods with diameters mostly ranging from ~15 to ~40 nm, and with aspect ratios of most nanorods in the range from 10 to 20. Figure 21c shows a single Te nanorod with a diameter of 32 nm and a length of 610 nm; its corresponding electron diffraction pattern is shown in Figure 21d. Electron diffraction patterns on different nanorods or different positions of a given single nanorod were essentially the same, indicating that the nanorod was single-crystalline in structure. Figure 21e shows the HRTEM micrograph of the same single nanorod, which shows that the nanorod was structurally single-crystalline with the periodic fringe spacing of 0.5927 nm along the longitudinal axis of the nanorod that corresponds to the interplanar spacing between the (001) planes of the hexagonal Te. Te nanorods had the preferential growth direction along the [001] zone axis. By controlling the experimental parameters, exclusive Te nanowires or nanorods could be produced. Figure 21f shows a TEM micrograph of Te nanowires. Most of these nanowires had diameters ranging from 20 to 100 nm with lengths of tens of micrometers. They have demonstrated that the microwave-assisted ionic liquid method is a fast, high-yield, and environmentally friendly route for the production of inorganic nanostructures.

The microwave-assisted ionic liquid method has been proven to be suitable for the rapid synthesis of a variety of elemental and compound nanostructures, including Au,[686−688] Co,[689,690] Mn,[689,690] Cr,[690] Mo,[690] W,[690] Re,[690] Ru,[690] Os,[690] Rh,[690] Ir,[690] Gd_4F_3,[691] Te,[685] C,[692] ZnO,[693−695] Fe_2O_3,[696−698] Fe_3O_4,[698,699] FeOOH,[698] SnO_2,[700] In_2O_3:Sn,[701] CuO,[697,702−705] MnO_2,[706] Mn_3O_4,[697] $3PbO·H_2O$,[697] PbO,[697] TiO_2,[707,708] CeO_2,[709] $ZnFe_2O_4$,[710] $PbCrO_4$,[711] Pb_2CrO_5,[711] MgF_2,[712] CaF_2,[712] SrF_2,[696,712] FeF_2,[696] CoF_2,[696] ZnF_2,[696] REF_3 (RE = La−Lu, Y),[696,713−715] $NaYF_4$,[716] Zn(OH)F,[717−719] β-$Co(OH)_2$,[697] β-$Ni(OH)_2$,[697] $Cd(OH)_2$,[697] $La(OH)_3$,[697] ZnS,[720,721] CdS,[721] Bi_2S_3,[722] Sb_2S_3,[722] Bi_2Se_3,[723] Bi_2Te_3,[724] CdTe,[725] LaPO_4:Ce,Tb,[726,727] $NH_4Fe_2(PO_4)_2OH·2H_2O$,[728] CoC_2O_4,[729] Cu/C,[730] Ni/C,[730] Pt/carbon nanotubes,[731] Rh/carbon nanotubes,[731] Pt−Ru/carbon nanotubes,[732] Ru/graphene,[733] Rh/graphene,[733] and cellulose/calcium silicate.[734]

4.2. Metals, Semimetals, Nonmetals, and Alloys

Much effort has been devoted to the microwave-assisted rapid preparation of a variety of metal nanostructures using an ionic liquid. Redel et al.[686] prepared Au nanoparticles by thermal, photolytic, or microwave-assisted decomposition/reduction under argon from Au(CO)Cl or $KAuCl_4$ in the presence of *n*-butylimidazole dispersed in the ionic liquid $[BMIm]^+[BF_4]^-$, $[BMIm]^+[OTf]^-$, or $[BtMA]^+[NTf_2]^-$ ($[BMIm]^+$ = *n*-butylmethylimidazolium, $[BtMA]^+$ = *n*-butyltrimethylammonium, $[OTf]^-$ = $^-O_3SCF_3$, $[NTf_2]^-$ = $^-N(O_2SCF_3)_2$). Uniform nanoparticles of ~1−2 nm in diameter were produced in $[BMIm]^+[BF_4]^-$ and increased in size with the molecular volume of the ionic liquid anion. Li et al.[735] prepared Au nanosheets using $HAuCl_4$ in an ionic liquid 1-butyl-3-methylimidazolium tetrafluoroborate ([BMIM][BF_4]) by microwave heating, and it was found that the ionic liquid could act as the template for the formation of Au nanosheets. Ren et al.[687] produced Au nanostructures and microstructures such as polyhedral crystals, single-crystalline nanoplates, hollow trapeziform crystals, holey polyhedra, and dendrites using $HAuCl_4·4H_2O$ in a variety of imidazolium- and pyridinium-based ionic liquids as the solvents without the addition of any capping agent or additional reducing agent via microwave heating. The influence of the ionic liquid anions and cations on the topology (size, shape, etc.) of the product was investigated. It was found that the anions of the ionic liquids controlled the topology of the product, whereas the cations of the ionic liquids had less influence. The $HAuCl_4$ concentration, reaction temperature, and heating method were key factors for the topological structures of the product. The thickness of single-crystalline nanoplates could be adjusted from 16 to 320 nm by varying the

dx.doi.org/10.1021/cr400366s | *Chem. Rev.* 2014, 114, 6462−6555

$HAuCl_4$ concentration and reaction temperature. Octahedral Au nanocrystals were also fabricated in an alcohol ionic liquid by the microwave-assisted ionic liquid method in the absence of any extra capping agent. This method is based on a chemical reaction of $HAuCl_4{\cdot}4H_2O$ in 1-(3-hydroxylpropyl)-3-methylimidazolium tetrafluoroborate ($[C_3OHmim][BF_4]$). Upon adjusting the $HAuCl_4{\cdot}4H_2O$ concentration and reaction temperature, Au nanoplates and micrometer-sized particles were obtained.[688]

Marquardt et al.[689] adopted the microwave-assisted ionic liquid method for the preparation of Co and Mn nanoparticles by decomposition of metal carbonyls of $Co_2(CO)_8$ and $Mn_2(CO)_{10}$, respectively, in the functionalized ionic liquid 1-methyl-3-(3-carboxyethyl)-imidazolium tetrafluoroborate $[EmimCO_2H][BF_4]$. The sizes of Co and Mn nanoparticles were 1.6 ± 0.3 and 4.3 ± 1.0 nm, respectively. In comparison, the sizes of Co and Mn nanoparticles produced in the nonfunctionalized ionic liquid $[BMIM][BF_4]$ were larger (5.1 ± 0.9 and 28.6 ± 11.5 nm, respectively). The as-prepared metallic nanoparticles were stable in the absence of capping ligands (surfactants) for more than 6 months, although the particle sizes were slightly changed. Vollmer et al.[690] prepared a variety of transition-metal nanoparticles of Cr, Mo, W, Mn, Re, Ru, Os, Co, Rh, and Ir by a rapid (3 min) and energy saving (10 W) microwave irradiation under argon atmosphere from metal−carbonyl precursors $[M_x(CO)_y]$ in the ionic liquid $[BMIM][BF_4]$. Most of the as-prepared metallic nanoparticles had sizes of ∼0.8−5 nm. The microwave preparation was compared to UV irradiation (1000 W, 15 min) or conventional thermal decomposition (180−250 °C, 6−12 h) of $[M_x(CO)_y]$ in the ionic liquid, and the metallic nanoparticles obtained by the microwave heating had smaller (<5 nm) and more uniform sizes.

Zhu et al.[685] have developed the microwave-assisted ionic liquid method for the rapid synthesis of Te nanorods and nanowires in the ionic liquid of *N*-butylpyridinium tetrafluoroborate. By controlling experimental parameters, exclusively Te nanorods or Te nanowires were obtained. Their experiments showed that both the ionic liquid and microwave heating played important roles in the formation of Te nanorods and nanowires.[685] Safavi et al.[692] prepared carbon nanodots with an average size of ∼6 nm via the microwave-assisted ionic liquid method. In this method, a desired amount of water-immiscible ionic liquid *N*-octylpyridinium hexafluorophosphate was heated in a microwave oven (450 W) for ∼2 min. The ionic liquid acted not only as an excellent medium for absorbing microwaves, but also as a carbon source.

4.3. Metal Oxides

In the microwave-assisted ionic liquid synthesis of metal oxide nanostructures, a metal compound is used as the metal source, an alkaline reagent is usually used to provide an alkaline environment, and an additive or a surfactant is sometimes adopted to control the morphology and size of the product. Nanostructures of metal oxides with various morphologies have been prepared in the presence of an ionic liquid by microwave heating, and some examples will be discussed below.

Wang et al.[693] synthesized ZnO structures with flower-like and needle-like shapes by the simple microwave-assisted approach using an ionic liquid $[BMIM][BF_4]$. Both the ionic liquid and microwave heating played important roles in the formation of different morphologies of ZnO. By controlling experimental conditions, exclusive ZnO needles or flowers could be synthesized at a temperature of 50, 90, or 125 °C in a short period of time (5 or 10 min). Flower-like ZnO nanosheet aggregates were prepared by microwave heating in an ionic liquid of 1-(2-hydroxylethyl)-3-methylimidazolium chloride.[694] Nanoparticle-constructed microspheres, plate-constructed stacks, rod-constructed flower-like structures, and complex ZnO aggregates were synthesized using $Zn(CH_3COO)_2{\cdot}2H_2O$ and an ionic liquid hydrate tetrabutylammonium hydroxide ($N(C_4H_9)_4OH{\cdot}30H_2O$) by microwave heating for 1 min. In this synthesis, the ionic liquid had multifunctions (solvent, absorber of microwaves, reactant, and template).[695]

Wang et al.[702] prepared CuO nanowhiskers using $CuCl_2{\cdot}2H_2O$ and NaOH in the presence of an ionic liquid $[BMIM][BF_4]$ by the rapid microwave-assisted ionic liquid approach at 80 °C. It was found that the ionic liquid $[BMIM][BF_4]$ had a significant influence on the morphology of CuO. CuO nanowhiskers were obtained in the presence of $[BMIM][BF_4]$, while CuO nanosheets were synthesized without using $[BMIM][BF_4]$. CuO nanostructures with leaf-like, chrysanthemum-like, and rod-like shapes were prepared using $Cu(CH_3COO)_2{\cdot}2H_2O$ and NaOH by the microwave-assisted approach using an ionic liquid $[BMIM][BF_4]$. By adjusting the concentration of $[BMIM][BF_4]$ and reaction time, different CuO nanostructures could be obtained in a short period of time.[703] Flower-like and leaf-like CuO nanostructures were synthesized using $CuCl_2{\cdot}2H_2O$ and NaOH in the presence of an ionic liquid of 1-octyl-3-methylimidazolium trifluoroacetate by microwave heating at 80 °C for 10 min. By controlling the concentration of the ionic liquid and reaction temperature, the morphology of CuO nanostructures could be adjusted.[705]

Cao et al.[698] reported the microwave-solvothermal ionic liquid synthesis of a variety of iron oxide nanostructures, such as α-FeOOH hollow microspheres constructed by self-assembly of nanoparticles, β-FeOOH architectures, and α-Fe_2O_3 nanoparticles. It was found that the ionic liquid $[BMIM][BF_4]$ had an influence not only on the crystal phase but also on the morphology of the product. The effects of the experimental parameters on the morphology and crystal phase of the product were studied, and the relationship between the morphology and crystal phase of the product was discussed. The formation mechanism of α-FeOOH hollow microspheres was proposed. A general thermal transformation strategy was designed for the preparation of α-Fe_2O_3 hollow microspheres using α-FeOOH hollow microspheres as the precursor and template, and by autocatalysis of the adsorbed Fe^{2+} ions on the α-FeOOH surface, Fe_3O_4 hollow microspheres were obtained.[698] Li et al.[699] prepared rhombic dodecahedral Fe_3O_4 nanocrystals via a rapid microwave-assisted route in the presence of a hydrophilic ionic liquid *N*-dodecylpyridinium perchlorate $[C_{12}Py]^+[ClO_4]^-$, and the reaction could be completed within 15 min at 90 °C. It was found that a proper amount of ionic liquid played a key role in the formation of rhombic dodecahedral Fe_3O_4 nanocrystals, and the shape of the product could be tuned by adjusting the experimental parameters. Cao et al.[710] reported the microwave-solvothermal ionic liquid synthesis of $ZnFe_2O_4$ nanoparticles using $Zn(CH_3COO)_2{\cdot}2H_2O$, $Fe(NO_3)_3{\cdot}9H_2O$, and $CO(NH_2)_2$ in the presence of an ionic liquid $[BMIM][BF_4]$ at 160 °C for 30 min, and it was found that the ionic liquid $[BMIM][BF_4]$ and microwave heating temperature had significant effects on the crystal phase of the product.

SnO_2 quantum dots with a narrow size distribution (4.27 ± 0.67 nm) were synthesized by microwave-assisted decom-

dx.doi.org/10.1021/cr400366s | Chem. Rev. 2014, 114, 6462−6555

position of tin(IV) *tert*-butoxide ($Sn(OtBu)_4$) in an ionic liquid [BMIM][BF_4] in a 10 mL sealed glass vessel under argon gas atmosphere at 180 °C for 1 min. The aqueous suspension of SnO_2 quantum dots was used for inkjet printing nanobridges between gold electrodes on polycarbonate and on silicon chip as well.[700] Bühler et al.[701] prepared In_2O_3:Sn nanoparticles with an average diameter of 25 ± 3 nm in an ionic liquid $[N(CH_3)(C_4H_9)_3][N(SO_2CF_3)_2]$ by a microwave-assisted route. Yang et al.[706] prepared single-crystalline nanoneedles and nanorods of cryptomelane-type manganese oxide octahedral molecular sieve (OMS-2) by the microwave-assisted ionic liquid approach using [BMIM][BF_4] at a relatively low temperature (90 °C) for a short period of time (10 min). [BMIM][BF_4] acted as a cosolvent, structure-directing agent, and reducing reagent in the reaction system. The multifunctional roles of [BMIM][BF_4] simplify the preparation procedure. On the basis of the redox reaction of $MnCl_2$ and $KMnO_4$ in the presence of [BMIM]BF_4, it was proposed that the formation of OMS-2 nanoneedles followed the rolling mechanism with the lamellae as an intermediate. In contrast, the direct reaction of $KMnO_4$ with [BMIM][BF_4] resulted in the formation of OMS-2 nanorods with diameters as small as 3−6 nm. Wang et al.[711] synthesized $PbCrO_4$ rods and Pb_2CrO_5 with bundle-like and rod-like morphologies adopting reactants of $Pb(CH_3COO)_2·3H_2O$, $K_2Cr_2O_7$, and [BMIM][BF_4], with or without NaOH by the rapid microwave-assisted ionic liquid method. In the presence of NaOH, Pb_2CrO_5 bundles and rods could be synthesized by microwave heating at 90 °C for 10 min. However, single-crystalline $PbCrO_4$ rods could be obtained by microwave heating at 50 °C for 10 min in the absence of NaOH.

4.4. Metal Chalcogenides

The remarkable merit of the microwave-assisted ionic liquid method for the synthesis of nanostructured metal sulfides is its rapidness (usually in minutes) as compared to the conventional heating methods (usually hours or even days), For example, only 10 min was needed for the microwave-assisted ionic liquid synthesis of ZnS or CdS nanoparticles using $Zn(CH_3COO)_2·2H_2O$ or $CdCl_2·2.5H_2O$ and $Na_2S·9H_2O$ in the presence of an ionic liquid [BMIM][BF_4] at 100 °C.[721] Single-crystalline Bi_2S_3 and Sb_2S_3 nanorods were synthesized using the starting reagents of Bi_2O_3 or Sb_2O_3, $Na_2S_2O_3$, HCl, and EG or ethanolamine in the presence of an ionic liquid [BMIM][BF_4] by the microwave-assisted ionic liquid method. It was found that the ionic liquid played an important role in the morphology of M_2S_3 (M = Bi, Sb). Bi_2S_3 nanorods could be prepared in a short period of time (only 30 s) in the presence of [BMIM][BF_4]; however, urchinlike Bi_2S_3 structures consisting of nanorods were obtained without using [BMIM]-[BF_4]. Sb_2S_3 nanorods were obtained in the presence of [BMIM][BF_4]; however, Sb_2S_3 nanosheets were obtained in the absence of [BMIM][BF_4].[722]

Jiang et al.[723] synthesized Bi_2Se_3 nanosheets with thicknesses of 50−100 nm using $Bi(NO_3)_3·5H_2O$, Se powder, HNO_3, ethylenediamine, or EG and an ionic liquid [BMIM][BF_4] by microwave heating. It was found that the ionic liquid [BMIM][BF_4] played an important role in the morphology of Bi_2Se_3. When ethylenediamine was used, both nanoparticles and irregularly shaped nanosheets were obtained without using [BMIM][BF_4], while exclusively irregularly shaped nanosheets formed in the presence of [BMIM][BF_4]. When EG was used, irregularly shaped nanosheets could be obtained in the absence of [BMIM][BF_4], while hexagonally shaped nanosheets were formed in the presence of [BMIM][BF_4].

Ji et al.[724] synthesized Bi_2Te_3 nanosheets via microwave heating a reaction system containing $Bi(NO_3)_3·5H_2O$, Te powder, KOH, EG, and an ionic liquid of 1-butyl-3-methylimidazolium bromide. By increasing the amount of the ionic liquid, a morphology evolution process of Bi_2Te_3 from a mixture of nanorods and nanoplates to hexagonally shaped nanoplates was observed. Hayakawa et al.[725] reported the microwave-assisted ionic liquid synthesis of highly luminescent thiol-capped CdTe nanocrystals with the zinc blende crystal structure using $CdCl_2·2.5H_2O$, H_2Te gas, and 2-(dimethylamino)ethanethiol hydrochloride in the presence of a hydrophobic ionic liquid of 1-methoxymethyl-1-methylpyrrolidinium bis(trifluoromethanesulfonyl)amide at 150 °C for different time periods. The average diameter of CdTe nanocrystals obtained by microwave irradiation at 150 °C for 80 min was 4.1 nm with a standard deviation of 14%.

4.5. Other Nanostructured Materials

Although some methods have been reported for the preparation of metal fluorides with diverse morphologies, either complicated and time-consuming processes or severe experimental conditions are needed in some methods. Furthermore, the fluoride reagents used in some methods are toxic fluorine-containing compounds such as CF_3COOH. Taking the fluorine-containing ionic liquids as examples, the anion $[BF_4]^-$ containing ionic liquids such as [BMIM][BF_4] can decompose thermally and hydrolyze under the microwave heating conditions to release F^- ions. Therefore, the ionic liquids containing the anion of $[BF_4]^-$ can be used as an environment-friendly fluorine source for the rapid microwave-assisted synthesis of nanostructured metal fluorides. On the basis of this strategy, Xu et al.[712] have demonstrated the microwave-assisted ionic liquid solvothermal method for rapid synthesis of CaF_2 double-shelled hollow microspheres using $Ca(NO_3)_2·4H_2O$ and $NaH_2PO_4·2H_2O$ in the presence of an ionic liquid [BMIM][BF_4] as the fluorine source at 120 °C for 10 min. This method is simple, time-saving, and environmentally friendly, and can be extended to prepare hollow microspheres of MgF_2 and SrF_2. MgF_2 hollow microspheres were prepared with a similar procedure using $Mg(NO_3)_2·6H_2O$ by microwave heating at 150 °C for 30 min, and SrF_2 hollow microspheres were prepared with a similar procedure using $Sr(NO_3)_2·4H_2O$ by microwave heating at 120 °C for 10 min. Jacob et al.[696] adopted the microwave-assisted ionic liquid method for the synthesis of metal fluoride nanostructures such as FeF_2, CoF_2, ZnF_2, LaF_3, YF_3, and SrF_2 with different morphologies using an ionic liquid [BMIM][BF_4] in a domestic microwave oven.

Li et al.[713] adopted the microwave-assisted ionic liquid method for the preparation of a series of binary rare earth fluorides REF_3 (RE = La−Lu, Y) nanostructures and microstructures using an ionic liquid [BMIM][BF_4] as a solvent, reactant, and template. Lorbeer et al.[714] prepared EuF_3 nanoparticles using $Eu(CH_3COO)_3·H_2O$, EG, and an ionic liquid by microwave heating with a single mode microwave reactor. Different tetrafluoroborate ionic liquids such as *N*-butyl-*N*-methyl-pyrrolidiniumtetrafluoroborate ([C_4mpyr]-[BF_4]), 1-butylpyridinium tetrafluoroborate ([C_4py][BF_4]), 1-hexylpyridinium tetrafluoroborate ([C_6py][BF_4]), (2-hydroxyethyl)-trimethylammoniumtetrafluoroborate ([choline]-[BF_4]), trihexyltetradecylphosphoniumtetrafluoroborate

dx.doi.org/10.1021/cr400366s | *Chem. Rev.* 2014, 114, 6462−6555

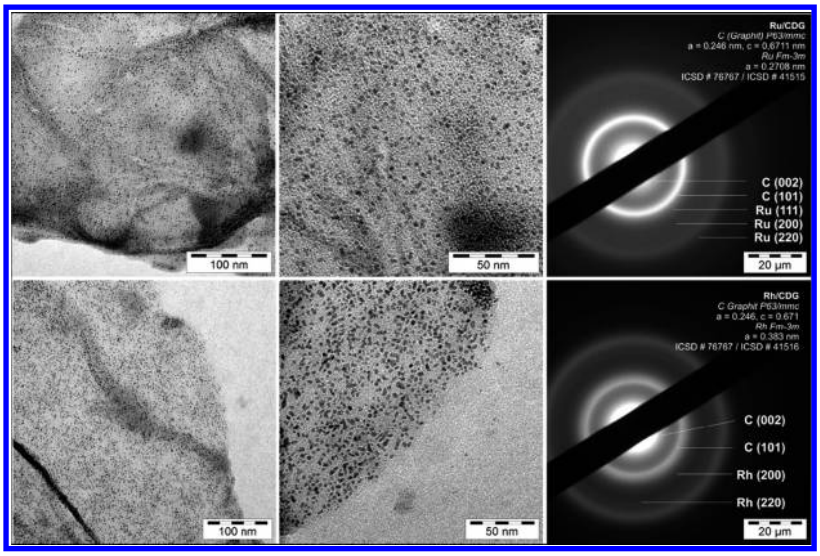

Figure 22. TEM characterization of Ru nanoparticles (top row) and Rh nanoparticles (bottom row) supported on chemically derived graphene surface from microwave-assisted decomposition of $Ru_3(CO)_{12}$ and $Rh_6(CO)_{16}$ in an ionic liquid $[BMIM][BF_4]$. Reprinted with permission from ref 733. Copyright 2010 Elsevier Ltd.

($[P_{66614}][BF_4]$), 1-butyl-3-methylimidazoliumhexafluorophosphate ($[C_4mim][PF_6]$), 1-methyl-3-butylimidazolium chloride $[C_4mim]Cl$, 1-methyl-3-butylimidazolium tetrafluoroborate $[C_4mim][BF_4]$, and tributyltetradecylphosphonium tetrafluoroborate $[P_{44414}][BF_4]$ were used. The experiments indicated a strong influence of the ionic liquid on the structure, morphology, and luminescent properties of the product. The morphology of the product varied from spherical nanoparticles to nanorods forming different types of aggregates, such as bundles, columns, or spherical aggregates. The comparison experiments were also conducted via the conventional ionothermal synthesis by heating the reaction mixture at 120 °C for 20 h in a furnace. The microwave synthesis was shown to be an extremely fast and facile synthesis route, and the reaction time could be as short as 30 s. In contrast, the conventional ionothermal synthesis took at least 2 h for a complete conversion of the starting reactants. In both cases, nanoparticles with sizes smaller than 15 nm were obtained. The size and shape of the as-prepared nanostructures varied in different ionic liquids. They also reported the microwave-assisted ionic liquid method for the synthesis of $GdF_3:Eu^{3+}$ nanoparticles with particle sizes ranging from 2 to 9.5 nm and an average size of ~6 nm using $Ln(CH_3COO)_3{\cdot}xH_2O$ (Ln = Gd, Eu) in the ionic liquid $[C_4mim][BF_4]$. In this method, the ionic liquid acted not only as the solvent but also as a fluoride source.[715]

Chen et al.[716] reported the microwave-assisted ionic liquid synthesis of $NaYF_4$ spheres formed by self-assembly of nanoparticles using an ionic liquid $[BMIM][BF_4]$ at 200 °C for 5 min. The diameters of $NaYF_4$ spheres could be tuned by changing the amounts of the precursors. It was found that the ionic liquid played key roles such as the solvent, absorbent of microwaves, and fluorine source for the formation of $NaYF_4$ spheres. Zn(OH)F nanofibers[717] and Zn(OH)F nanobelts[718] were synthesized under microwave irradiation in the presence of an ionic liquid of 1,2,3-trimethylimidazolium tetrafluoroborate. Zn(OH)F nanostructures with a flower-like morphology were prepared using an ionic liquid $[BMIM][BF_4]$ via a microwave-assisted ionic liquid route at 320 W for 5 min; the flower-like Zn(OH)F had six petals, and every petal was composed of lots of acicular nanostructures.[719] Pang et al.[697] used the structurally similar ionic liquid precursors tetrabutylammonium hydroxide and tetraethylammonium hydroxide for the synthesis of nanostructures of metal hydroxides including β-$Co(OH)_2$, β-$Ni(OH)_2$, $Cd(OH)_2$, and $La(OH)_3$ by microwave heating for 1 min.

Bühler et al.[726] prepared $LaPO_4$:Ce,Tb nanoparticles with sizes of 9−12 nm based on the use of an ionic liquid of tributylmethylammonium triflylimide $[NCH_3(C_4H_9)_3][(SO_2CF_3)_2N]$ under microwave irradiation at 300 °C for ~10 s. According to the noncoordinating properties of the ionic liquid, the phase transfer of $LaPO_4$:Ce,Tb nanoparticles from polar to nonpolar dispersants was performed. Microwave heating was extremely fast, resulting in almost instantaneous crystallization of nanoparticles. Dispersions of $LaPO_4$:Ce,Tb nanoparticles in ethanol were applied for inkjet printing of transparent luminescent layers on polymer substrates. Ethanolic dispersions of $LaPO_4$:Ce,Tb nanoparticles were used to realize a fully transparent dielectric barrier discharge lamp as a prototype of a "luminescent window".[727] Cao et al.[728] prepared iron hydroxyl phosphate ($NH_4Fe_2(PO_4)_2OH{\cdot}2H_2O$) nanostructures with a variety of morphologies such as solid microspheres, microspheres with the core in the hollow shell, and double-shelled hollow microspheres by the one-step microwave-solvothermal ionic liquid method. In this method, $Fe(NO_3)_3{\cdot}9H_2O$ and $(NH_4)_2HPO_4$ were used as the reactants in the presence of an ionic liquid $[BMIM][BF_4]$. The resultant reaction system was microwave-heated at 160 °C for 1 h. The effects of the experimental parameters on the morphology and crystal phase of the products were investigated. The ionic liquid $[BMIM][BF_4]$ significantly influenced the morphology and crystal phase of the product. Starlike structures of $Fe_5(PO_4)_4(OH)_3{\cdot}2H_2O$ were obtained without $[BMIM][BF_4]$. Rich morphologies of $NH_4Fe_2(PO_4)_2OH{\cdot}2H_2O$ obtained by this synthetic method enabled the investigation of structural-dependent properties such as photoluminescence, which is important for various applications, especially in light emitting diodes. Structural-dependent photoluminescence was observed, and photoluminescence was observed from the double-shelled hollow microspheres of $NH_4Fe_2(PO_4)_2OH{\cdot}2H_2O$ while the

dx.doi.org/10.1021/cr400366s | Chem. Rev. 2014, 114, 6462−6555

other nanostructures did not exhibit photoluminescence, and the underlying mechanisms were discussed.

Cobalt oxalate nanorods with diameters of ~50 nm were prepared using $Co(CH_3COO)_2{\cdot}4H_2O$, $H_2C_2O_4$, and NaOH as the reactants in the presence of an ionic liquid [BMIM][BF_4] by the rapid microwave-assisted ionic liquid method at 90 °C for 10 min. These nanorods self-assembled to form bundles of nanorods. It was found that both [BMIM][BF_4] and microwave heating played an important role in the formation of cobalt oxalate nanorods.[729]

The microwave-assisted ionic liquid method has also been adopted for rapid synthesis of nanocomposites. Jacob et al.[730] reported a microwave-assisted ionic liquid route to the preparation of carbon-coated Cu or Ni nanoparticles using an ionic liquid [BMIM][BF_4] for 10 min. Liu et al.[731] reported the preparation of metal (such as Pt, Rh, etc.) nanoparticles deposited on carbon nanotubes in an ionic liquid via microwave heating. In this method, an inorganic salt (such as $H_2PtCl_6{\cdot}4H_2O$, $RhCl_3{\cdot}2H_2O$, etc.) as the metal source was reduced to metal nanoparticles by glycol in 1,1,3,3-tetramethylguanidinium trifluoroacetate or 1,1,3,3-tetramethylguanidinium lactate by microwave heating.

Marquardt et al.[733] reported the rapid microwave-assisted preparation (6 min, 20 W) of Ru or Rh nanoparticles deposited on chemically derived graphene surface with relatively uniform particle sizes (Ru 2.2 ± 0.4 nm and Rh 2.8 ± 0.5 nm) by decomposition of the corresponding metal carbonyl precursors under argon atmosphere in a suspension of graphene in an ionic liquid [BMIM][BF_4]. The TEM micrographs of the products (Figure 22) show that small metal nanoparticles of Ru and Rh with sizes of 2−3 nm were uniformly dispersed on the graphene surface. The graphene-supported metal nanoparticles were active and could be reused at least 10 times as catalysts for the hydrogenation of cyclohexene and benzene under organic-solvent-free conditions.

5. MICROWAVE-ASSISTED PREPARATION OF NANOSTRUCTURES IN OTHER SOLVENTS

In addition to the solvents of water, polyols, and ionic liquids that have been discussed above, many other solvents have also been investigated for the microwave-assisted preparation of inorganic nanostructures, which have greatly widened the applications of microwave heating in the preparation of nanostructured materials. A variety of organic solvents have been adopted for the microwave-assisted preparation of inorganic nanostructures, such as alcohols,[736−776] ethylene glycol monoalkyl ethers,[777] propylene carbonate,[778] ethylenediamine,[767,779−785] PEG with low molecular weights,[786−789] methacrylate,[790] DMF,[770,791−799] trioctylphosphine,[530] nonadecane,[800] octyl ether,[800] dimethyl sulfoxide,[801] acetonitrile,[802] tetrahydrofuran,[770] formaldehyde,[803] cyclohexanone,[804] hexadecylamine,[805,806] diethanolamine,[807] oleylamine,[808−813] 1,2-dichlorobenzene,[814] toluene,[815] and pyridine.[816] Various inorganic nanostructures have been prepared by the microwave-assisted method in the above-mentioned solvents, and these nanostructures include Au,[736] Ag,[736,737,777,790] Cu,[740,741] Pd,[738,739] Ru,[778,814] Rh,[778] Ir,[778] Mo,[778] W,[778] Re,[778] Os,[778] Fe,[778] Co,[778] Ge,[812] Cu−Ag,[742] Fe−Pt,[800] Fe−Pd,[800] Ni−Co,[811] C,[743] graphene,[817] Si,[792] Se,[779] Ga_2O_3,[753] ZnO,[744−746,751,772,787] Al-doped ZnO,[776] CuO,[747] α-Fe_2O_3,[748,749] Fe_3O_4,[748,751,773] TiO_2,[752,766] Mn_3O_4,[750,751] CoO,[751] WO_3,[754] CeO_2,[763] ZrO_2,[764] Eu^{3+}:Y_2O_3,[805] α-Ni(OH)$_2$,[755] $BaTiO_3$,[751] $NiFe_2O_4$,[761] $MnFe_2O_4$,[762] PbS,[768,786,803] Bi_2S_3,[793,795,803] HgS,[768,770,786,803] CdS,[767,779−781,791,794,796,801,806] ZnS,[782,803] CuS,[803,807] EuS,[802] Cu_3Se_2,[797] CdSe,[804,808] $CuInS_2$,[809] Cu_2ZnSnS_4,[810,813] $CuInSe_2$,[784,785] Cu_2SnSe_4,[788] $CuCr_2Se_4$,[789] $Cu_{2-x}Te$,[783] HgTe,[783] Ni_3P,[530] Eu^{3+}-doped amorphous calcium phosphate,[799] Pd/carbon nanotube,[815] Ag/graphene,[798] Au/CeO_2,[760] Pt/TiO_2,[765] Pd/CeO_2,[760] α-Fe/$Fe_{3-x-y}Mn_xZn_yO_4$,[756] $Fe_yCo_{1-y}/Fe_{3-x}Co_xO_4$,[771] SiO_2/Cd(OH)$_2$,[757] Ag/Ag_2S,[769] poly(ε-caprolactone)/clay,[818] and CdS/poly(*N*-vinylcarbazole).[816]

Among these solvents, alcohols have been most frequently used as the solvents for the microwave-assisted synthesis of inorganic nanostructures. Alcohols have high loss tangent (tan δ) values; for example, ethanol has a high loss tangent value of 0.941 at 20 °C and 2.45 GHz, much larger than that of water (0.123 at room temperature). Therefore, alcohols are excellent microwave absorbents. Gabriel et al.[25] discussed in detail the dielectric properties of alcohols for microwave heating. Alcohols are able to form hydrogen bonds in a way similar to that of water at a lesser extent; thus their dielectric properties are similar to those of water. The aliphatic alcohols also have dipole moments that are similar to those of water. As the chain length of the alcohol increases, the relaxation time becomes longer. The relaxation time is not greatly influenced by the position of the OH group in the molecule, but it significantly decreases when the hydrocarbon chain contains a double bond or a phenyl ring adjacent to the $-CH_2OH$ fragment.[25] The standard microwave frequency for dielectric heating of 2.45 GHz corresponds to a relaxation time of 65 ps. The commonly used alcohols have relaxation properties that enable them to couple effectively with this fixed microwave frequency, and they are effective solvents for microwave heating. Because alcohols especially with low molecular weights have usually relatively low boiling points, the open reaction systems allow only low-temperature chemical reactions, and the solvothermal reactions in closed systems are beneficial for relatively high-temperature microwave-assisted synthesis.

Abargues et al.[736] reported the microwave-solvothermal preparation of Au and Ag nanoparticles by the reduction of $HAuCl_4$ and $AgNO_3$ with PVA in the solvent of a short-chain alcohol. The reaction kinetics was especially very fast because upon microwave exposure of only 30 s the reaction was completed. The best results were obtained using alcohols with lower chain lengths. Pal et al.[737] prepared Ag nanoparticles with diameters of 10 ± 5 nm using $AgNO_3$ and PVP in ethanolic medium under microwave irradiation at 800 W for a very short period of time (5 s). Galletti et al.[739] reported the microwave-assisted solvothermal preparation of Pd nanoparticles with an average size of ~3.8 nm using $Pd(CH_3COO)_2$ and PVP in the solvent of ethanol in a single-mode microwave oven at 100 °C for 5 min. Nakamura et al.[740] prepared Cu nanoparticles with sizes of 5−6 nm (with the surface plasmon absorption) and 2−3 nm (without the surface plasmon absorption) using copper(II) octanoate and copper(II) myristate, respectively, as the copper precursors by reduction with alcohols by microwave heating at 170 °C for 20 min. Dar et al.[741] prepared Cu nanostructures by microwave heating a solution of copper acetylacetonate in benzyl alcohol at 800 W for 3 min. The as-prepared Cu nanostructures were stable against oxidation in ambient air for several months. The Cu sample was composed of nanospheres with diameters of ~150 nm, and each nanosphere was made of nanocrystals with sizes of ~7.7 nm.

dx.doi.org/10.1021/cr400366s | *Chem. Rev.* 2014, 114, 6462−6555

There have been many reports on the preparation of metal nanostructures using the microwave-assisted polyol process by reduction of metal salts with ethylene glycol, as discussed in the previous section. Darmanin et al.[777] adopted a reducing agent as well as a solvent containing only one hydroxyl group to prepare Ag nanostructures by microwave heating. They demonstrated the rapid microwave-assisted production of Ag nanoprisms/nanoplates by a careful choice of the reducing agent containing only one hydroxyl group such as ethylene glycol monoalkyl ethers at 140 °C for 30 min. Careful optimization of the reducing agent, microwave heating time, temperature, or the ratio of PVP to $AgNO_3$ allowed complete conversion of nanoparticles into nanoplates/prisms. They proposed that nanoprisms formation passes through the formation of intermediate particles (seeds) from silver spherical particles followed by the formation of small nanoprisms and their growth into larger nanoprisms.

Druzhinina et al.[743] investigated the microwave-assisted solvothermal preparation of carbon nanofibers and nanotubes. The analysis of the temperature and pressure kinetics during microwave irradiation revealed in particular a strong influence of the applied pressure on the formation of the product. Different metal salt (Fe, Ni, Co) solutions in ethanol were drop-cast or spin-coated over the Si wafer and dried in the air. The modified substrates were exposed to microwave irradiation (5 min at 200 W) in the presence of different carbon sources (ethanol, butanol, 2-propanol, and EG). Ni was the most favorable catalyst to obtain small diameters of carbon nanofibers down to 14 nm for a short microwave heating time of 2 min.

Schneider et al.[744] prepared ZnO nanoparticles by thermal decompostion of zinc acetylacetonato and zinc oximato complexes, respectively, in alkoxyethanols (methoxyethanol, ethoxyethanol, or *n*-butoxyethanol) by microwave heating. ZnO hierarchical hollow spheres consisting of nanoparticles were prepared using $Zn(CH_3COO)_2{\cdot}2H_2O$ as the zinc source and ethanol as the solvent by the rapid one-pot microwave-assisted solvothermal method at 200 °C for 30 min.[745] Cu-doped ZnO nanoparticles were synthesized using $Cu(CH_3COO)_2$, $Zn(CH_3COO)_2$, and PVP in the solvent of ethanol by microwave refluxing for 6 min.[746]

Flower-like α-Fe_2O_3 microspheres constructed with nanosheets were synthesized using $FeCl_3{\cdot}6H_2O$ and urea in the solvent of ethanol via the microwave-assisted solvothermal method at 150 °C for 30 min.[749] Tetragonal Mn_3O_4 nanoparticles with sizes of ∼30 nm were synthesized using $KMnO_4$ in ethanol by the microwave-assisted solvothermal method at ∼190 °C for 5 min.[750] Metal oxide nanoparticles such as CoO, ZnO, Fe_3O_4, MnO, Mn_3O_4, and $BaTiO_3$ were synthesized by reacting metal alkoxides, acetates, or acetylacetonates in benzyl alcohol by microwave heating at 200 °C for 0.5−3 min.[751] Deshmane et al.[753] synthesized mesoporous Ga_2O_3 nanoparticles employing triblock copolymer (F127) and CTAB in ethanol via microwave heating at 130 °C for 15−200 min followed by calcination at 350 or 400 °C for 10 h. The transition from semicrystalline to fully crystalline mesophases was observed as the microwave heating time increased from 15 to 120 min. These mesophases consisted of 3−8 nm crystallites and unimodal pores with sizes of 3−7 nm with a specific surface area of 360 $m^2\ g^{-1}$. Le Houx et al.[754] prepared WO_3 nanoparticles with sizes of 5−30 nm by microwave-solvothermal treatment of tungsten chloride in benzyl alcohol up to 210 °C followed by annealing in air. The solvothermal treatment was carried out by resistive or microwave heating. When the resistive heating was used, the specific surface areas were in the range of 20−90 $m^2\ g^{-1}$; however, 140 $m^2\ g^{-1}$ of specific surface area was obtained by fast microwave heating. CeO_2 nanoparticles were prepared via a microwave-assisted solvothermal process using $Ce(NO_3)_3$, H_2O_2, and PVP in isopropanol at 250 °C for 20 min, and the obtained powder was calcined at 400 °C for 2 h.[763] Flower-like TiO_2 nanostructures were prepared using commercial TiO_2 and $TiCl_4$ in benzyl alcohol by microwave heating at 100 °C for 1 h.[766] Yttria-stabilized zirconia nanocrystals with mean sizes between 5 and 10 nm were prepared in alcoholic solutions of yttrium and zirconium chloride and sodium ethoxide under argon gas by microwave solvothermal treatment at ∼160 °C for 2 min.[764]

Bousquet-Berthelin et al.[761] prepared $NiFe_2O_4$ nanoparticles with sizes of 4−5 nm using $NiCl_2{\cdot}6H_2O$, $FeCl_3{\cdot}6H_2O$, and sodium ethoxide in ethanol by the microwave-solvothermal method at 160 °C for 5 min. Pascu et al.[762] reported a fast microwave-assisted sol−gel chemical approach to produce magnetic nanostructured coating of $MnFe_2O_4$ on polystyrene beads covered with a thin Al_2O_3 layer at 160 °C in just a few minutes. The reaction system contained iron(III) acetylacetonate [$Fe(acaca)_3$] and $Mn(CH_3COO)_2$ (Fe/Mn molar ratio = 2:1) in anhydrous benzyl alcohol. The method can fabricate a stoichiometric and homogeneous $MnFe_2O_4$ on the polystyrene template over an area of half a square centimeter on a glass slide substrate.

Alcohols have been proven to be suitable solvents for the microwave-assisted preparation of a variety of nanocomposites. For example, Feng et al.[765] prepared Pt nanoparticles using H_2PtCl_6 in the solvent of methanol by the microwave-assisted solvothermal approach at 120 °C for 20 min and deposited Pt nanoparticles in situ within TiO_2 nanotube arrays, and the sizes of Pt nanoparticles could be adjusted by changing the initial concentration of metal precursor. Caillot et al.[756] prepared α-$Fe/Fe_{3-x-y}Mn_xZn_yO_4$ nanocomposites by microwave-solvothermal treatment of alcoholic solutions of chloride precursors and sodium ethoxide in a short period of time (e.g., 15 s). The nanocomposites of Fe−Co alloy/cobalt ferrite ($Fe_{3-x}Co_xO_4$) were prepared in alcoholic solutions of ferrous chloride, cobalt chloride, and sodium ethoxide by the microwave solvothermal method at 160 °C.[771] As compared to the conventional synthesis, smaller grains (100 nm as compared to 1 μm) could be produced by microwave heating in a short period of time (e.g., 10 s) using a less basic medium. In all of the cases, the microstructure and the amount of metal inside the composite were very different from the product obtained via a conventional heating route.[771] Liu et al.[757] prepared $SiO_2/Cd(OH)_2$ composite nanotubes using water-dissolvable $KCdCl_3$ nanowires, NaOH, and ethyl silicate in the solvent of ethanol by the microwave-assisted solvothermal method at 100 °C for 1 h. $KCdCl_3$ nanowires were prepared by adding an aqueous solution containing $CdCl_2$ and KI into anhydrous ethanol at room temperature. $KCdCl_3$ nanowires, which are water-dissolvable and can be easily removed by washing with water, act as both the precursor and the template for the preparation of $SiO_2/Cd(OH)_2$ composite nanotubes in an alkaline ethanol solution. Gonzalez-Arellano et al.[758] prepared supported iron oxide nanoparticles using $FeCl_2{\cdot}4H_2O$ in ethanol by microwave heating at 200 W for 15 min (average temperature 100 °C). The supports used were porous (silica, MCM-41, and a mild acidic montmorillonite clay) and nonporous biomaterials (cellulose and chitosan). Balu et al.[759] reported the micro-

dx.doi.org/10.1021/cr400366s | Chem. Rev. 2014, 114, 6462−6555

wave-assisted preparation of iron oxide nanoparticles (Fe_2O_3, hematite) with sizes of 3−5 nm on silica-type mesoporous material Si-SBA-15 as a support using $FeCl_2·4H_2O$ as the iron precursor and ethanol as the solvent at 150−200 °C for 3−5 min. They found that, in contrast to the chosen reaction temperature, the reaction time and stirring efficiency were of critical importance in the preparation of the supported nanoparticles. Extended reaction time (>10 min) led to a significant proportion of larger aggregates, while inefficient stirring also produced low-quality nanoparticles as a result of poor dispersion and delivery of the iron precursor to the mesoporous support. Yang et al.[769] prepared porous Ag/Ag_2S hybrid nanotubes by microwave-assisted surface sulfidation of Ag_2CO_3 nanorods. This process is facile and rapid, and only involves the reaction of Ag_2CO_3 nanorods with thioacetamide in ethanol under microwave irradiation at 400 W for 15 min. The Ag content in porous Ag/Ag_2S hybrid nanotubes could be tuned by varying experimental parameters such as the thioacetamide concentration.

In addition to alcohols, which have been commonly used as the solvents, other solvents have also been adopted for the microwave-assisted preparation of inorganic nanostructures. Vollmer et al.[778] reported the microwave-assisted preparation of nanoparticles of transition metals by using propylene carbonate as the solvent, which is an established industrial and low-priced solvent. They have demonstrated that biodegradable propylene carbonate can be used as a solvent and stabilizing medium for the preparation of nanoparticles of transition metals including Ru, Rh, Ir, Mo, W, Re, Os, Fe, and Co. Stable nanoparticles with small and uniform particle sizes (typically <5 ± 1 nm) were obtained by rapid (3 min) and energy-saving (50 W) microwave heating under argon atmosphere from the metal−carbonyl precursors in propylene carbonate. Nguyen et al.[800] reported the microwave-assisted preparation of Fe−Pt and Fe−Pd nanoparticles using $Na_2Fe(CO)_4$ and platinum acetylacetonate $Pt(acac)_2$/$Pd(acac)_2$ in nonadecane or octyl ether. By varying the solvent and surfactant, the microwave-assisted reactions were advantageous for the rapid production of monodisperse face centered cubic (fcc) Fe−Pt nanoparticles, which could be converted to the face centered tetragonal (fct) phase at 364 °C. Microwave reactions at a high pressure in a closed system led to the direct formation of a mixture of fcc and fct Fe−Pt nanoparticles. The fct nanoparticles had a particle size of ∼24 nm and a strong coercivity, indicating ferromagnetic behavior.

Sridhar et al.[817] prepared graphene sheets by combining chemical treatment and microwave irradiation using natural graphite, ammonium peroxy disulfate, and H_2O_2 in a domestic microwave oven at 500 W for 1.5 min to produce strong expansion of the graphite worm in the thickness direction. Under microwave irradiation, the precursors exfoliated rapidly, accompanied by lightening. Atkins et al.[792] reported the microwave-assisted production of amine-terminated Si nanoparticles through the reaction of Na_4Si_4 or Mn-doped Na_4Si_4 with NH_4Br in the presence of the capping ligand C_3H_5N, C_3H_7N, or $C_{11}H_{23}N$ in the solvent of DMF. Uniform 3-aminopropyl-terminated and 3-aminopropenyl-terminated Si nanoparticles with average diameters of 2−3 nm were obtained. Reaction temperature of 250 °C for 10 min or reactions with a power of 200 W for 20 min were found to be the optimal conditions for the formation of Si nanoparticles. The microwave-assisted solvothermal method was reported for the preparation of Se nanorods with diameters in the range of 30−150 nm using sodium selenite and $NaBH_4$ in ethylenediamine at 100 °C for 1 h.[779]

Ethylenediamine has been adopted as the solvent to prepare metal chalcogenide nanostructures by microwave heating. For example, CdS nanorods were prepared using $CdCl_2$, thiourea, and glutathione in ethylenediamine by the microwave-assisted solvothermal method at 160 °C for 3 h.[779] CdS nanowires with diameters of ∼4 nm were prepared using a complex of cadmium-1-pyrrolidine dithiocarboxylic acid ammonium in ethylenediamine under microwave irradiation in ambient air for 1 min.[780] CdS nanoribbons were prepared using $CdCl_2·2.5H_2O$ and 1-pyrrolidine dithio carboxylic acid ammonium salt in ethylenediamine under microwave irradiation for 10 min in ambient air.[781] Radial ZnS nanoribbons with widths of 10−20 nm and a typical thickness of 3 nm were synthesized in ethylenediamine via the microwave-solvothermal method, combined with the thermal treatment in nitrogen gas flow.[782] Palchik et al.[783] synthesized nanoparticles of $Cu_{2-x}Te$ and HgTe adopting elemental Te, CH_3COOCu, and mercury acetate in the solvent of ethylenediamine by microwave refluxing for 1−2 h. In the case of the preparation of $Cu_{2-x}Te$, the product was a complex of Cu, Te, and ethylenediamine, which decomposed into $Cu_{2-x}Te$ by annealing at 280 °C under Ar for 2 h. $CuInSe_2$ nanostructures with a rodlike or platelike morphology were prepared in ethylenediamine by the microwave-assisted solvothermal method at 180 °C for 5−30 min.[784]

DMF has also been adopted as the solvent for the microwave-assisted synthesis of nanostructured metal chalcogenides. Majumder et al.[794] reported the microwave-assisted synthesis of CdS nanocrystals through the reaction of $Cd(CH_3COO)_2$ with thiourea in the presence of capping agents (1-butanethiol and 2-mercaptoethanol) in DMF; the number of microwave heating was varied to control the size and size distribution of the thiol-capped CdS nanocrystals. Karan et al.[796] reported the microwave-assisted synthesis of CdS quantum dots with sizes of 2.9−5.5 nm using $Cd(CH_3COO)_2·2H_2O$, thiourea, and poly(methyl methacrylate) in DMF at 900 W for 20−30 s. He et al.[793] prepared Bi_2S_3 nanowhiskers through the reaction between $Bi(NO_3)_3·5H_2O$ and thiourea in the presence of PVP in the solvent of DMF via a microwave-assisted route. Bi_2S_3 nanorods were prepared using bismuth citrate, thiourea, and CTAB in the solvent of DMF by microwave heating at 200 °C for 5 min.[795] β-HgS nanoparticles with sizes of 8−23 nm were prepared using $Hg(CH_3COO)_2·2H_2O$ and thiourea in different solvents by microwave refluxing, and the solvents used were absolute ethanol, tetrahydrofuran, distilled water, DMF, and 20% DMF aqueous solution, respectively.[770] Cu_3Se_2 nanoplates with a thickness of 17 nm were synthesized through a microwave-enhanced reaction between Se and copper(I) oleate in DMF at 100 °C for 1 h.[797]

Other solvents have also been used in the microwave-assisted synthesis of nanostructured metal chalcogenides. Ferrer et al.[801] reported turning "on" and "off" nucleation and growth of CdS clusters and nanoparticles with diameters ranging from 1.6 to over 250 nm from the microwave-assisted reaction of $Cd(CH_3COO)_2$ with dimethyl sulfoxide. Dimethyl sulfoxide acted as the solvent and a source of sulfide ions. The formation of CdS was controlled by turning on and off microwave energy supply. The extent of the nucleation and growth was controlled by the supply of sulfide ions from the reaction of Cd^{2+} ions and dimethyl sulfoxide during exposure to microwave radiation. Marx Nirmal et al.[806] used the complex of cadmium with

dx.doi.org/10.1021/cr400366s | Chem. Rev. 2014, 114, 6462−6555

pyrrolidine dithiocarbamate $Cd(pdtc)_2$ as a single source precursor for the synthesis of CdS nanoparticles by microwave-assisted thermal decomposition of the complex in the solvent of hexadecylamine. The microwave irradiation failed to decompose the complex $Cd(pdtc)_2$ without the addition of a polar solvent even after heating for 5 min. However, the addition of a small amount of DMF to the reaction system and microwave heating for 1 min with a power of 800 W resulted in the formation of CdS nanoparticles. CdS nanoparticles with a disordered close-packed structure and an average size of 5 nm were obtained under microwave irradiation; in contrast, wurtzite hexagonal CdS nanorods with an average size of ~3 nm in width and 15 nm in length were obtained by the conventional heating at 150 °C for 30 min. In the case of the conventional heating, the decomposition rate was very slow, and the nanoparticles grew in a direction leading to nanorods.

Low molecular weight PEG-200 was also used as a solvent for the preparation of PbS and HgS nanoparticles with average sizes from 20 to 30 nm using the reactants of $Pb(CH_3COO)_2 \cdot 3H_2O$, $Hg(CH_3COO)_2$, and S powder by microwave heating for 20 min.[786] Liu et al.[807] reported a microwave-assisted Cu-complex transformation route for the preparation of CuS nanotubes. Using Cu-complex $Cu(TU)Cl \cdot 0.5H_2O$ (TU = thiourea) nanowires as the self-sacrificial template formed under ambient conditions, CuS nanotubes with a rectangular cross-section were synthesized in diethanolamine. The diameter of CuS nanotubes with a rectangular cross-section could be tuned through changing experimental parameters. Furthermore, cone-like CuS nanotubes were also prepared by adopting Cu-EBT (EBT = eriochrome black T) complex nanorods as precursors. CuS nanotubes with rectangular cross sections were found to be effective as nonenzymatic glucose sensors. Liao et al.[803] reported the microwave-assisted synthesis of nanocrystalline metal sulfides including CuS, HgS, ZnS, Bi_2S_3, and PbS with different shapes and different particle sizes using corresponding metal salts and thioacetamide in the solvent of formaldehyde. Hasegawa et al.[802] prepared EuS nanoparticles with an average size of 8 nm by microwave refluxing decomposition of a single source precursor $(PPh_4)[Eu(S_2CNEt_2)_4] \cdot 2H_2O$ in acetonitrile for 6 h. Firth et al.[804] reported the microwave-assisted synthesis of CdSe nanocrystals using $Cd(CH_3COO)_2 \cdot H_2O$ and Se in cyclohexanone, and the reaction mixture was heated to 145 °C for varying lengths of time (between 30 s and 15 min). The particle size was regulated by adjusting the reaction time. When the reaction time was restricted to less than 1 min, it was possible to isolate CdSe nanocrystals with an average diameter of 2 nm, while 6 nm CdSe nanocrystals were produced for longer than 10 min. Wang et al.[808] prepared red-emitting CdSe quantum dots with sizes ranging from 6.0 to 13.4 nm adopting B_2Se_3 and $CdCl_2$ as the reactants in oleylamine by microwave heating; the particle size was controlled mainly by changing reaction temperatures from 190 to 270 °C. The smallest quantum dots exhibited the zinc blende structure, while larger particles showed the wurtzite structure.

Nanostructured ternary and multinary metal chalcogenides have also been prepared in various solvents by the microwave-assisted method. Pein et al.[809] prepared $CuInS_2$ nanoparticles using CuI, $InCl_3$, and elemental S in the solvent of oleylamine, and a microwave heating time of only 1.5 min resulted in the rapid formation of $CuInS_2$ nanoparticles with sizes of 3−4 nm. Yang et al.[810] prepared Cu_2ZnSnS_4 nanoparticles with sizes of ~10−15 nm using $Cu(NO_3)_2 \cdot 3H_2O$, $Zn(NO_3)_2 \cdot 6H_2O$, $SnCl_4 \cdot 5H_2O$, and S powder in oleylamine by microwave heating at 260 °C for 30 min followed by annealing at 350 °C under nitrogen gas flow. Lee et al.[785] prepared $CuInSe_2$ nanostructures with different morphologies using $CuCl_2$, $InCl_3 \cdot 4H_2O$, and Se powder in ethylenediamine by a microwave-assisted solvothermal process at 180 °C for 1 h. The optimum crystallinity was obtained at 180 °C with 0.02 M Cu^{2+} ions. When $Cu(CH_3COO)_2$ was used as the copper source, $CuInSe_2$ particle size was dramatically reduced. Moreover, the synthesis at 1 L scale of the reactants gave the particle size of 20 nm, which was smaller than that of small scale synthesis (23−35 nm). Grisaru et al.[788] prepared Cu_2SnSe_4 nanoparticles using CuCl (or $CuCl_2 \cdot 2H_2O$), Sn, and Se in PEG as the solvent by microwave heating at 900 W for 2 h, and the precursor was annealed under argon at 450 °C for 12 h. It was found that the reactants did not react in EG, tri-, or tetraethylene glycol. Kim et al.[789] prepared $CuCr_2Se_4$ nanoparticles from the chemical reactions of CuCl, $Cr(CH_3COO)_3$, and Se in PEG-400 under microwave irradiation at 540 W for 1 h in argon atmosphere.

Different kinds of nanocomposites have been prepared by the microwave-assisted method in various solvents. Yamauchi et al.[811] reported the microwave-assisted synthesis of face-centered cubic Ni/Co (core/shell) nanoparticles using Ni-$(CH_3COO)_2$ and cobalt(II) formate complexes in oleylamine. The as-prepared product was composed of a Co-rich shell and a Ni-rich core. The shape of Ni/Co nanoparticles could be varied using different nickel precursors (acetate or formate complexes), and the shape of the Ni core played a key role in determining the final shape of Ni/Co nanostructures. Liu et al.[798] prepared the Ag nanoparticles/graphene nanocomposite by one-pot microwave-assisted reduction using a DMF solution of graphene oxide and $AgNO_3$. Cano et al.[815] reported a fast one-step microwave refluxing synthesis of the nanocomposite of Pd nanoparticles/multiwalled carbon nanotubes by decomposition of the complex $Pd_2(dba)_3CHCl_3$ (dba = *trans,trans*-dibenzylideneacetone) in the presence of carbon nanotubes in the solvent of toluene under argon atmosphere. High loadings of Pd nanoparticles (up to 40 wt %) having sizes between 3 and 5 nm were deposited on the surface of carbon nanotubes within 2 min. The reaction time was significantly shortened by microwave heating (only 2 min), which required 2 h under the conventional heating at the same temperature (115 °C). Wada et al.[790] prepared Ag nanoparticles using $C_{13}H_{27}COOAg$ in reactive methacrylate monomer under microwave irradiation. Successive polymerization of the monomer containing the resulting Ag nanoparticles produced the nanocomposite comprising Ag nanoparticles dispersed in the polymer matrix. He et al.[816] prepared CdS/poly(*N*-vinylcarbazole) nanocomposites by microwave heating at 300 W for 5 min in which the polymerization of *N*-vinylcarbazole and the formation of CdS nanoparticles with sizes of ~10−20 nm occurred simultaneously, using *N*-vinylcarbazole, azobisisobutryonitrile, $Cd(CH_3COO)_2 \cdot 2H_2O$, and thiourea as the reactants and pyridine as the solvent. Chen et al.[799] prepared amorphous calcium phosphate (ACP)/polylactide-*block*-monomethoxy-(poly(ethylene glycol)) (PLA−mPEG) hybrid nanoparticles using $CaCl_2$, $Na_2HPO_4 \cdot 12H_2O$, and PLA-mPEG in aqueous solution (pH value was adjusted to 10 using ammonia). Subsequently, the microwave-assisted solvothermal approach was adopted for the preparation of ACP porous nanospheres by using ACP/PLA−mPEG hybrid nanoparticles in DMF at 200 °C for 1 h, europium-doping was performed to enable photoluminescence function of ACP porous nanospheres, and

dx.doi.org/10.1021/cr400366s | *Chem. Rev.* 2014, 114, 6462−6555

a high specific surface area of the europium-doped ACP (Eu^{3+}:ACP) porous nanospheres was achieved (126.7 m^2 g^{-1}). In vitro drug release experiments indicated that the ibuprofen-loaded Eu^{3+}:ACP porous nanospheres had a slow and sustained drug release property in simulated body fluid. It was found that the cumulative amount of released drug had a linear relationship with the natural logarithm of release time ($\ln(t)$). The as-prepared Eu^{3+}:ACP porous nanospheres were bioactive, and could transform to hydroxyapatite during drug release in simulated body fluid.

6. MICROWAVE-ASSISTED PREPARATION OF NANOSTRUCTURES IN MIXED SOLVENTS

The properties of the solvents have significant effects on the formation of inorganic nanostructures under microwave heating conditions. Different solvents interact very differently with microwaves because of variations in solvent polarities, dielectricity, and other properties. The appropriate selection and use of mixed solvents will greatly expand the application range of the microwave-assisted rapid preparation of inorganic nanostructures. The different combination and the volume ratio of the selected mixed solvents will also provide additional experimental parameters for control over the chemical composition, structure, size, morphology, and self-assembly of microwave-synthesized inorganic nanostructures.

6.1. Binary Solvent Systems

6.1.1. Water/Polyols. Polyols have several −OH functional groups attached to the carbon backbone, they are excellent solvents for microwave heating with high loss tangent (tan δ) values, and their abilities to absorb microwaves are generally much better than that of water. The combination of water and polyols will certainly enhance the absorption of microwaves as compared to that in the case of using water as the only solvent. On the other hand, polyols are highly miscible with water, and polyol molecules are able to form intermolecular hydrogen bonds with each other and with neighboring water molecules in solution. The polyol compounds usually have high viscosities due to strong hydrogen bonding.[25] However, some reactants have limited solubilities in polyols as the solvents especially with high molecular weights. The addition of water in polyols will greatly increase the solubilities of many reactants.

Because of their advantages, the mixed solvents of polyols and water have been frequently used for the microwave-assisted preparation of inorganic nanostructures, including Pt,[819] Cu,[820] Ni,[821,822] Co,[823] carbon,[824,825] Pt−Ru,[819] Pt/C,[826−832] Pt/diamond,[833] Pt/carbon nanotube,[832,834−836] Pt/carbon nanotube/carbon paper,[837] Pt/graphene,[838−840] Pt−Ru/graphene,[841] Pd/C,[828] Ag/carbon paper,[842] ruthenium oxide/carbon nanotube,[843] α-Fe_2O_3,[844,845] Fe_3O_4,[846] ZnO,[847−849] copper oxide,[850−852] TiO_2,[853] CeO_2,[854,855] In_2O_3:Sn,[856] SnO_2:F,[857] $WO_3{\cdot}(H_2O)_{0.33}$,[858] cobalt(II) acetate hydroxide,[369] $Cd(OH)_2$,[859] Bi_2S_3,[860] Ru_xSe_y,[861] $Ru_{85}Se_{15}$,[862] Bi_2Te_3,[863,864] Sb_2Te_3,[865,866] $CaCO_3$,[867,868] $CaHPO_4$,[869] $BiPO_4$,[380] RE:YPO_4 (RE = Eu, Ce, Tb, and Ce + Tb),[870] Tb:$CePO_4$,[871] $GdPO_4$,[872] Eu:$GdPO_4$,[872] $LiFePO_4$,[873] $LiFe_{1-x}(VO)_xPO_4$,[874] $BaTiO_3$,[875] Nd-doped $SrTiO_3$,[876] $(Ba,Sr)TiO_3$,[877] $CaMoO_4$,[878] $FeMoO_4$,[879] $Zn_{1-x}Co_xAl_2O_4$,[880] $CoFe_2O_4$,[881,882] $MnFe_2O_4$,[882] Bi_2GeO_5,[883] ZrO_2-doped Al_2O_3,[448] $Co_x(OH)_y(X)_z{\cdot}nH_2O$ (X = anion),[884] $NaYF_4$:Yb,Er,[885] Ce- and Tb-doped $BaYF_5$,[886] SnO_2/graphene,[841] Ir_xSe_y/C,[887] $Ru_{85}Se_{15}$/carbon nanotube,[888] Pt_3Te/C,[889] Pt/CeO_2/C,[890] Fe_3O_4/HAP,[891] Fe_3O_4/zeolite,[892] ZnO/zeolite,[892] and SnS_2/SnO_2.[893]

Various metal nanostructures have been successfully prepared by the microwave-assisted method in mixed solvents of EG and water. Liu et al.[819] prepared Pt (4.7 nm) and Pt−Ru (4.5 nm) nanoparticles using H_2PtCl_6 and/or $RuCl_3$ in mixed solvents of EG and water by a microwave-assisted process at 170 °C for 1 min. Xu et al.[820] prepared dimethylglycoxime functionalized Cu nanoparticles using $Cu(CH_3COO)_2{\cdot}H_2O$ and dimethylglycoxime in mixed solvents of EG and water by microwave refluxing heating under ambient air at a power of 365 W for 30 min, and the as-prepared Cu nanoparticles were used to construct a glucose sensor. The microwave-assisted preparation of Ni nanowires with a necklace-like morphology was reported by Tang et al.[821] $NiCl_2{\cdot}6H_2O$, hydrazine monohydrate, and PVP were used as starting reagents, and EG and water were used as the mixed solvent. The as-prepared Ni nanowires consisted of many nanoparticles with an average size of ∼25 nm. Ni nanostructures with various morphologies including spheres, chains, and irregular particles with porous surfaces were also obtained by adjusting experimental parameters. Tang et al.[822] prepared polycrystalline Ni nanowires using $NiCl_2{\cdot}6H_2O$, PVP, hydrazine (85 wt %), and EG by microwave heating at a power of 400 W for 2 min and another 4 min at 150 W. The diameters of Ni nanowires were controllable in a wide range of 70−380 nm via the concentration of precursor solutions, and the diameters of the nanowires as well as those of the contained particles increased linearly with the concentration. The nanowires had rough surfaces at low concentrations but became smoother at high concentrations. Shojaee et al.[823] prepared flower-like Co nanostructures constructed by nanosheets in mixed solvents of water and EG under microwave irradiation at 900 W for less than 10 min.

There have been many papers in the literature reporting on the microwave-assisted synthesis of nanocomposites consisting of Pt nanoparticles and carbon-based support in mixed solvents of water and polyols. Chen et al.[826] prepared Pt nanoparticles (3.5−4.0 nm) supported on commercial carbon using $H_2PtCl_6{\cdot}6H_2O$ and KOH in mixed solvents of EG and water by a microwave-assisted process at 700 W for 1 min. Wang et al.[827] adopted a similar microwave-assisted method for the preparation of the Pt/C nanocomposite. It was found that the particle size and size distribution of Pt nanoparticles were greatly influenced by the microwave irradiation duration (heating temperature). Temperature in the reacting beaker was 132 ± 2, 163 ± 2, 175 ± 2, and 186 ± 2 °C for microwave heating times of 0.5, 1, 1.5, and 2 min, respectively. Liu et al.[828] prepared Pt or Pd nanoparticles supported on commercial carbon using $H_2PtCl_6{\cdot}6H_2O$ or $PdCl_2$ in mixed solvents of EG and water by a microwave-assisted process for 50 s, and the average particle size of Pt and Pd nanoparticles was 4 and 5 nm, respectively. Zhou et al.[829] fabricated Pt nanoparticles supported on the mesoporous carbon using H_2PtCl_6, NaOH, and CTAB in mixed solvents of EG and water by a microwave-assisted process at 700 W for 1 min, wherein CTAB was expected to improve the wettability of carbon support as well as the dispersion of Pt nanoparticles. It was found that Pt nanoparticles were uniform in size and highly dispersed on the mesoporous carbon support. Zhao et al.[831] reported that CH_3COONa had an effect on the size of Pt nanoparticles prepared in mixed solvents of EG and water under microwave irradiation. Acetate-stabilized Pt nanoparticles supported on commercial carbon were obtained using $H_2PtCl_6{\cdot}6H_2O$ and CH_3COONa by microwave heating at 800 W for 1 min, and

dx.doi.org/10.1021/cr400366s | Chem. Rev. 2014, 114, 6462−6555

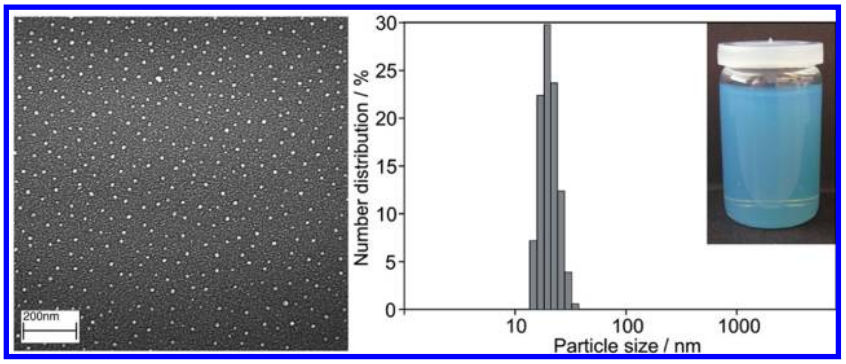

Figure 23. SEM micrograph of as-prepared indium tin oxide (In_2O_3:Sn) nanocrystals and size distribution. Reprinted with permission from ref 856. Copyright 2008 Elsevier B.V.

the mean size of Pt nanoparticles was 5.1, 4.3, 3.5, and 2.8 nm, respectively, when 0, 0.1, 0.3, and 0.5 mL of 1.0 M CH_3COONa solution was used. Li et al.[834] prepared Pt nanoparticles with different sizes supported on carbon nanotubes using K_2PtCl_6 and KOH in the presence of carbon nanotubes in mixed solvents of EG and water with different pH values by a microwave-assisted process at 800 W for 1 min. It was found that the pH value had an effect on the particle size, and that Pt nanoparticles became smaller and more uniform when the pH value increased from 3.4 to 9.2. Sharma et al.[838] prepared the nanocomposite consisting of Pt nanoparticles with sizes of several nanometers and graphene using graphene oxide, K_2PtCl_6, and KOH in mixed solvents of EG and water by a microwave-assisted process at 700 W for 50−100 s. Guo et al.[839] prepared the Pt nanoparticle/graphene nanocomposite using graphene oxide, Pt precursor, and poly(methacrylic acid sodium salt) in mixed solvents of EG and water by a microwave-assisted process at 800 W for 1.5 min. Liao et al.[840] prepared the Pt/graphene nanocomposite in mixed solvents of 1,2-propanediol and a small amount of water by one-pot microwave-assisted process at 170 °C for 5−20 min. For short reaction times, the as-prepared Pt nanoparticles were small, well separated, and uniformly deposited on graphene. Prolonged microwave irradiation led to dense dispersion of Pt nanoparticles and the formation of some aggregated nanoparticles, and eventually to continuous connecting agglomerates.

Nanostructures of metal oxides have also been prepared by the microwave-assisted method in mixed solvents of water and polyols. Deshmukh et al.[844] prepared bundles of α-Fe_2O_3 nanorods using $Fe(NO_3)_3{\cdot}9H_2O$ in mixed solvents of water and pentaerythritol by a microwave-assisted solvothermal route at 130 °C for 15 min. Wang et al.[846] prepared Fe_3O_4 nanosheets using $FeSO_4{\cdot}7H_2O$ and NaOH in mixed solvents of EG and water by microwave refluxing heating, and the iron salt, ratio of OH^- to iron ions, and heating method had effects on the morphology or crystalline phase of the product.

For the microwave-assisted synthesis of ZnO nanostructures, Zhu et al.[847] prepared ZnO hierarchical nanostructures with straw-bundle-like, chrysanthemum-like, and oat-arista-like morphologies and nanorod-based microspheres using $Zn(CH_3COO)_2{\cdot}H_2O$ in mixed solvents of EG and water via microwave heating. Zhang et al.[848] reported the microwave-assisted solvothermal synthesis of ZnO structures with a variety of morphologies using $Zn(CH_3COO)_2{\cdot}2H_2O$ in a mixture of water and EG in a short period of time. By changing the volume ratio of water to EG, the morphology of ZnO could be controlled, and different morphologies of ZnO, such as rods, hexagonal prisms, peanuts, butterflies, and hierarchical nanospheres, could be obtained. Edrissi et al.[849] prepared deer horn-like ZnO nanostructures via microwave heating bis(2-pyridinethiol *N*-oxide) zinc(II) complex in a mixture of EG and water.

Well-crystallized birnessite nanosheets containing K^+ in the interlayers were prepared using $KMnO_4$ and KOH in mixed solvents of EG and water by microwave heating at 90 °C for 10 min, and ethylene glycol was used as both a solvent and a reducing agent.[894] Mn_3O_4 nanoparticles with sizes less than 50 nm were prepared using $MnCl_2{\cdot}4H_2O$ and NaOH in mixed solvents of distilled water and EG by microwave refluxing with a power of 20 W for the total pulsed microwave irradiation time of 5 min.[895] Shirke et al.[854] synthesized cerium oxide nanoparticles with an average particle size of 9 nm using cerium nitrate, propylene glycol, and ammonia by microwave heating. Zawadzki et al.[855] prepared CeO_2 nanoparticles with an average particle size of ∼3 nm using $Ce(NO_3)_3{\cdot}6H_2O$ and hexamine ($C_6H_{12}N_4$) in mixed solvents of diethylene glycol and water by the microwave-solvothermal method under the pressure of 10 bar for 1 h.

Hammarberg et al.[856] prepared indium tin oxide (ITO) nanoparticles using $InCl_3{\cdot}4H_2O$, $SnCl_4{\cdot}5H_2O$, and $N(CH_3)_4OH{\cdot}5H_2O$ in mixed solvents of diethylene glycol and water by microwave heating at 200 °C for 2 h under ambient pressure. The SEM micrograph of as-prepared ITO nanocrystals and size distribution are shown in Figure 23. The as-prepared suspension of ITO in diethylene glycol was colloidally stable within weeks and exhibited a transparent appearance with a bright blue color (Figure 23). The average particle diameter of ITO nanocrystals was 15 nm with a narrow size distribution (Figure 23). The BET specific surface area of powdered ITO nanocrystals was measured to be 56.1 $m^2\ g^{-1}$. Avadhut et al.[857] prepared fluorine-doped tin oxide (SnO_2:F) nanoparticles with different doping levels in mixed solvents of diethylene glycol and water by the microwave-assisted approach at 200 °C for 1 h, and $SnCl_4{\cdot}5H_2O$, $N(CH_3)_4F{\cdot}4H_2O$, and $N(CH_3)_4OH{\cdot}5H_2O$ were adopted as the reactants.

Nanostructures of ternary and multinary metal oxides have also been successfully prepared in mixed solvents of water and polyols by the microwave-assisted method. Lee et al.[875] prepared $BaTiO_3$ nanoparticles using $Ba(OH)_2{\cdot}8H_2O$ and amorphous titanium hydrous gel as precursors in mixed solvents of 1,4-butanediol and water by a microwave-assisted solvothermal process for a short period of time. Typically, the microwave-assisted reaction was accomplished within 2 h at

220 °C against 12 h required in the conventional heating approach. They detected the metastable cubic phase by XRD while locally symmetric tetragonal phase by Raman spectroscopy in the case of the conventional processing. In contrast, they detected the coexistence of tetragonal and cubic phases by XRD and only tetragonal phase by Raman spectroscopy in the case of the microwave-assisted processing. The TEM analysis indicated typical particle size distribution in the range of ~20−80 nm for conventionally processed powder while that in the range of ~20−50 nm for the microwave processed powder. Zheng et al.[876] synthesized mesoporous Nd-doped $SrTiO_3$ nanospheres and nanoplates with high specific surface areas using tetra-*n*-butyltitanate, $Sr(NO_3)_2$, $Nd(NO_3)_3$, and NaOH in mixed solvents of EG and deionized water by the microwave-assisted solvothermal method at 200 °C for 10 min. Mesoporous Nd-doped $SrTiO_3$ nanospheres were obtained at lower concentrations of the reactants. However, the product consisted of nanoplates when the concentrations of the reactants were increased. Yang et al.[877] synthesized $(Ba,Sr)TiO_3$ nanocrystals with average particle sizes ranging from 20 to 80 nm using $TiOCl_2$, $Ba(OH)_2$, $Sr(NO_3)_2$, and ammonia in mixed solvents of 1,4-butanediol and water through a microwave-assisted approach at 800 W within a short reaction time (~1 min).

Marques et al.[878] synthesized nanostructure-assembled $CaMoO_4$ materials using $Ca(CH_3COO)_2{\cdot}H_2O$ and H_2MoO_4 in mixed solvents of deionized water and EG with different ratios by the microwave-assisted solvothermal method at 140 °C for 1 h. Corn-cob-like $CaMoO_4$ structures were obtained in only aqueous solution, and these structures essentially consisted of small aggregated particles with an octahedral shape. In the synthesis containing 25 mL of EG and 75 mL of water, two distinct types of microcrystals (corn cob and dumbbell shapes) were observed. Zhang et al.[879] synthesized $FeMoO_4$ hierarchical hollow microspheres by the reaction between $Fe(NO_3)_3{\cdot}9H_2O$ and $(NH_4)_6Mo_7O_4{\cdot}4H_2O$ in mixed solvents of water and glycerol via microwave heating at 190 °C for 10 min. The as-prepared hierarchical microsphere had a hollow interior, and the shell was composed of many irregular nanoparticles. It was proposed that the self-assembly of $FeMoO_4$ nanoparticles at the water/gas interface was responsible for the formation of hierarchical hollow microspheres.

$Zn_{1-x}Co_xAl_2O_4$ (x = 0, 0.5, 1.0) nanoparticles were synthesized using $Zn(CH_3COO)_2{\cdot}2H_2O$, $Co(CH_3COO)_2{\cdot}2H_2O$, and $Al[OCH(CH_3)_2]_3$ in mixed solvents of 1,4-butanediol and water under microwave-assisted solvothermal conditions at 200 °C for 1 h, and the obtained precursors were calcined at 550 and 1100 °C for 3 h.[880] $CoFe_2O_4$ nanoparticles with an average size of ~5 nm were obtained by coprecipitation using $Co(CH_3COO)_2{\cdot}4H_2O$, $FeCl_3$, and $CH_3COONa{\cdot}3H_2O$ in mixed solvents of 1,2-propanediol and deionized water by microwave heating at 160 °C for 1 h.[881] MFe_2O_4 (M = Mn, Co) nanoparticles with diameters less than 10 nm were prepared using ferric salts in mixed solvents of EG and water by microwave refluxing for 10 min.[882] A microwave-assisted refluxing route has been used to synthesize 5 nm thickness nanoflake-assembled flower-like microspheres of cobalt hydrotalcite such as the compound $Co_x(OH)_y(X)_z{\cdot}nH_2O$ (X = anion) using $Co(NO_3)_2{\cdot}6H_2O$ and urea in mixed solvents of EG and deionized water at 85 °C for various periods of times (15, 30, and 90 min).[884]

Spheroidal vaterite $CaCO_3$ structures composed of irregular nanoparticles with an average size of ~70 nm were synthesized by a microwave-assisted reaction between $Ca(CH_3COO)_2$ and $(NH_4)_2CO_3$ in mixed solvents of EG and water at 90 °C for 10 min.[867] Vaterite $CaCO_3$ structures with various morphologies were rapidly synthesized via the reaction between $Ca(CH_3COO)_2$ and Na_2CO_3 in the presence of CTAB or SDS in the water/EG system by the microwave-assisted method at 100 °C for 8−30 min.[868] It was found that the microwave heating, reaction time, surfactant, and solvent played important roles in the morphology of vaterite. Various vaterite structures with dagger-like, bicone-like, shuttle-like morphologies and microspheres self-assembled from nanoparticles were obtained by adjusting the experimental parameters. The experiments indicate that when the reaction time is prolonged, vaterite, as a less stable polymorph that is stabilized kinetically, will transform into calcite.[868]

Ma et al.[869] reported the microwave-assisted synthesis of $CaHPO_4$ with flower-like and bundle-like morphologies using $CaCl_2{\cdot}2.5H_2O$ and NaH_2PO_4 in the presence of SDS in mixed solvents of EG and water at 95 °C for 1 h. It was found that the molar ratio of water to EG and reaction time had significant effects on the size and morphology of the product. $BiPO_4$ nanoparticles and nanorods were synthesized using $Bi(NO_3)_3{\cdot}5H_2O$ and $NaH_2PO_4{\cdot}2H_2O$ in mixed solvents of glycerol and water by microwave heating for 15 min (80% of 800 W). However, the rice-like morphology of $BiPO_4$ was obtained in mixed solvents of EG/water or diethylene glycol/water.[380] Rodriguez-Liviano et al.[870] prepared mesoporous tetragonal RE:YPO_4 nanostructures (RE = Eu, Ce, Tb, and Ce + Tb) with a lenticular morphology by a microwave-assisted homogeneous precipitation process at temperatures ranging from 80 to 120 °C from EG solutions containing yttrium acetylacetonate and H_3PO_4 (85%). Rodriguez-Liviano et al.[872] reported the microwave-assisted solvothermal synthesis of $GdPO_4$ and Eu:$GdPO_4$ nanocubes using gadolinium (europium) acetylacetonate and H_3PO_4 in mixed solvents of butylene glycol and water at 120 °C (heating rate 14 °C min^{-1}) for 1 h. Figure 24 shows TEM micrographs of $GdPO_4$ and Eu:$GdPO_4$ nanocubes obtained using butylene glycol solutions containing $Eu(acac)_3$, $Gd(acac)_3$ and H_3PO_4 by microwave heating at 120 °C for 1 h. The as-prepared $GdPO_4$ and Eu:$GdPO_4$ nanocubes were uniform in size with edge sizes of ~75 ± 10 nm, and were highly crystalline with a tetragonal structure. In comparison, when keeping the same concentrations of reagents and reaction conditions but using the conventional heating, long nanowires with a hexagonal structure were obtained, although a small

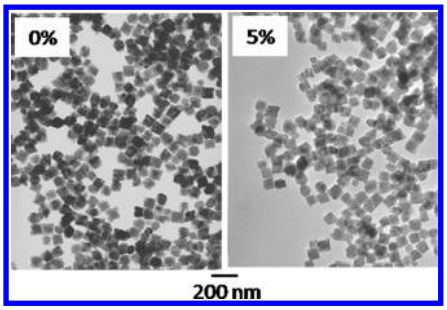

Figure 24. TEM micrographs of $GdPO_4$ and Eu:$GdPO_4$ nanocubes prepared by microwave heating at 120 °C for 1 h using buthylene glycol solutions containing $Eu(acac)_3$, $Gd(acac)_3$ (Gd + Eu = 0.02 mol L^{-1}), and H_3PO_4 (0.15 mol L^{-1}) with different Eu content: 0% ($GdPO_4$) and 5% ($Eu_{0.05}Gd_{0.95}PO_4$). Reprinted with permission from ref 872. Copyright 2012 American Chemical Society.

dx.doi.org/10.1021/cr400366s | *Chem. Rev.* 2014, 114, 6462−6555

number of nanocubes were also formed. The nature of the polyol solvent was another key factor for the formation of nanocubes. When butylene glycol was replaced by EG, the product was composed of bigger spheroidal particles with relatively uniform sizes, and a mixture of crystalline phases (tetragonal and monoclinic) was obtained. Murugan et al.[873] synthesized olivine $LiFePO_4$ nanorods using LiOH, $Fe(CH_3COO)_2$, and H_3PO_4 in tetraethylene glycol by a rapid microwave-solvothermal approach at 300 °C for 5 min. Harrison et al.[874] synthesized $LiFe_{1-x}(VO)_xPO_4$ ($x = 0-0.25$) nanostructures using stoichiometric ratios of LiOH, $Fe(CH_3COO)_2$, H_3PO_4, and $VO(OC_3H_7)_3$ in tetraethylene glycol by the microwave-solvothermal process at the temperatures between 260 and 280 °C (power 600 W) within 10 min. The morphologies of $LiFe_{1-x}(VO)_xPO_4$ had several types including rods, plate-like particles, and spheres. $LiFe_{1-x}(VO)_xPO_4$ is thermally unstable and a metastable phase that is difficult to be synthesized by the conventional method.

Nanostructured chalcogenides have also been prepared by the microwave-assisted method in mixed solvents of water and polyols. Jiang et al.[860] prepared Bi_2S_3 nanostructures with urchin-like and rod-like morphologies using Bi_2O_3, HCl, and $Na_2S_2O_3·5H_2O$ in mixed solvents of EG and water by microwave heating at 190 °C for 30 s. Urchin-like Bi_2S_3 nanostructures were obtained using SDS or in the absence of any surfactant; however, Bi_2S_3 nanorods were obtained in the presence of CTAB. Liu et al.[862] prepared $Ru_{85}Se_{15}$ nanoparticles with an average size of ∼1.8 nm using $RuCl_3$ and Na_2SeO_3 in mixed solvents of EG and a small amount of water via a rapid microwave-assisted process at 700 W for 1.5 min. Nekooi et al.[861] synthesized Ru_xSe_y nanoparticles using $RuCl_3·0.5H_2O$, $Na_2SeO_3·5H_2O$, and KOH in mixed solvents of EG and water by microwave refluxing heating at 1000 W for 75 s under stirring.

Bi_2Te_3 hollow nanospheres with diameters of 50−100 nm were prepared using TeO_2, $Bi(NO_3)_3$ and HNO_3 in mixed solvents of water and EG by microwave heating at 150 °C for 30 min.[863] Bi_2Te_3 nanosheets and nanotubes were prepared using $Bi(NO_3)_3·5H_2O$ and TeO_2 in mixed solvents of EG and water via the microwave-assisted method at 170−195 °C for 30−60 min. It was found that both the nanosheets and the nanotubes were well-crystallized single crystals, and morphologies of the products were greatly affected by the microwave heating temperature. A possible formation mechanism related to the layer structure rolling was also proposed.[864] Dong et al.[865] synthesized Sb_2Te_3 single-crystalline nanosheets with thicknesses of 50−70 nm using $SbCl_3$, Na_2TeO_3, hydrazine hydrate, and EG by the microwave-assisted method at 200 °C for 15 min, and the reaction mechanism was proposed. The bulk sample of Sb_2Te_3 nanosheets was prepared by the spark plasma sintering, which still consisted of Sb_2Te_3 nanosheets after the spark plasma sintering and thermoelectric property measurements, and a relatively high ZT value of 0.58 at 420 K was obtained. They also reported the rapid microwave-assisted solvothermal synthesis of Sb_2Te_3 nanostructures with a variety of morphologies including single-crystalline nanorods, individual nanosheets, nanorods with branched ultrathin nanosheets, and half-nanotubes constructed by self-assembly of nanocrystals.[866] In this method, $SbCl_3$, TeO_2, hydrazine hydrate, PEG, and EG were used as starting reagents, and the reaction system was heated by microwaves at 200 °C for 15 min. The morphology of Sb_2Te_3 nanostructures could be controlled by simply altering the amount of hydrazine hydrate and PEG. The tablet samples of Sb_2Te_3 nanostructured powders with different morphologies were prepared by a room-temperature pressurized method, and they exhibited high Seebeck coefficients, which were much higher than those of Sb_2Te_3 bulk crystals.

Mi et al.[885] reported the microwave-assisted solvothermal synthesis of $NaYF_4$:Yb,Er nanoparticles adopting mixed solvents of EG and water at 160 °C for 1 h. Rare earth acetates were used as rare earth precursors, and NH_4F (or NH_4HF_2, NaF, ionic liquid $[BMIM][BF_4]$) and NaCl were used as the sources of fluorine and sodium, respectively. The as-prepared nanoparticles were nearly ellipsoidal or spherical, with an average size of ∼41 nm and with mixed hexagonal and cubic structures. Lei et al.[886] prepared Ce^{3+}- and Tb^{3+}-doped $BaYF_5$ nanocrystals using $Ba(CH_3COO)_2$, $Y(NO_3)_3$, NH_4F, $Ce(NO_3)_3$, and $Tb(NO_3)_3$ in mixed solvents of EG and water by microwave heating for 10 min.

In addition to the single-phase nanostructured materials, various nanocomposites have been successfully prepared by the microwave-assisted method in mixed solvents of water and polyols. Wang et al.[841] prepared Pt−Ru/graphene and SnO_2/graphene nanocomposites in a mixture of EG and water by a microwave-assisted process at 700 W for a total time of 4 min. One of the advantages of this method is that the reduction of graphene oxide to graphene and the formation of Pt−Ru nanoparticles from metal precursors and SnO_2 nanoparticles from $SnCl_2$ precursor can be realized simultaneously. Zhao et al.[890] prepared $Pt/CeO_2/C$ nanocomposites using H_2PtCl_6 and $(NH_4)_2Ce(NO_3)_6$ in the presence of commercial carbon in mixed solvents of EG and water by one-step pulsed microwave refluxing at 650 W for 10 min. Pt nanoparticles as well as CeO_2 nanoparticles were relatively uniform in size and highly dispersed on the carbon support. Carbon-supported Ir_xSe_y nanocomposites with different Se/Ir atomic ratios were synthesized using H_2IrCl_6 and Na_2SeO_3 in mixed solvents of EG and a small amount of water via a microwave-assisted process. Ir_xSe_y nanoparticles were well dispersed on the surface of the carbon support with a narrow particle size distribution at $y/x \leq 1/3$.[887] $Ru_{85}Se_{15}$ nanoparticles supported on multiwalled carbon nanotubes were synthesized using $RuCl_3$, Na_2SeO_3, and carbon nanotubes in mixed solvents of EG and water by microwave heating at 900 W for 1.5 min.[888] Pt_3Te nanoparticles with an average size of ∼2.8 nm well dispersed on commercial carbon were prepared using $H_2PtCl_6·6H_2O$ and $Na_2TeO_4·2H_2O$ in mixed solvents of EG and water by microwave refluxing within a few minutes.[889]

Chen et al.[891] reported the rapid microwave-assisted synthesis of the magnetic nanocomposite consisting of HAP ultrathin nanosheets and magnetic Fe_3O_4 nanoparticles at 120 °C for 30 min. In this method, $Ca(CH_3COO)_2$, $NaH_2PO_4·2H_2O$, block copolymer PLA−mPEG, and preformed Fe_3O_4 nanoparticles were used as the starting materials in mixed solvents of deionized water and EG. For the synthesis of Fe_3O_4 magnetic nanoparticles, tris(acetylacetonato) iron(III) ($Fe(acac)_3$) and tris(acetylacetonato) iron(II) ($Fe(acac)_2$) were used as the reactants in dibenzyl ether, oleic acid, and ionic liquid $[BMIM][BF_4]$, and the suspension was microwave-heated to 200 °C and maintained at this temperature for 5 min; then, the reaction system was heated to 230 °C and maintained at this temperature for 10 min. The as-prepared nanocomposite was investigated as the drug nanocarrier using hemoglobin (Hb) and docetaxel as model drugs. It was found that the adsorption amount of Hb on the nanocomposite increased with increasing Hb initial concentration. The release of Hb from the

nanocomposite was essentially governed by a diffusion process. The nanocomposite had a good sustained release profile of docetaxel, and showed the property of pH-responsive drug release, which can be explained by gradual dissolution of HAP in a low pH environment. The nanocomposite had a high biocompatibility and also a high in vitro anticancer effect after loading docetaxel. Because of the high biocompatibility, magnetic response property, pH-controlled sustained drug release, and the ability to enter cells, the as-prepared nanocomposite is promising for the application in drug delivery.

Heuser et al.[892] reported the microwave-assisted synthesis of nanoparticles of Fe_3O_4 or ZnO coated on zeolite A at 150 °C for 10 min. Glycerin (60% v/v) was added to a $FeSO_4$/zeolite/NaOH solution to increase the solution viscosity and affect Fe_3O_4 nucleation and growth. The microwave irradiation assisted in displacing either ferrous or zinc ions from the preloaded zeolite network and increasing the reaction rate. These experiments showed the ability of using zeolite ion-exchange as a means of delivering cations in reactions where the zeolite served as a microreactor. Microwave radiation increased the ion exchange rate in a controlled manner to displace ions from the zeolite network to form Fe_3O_4 or ZnO by reactions of $FeSO_4$ or $Zn(NO_3)_2$ with NaOH. Chang et al.[893] prepared the SnS_2/SnO_2 nanocomposite adopting $SnCl_4$ and L-cysteine as the reactants in mixed solvents of EG and water by a microwave-assisted reaction at 700 W for 3 min. The influence of the molar ratio of $SnCl_4$ to L-cysteine on the product was investigated. It was found that SnS_2/SnO_2 nanoparticles were obtained when the molar ratio of $SnCl_4$ to L-cysteine was 1:2, and nanosheets instead of nanoparticles were formed at higher content of L-cysteine.

6.1.2. Water/Alcohols. Alcohols are good solvents for microwave heating, and their abilities to absorb microwaves are generally better than that of water, as was shown in Table 1. For example, the loss tangent (tan δ) value of ethanol is 0.941 at 2.45 GHz and 20 °C, much higher than that of water (0.123). The mixed solvents of water and alcohols will certainly enhance the abilities to absorb microwaves as compared to that in the case of using water as the only solvent. Alcohols are highly miscible with water and are able to form intermolecular hydrogen bonds with each other and with neighboring water molecules in solution.[25] Because alcohols especially with low molecular weights have usually relatively low boiling points, the open reaction systems with mixed solvents of water and alcohols will allow only low-temperature chemical reactions, and the solvothermal reactions in closed systems are needed for relatively high-temperature microwave-assisted synthesis.

A variety of inorganic nanostructures have been prepared by the microwave-assisted method in mixed solvents of water and alcohols, including noble metals,[896,897] iron oxides,[898,899] SnO_2,[900,901] Eu^{3+}-doped SnO_2,[902] TiO_2,[903−906] La^{3+} and Zr^{4+} codoped TiO_2,[907] CuO,[908] ZnO,[901] SiO_2,[909] $Ni(OH)_2$,[910,911] $Co(OH)_2$,[912] $Cd(OH)_2$,[913] $PbTiO_3$,[271] N-doped titanate,[914] Sn^{2+}-doped $BaTiO_3$,[915] ZnS:Mn^{2+},[916] CdSe,[917] WC,[39] YF_3 and lanthanide-doped YF_3,[918] aluminum hydroxyfluoride,[919] $Sn_{1.24}Ti_{1.94}O_{3.66}(OH)_{1.50}F_{1.42}$,[920] Au/$SiO_2$,[921] Ag/mesoporous SBA-12,[922] Co_3O_4/graphene,[923] C/TiO_2,[924] silica/iron oxide,[925] SiO_2-coated Ag,[926] SiO_2-coated γ-Al_2O_3,[927] TiO_2-coated ZnO,[928] $Fe_3O_4/SiO_2/NH_2$,[929] TiO_2/polystyrene,[930] and polystyrene/CdS.[931]

Tu et al.[896] reported the microwave-assisted preparation of PVP-stabilized colloidal nanoparticles of a variety of noble metals including Pt, Ir, Rh, Pd, and Au in mixed solvents of methanol and water using a modified domestic microwave oven. The reactants used were $H_2PtCl_6·6H_2O$, $H_2IrCl_6·6H_2O$, $RhCl_3·3H_2O$, $H_2PdCl_4·nH_2O$, $HAuCl_4·3H_2O$, NaOH, and PVP. The as-prepared colloidal solutions of noble metal nanoparticles were stable for several months. The colloidal noble metal nanoparticles synthesized by microwave heating had smaller relative standard deviations than those prepared by the conventional oil bath heating, implying a better dispersity of nanoparticles obtained by microwave heating.

Many papers have been published reporting on the microwave-assisted synthesis of nanostructured metal oxides in mixed solvents of water and alcohols. Cao et al.[899] reported the one-step NaCl-assisted microwave-solvothermal synthesis of monodisperse α-Fe_2O_3 mesoporous microspheres formed by oriented assembly of nanocrystals. In this method, $Fe(NO_3)_3·9H_2O$ was used as the iron source, and PVP acted as a surfactant in the presence of NaCl in mixed solvents of water and ethanol. NaCl was found to play an important role in the formation of monodisperse α-Fe_2O_3 mesoporous microspheres. One of the advantages of this method is that the size of α-Fe_2O_3 mesoporous microspheres can be adjusted in the range from ∼170 to ∼260 nm by adjusting the experimental parameters. α-Fe_2O_3 mesoporous microspheres exhibited a high photocatalytic activity in the degradation of salicylic acid. The combination of the mesoporous structure with monodisperse microspheres is beneficial for the enhancement of the photocatalytic property of α-Fe_2O_3.

Zhang et al.[901] reported the microwave-assisted solvothermal synthesis of SnO_2 or ZnO nanostructured microspheres self-assembled by nanocrystals using $SnCl_4·5H_2O$, or $Zn(CH_3COO)_2·2H_2O$, NaOH, ethyl acetate, and CTAB in mixed solvents of deionized water and methanol at 160 °C for 30 min. The photocatalytic activity for methyl orange in aqueous solution was significantly enhanced by simply mixing as-prepared SnO_2 and ZnO nanostructured microspheres as compared to the single-phase ZnO or SnO_2. Birkel et al.[900] prepared SnO_2 nanocrystals using $SnCl_4·5H_2O$ and an alkali (NaOH, KOH, tetramethylammonium hydroxide, or ammonia) in mixed solvents of ethanol and water by a microwave-assisted solvothermal process at 240 °C for 2 h. The morphology of the product could be controlled by the use of different alkalis. SnO_2 bundles of nanorods (5−10 nm in diameter) were obtained in the presence of NaOH, and SnO_2 nanocrystals with mixed morphologies of rods, spherical particles, and plates were obtained using KOH. The use of tetramethylammonium hydroxide led to the formation of a mixture of spherical, plate, and rod-like structures; however, very small nanoparticles were obtained in the presence of ammonia. Kar et al.[902] prepared Eu^{3+}-doped SnO_2 nanocrystals adopting $SnCl_4·5H_2O$, $Eu(NO_3)_3·6H_2O$, and NaOH in mixed solvents of water and ethanol by microwave heating at 100 °C for 5 min followed by calcination at 200−800 °C for 1 h. Zhu et al.[908] prepared CuO hierarchical hollow nanostructures assembled by nanosheets using $Cu(NO_3)_2·3H_2O$ and ammonia in mixed solvents of *n*-octanol and water through pulsed microwave heating at 1000 W for 3 min, and the morphology and size of building blocks and final products could be tuned by adjusting experimental parameters.

Wilson et al.[903] prepared anatase TiO_2 nanoparticles with sizes of 3−5 nm using titanium isopropoxide and HNO_3 in mixed solvents of water and isopropanol by microwave-solvothermal treatment for 5−10 min. Periyat et al.[904] prepared

dx.doi.org/10.1021/cr400366s | Chem. Rev. 2014, 114, 6462−6555

spherical aggregates of mesoporous nanocrystalline TiO_2 using titanium butoxide in mixed solvents of deionized water and an alcohol (isopropanol, ethanol, or butanol) by microwave heating at a power of 300 W for 2 min. The as-prepared materials possessed high specific surface areas up to 240 $m^2 g^{-1}$, which are higher than those of similar traditional sol−gel prepared or commercial samples. Wang et al.[905] prepared porous anatase TiO_2 spheres using titanium glycolate precursors (obtained by an EG-mediated sol−gel process) in mixed solvents of ethanol and water by microwave heating at 150 °C for 10 min. The effects of experimental conditions on the formation of titanium glycolate precursors and final TiO_2 spheres were investigated. Zhu et al.[906] prepared TiO_2 porous hollow microspheres formed by self-assembly of nanosized building blocks using tetrabutyl titanate as the titanium source in mixed solvents of ethanol and deionized water by microwave-assisted solvothermal treatment at 180 °C for 1 h.

The continuous flow microwave reactors have also been used for the synthesis of metal oxide nanostructures in mixed solvents of water and alcohol. Corradi et al.[909] prepared SiO_2 spherical nanoparticles from the hydrolysis and condensation of tetraethyl orthosilicate (TEOS) in mixed solvents of methanol and water by using a continuous flow microwave synthesis process. The flow rate was varied from 43 to 101 mL min^{-1}. The mean particle diameter became smaller than 50 nm as the residence time was decreased by increasing the flow rate to 101 mL min^{-1}.

Zhu et al.[271] prepared $PbTiO_3$ nanowires with diameters of 40−60 nm and lengths up to several micrometers and the aspect ratio close to 90 using $Pb(CH_3COO)_2{\cdot}3H_2O$, $Ti(OC_4H_9)_4$, and KOH in mixed solvents of water and ethanol by a microwave-solvothermal process at 200 °C for 90 min. The as-prepared nanowires tended to grow into a regular structure with parallel arrangement along their long axis in the [001] direction. Nitrogen-doped titanate nanotubes were prepared using preformed titanate nanotubes dispersed in mixed solvents of ethanol and water containing NH_4Cl by a microwave-solvothermal process at 130 °C for 2 h.[914] Sn^{2+}-doped $BaTiO_3$ nanopowder was synthesized using $BaCl_2$, $SnCl_2{\cdot}2H_2O$, $Ti(i\text{-}C_3H_7O)_4$, and KOH in mixed solvents of water and i-propanol by the microwave-assisted solvothermal method at 200 °C for 1 h. The particle sizes of $Ba_{1-x}Sn_xTiO_3$ were 20−40 nm and increased with increasing amount of doped Sn^{2+}.[915]

Metal hydroxide nanostructures have also been prepared by the microwave-assisted method in mixed solvents of water and alcohols. Xu et al.[910] prepared nanostructured flower-like α-$Ni(OH)_2$ architectures consisting of aggregated nanoflakes using $Ni(NO_3)_3{\cdot}6H_2O$ and urea in mixed solvents of distilled water and ethanol by the microwave-assisted solvothermal method at 90 °C for 15 min. The nanoflakes as the building blocks were built up from many nanocrystals with diameters of 2−3 nm. The as-prepared α-$Ni(OH)_2$ flower-like nanostructures had a higher electrochemical activity in the electrochemical reduction of O_2 as compared to α-$Ni(OH)_2$ synthesized by the conventional solvothermal method. $Ni(OH)_2$ flower-like architectures assembled with nanosheets with thicknesses of 10−20 nm were synthesized using $Ni(NO_3)_2{\cdot}6H_2O$, urea, $NH_3{\cdot}H_2O$, and PEG in mixed solvents of water and ethanol through the microwave-assisted solvothermal method at 160 °C for 30 min.[911] The microwave-assisted synthesis of $Co(OH)_2$ nanostructures was reported using $CoCl_2{\cdot}6H_2O$ and HMTA in mixed solvents of water and ethanol at 90 °C for 1−4 min.[912] Ultralong and flexible necklace-like nanostructures of $Cd(OH)_2$ were prepared in the *n*-octanol/aqueous liquid system by microwave heating, and a mechanism based on the synergistic effect of bubble-template and interface-assistance was proposed.[913]

Nanostructured metal chalcogenides have also been prepared in mixed solvents of water and alcohols by the microwave-assisted method. Ayele et al.[917] developed the low-temperature microwave-assisted synthesis of CdSe quantum dots with tunable sizes without adopting the hot injection technique. In their synthesis, $Cd(CH_3COO)_2{\cdot}2H_2O$, Na_2SeSO_3, and NaOH were used as reactants, a mixture of ethanol and deionized water was used as the solvent, and oleic acid was used as a capping ligand. By simply adjusting the experimental conditions such as temperature, time, and microwave power, CdSe quantum dots with sizes ranging from 2.3 to 2.8 nm were obtained.

The microwave-assisted method has been proven to be successful for the preparation of nanostructures of many other compounds in mixed solvents of water and alcohols. YF_3 and lanthanide-doped YF_3 nanocrystals were prepared in mixed solvents of ethanol and water by the microwave-assisted approach at 90 W for 15 min. The as-prepared nanocrystals had diameters of ∼6−10 nm, and these nanoparticles aggregated to form bigger assemblies with diameters of ∼40−60 nm. The as-prepared YF_3 nanocrystals could well disperse in water, forming a stable and transparent colloidal solution.[918] Dambournet et al.[919] reported the two-step microwave-assisted solvothermal synthesis of platelet-shaped aluminum hydroxyfluorides derived from β-AlF_3 using $Al(NO_3)_3{\cdot}9H_2O$ and HF in mixed solvents of water and isopropanol at 100 °C for 10 min and then at 160 °C for 2 h.

The surface modification of various nanoparticles with silica was investigated for biomedical applications. However, silica encapsulation through the conventional methods requires long reaction times (hours to days). Bahadur et al.[921] reported rapid one-step microwave-assisted preparation of silica-coated gold (Au/SiO_2) nanoparticles with tunable silica shell thickness and surface functionalization (Figure 25). Figure 25a shows the

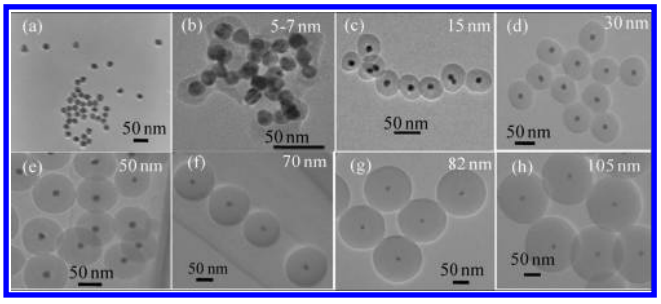

Figure 25. TEM micrographs: (a) uncoated Au nanoparticles; (b)−(h) $Au@SiO_2$ nanoparticles with different silica shell thicknesses prepared by the microwave-assisted method at different TEOS concentrations: (b) 1 mM, (c) 2 mM, (d) 3 mM, (e) 5 mM, (f) 10 mM, (g) 15 mM, and (h) 20 mM. $[H_2O]$ = 11 M, $[NH_3{\cdot}H_2O]$ = 0.8 M. Reprinted with permission from ref 921. Copyright 2011 Elsevier B.V.

TEM micrograph of uncoated Au nanoparticles prepared by the citrate reduction method, and the sizes of uncoated Au nanoparticles were uniform with an average diameter of ∼16 nm. Silica coating was carried out by microwave heating a reaction system containing Au nanocrystals, TEOS, and ammonia in mixed solvents of water and ethanol at 50 °C for

5 min. Au/SiO_2 nanoparticles with a wide range of silica shell thicknesses (5−105 nm) were prepared within 5 min of microwave irradiation by only changing the concentration of TEOS. The size uniformity and monodispersity of Au/SiO_2 nanoparticles were found to be better as compared to the product prepared by the conventional method. The microwave irradiation significantly reduced the preparation time (within 5 min) as compared to that of the conventional methods (hours to days). TEM micrographs of $Au@SiO_2$ nanoparticles with different silica shell thicknesses prepared by the microwave-assisted method (Figure 25b−h) show that almost all of the nanoparticles contained a single core of Au nanoparticle (∼16 nm) in the center. The as-prepared Au/SiO_2 nanoparticles were further functionalized with amino, carboxylate, and alkyl groups. Park et al.[925] demonstrated that uniform and spherical silica encapsulation of magnetic iron oxide nanoparticles could be achieved within 10 min via microwave irradiation after tetramethylammonium hydroxide-mediated phase transfer of monodisperse magnetic nanoparticles from the organic phase (2-propanol) to the water phase using TEOS.

Siddiquey et al.[927] prepared SiO_2-coated γ-Al_2O_3 nanoparticles by microwave heating. They first obtained the ethanol dispersion of γ-Al_2O_3 nanoparticles with diameters of ∼30 nm by the ball-milling technique. The γ-Al_2O_3 dispersion together with TEOS and aqueous ammonia in mixed solvents of ethanol and water then were heated by microwaves at 70 °C for 2 min in an open system, leading to rapid coating of γ-Al_2O_3 nanoparticles with a homogeneous silica shell with the thicknesses of ∼3−4 nm. This work demonstrates that the microwave heating can not only enhance chemical reactions, but also realize the homogeneous coating on nanoparticles. Thus, microwave heating is suitable for in situ synthesis of the core/shell nanostructures. A similar method was also applied to the coating of SiO_2 on Ag nanoparticles using preobtained colloidal Ag, TEOS, and dimethylamine in mixed solvents of water and ethanol by microwave heatng at 50 °C for 2 min.[926] The nanocomposite of amorphous TiO_2 layer (6−10 nm) coated on ZnO was prepared using titanium tetra-*n*-butoxide as the titanium source and commercial ZnO nanoparticles in mixed solvents of ethanol and water by the rapid microwave-assisted method at 70 °C for 2 min.[928] Stutz et al.[929] prepared $Fe_3O_4/SiO_2/NH_2$ core−shell nanoparticles by a three-step microwave-assisted route. They first prepared Fe_3O_4 nanoparticles using iron(III) acetylacetonate in benzyl alcohol under inert atmosphere by microwave heating at 170 °C for 12 min. In the next steps, they prepared Fe_3O_4/SiO_2 and $Fe_3O_4/SiO_2/NH_2$ core/shell nanoparticles using dispersed Fe_3O_4 or Fe_3O_4/SiO_2, TEOS, and ammonia in mixed solvents of ethanol and water by microwave heating at 60 °C for 3 min.

A combined procedure of sol−gel and microwave-assisted emulsion polymerization has been developed to prepare TiO_2/polystyrene core−shell nanospheres with TiO_2 nanoparticle as the core and polystyrene as the shell. $Ti(OC_4H_9)_4$ and NaOH were used as the reactants in mixed solvents of water and ethanol by microwave heating at 40 °C for 40 min. The resulting TiO_2 colloid was heated to 70 °C under nitrogen atmosphere, and then sodium dodecyl sulfonate, ammonium persulfate, and styrene monomer were added to initiate the emulsion polymerization on the surface of TiO_2 colloidal nanoparticles. It was found that the diameter of the TiO_2/polystyrene core−shell nanospheres could be regulated by the concentration of styrene monomer.[930] Polystyrene/CdS core−shell nanostructures were fabricated using $CdCl_2·2.5H_2O$, thioacetamide, and PVP in the presence of polystyrene microspheres in mixed solvents of deionized water and alcohol under microwave irradiation at 70 °C for 1.5 h.[931]

6.1.3. Water/*N*,*N*-Dimethylformamide. The mixed solvents of water and *N*,*N*-dimethylformamide (DMF) have been less reported for the microwave-assisted preparation of inorganic nanostructures. Xu et al.[932] reported the microwave-solvothermal synthesis combined with thermal treatment for the preparation of $Y_4Al_2O_9$ hierarchically nanostructured microspheres assembled with nanosheets. First, the microwave-assisted solvothermal method was used to prepare the precursor using $Y(NO_3)_3$ and $Al(NO_3)_3$ at 200 °C for 1 h in mixed solvents of water and DMF without any surfactant (pH ∼9 adjusted by aqueous ammonia). The thermal treatment of the precursor at 900 °C in air for 2 h then was performed to obtain $Y_4Al_2O_9$ hierarchically nanostructured microspheres, and the morphology of the precursor could be well preserved. The photocatalytic activity of as-prepared $Y_4Al_2O_9$ hierarchically nanostructured microspheres over phenol was investigated, and the degradation rate of phenol reached 91.2% in a time period of 4 h.

6.1.4. Water/1,2-Ethylenediamine. The mixed solvents of water and 1,2-ethylenediamine have also been adopted for the microwave-assisted preparation of inorganic nanostructures. Apte et al.[933] prepared Mn_3O_4 nanostructures using manganese nitrate in mixed solvents of water and ethylenediamine by microwave heating. The nanostructures were mostly spherical/cubic in shape and had sizes in the range of 10−50 nm; Mn_3O_4 nanorods with diameters of 9−10 nm were also obtained. Yan et al.[446] synthesized α-Fe_2O_3 spindle-like structures using $Fe(NO_3)_3·9H_2O$ in mixed solvents of ethylenediamine and distilled water by the microwave-assisted solvothermal method at 500 W for 50 min.

Limaye et al.[934] prepared ZnS nanorods with diameters of ∼50−100 nm using $ZnCl_2$ and thiourea in mixed solvents of water and ethylenediamine by microwave heating. It was revealed that the microwave refluxing time played an important role in determining the diameter of the nanorods. Li et al.[935] synthesized $Zn_xCd_{1-x}S$ nanorods with diameters of ∼10 nm using a preformed Zn−Cd precursor in mixed solvents of ethylenediamine and water by microwave heating at 140−160 °C for 10 min. $Zn_{0.28}Cd_{0.72}S$ exhibited the best photocatalytic activity for the degradation of methyl orange under visible light with a conversion ratio up to 96% after 6 h irradiation, which was higher than that of the sample prepared by the conventional solvothermal method.

Ma et al.[936] synthesized $SrCO_3$ one-dimensional nanostructures assembled from nanocrystals using $Sr(NO_3)_2$, $(NH_4)_2CO_3$, ethylenediamine, and water by the microwave-assisted solution method at 90 °C. The experiments showed that the microwave heating time played an important role in the size and morphology of $SrCO_3$. Zn_2GeO_4 nanorod bundles consisting of nanorods of 40−70 nm in diameter were prepared using $Zn(CH_3COO)_2·2H_2O$ and GeO_2 in the presence of PEG in mixed solvents of water and ethylenediamine via the microwave-assisted approach at 170 °C for 15 min.[937]

6.1.5. Other Binary Solvents. A variety of other binary solvents have also been applied to the microwave-assisted preparation of inorganic nanostructures. Examples for the microwave-assisted preparation of elemental nanostructures are discussed below. Doolittle et al.[938] adopted a water−sodium bis(2-ethylhexyl) sulfosuccinate (AOT)-heptane reverse micelle system for the preparation of Au nanoparticles by hydrazine

dx.doi.org/10.1021/cr400366s | *Chem. Rev.* 2014, 114, 6462−6555

reduction of $HAuCl_4$ under microwave radiation at 300 W, typically for 2 min. Chen et al.[939] prepared Pd nanoparticles via thermal decomposition of palladium acetate in the presence of an alkali in methyl isobutyl ketone and butanol under microwave irradiation for 1 min. The average diameters of Pd nanoparticles increased from 30 to 40 nm with the increase in the concentration of palladium acetate, and the as-prepared Pd colloidal nanoparticles were agglomerates from hundreds of smaller nanoparticles with sizes of 3−4 nm. Tong et al.[940] prepared 28−81 nm Pd pompon-like nanostructures formed by self-assembly of nanoparticles with an average size of ∼2.4 nm by thermal decomposition of palladium acetate in methyl isobutyl ketone and a small amount of EG under microwave irradiation at 900 W for 1 min. The sizes of Pd pompon-like nanostructures could be controlled by adjusting the concentration of palladium acetate. Rapid microwave-assisted thermal reduction of graphene oxide to graphene was achieved in mixed solvents of *N*,*N*-dimethylacetamide and water at the temperature up to 165 °C for 1−10 min.[941]

Nanostructured metal oxides have been successfully prepared by the microwave-assisted method in a variety of binary solvents. For example, microporous SnO_2 nanostructures were prepared using $SnCl_4{\cdot}5H_2O$ amd CTAB in mixed solvents of water and ethanolamine via microwave heating at 160 °C for 10 min, and different SnO_2 nanostructures could be obtained by adjusting the concentration of CTAB.[942] ZnO nanoparticles and nanorods were synthesized from the reaction between $Zn(NO_3)_2{\cdot}6H_2O$ and NaOH in water and PEG with low molecular weights under 180 W microwave irradiation for 30 min.[943] ZnO micro- and nanostructures with a variety of morphologies were synthesized using $Zn(NO_3)_2{\cdot}6H_2O$, pyridine, and water by the microwave-assisted method at 90 °C for 10 min. The pyridine had a significant influence on the morphology of ZnO. Various morphologies of ZnO (hexagonal columns, linked hexagonal needles, hollow structures, and hexagonal nanorings) were obtained by adjusting the concentration of pyridine. The effects of other alkaline additive (aniline and triethanolamine) on the morphology of ZnO were also investigated.[944] α-Fe_2O_3 nanoparticles were synthesized using $FeCl_3$ in mixed solvents of absolute ethanol and acetic acid by the combination of microwave irradiation and esterification at 150 °C for 15 min. In this method, water produced by the esterification between ethanol and acetic acid leads to the forced hydrolysis of Fe^{3+} ions. Microwave irradiation greatly promoted the growth of α-Fe_2O_3 nanoparticles as compared to the conventional solvothermal approach, agitation could ensure the formation of pure hematite phase, and the akaganeite phase was formed without stirring.[945] By using a similar method, TiO_2 nanoparticles with sizes of ∼9−12 nm were obtained.[946] Szeifert et al.[947] prepared highly dispersible anatase TiO_2 nanoparticles with sizes of ∼3 nm using $TiCl_4$ in mixed solvents of *tert*-butyl alcohol and toluene. Microwave heating could enhance the crystallinity of the nanoparticles and drastically shorten the reaction time to less than 1 h at a temperature as low as 50 °C. Parmar et al.[948] reported the rapid (10 min) microwave-solvothermal synthesis of TiO_2 nanorice nanoparticles (6−15 nm wide, 30−100 nm long) using Ti-isopropoxide in mixed solvents of acetylacetone and deionized water (pH ∼11.7 adjusted by 30% ammonia) at 180 °C. In addition, the as-synthesized TiO_2 nanorice nanoparticles showed a high stability against annealing treatment, retaining high surface area and large pore volume.

Nyutu et al.[949] produced multigram quantities of cryptomelane-type manganese oxide (K-OMS-2) nanostructured materials in the size range of 4−20 nm and with high surface areas up to 227 $m^2\ g^{-1}$ via an open-vessel microwave-refluxing route in aqueous and nonaqueous mixed solvents. The solvents used were dimethyl sulfoxide, DMF, EG, propylene glycol, sulfolane, dimethylacetamide, ethanol, *N*-methyl pyrrolidone, and ethyl acetate. The OMS-2 nanofiber diameter could be controlled by varying the amount of the cosolvent or type of the cosolvent. Opembe et al.[950] reported the continuous flow microwave synthesis of cryptomelane-type K-OMS-2 nanofibers with a specific surface area of 213 $m^2\ g^{-1}$ in the mixed aqueous/organic solvent system. Panda et al.[951] reported the rapid microwave-assisted production of nanorods, nanowires, and nanoplates of rare earth oxides (M_2O_3, M = Pr, Nd, Sm, Eu, Gd, Tb, Dy). Metal acetate or acetylacetonate was used as the starting reagent in oleic acid and oleylamine, and the resulting solution was placed in a microwave oven with the power set to 70% of 650 W and operated in 3 min cycles (on for 2.5 min, off and stirring for 0.5 min). The uniformity of the nanorods and nanowires was demonstrated from their spontaneous assembly into highly ordered 2-D superstructures.

Nanostructured metal chalcogenides have been successfully prepared by the microwave-assisted method in a variety of mixed solvents. Caponetti et al.[952] adopted microwave irradiation in a water−sodium bis(2-ethylhexyl) sulfosuccinate−heptane microemulsion system to prepare CdS nanoparticles. The reaction was carried out in an open system, and the temperature was maintained at 35 °C by using a low microwave power ranging between 22 and 30 W. Under these circumstances, water was selectively driven off the aqueous core of reverse micelles, and, as a consequence, small, crystalline, and anhydrous CdS nanoparticles could be obtained. It was observed that microwave-irradiated nanoparticles grew faster and their size reached a constant value, and the final mean particle diameter was 2.7 nm, smaller than that observed in a nonirradiated sample. Shinde et al.[953] prepared CdS nanorod bundles as well as sea urchin-like and starfish-like hierarchical nanostructures using $Cd(CH_3COO)_2$ and thiourea in diethylene triamine and water by the microwave-assisted method at 140 °C for 10 min. Amalnerkar et al.[954] reported the microwave-assisted solvothermal synthesis of hierarchical CdS nanostructures including entangled nanorods, nanosticks, and nanoflowers using $Cd(CH_3COO)_2$ and thiourea in binary solvents of diethylenetriamine and deionized water typically within 5 min. Patra et al.[955] reported a microwave-assisted route to nanoflakes and dendrite-type β-In_2S_3 in high yield (>97%) using $InCl_3$ and thiourea in mixed solvents of EG and PEG-400, and the length and width of the resulting nanoflakes were in the range of 70−600 and 4−10 nm, respectively. Yan et al.[956] prepared amorphous α-Ag_2S nanowires using $AgNO_3$ in thioglycolic acid and water under microwave irradiation at various powers for 3 or 5 min. Wang et al.[957] reported a two-phase microwave-assisted synthesis of Cu_2S nanocrystals in the toluene−water system using $CuSO_4$ and dodecanethiol as the reactants at 190 °C for 4 h under a dynamic mode with a microwave power output of 125 W. The formation of Cu_2S nanocrystals was strongly correlated with the reaction temperature and time. The size of Cu_2S nanocrystals could be controlled from 3 to 8 nm by varying the concentration of alkyl-thiol. Panigrahi et al.[958] prepared WS_2 nanowires using tungstic acid and sulfur in monoethanolamine and water through a microwave-assisted route at 800 W for 5−6 min in

dx.doi.org/10.1021/cr400366s | *Chem. Rev.* 2014, 114, 6462−6555

cycles of 30 s. Acidification of the precursor solution yielded amorphous precipitate, which led to the formation of WS_2 nanowires with diameters of ~5−10 nm when heated at 750 °C under argon atmosphere for 1.5 h. $CuInS_2$ nanoparticles were synthesized by decomposition of a single source precursor $(Ph_3P)_2Cu(\mu\text{-}SEt)_2In(SEt)_2$ in dioctyl phthalate or benzyl acetate in the presence of 1,2-ethanedithiol via microwave irradiation at a reaction temperature as low as 100 °C and reaction times as short as 30 min. The particle sizes were 1.8−10.8 nm as reaction temperatures were varied from 100 to 200 °C with good size control and high yield (up to 95%).[959]

Sliem et al.[960] reported the synthesis of PbSe nanocrystals by the conventional hot injection process and also microwave irradiation using lead acetate, selenourea, and oleic acid in phenyl ether and DMF. They investigated the shape evolution of PbSe nanocrystals during microwave synthesis. The mechanism of morphology evolution from spherical to cubic shape was discussed. They proposed that the formation of PbSe nanocubes is attributed to the higher growth rate in the [111] direction as compared to that in the [100] direction. Han et al.[961] reported the microwave-assisted synthesis of ZnSe nanostructures with different morphologies including nanoparticles, rice-like nanocrystals, and rods using a solution of $Zn(CH_3COO)_2{\cdot}2H_2O$ in octylamine or octyldecylamine and a solution of Se in Tri-*n*-butylphosphine at 180 °C for 1−20 min. Panda et al.[962] reported the rapid microwave-assisted synthesis of aligned nanorods and nanowires of ZnS, ZnSe, CdS, and CdSe in a mixture of alkylamines (C_6−C_{18}) and DMF. For the synthesis of sulfides, a single precursor metal ethyl xanthate was used; and for selenides, a mixture of metal acetate and selenourea precursors was used.

Nanostructured metal fluorides have also been successfully prepared by the microwave-assisted method in a variety of mixed solvents. A variety of monodisperse GdF_3:Yb,Er upconversion nanocrystals with different shape, size, and dopants were synthesized by the microwave-assisted method at 290 °C for 10 min. In this method, lithium trifluoroacetate (TFA), gadolinium TFA, ytterbium TFA, and erbium TFA were used as the reactants in a 1:1 (v:v) mixture of oleic acid and octadecene in nitrogen atmosphere. In addition to monodisperse spherical nanoparticles, rhombic-shaped slices that showed a tendency for self-assembly into stacks were also obtained.[963] Wang et al.[964] synthesized monodisperse $NaYF_4$ nanocrystals using corresponding metal trifluoroacetates in mixed solvents of 1-octadecene and oleic acid by the microwave-solvothermal method at 290 °C for 5 min. Doping with Li^+ ions resulted in a significant increase in upconversion efficiency and a transition from cubic to tetragonal crystal lattice. AYF_4:Yb,Er (A = Na, Li) nanocrystals were synthesized in mixed solvents of 1-octadecene and oleic acid using a microwave-assisted process at 290 °C for 10 min.[965] It was found that the size of the nanocrystals could be controlled by adjusting the growth time, and the morphology of the nanocrystals could be controlled by the reactant concentration and composition. Low reactant concentrations resulted in monodisperse spherical nanocrystals; however, at high concentrations, nanocrystals grew into flowers when the crystallographic lattice was cubic, into wires at a Na/Li ratio of 1:4, and into rhombic shape for $LiYF_4$:Yb,Er nanocrystals. $KMgF_3$ nanocrystals were synthesized via the thermolysis of metal trifluoroacetate precursors in mixed solvents of oleic acid and oleylamine under microwave irradiation at 290 °C for 30 min. The crystal phase and shape of nanocrystals could be controlled by the variation of the ratio of oleic acid/oleylamine, resulting in the formation of near-spherical nanoparticles, and nanoplates of cubic-phased $KMgF_3$, as well as nanorods of tetragonal-phased MgF_2. Tb^{3+}-doped $KMgF_3$ nanocrystals were also prepared by this method, and they exhibited a strong green emission.[966]

Liu et al.[967] reported that photoluminescent carbon nitride dots could be prepared using CCl_4 and 1,2-ethylenediamine as both reactants and solvents by a simple heat treatment-based strategy. The formation of carbon nitride dots was attributed to the polymerization of CCl_4 and 1,2-ethylenediamine under refluxing by microwave heating or solvothermal heating. The as-prepared carbon nitride dots exhibited a strong fluorescence.

Various nanocomposites can also be prepared by the microwave-assisted method in a variety of mixed binary solvents. Campelo et al.[922] prepared nanocomposites of Au or Pd nanoparticles/mesoporous SBA-12 using gold bromide or palladium acetate in mixed solvents of ethanol and acetone by microwave heating at 100−140 °C for different times (2, 5, 10, and 20 min). The metal nanoparticles had different sizes depending on the metal and the time of microwave irradiation. Herring et al.[968] prepared ZnO nanopyramids supported on reduced graphene oxide nanosheets by microwave heating $Zn(CH_3COO)_2$ and graphene oxide in a mixture of oleic acid and oleylamine. Highly active $Pt/TiO_2/C$ nanocomposite was synthesized in mixed solvents of EG and isopropyl alcohol by a microwave-assisted process.[969]

Herring et al.[970] reported a fast one-pot microwave-assisted synthesis route to Au/ZnO hybrid hexagonal nanopyramids by sequential homogeneous−heterogeneous nucleation steps. The rapid decomposition of $Zn(CH_3COO)_2$ by microwave heating in the presence of a mixture of oleic acid and oleylamine resulted in the formation of hexagonal ZnO nanopyramids. In the presence of Au ions, the initially formed Au nanocrystals acted as heterogeneous nuclei for the nucleation and growth of ZnO nanopyramids. Using preformed Au nanoparticles instead of Au ions resulted in a narrow size distribution of uniform Au/ZnO nanopyramids, each consisting of a gold nanoparticle embedded in the center of the hexagonal base of the ZnO nanopyramid. ZnO did not form by microwave heating the reaction mixture for 10 min with powers ranging from 100 to 500 W, and the first sign of ZnO growth was observed after 10 min of microwave heating at a power of 600 W (126 °C). ZnO spindles began to grow from gold nanoparticles resulting in Au−ZnO nanocomposites that consisted of a spherical gold nanoparticle attached to a small ZnO rod. As the microwave power was increased to 700 W (149 °C), the ZnO spindles attached to gold nanoparticles increased in size. By increasing the microwave power to 800 W (160 °C), the ZnO spindles began to encapsulate the gold nanoparticle in the center of the hexagonal base, and the development of the ZnO nanopyramid could be clearly observed. Further increase of the microwave power to 900 W (184 °C) resulted in a sudden increase in the number density of the Au/ZnO nanostructures, and most of the nanopyramids appeared to be fully developed. Finally, with full microwave power of 1000 W (214 °C), well-defined hexagonal pyramids, with each pyramid containing a single Au nanoparticle in the center of its hexagonal base, were formed as shown in Figure 26.

Bensebaa et al.[971] prepared Pt−Ru nanoparticles with an average size of 2.8 nm stabilized within a conductive polymer matrix polypyrrole di(2-ethylhexyl) sulfosuccinate by microwave refluxing heating at 163 °C for 3 min, and H_2PtCl_6, $RuCl_3$,

dx.doi.org/10.1021/cr400366s | Chem. Rev. 2014, 114, 6462−6555

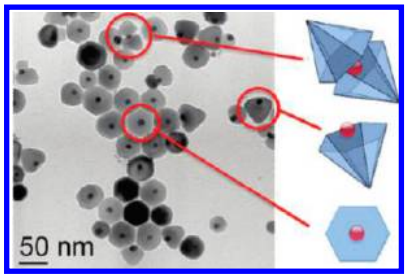

Figure 26. TEM micrograph of Au/ZnO nanostructures obtained from a reaction mixture containing 0.05 M $Zn(CH_3COO)_2$, 0.5 mL solution of preformed Au nanoparticles, and 1:2 molar ratio of oleic acid/oleylamine after 10 min microwave irradiation at a power of 1000 W (214 °C). Reprinted with permission from ref 970. Copyright 2011 American Chemical Society.

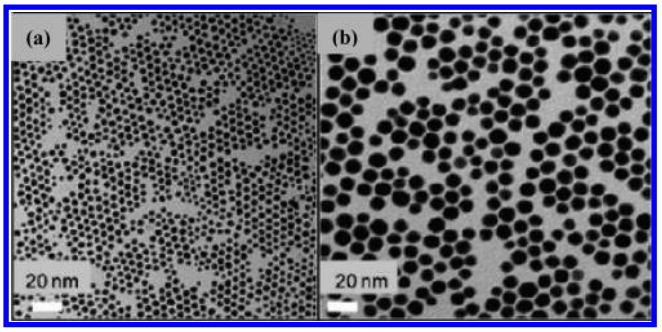

Figure 27. TEM micrographs of Au nanoparticles prepared using oleylamine (a) and in 1:1 ratio of oleic acid/oleylamine (b). Reprinted with permission from ref 973. Copyright 2010 American Chemical Society.

and polypyrrole di(2-ethylhexyl) sulfosuccinate were used as the starting materials in methanol and EG. Kate et al.[972] synthesized the polypyrrole/Ag nanocomopposites under microwave irradiation based on interfacial polymerization at a water/chloroform interface using pyrrole and $AgNO_3$ solutions at 20% microwave power of 800 W for 1, 2, and 3 min. Pyrrole was partially dissolved in chloroform and $AgNO_3$ was completely dissolved in distilled water, and the reaction proceeded at the water/chloroform interface, leading to the formation of Ag nanoparticles with sizes of ~20 nm dispersed in the polypyrrole matrix.

6.2. Ternary and Multinary Solvent Systems

In recent years, some researchers have adopted ternary and multinary solvent systems for the microwave-assisted preparation of a variety of inorganic nanostructures, including Au,[973] Ag,[974] ZnO,[975] α-Fe_2O_3,[976] γ-Fe_2O_3,[977] Fe_3O_4,[978] Co_3O_4,[979] TiO_2,[980] CeO_2,[981] ZrO_2,[982] ZnS,[983] Ag_2S,[974] CdSe,[984,985] CdTe,[986] pnictogen chalcogenide,[987] $SrTi_{1-x}Cr_xO_3$,[988] MFe_2O_4 (M = Ni, Co, Mn),[977] AlOOH,[989] AlOOH:Tb^{3+},[990] aluminum hydroxyfluoride,[991] $NaGdF_4$:Ln^{3+} (Ln = Yb, Er/Tm/Ho),[992] Eu^{3+}-doped HAP,[993] zeolite,[994] Au/carbon nanotubes,[995] TiO_2/graphene,[996] Pt/WO_3/C,[997] Pt/polypyrrole,[998] La_2O_3/$BaCO_3$,[999] CdSe/graphene,[1000] CdSe/ZnS,[1001,1002] and ZnO/ZnS/γ-Fe_2O_3.[1003]

For the microwave-assisted preparation of metal nanostructures in ternary and multinary solvent systems, two examples are discussed below. Mohamed et al.[973] reported the fast one-pot microwave-assisted preparation of Au nanoparticles with different shapes capped with a mixture of oleylamine and oleic acid. In this method, an appropriate amount of $HAuCl_4$ in HCl solution was mixed with oleylamine and oleic acid, and the reaction system was microwave heated for only ~1 min. The size and morphology of the nanocrystals could be tailored by varying the ratio of oleylamine to oleic acid, microwave heating time, and concentration of $HAuCl_4$. Pure oleylamine led to the formation of only spherical Au nanoparticles, and addition of oleic acid increased the growth rate and enhanced the formation of anisotropic shapes. Figure 27 shows the TEM micrographs of Au nanoparticles prepared in the presence of oleylamine and in a 1:1 ratio of oleylamine to oleic acid, indicating that in both cases the resulting Au nanoparticles were spherical but exhibited clearly different sizes. The average sizes of the nanoparticles prepared in pure oleylamine and in a 1:1 ratio of oleylamine to oleic acid were ~8.0 ± 1.0 and 15.0 ± 2.0 nm, respectively. Gao et al.[974] reported the preparation of hexagonally arranged spherical Ag nanocrystals by one-step microwave-assisted solvothermal interface reaction at 160−170 °C for 3 h using $AgNO_3$, dodecylthiol, EG, and toluene. The ratio of EG/dodecylthiol had an effect on the morphology and arrangement of the obtained Ag nanoparticles. At a low volume ratio, Ag nanocrystals with a rectangular shape arranged in orthogonal arrays could be observed.

Metal oxide nanostructures have also been prepared by the microwave-assisted method in ternary and multinary solvent systems. Erten-Ela et al.[975] prepared ZnO nanorods using $Zn(CH_3COO)_2{\cdot}2H_2O$ and NaOH in mixed solvents of water, PEG-400, and absolute ethanol by microwave heating at 140 °C for 30 min. α-Fe_2O_3 nanocubes were prepared by thermal decomposition of iron oleate complex in mixed solvents of oleic acid, triethylene glycol, ethanol, and water via the microwave-assisted solvolthermal method at 400 W for 6 min, followed by the Ostwald ripening process, and the primary nanoparticles synthesized by microwave heating were low crystalline with an average diameter of ~6 nm.[976] Co_3O_4 nanocubes with sizes of ~20 nm were prepared using $Co(NO_3)_2{\cdot}6H_2O$ and sodium oleate in mixed solvents of ethanol, hexane, and deionized water by the microwave-assisted solvothermal method at 200 °C for 20 min.[979] Hierarchical nanostructures of TiO_2 were prepared using TiF_4, urea, and CTAB in mixed solvents of water, cyclohexane, and 1-pentanol by the microwave-assisted method at 120 °C for different time periods.[980] CeO_2 nanoparticles, nanocubes, and nanorods were synthesized using $Ce(NO_3)_3$ in mixed solvents of water, EG, oleic acid, and *tert*-butylamine by microwave heating for 2−30 min, and the shape of CeO_2 nanostructures could be adjusted simply by varying the microwave irradiation time.[981] ZrO_2 nanoparticles were synthesized from the hydrolysis and condensation of tetra-*n*-propylzirconate in mixed solvents of ethanol, caproic acid, and water by a continuous microwave synthesis process.[982]

Sulaeman et al.[988] reported the microwave-assisted solvothermal synthesis of Cr-doped $SrTiO_3$ ($SrTi_{1-x}Cr_xO_3$, x = 0−0.2) nanoparticles (15−20 nm) using $SrCl_2{\cdot}6H_2O$, $Cr(NO_3)_3{\cdot}9H_2O$, $Ti(OC_3H_7)_4$, and KOH in mixed solvents of water, 2-propanol, methanol, and oleic acid at 200 °C for 3 h. Baruwati et al.[977] synthesized MFe_2O_4 (M = Ni, Co, Mn) and γ-Fe_2O_3 nanoparticles with sizes of 5−10 nm at the water−toluene interface in the presence of oleic acid under the conventional as well as microwave hydrothermal conditions using nitrate or chloride salts. AlOOH hierarchically nanostructured microspheres constructed by nanosheets were prepared by the microwave-assisted solvothermal method using $AlCl_3{\cdot}6H_2O$, NaOH, and CTAB in a mixture of deionized water, methanol, and ethyl acetate at 160 °C for 30 min. γ-Al_2O_3 hierarchically

dx.doi.org/10.1021/cr400366s | *Chem. Rev.* 2014, 114, 6462−6555

nanostructured microspheres were obtained by heating AlOOH hierarchically nanostructured microspheres to 500 °C in air, and the morphology could be well preserved during the thermal transformation process.[989] AlOOH:Tb^{3+} microspheres constructed by nanosheets were prepared using $AlCl_3 \cdot H_2O$, $Tb(NO_3)_3 \cdot H_2O$, NaOH, and CTAB in a mixture of deionized water, methanol, *n*-butyl alcohol, and ethyl acetate via the microwave solvothermal approach at 160 °C for 30 min.[990] Dambournet et al.[991] synthesized pyrochlore-type aluminum hydroxyfluoride nanoparticles with an average size of 12 nm using a microwave-solvothermal process. The reactants used in the synthesis were Al(III) isopropoxide and HF in mixed solvents of isopropanol, ether, and distilled water. In the first step, a temperature of 200 °C was rapidly reached by keeping the microwave power at 300 W; thereafter, the temperature was kept at 160 °C for 1 h. The optimization of the crystallite size and surface area of the product was performed by varying experimental parameters including the nature of the aluminum precursor, choice of solvents, and addition of a small amount of ether.

Wang et al.[992] adopted the microwave-solvothermal method for the rapid synthesis of nanocrystals of lanthanide-doped hexagonal phase $NaGdF_4:Ln^{3+}$ (Ln = Yb, Er/Tm/Ho) with multicolour upconversion luminescence and paramagnetic properties. $LnCl_3$, NaF, and NaOH were used as the starting reagents in mixed solvents of deionized water, oleic acid, and alcohol. The shape of the nanocrystals could be manipulated from rod-like to spherical just by tuning the initial concentration of reactants. The product obtained at 160 °C for 5 min was relatively uniform nanorods with the average sizes of 76.4 ± 1.3 nm in length and 17.1 ± 0.6 nm in diameter. When the reaction temperature was kept at 160 °C and the reaction time changed, the as-prepared product exhibited a uniform rod-like morphology, while the aspect ratio of nanorods varied obviously with the reaction time. For example, the average length increased from 76.4 to 121.5 nm when prolonging the holding time from 5 to 90 min. Yang et al.[993] prepared Eu^{3+}-doped HAP nanostructures including nanorods and nanoparticles using $Eu(NO_3)_3$, $Ca(NO_3)_2 \cdot 4H_2O$, $(NH_4)_2HPO_4$, and CTAB in mixed solvents of *n*-butanol, *n*-octane, and water via a microemulsion-mediated microwave-assisted process, and the morphology of the product could be adjusted by altering the pH value.

Various nanocomposites have been successfully prepared by the microwave-assisted method in ternary and multinary solvent systems. For example, the microwave-assisted microemulsion synthesis of carbon-supported Pt−WO_3 nanoparticles was reported by Yang et al.[997] Amorphous WO_3 nanoparticles of 1 nm in size were first deposited onto carbon from an alkaline tungstate containing microemulsion via mixing with an acid-containing microemulsion under microwave exposure. Pt nanoparticles with an average size of 2.5 nm were subsequently deposited onto the carbon-supported WO_3 nanoparticles by reducing H_2PtCl_6 in microemulsion by microwave heating. Jeon et al.[998] synthesized polypyrrole nanospheres (~80 nm) using micelles composed of tetradecyl trimethylammonium bromide and decyl alcohol. Pt nanoparticles (~3.2 nm) supported on polypyrrole nanospheres were prepared using $H_2PtCl_6 \cdot 3H_2O$ and polypyrrole nanospheres in mixed solvents of EG, 2-propanol, and water by a microwave-assisted process at 800 W for 7 min, and the pH value was adjusted between 7 and 8 using 0.4 M KOH. He et al.[999] synthesized $La_2O_3/BaCO_3$ nanocomposites using lanthanum nitrate, barium nitrate, methyl oxalate, and CTAB in 1-hexyl alcohol, *n*-hexane, and water from a coupling route of homogeneous precipitation with microemulsion by pulsed microwave heating for 10 min. Finally, the precursor was calcined at 800 °C for 1 h.

Zedan et al.[1000] reported the microwave-assisted synthesis of the nanocomposite consisting of CdSe nanocrystals dispersed on graphene sheets using oleic acid, dimethyl sulfoxide, and tributylphosphine. The reduction of graphite oxide into graphene occurred within 2 min of microwave irradiation as opposed to 12 h of the conventional heating at 180 °C. Cubic and hexagonal CdSe nanocrystals with average sizes of 2−4 and 5−7 nm, respectively, were prepared by the proper choice of the capping agent within a few minutes of microwave irradiation. Ziegler et al.[1001] reported a fast microwave-assisted procedure for the preparation of highly luminescent CdSe nanoparticles with ZnS shells. The effects of experimental parameters such as the temperature, time, and shell thickness on the luminescence quantum yield and stability of the ZnS shell were investigated. Roy and co-workers[1002] synthesized CdSe/ZnS nanoparticles by the two-step microwave-assisted method. In this method, CdSe cores were prepared using $Cd(CH_3COO)_2$ and elemental Se powder in trioctyl phosphine oxide, hexadecylamine, and trioctylphosphine. The second step was the addition of the zinc sulfide shell using CdSe nanoparticles as the core, and iethyl zinc (in heptane) in 1-methyl-2-pyrrolidinone, 3-mercaptopropionic acid, hexamethyldisilathiane, and butylamine. Zhu et al.[1003] prepared ZnO/ZnS/γ-Fe_2O_3 hollow spheres using zinc acetylacetonate, ferric acetylacetonate, and sodium bis (2-ethylhexyl) sulfosuccinate in mixed solvents of PEG-300, oleic acid, and ethylenediamine via microwave heating at 100 °C for 30 min. The hollow spheres were composed of ZnO, ZnS, and γ-Fe_2O_3 nanoparticles, and each hollow sphere had a distinct surface hole with the pore size of tens of nanometers or hundreds of nanometers.

7. MICROWAVE-ASSISTED SELF-ASSEMBLY OF NANOSTRUCTURES

Many successful examples for microwave-assisted self-assembly of nanostructures in liquid phase have been reported, including Pd,[940] Ag,[974,1004] Al,[1005] Ni,[528] SnO_2,[901] CuO,[186,851] α-Fe_2O_3,[169,295,899] Fe_3O_4,[522] ZnO,[901] Sm_2O_3,[951] Nd_2O_3,[951] Gd_2O_3,[951] NiO precursor,[1006] $Cd(OH)_2$,[859] α-FeOOH,[698] ZnS,[962] ZnSe,[962] $CaCO_3$,[868] $BaCO_3$,[391] GdF_3,[963] $NaYF_4$,[716,964] BiOBr,[618] hydroxyapatite,[350] and $FeMoO_4$.[879]

Gao et al.[974] prepared hexagonally arranged Ag nanoparticles using $AgNO_3$, dodecylthiol, EG, and toluene by one-step microwave-assisted solvothermal interface reaction at 160−170 °C for 3 h, and a thin layer of black product formed between the polar and the nonpolar solvents. A small amount of the black sample was dispersed in toluene, and then a drop of this solution was deposited on an amorphous carbon film on 300 mesh Cu grid for TEM observation directly without the technique of size-selective precipitation. The ratio of EG/dodecylthiol had an effect on the morphology and arrangement of the obtained Ag nanocrystals. At a low volume ratio, Ag nanoparticles with a rectangular shape arranged in orthogonal arrays were observed. The TEM micrographs of the as-prepared Ag nanocrystals are shown in Figure 28. The product consisted of hexagonal-like ordered superstructures of monodisperse Ag nanoparticles. The SAED pattern (Figure 28b) shows polycrystalline diffraction rings, which can be indexed to Ag with a cubic structure. A magnified TEM micrograph (Figure

dx.doi.org/10.1021/cr400366s | Chem. Rev. 2014, 114, 6462−6555

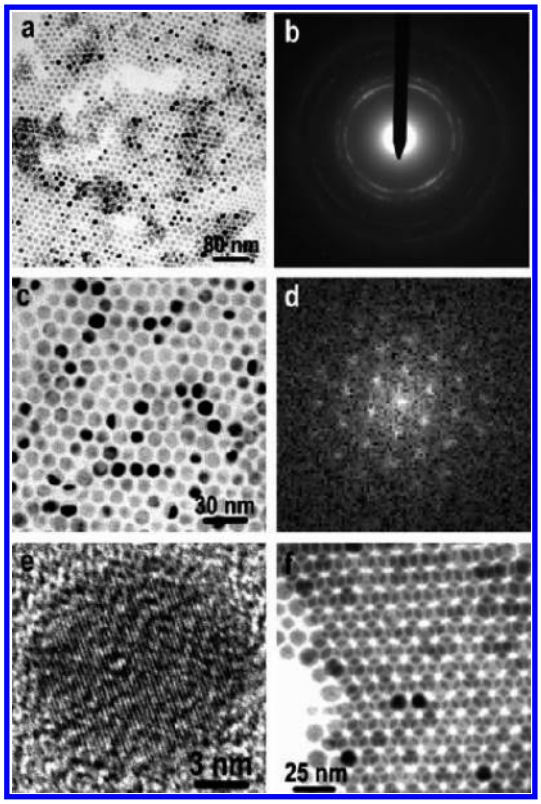

Figure 28. TEM micrographs, SAED pattern, Fourier transform power spectrum, and HRTEM image of the as-prepared Ag nanocrystals. Reprinted with permission from ref 974. Copyright 2005 American Chemical Society.

28c) displays monodisperse spherical nanoparticles with an average diameter of ~10 nm and interparticle spacings of ~2 nm. Fourier transform power spectrum (Figure 28d) shows ordered hexagonal-like spot arrays. The HRTEM image (Figure 28e) exhibits clear lattice planes in a nanocrystal. Figure 28f shows a TEM micrograph of two/three layers of superlattices, the upper layer was hexagonally arranged, and these nanocrystals were laid on the interspaces of the hexagonally arranged nanocrystals of the lower layer.

Olgun[1005] demonstrated the evaporation-induced rapid self-assembly of 52 nm Al nanoparticles and 19 nm Ag nanoparticles for the formation of microwires using different surfactant−solvent formulations by microwave heating at 51−55 °C. The formation of microwire patterns was due to stick−slip dynamics of the contact line on the surface of the substrate. By using microwave energy, the rapid self-assembly from metal nanoparticles was achieved within a few minutes. Poly(dimethylsiloxane) was used for the purpose of promoting microwire deposition, while Tween-20 was added as a stabilizer for Ag nanoparticles to prevent further agglomeration and growth in solution. The microwire deposition process presented in this study is relatively simple as compared to the previous patterning techniques. The use of a photoresist layer, a micropatterned mask, a monolayer coating, and molded patterns is not required in this method.

Cao et al.[899] reported a one-step NaCl-assisted microwave-solvothermal method for the preparation of monodisperse α-Fe_2O_3 mesoporous microspheres formed by self-assembly of nanocrystals using $Fe(NO_3)_3{\cdot}9H_2O$, PVP, and NaCl in mixed solvents of water and ethanol. NaCl was found to play an important role in the formation of monodisperse α-Fe_2O_3 mesoporous microspheres. Figure 29 shows the SEM and TEM characterization of the sample prepared at a microwave-

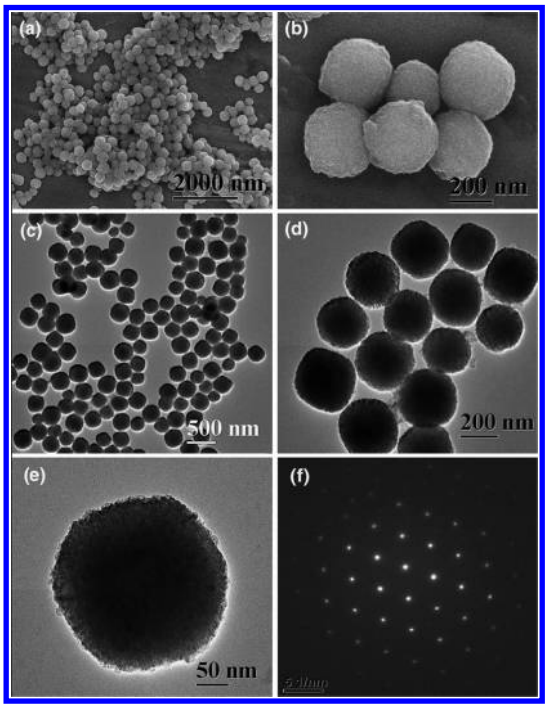

Figure 29. SEM and TEM characterization of monodisperse α-Fe_2O_3 mesoporous microspheres formed by self-assembly of nanocrystals using $Fe(NO_3)_3{\cdot}9H_2O$, PVP, and NaCl in mixed solvents of water and ethanol by the microwave-solvothermal method at 140 °C for 30 min. (a,b) SEM micrographs; (c−e) TEM micrographs; and (f) the SAED pattern of a single microsphere. Reprinted with permission from ref 899. Copyright 2010 Springer.

solvothermal temperature of 140 °C for 30 min. Almost exclusive α-Fe_2O_3 mesoporous microspheres assembled with nanocrystals were obtained. Figure 29f shows the SAED pattern of a single microsphere, revealing the single-crystal-like feature of the mesoporous microsphere formed via self-assembly of α-Fe_2O_3 nanocrystals. The size of α-Fe_2O_3 mesoporous microspheres could be controlled in the range from ~170 to ~260 nm by changing the experimental parameters such as the microwave-solvothermal time and concentration of PVP. The BET specific surface area of α-Fe_2O_3 mesoporous microspheres reached as high as 114 $m^2\ g^{-1}$. α-Fe_2O_3 mesoporous microspheres obtained at a lower temperature (120 °C) had a much higher specific surface area and narrower pore size distribution than those of the sample prepared at a higher temperature (140 °C). The oriented organization of smaller nanocrystals in α-Fe_2O_3 mesoporous microspheres obtained at a lower temperature (120 °C) led to a smaller average pore size (4.3 nm); in contrast, the bigger nanocrystals in α-Fe_2O_3 mesoporous microspheres obtained at a higher temperature (140 °C) resulted in a larger average pore size (7.9 nm).

Hu et al.[169] adopted a microwave-assisted hydrothermal process for the rapid synthesis of α-Fe_2O_3 self-assembled hierarchically nanostructured architectures using an aqueous solution containing $K_3[Fe(CN)_6]$. Several kinds of nanostructures, such as nanoparticles, dendritic crystals with different sizes, plates, and self-organized nanorods, could be obtained under different conditions. Figure 30a shows a low-magnification TEM micrograph of a star-shaped α-Fe_2O_3 crystal with a 6-

dx.doi.org/10.1021/cr400366s | Chem. Rev. 2014, 114, 6462−6555

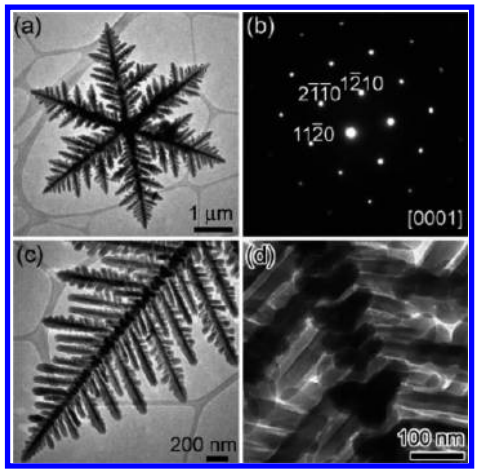

Figure 30. (a) TEM micrograph of a 6-fold-symmetric α-Fe_2O_3 dendrite; (b) electron diffraction pattern taken from a single dendrite, which shows the single-crystal nature of the entire dendritic structure; and (c and d) high-magnification TEM micrographs of the dendrite. Reprinted with permission from ref 169. Copyright 2007 American Chemical Society.

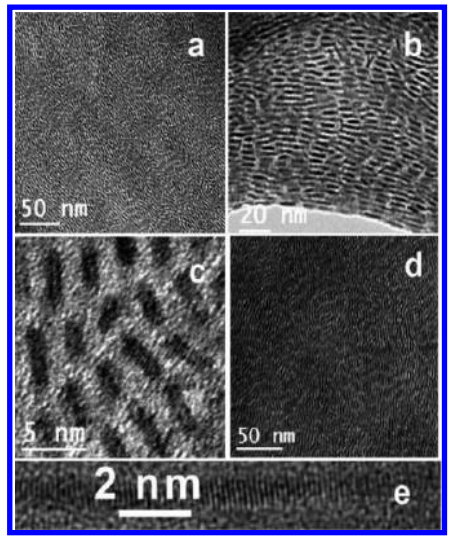

Figure 31. TEM micrographs: (a and b) Sm_2O_3 nanorods forming 2-D supercrystalline assembly; (c) HRTEM of Nd_2O_3 nanorods, (d) Gd_2O_3 nanowires; and (e) HRTEM of a Gd_2O_3 nanowire. Reprinted with permission from ref 951. Copyright 2007 American Chemical Society.

fold symmetry standing on the copper grid, and its corresponding electron diffraction pattern is shown in Figure 30b. The electron diffraction patterns on different α-Fe_2O_3 dendrites or different positions of a given single star-shaped crystal were essentially identical, suggesting that the α-Fe_2O_3 dendrite was single-crystal in nature. A close-up view of the hierarchically nanostructured architectures revealed that the central trunk exhibited a pagodas-like shape instead of a solid-rod shape. Tripod-like nanocrystals of ~100 nm as building blocks self-assembled in a head-to-head fashion into the central trunk. Figure 30c and d shows the high-magnification TEM micrographs of a trunk.

Panda et al.[951] prepared uniform nanorods, nanowires, and nanoplates of rare earth oxides (M_2O_3, M = Pr, Nd, Sm, Eu, Gd, Tb, Dy) using metal acetate or acetylacetonate in oleic acid and oleylamine by the rapid microwave-assisted method with the power set to 70% of 650 W and operated in 3 min cycles (on for 2.5 min, off and stirring for 30 s). The reported method allows the control of the size and shape of the rare earth oxide nanostructures by varying the microwave reaction time and the concentrations of the organic surfactants. The uniformity of the nanorods and of nanowires is demonstrated in their spontaneous assembly into highly ordered 2-D supercrystals. To compare the effect of the microwave heating with the conventional heating, the control experiments were performed under reaction conditions identical to those of the microwave experiments but using conventional thermal heating. The resulting nanorods were significantly less uniform than those obtained under microwave irradiation. Figure 31 shows TEM micrographs of the self-assembly of as-synthesized Sm_2O_3, Nd_2O_3, and Gd_2O_3 nanorods and nanowires. The nanorods with an average diameter of 1.2 nm and average lengths of 4−5 nm were self-assembled into large regions of highly ordered 2-D superstructures, as shown in Figure 31a and b. HRTEM was used to further investigate the crystallinity and crystal structure of the synthesized nanostructures. Distinct lattice planes in the HRTEM image indicated that the nanostructures were single crystals. The HRTEM image of the individual nanowire (Figure 31e) shows well-resolved lattice planes perpendicular to the long axis with an interplanar distance corresponding to the *d* spacing of the (400) plane of the cubic *Ia*3 space group. The growth mechanism for the 1-D rare earth nanostructures was proposed.[951] It was attributed to the kinetic growth, which determined the final morphology of nanocrystals rather than thermodynamic growth. The competitive adsorption of oleic acid and oleylamine could inhibit the growth of the nanocrystal in all but enhance the favorable crystallographic plane, thus resulting in 1-D nanostructures. The crystal plane with a higher surface energy is expected to have a faster growth rate. To verify this mechanism, the relative concentrations of oleic acid and oleylamine were varied. When the molar ratio of the metal precursor/oleic acid/oleylamine was 1:17:17, spherical particles were formed in the case of Eu_2O_3 nanocrystals, implying the stronger binding capability of oleic acid relative to oleylamine. The nanorods were formed when the molar ratio of oleylamine to oleic acid was about 1.5 for Eu_2O_3 nanocrystals. However, when oleylamine was present in much excess, square nanoplates of Sm_2O_3 and Eu_2O_3 were formed. It was found that the nanorods and square nanoplates were predominantly formed when the molar ratio of metal acetate/oleic acid/oleylamine was 1:14:22 and 1:9:27, respectively. These results demonstrate that the control over the shape of the resulting nanocrystals can be achieved by adjusting the capping ligands.[951]

Pancake-like $Cd(OH)_2$ superstructures were prepared via the rapid microwave-assisted hydrothermal method at 150 °C for 10 min, adopting $Cd(CH_3COO)_2{\cdot}2H_2O$ and hydrazine hydrate in mixed solvents of water and glycerol. The SEM and TEM micrographs of $Cd(OH)_2$ multilayer stacked nanostructures are shown in Figure 32, indicating that each architecture is constructed by many nanoflakes via layer-by-layer self-assembly. The SAED pattern displays ordered electron diffraction spots and confirms the high crystallinity of the product (Figure 32d). Several influencing factors, such as the volume ratio of hydrazine hydrate to glycerol, reaction time, temperature, and cadmium source, were found to play important roles in the formation of $Cd(OH)_2$ multilayer stacked structures. The layer-by-layer self-assembly of nanosheets was proposed for the formation of these superstructures.[859]

dx.doi.org/10.1021/cr400366s | *Chem. Rev.* 2014, 114, 6462−6555

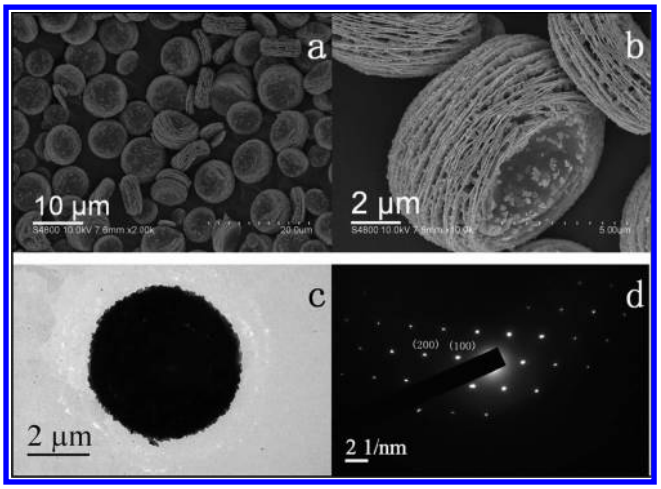

Figure 32. SEM micrographs (a and b), TEM micrograph (c), and SAED pattern (d) of $Cd(OH)_2$ multilayer stacked structures prepared under microwave irradiation at 150 °C for 10 min. Reprinted with permission from ref 859. Copyright 2012 The Royal Society of Chemistry.

The El-Shall group reported the rapid microwave-assisted synthesis of uniform and highly aligned nanorods and nanowires of ZnS, ZnSe, CdS, and CdSe in a mixture of alkylamines (C_6–C_{18}) and DMF. The stepwise formation of the nanowires from small spherical nuclei to short aligned nanorods to long assemblies of nanowires was observed by varying the microwave heating time from 0.5–1 min to 1–2 min to >3 min, respectively. These uniform nanorods and nanowires spontaneously assembled into highly ordered two-dimensional superstructures. Figure 33 displays a TEM

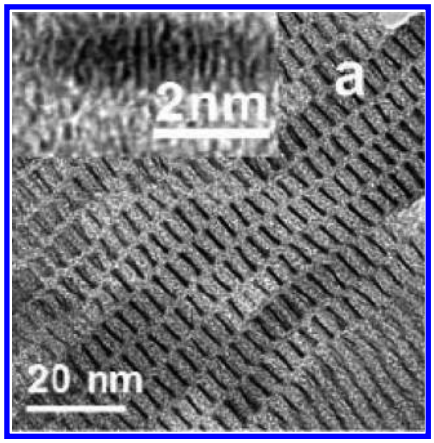

Figure 33. TEM micrograph of ZnS nanorods. Higher resolution image is shown in the inset. Reprinted with permission from ref 962. Copyright 2006 American Chemical Society.

micrograph of the as-prepared ZnS nanorods with an average diameter of 1 nm and an average length of 5 ± 0.05 nm synthesized with a reaction time of 2 min. The nanorods self-assembled into arrays of highly ordered two-dimensional superstructures.[962]

Wang et al.[963] prepared a variety of monodisperse GdF_3:Yb,Er nanocrystals with different shapes, sizes, and dopants by the microwave-assisted method. In addition to monodisperse spherical nanoparticles, rhombic-shaped slices that self-assembled into stacks were also obtained. Figure 34

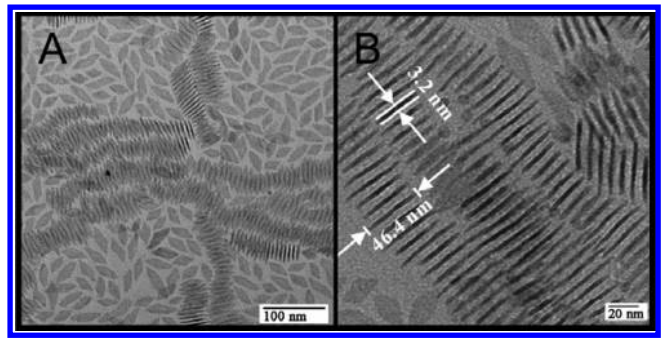

Figure 34. TEM micrographs of GdF_3 rhombic nanoplates. (A) Overview of rhombic nanoplates and "stacks"; (B) blow-up of self-assembled rhombic nanoplates. Reprinted with permission from ref 963. Copyright 2011 Springer.

shows TEM micrographs of the as-prepared regularly shaped GdF_3 rhombic nanoplates with ~3.2 nm in thickness and ~45 nm in length. The nanoplates had a strong tendency to form 2-D assemblies. Wang et al.[964] synthesized monodisperse $NaYF_4$ nanocrystals using corresponding metal trifluoroacetates in mixed solvents of 1-octadecene and oleic acid by the microwave-solvothermal method at 290 °C for 5 min. Figure 35A shows the TEM micrograph of $NaY_{0.78}F_4:Yb^{3+}_{0.2},Er^{3+}_{0.02}$

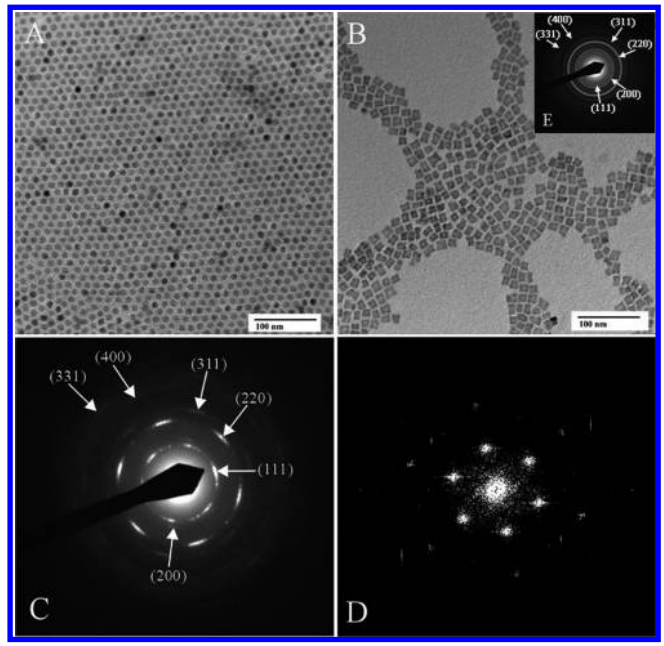

Figure 35. (A,B) TEM micrographs of $NaY_{0.78}F_4:Yb^{3+}_{0.2},Er^{3+}_{0.02}$ and $NaY_{0.78}F_4:Yb^{3+}_{0.2},Tm^{3+}_{0.02}$ nanocrystals. (C) SAED pattern of $NaY_{0.78}F_4:Yb^{3+}_{0.2},Er^{3+}_{0.02}$ nanocrystals. (D) Fast-Fourier transform (FFT) image of picture (A). (E) SAED pattern of $NaY_{0.78}F_4:Yb^{3+}_{0.2},Tm^{3+}_{0.02}$ nanocrystals. Reprinted with permission from ref 964. Copyright 2009 American Chemical Society.

monodisperse nanocrystals (~11 nm). The cubic crystal lattice was confirmed by SAED in Figure 35C. These nanocrystals self-assembled into a regular, hexagonal 2-D arrangement over a large area. Figure 35D shows the fast Fourier transform of Figure 35A that confirms the hexagonal assembly of the nanoparticles. Under the identical synthesis conditions, small and monodisperse nanocrystals, doped with Yb^{3+} and Tm^{3+} ions, were obtained in a "cubic" morphology with a side length

dx.doi.org/10.1021/cr400366s | Chem. Rev. 2014, 114, 6462–6555

of ~10 nm (Figure 35B). Figure 35E (the inset of (B)) shows that these nanocrystals had a crystalline and cubic crystal lattice.

8. COMPARISON OF MICROWAVE HEATING WITH CONVENTIONAL HEATING

Microwave energy can significantly enhance the chemical reaction rate, selectivity, and yield of the product. As discussed above, the microwave-assisted synthesis can exhibit order-of-magnitude enhancement in reaction rate as compared to the conventional synthesis. However, the fundamental difficulties facing all comparative studies between the microwave heating and conventional heating, as well as between various microwave heating studies themselves, are the accurate determination of temperature and the inconsistencies between different experiments in terms of microwave field homogeneity, reactor size and geometry, microwave power, heating rate, heating temperature and time, and volume of reaction systems, etc.[44] The distribution of microwave energy within the reaction mixture is also dictated by the nature and configuration of the reactor employed. For example, the rates of nucleation and crystallization are higher in a multimode microwave oven than those in a single mode microwave oven with a more uniform microwave field.[2] The microwave reactor system can be operated in various ways, such as by varying the rate at which the temperature is increased, microwave power, stirring of the reaction system, etc. Unfortunately, in many cases, the comparisons have been made under different experimental conditions such as different reaction temperatures and times. Only a small number of researchers have taken these into account when comparing their studies with previous microwave syntheses and/or with conventional syntheses. In brief, comparative studies between the microwave heating and conventional heating should be conducted under exactly identical experimental conditions.

It is well-known that the use of microwaves saves energy because of fast kinetics, rapid heating, and short reaction time, but few studies have reported the quantitative energy consumption by microwave heating. Katsuki et al.[46] investigated the approximate energy consumption calculated from the output power. They prepared cubic $BaTiO_3$ nanoparticles using 8.2693 g of commercial TiO_2 and 17.8935 g of $Ba(OH)_2$ in 195 mL of distilled water at 90 °C by a home-built single-mode semicontinuous microwave-assisted reactor. It took 1.5 min to heat the reaction system to 90 °C. Cubic $BaTiO_3$ nanoparticles with sizes of 30−50 nm were obtained at 90 °C for 5 min. The conversion ratio of TiO_2 to $BaTiO_3$ was 97.6% and 100% for 5 and 15 min, respectively. However, the conversion ratio was 62−65% at 90 °C for 15 min without stirring, and the stirring treatment at 250 rpm was found to be a very important factor for uniform microwave heating of the reaction system in a large glass vessel. They found that from 22 to 90 °C, 1000 W of output (100%) was applied, and the heating rate of the reaction system was 0.54 °C s^{-1}. After reaching 90 °C, the output was changed from 65 to 115 W at 90 °C for 5 min. The approximate energy consumption from room temperature to 90 °C was 89 kJ, and 29 kJ at 90 °C for 5 min, and the total energy for the microwave-assisted synthesis of $BaTiO_3$ was 118 kJ. In comparison, 195 mL of distilled water was treated at 90 °C for 5 min using the same reactor system, the approximate energy consumption from room temperature to 90 °C was 93 kJ, and 32 kJ at 90 °C for 5 min, respectively, and the approximate total energy consumption was 125 kJ. To evaluate the approximate total energy consumption by the conventional heating, 195 mL of water in a polyethylene vessel was put in the oven and heated from 23 to 90 °C with the heating rate of 5.6 °C min^{-1} and kept at 90 °C for 5 min. For the conventional heating, 648 and 144 kJ were needed from 23 to 90 and 90 °C for 5 min, respectively, and total energy consumption was 792 kJ. The conventional heating system needed more than 6 times energy consumption of the microwave heating system.

Horikoshi et al.[111] examined the effects of the 2.45 GHz microwave radiation on the preparation of Ag nanoparticles in aqueous medium by reduction of $[Ag(NH_3)_2]^+$ with carboxymethylcellulose (CMC) in both batch-type and continuous-flow reactor systems. The microwave-assisted preparation was compared to the conventional heating method, both at the same reaction temperature of 100 °C. A flow-through microwave reactor system was used for the continuous production of Ag nanoparticles. The flow reactor system with a flow rate of 600 mL min^{-1} coupled with 1200 W microwave radiation generated Ag nanoparticles with a size distribution of 0.7−2.8 nm (average size ~1.5 nm). They made a comparison of used power and heating rate between the single mode microwave apparatus and conventional oil bath. Continuous 64 W microwave irradiation showed a rate of temperature rise of 0.51 °C s^{-1} for the CMC/$[Ag(NH_3)_2]^+$ aqueous solution, whereas for the oil-bath heating the rate was 0.09 °C s^{-1} for a power consumption of 400 W. The much lower power of the microwaves led to a significant enhancement of the heating rate relative to the oil bath heating. Nishioka et al.[503] reported the continuous production of Ag nanoparticles using a homogeneous flow-type microwave reactor system based on a polyol process. They also compared the performance of the flow-type microwave heating process with that of flow-type heating by immersion of the reactor tube in an oil bath. They prepared Ag nanoparticle dispersions using two methods at the same concentration of reactants, reaction temperature, and time. For the 10 mL h^{-1} flow rate, the UV−vis absorption peak intensity of the dispersion obtained by microwave heating was almost twice that of the conventional heating, indicating the higher yield of Ag nanoparticles by microwave heating. When the flow rate was increased to 100 mL h^{-1}, this effect was more pronounced. As compared to the microwave heating, no appreciable UV−vis absorption peak was observed for the sample obtained by the conventional heating, suggesting that the reaction did not occur practically by the conventional heating at this high flow rate.

Horikoshi et al.[111] reported the dielectric loss factor of the $[Ag(NH_3)_2]^+$ aqueous solution, which was 1.4-fold greater than that of pure water, and higher than that of the CMC aqueous system, indicating that preferential microwave heating occurred at the $[Ag(NH_3)_2]^+$ complex. By contrast, the dielectric constants remained rather constant relative to water, whereas the dielectric loss tangents of the initial solution and of the $[Ag(NH_3)_2]^+$/water system were otherwise identical to the Ag colloidal solution after the 5 min microwave heating period but somewhat greater than those of pure water and the CMC/water solution.[111] The 2.45 GHz microwaves penetrated the aqueous medium; the microwave energy was supplied directly and preferentially to the $[Ag(NH_3)_2]^+$ complex. On the other hand, the aqueous solution was heated by the oil bath heating nonselectively by thermal conduction and convection through the reactor walls to the reaction system. Thus, mechanistic variations in microwave heating versus conventional heating are expected to cause differences in heat interchange at the

dx.doi.org/10.1021/cr400366s | Chem. Rev. 2014, 114, 6462−6555

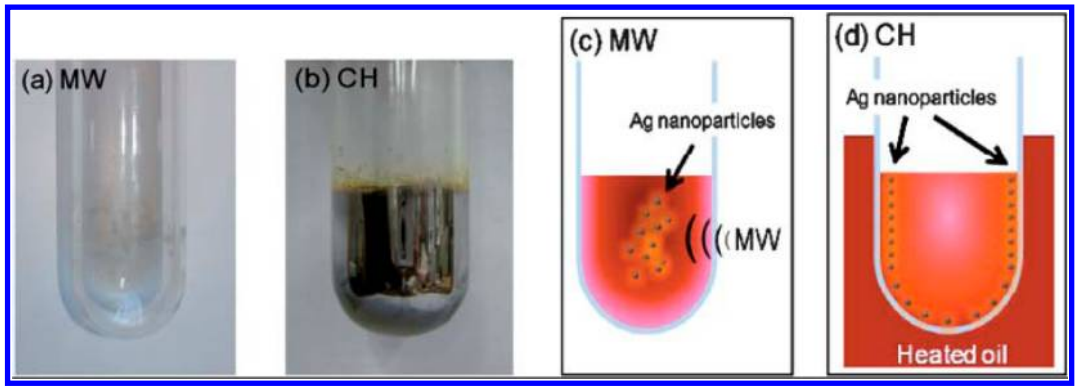

Figure 36. Photograph of the reactor after the reaction system was heated by two different methods: (a) microwave irradiation for 4 min; and (b) oil bath heating for 4 min. The cartoons show the temperature distribution in the reactor: (c) after the 4 min of microwave heating; and (d) after the 4 min of oil bath heating. Experiments were carried out under nonstirring conditions. Concentrations: 0.05% w/v CMC, and 60 mM $[Ag(NH_3)_2]^+$ aqueous solution. Reprinted with permission from ref 111. Copyright 2010 The Royal Society of Chemistry.

microscopic level, which leads ultimately to variations in size distributions of Ag nanoparticles.[111]

The differences between the microwave heating and conventional heating are clearly shown in Figure 36.[111] The microwave irradiation for 4 min of the $[Ag(NH_3)_2]^+$/CMC aqueous solution led to a slightly yellow-colored solution in the reactor (Figure 36a), and Ag nanoparticles that adsorbed on the reactor walls could be easily removed by simple washing with water. In contrast, the Ag film (mirror) coating the inner reactor walls formed after 4 min by the conventional heating (Figure 36b). The initial temperature distributions and formation of Ag nanoparticles under nonstirring conditions by both the microwave and the conventional heating are shown in the cartoons of Figure 36c and d.[111] In the former case, microwave radiation penetrated the $[Ag(NH_3)_2]^+$/CMC aqueous solution causing the temperature to rise by dielectric loss and to some extent by conduction heating, followed by subsequent loss of heat to the surroundings through the reactor walls. As a result, the temperature near the inner walls of the reactor tended to be lower than that at the center of the reactor. That is, the preparation of Ag nanoparticles by the microwave-assisted process progressed outward from the center of the reactor to the inner reactor walls due to a temperature gradient that gave rise to a concentration gradient. In contrast, heat from the oil bath was most prominent at the reactor walls and was subsequently transmitted to the solution by the thermal conduction and convection mechanism, leading to the formation of a Ag film at the reactor inner walls due to higher concentration of the nanoparticles. Schanche[28] and Kappe[29] discussed temperature distributions produced by microwave and conventional heating methods in organic syntheses.

Horikoshi et al.[111] investigated the effect of the heating methods on the formation of Ag nanoparticles in aqueous solution by reduction of $[Ag(NH_3)_2]^+$ with CMC. Figure 37a and b shows the TEM micrographs of the resulting Ag nanoparticles. A fairly monodispersed particle size distribution was observed by microwave heating (1.8−3.6 nm, average size ~3 nm) under temperature conditions otherwise identical to those of the conventional heating, which produced a broader size distribution (1−5 nm). By contrast, light scattering measurements indicated a size distribution by microwave heating in the range of 1−2.3 nm (Figure 37c), whereas the conventional heating led to polydipsersed nanoparticles mostly in the range of 3−5.7 nm (Figure 37d) with some nanoparticles up to 30 nm. These experimental results indicate that even

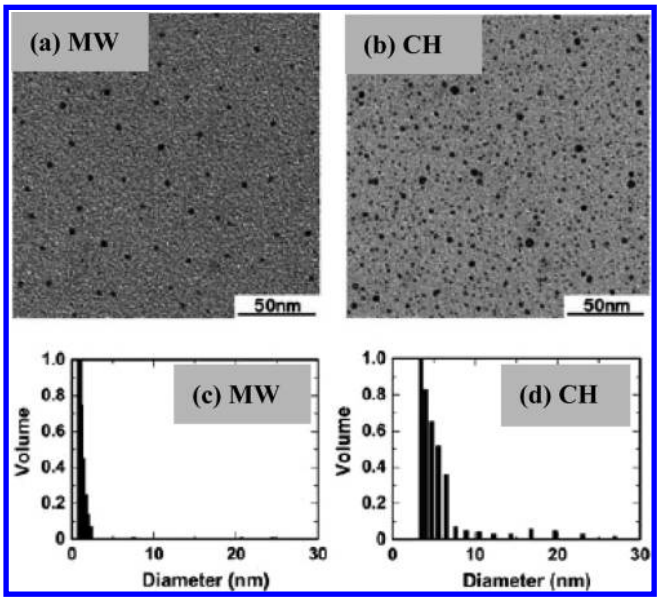

Figure 37. TEM micrographs and particle size distributions of Ag nanoparticles produced under microwave irradiation (a and c) and oil bath heating (b and d). Concentrations: 0.05% w/v CMC, and 60 mM $[Ag(NH_3)_2]^+$ aqueous solution. Reprinted with permission from ref 111. Copyright 2010 The Royal Society of Chemistry.

though the reaction temperature conditions for the microwave heating and oil bath were identical, there was a noticeable difference in the formation rate of Ag nanoparticles and their size distributions.

Katsuki et al.[164] prepared monodisperse α-Fe_2O_3 nanoparticles using $Fe(NO_3)_3{\cdot}9H_2O$ solutions by the microwave-hydrothermal and conventional-hydrothermal reactions. As compared to the conventional-hydrothermal reaction, the microwave-hydrothermal reaction led to increased formation rate by 3 times at 120 °C and 5 times at 140 °C from 0.1 M $Fe(NO_3)_3{\cdot}9H_2O$ solutions. Kijima et al.[1007] synthesized α-Fe_2O_3 nanoparticles with an average diameter of less than 10 nm using $Fe(NO_3)_3{\cdot}9H_2O$ as the only starting reagent in aqueous solution by continuous microwave heating for 2 min in a modified household microwave oven. Figure 38 shows the photographs of the reaction solutions that were microwave-heated and conventionally heated. When the solution was irradiated with microwaves continuously, the temperature of the solution was increased rapidly to 100 °C within 80 s, and

dx.doi.org/10.1021/cr400366s | Chem. Rev. 2014, 114, 6462−6555

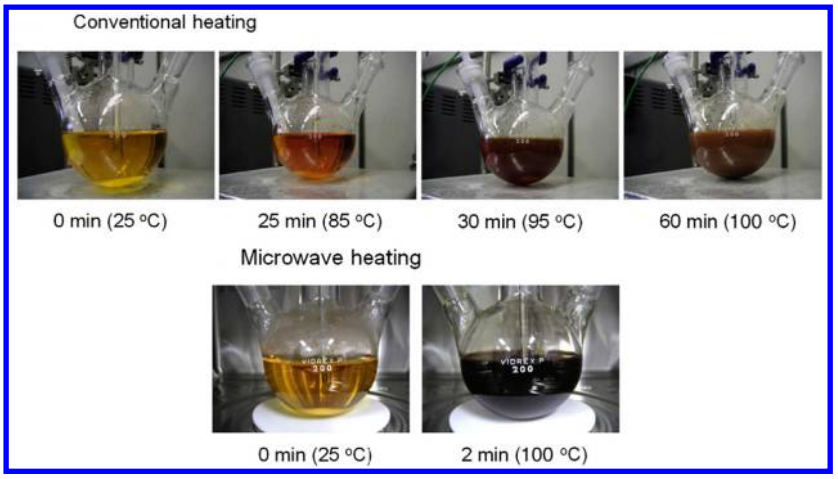

Figure 38. Time course of the color of the reaction solutions that were microwave-heated and conventionally heated. Reprinted with permission from ref 1007. Copyright 2010 Elsevier B.V.

the color of the solution changed from bright yellow to wine red, indicating that a colloidal dispersion formed. Although no stabilizer existed in the solution, the colloidal dispersion was stable. In contrast, when the solution was heated by a magnetic hot-stirrer, the temperature of the solution was increased gradually. After 30 min, a reddish-brown suspension was obtained. The XRD pattern confirmed that α-Fe_2O_3 rapidly formed by microwave heating. Even if the microwave heating was 1 h, α-FeOOH was not observed in the product. In contrast, a mixture of α-Fe_2O_3 and α-FeOOH was obtained by the conventional heating for 1 h.

Katsuki et al.[269] prepared $BaTiO_3$ nanoparticles using commercial TiO_2 and $Ba(OH)_2$ in distilled water by the microwave heating and conventional heating at 90 °C. As compared to the formation of $BaTiO_3$ nanoparticles using the conventional heating process, the microwave-assisted process led to increased formation rate by about 6 times. For a reaction time of 1 min, the conversion ratio of TiO_2 to cubic $BaTiO_3$ powder was 73.7% and 0% by microwave heating and conventional heating, respectively. For a reaction time of 5 min, the conversion ratio of TiO_2 to cubic $BaTiO_3$ reached 95.8% by microwave heating; however, the conventional heating still led to 0% conversion ratio. The conversion of TiO_2 to $BaTiO_3$ reached 100% after only 10 min via microwave irradiation but after 1 h via the conventional process. $BaTiO_3$ nanoparticles with an average size of 29 nm were obtained after treatment for 15 min by microwave heating. The experiments showed that the use of microwaves led to the formation of smaller nanoparticles with a narrower size distribution as compared to that of the conventional heating process.

Zhu et al.[470] prepared the nanocomposites of polyacrylamide (PAM)/metal (Pt, Ag, Cu) with metal nanoparticles homogeneously dispersed in the polymer matrix using the corresponding metal salt and acrylamide monomer in EG by the rapid microwave-assisted polyol method. The diameters of Ag nanoparticles in the PAM/Ag nanocomposite were in the range of 6−18 nm with an average diameter of 11.3 nm prepared by microwave heating the EG solution of 0.01 M $AgNO_3$ and 3 M acrylamide at 125 °C for 15 min, as shown in Figure 39a,b. For comparison, the synthesis of the PAM/Ag nanocomposite was also conducted by the conventional oil bath at 125 °C; however, much longer reaction time (about 2.5 h) was needed to obtain the PAM/Ag nanocomposite with an average Ag diameter of 16.9 nm and a wide size distribution of

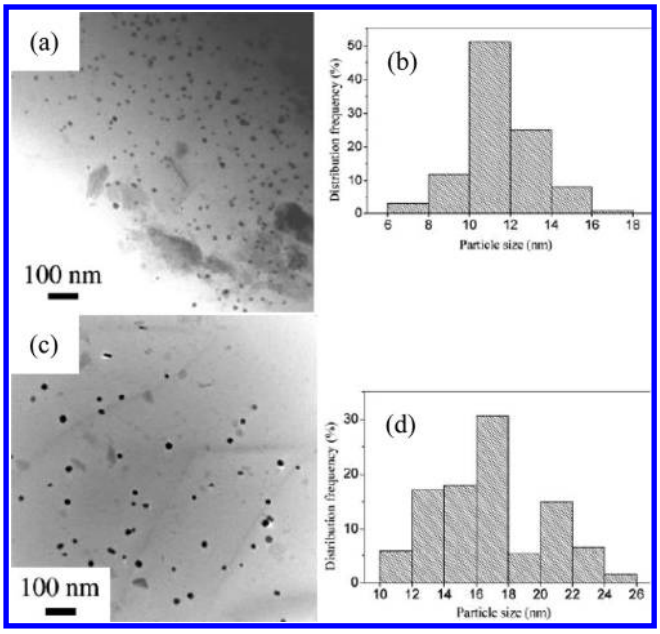

Figure 39. (a) TEM micrograph and (b) the histogram of Ag particle size distribution of the PAM/Ag nanocomposite prepared by microwave heating an EG solution of 0.01 M $AgNO_3$ and 3 M acrylamide at 125 °C for 15 min. (c) TEM micrograph and (d) the particle size distribution of the PAM/Ag nanocomposite prepared by oil bath heating an EG solution of 0.01 M $AgNO_3$ and 3 M acrylamide at 125 °C for 150 min. Reprinted with permission from ref 470. Copyright 2006 American Chemical Society.

10−26 nm (Figure 39c,d), which were larger than those prepared by microwave heating at the same temperature with the same reaction solution. The PAM/Ag nanocomposite with a larger average Ag particle size and a broader particle size distribution was obtained by microwave heating at a higher temperature for 15 min or at 125 °C for a longer reaction time.

Katsuki and Komarneni[1008] prepared monodisperse α-Fe_2O_3 nanoparticles using 0.018 M $FeCl_3 \cdot 6H_2O$ and 0.01 M HCl solutions in the temperature range of 100−160 °C via the microwave-hydrothermal (M-H) and conventional-hydrothermal (C-H) method. Acicular β-FeOOH structures with 300 nm in length and 40 nm in thickness were dominantly formed at 100 °C for 2−3 h, while spherical α-Fe_2O_3 particles with 100−180 nm in diameter were preferentially formed for 13 h using

dx.doi.org/10.1021/cr400366s | Chem. Rev. 2014, 114, 6462−6555

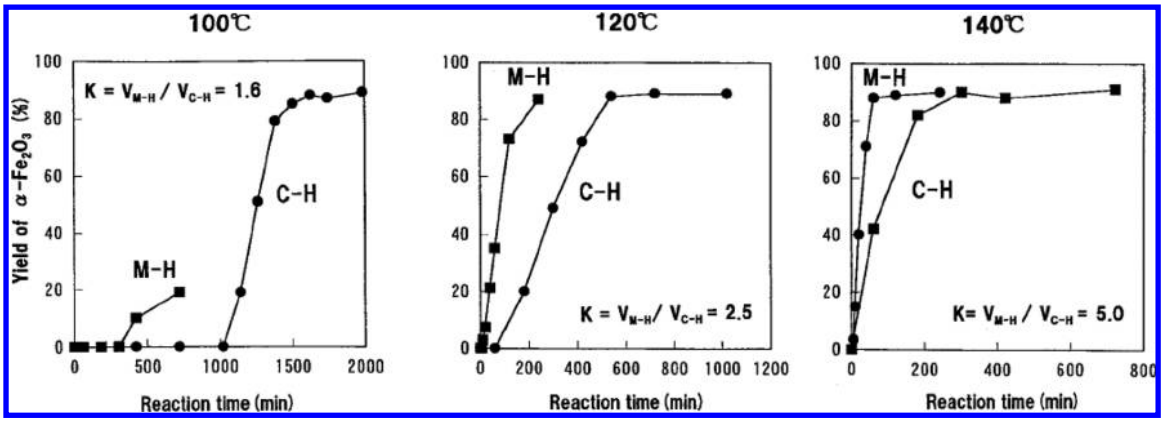

Figure 40. Effect of microwave heating on the kinetics of hydrothermal formation of α-Fe_2O_3 nanoparticles at 100, 120, and 140 °C. Reprinted with permission from ref 1008. Copyright 2001 American Ceramic Society.

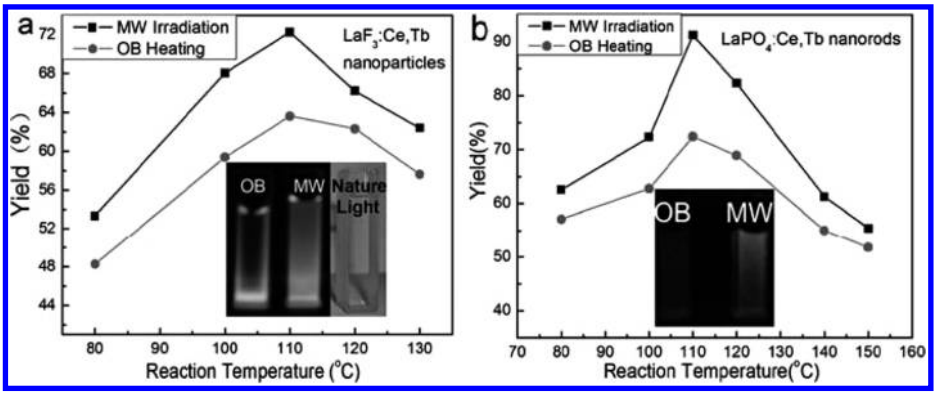

Figure 41. Yields of LaF_3:Ce,Tb nanoparticles (a) and $LaPO_4$:Ce,Tb nanorods (b) at different reaction temperatures using different heating sources. The inset images show the appearance of samples obtained from microwave heating and oil bath under a 254 nm ultraviolet lamp and natural light. Reprinted with permission from ref 616. Copyright 2010 The Royal Society of Chemistry.

the conventional-hydrothermal method. In contrast, the microwave-hydrothermal reaction at 100 °C led to monodisperse α-Fe_2O_3 nanoparticles with 30−66 nm in diameter after 2 h without the formation of β-FeOOH. Figure 40 shows the yields of α-Fe_2O_3 at 100−140 °C for different reaction times via the C-H and M-H reactions. From Figure 40, one can see that the ratios of the kinetics $K = V_{M\text{-}H}/V_{C\text{-}H}$ were 1.6 and 2.5 at 100 and 120 °C, respectively, but increased to ∼5 at 140 °C. The yields of α-Fe_2O_3 particles obtained by the M-H reaction reached 83%−95% at 140−160 °C after 2−4 h.

Zhu et al.[616] reported the rapid synthesis of LaF_3:Ce,Tb and $LaPO_4$:Ce,Tb nanocrystals using EG as the solvent by adopting a microwave-heated microfluidic reactor. They performed comparative experiments between the microwave heating and oil bath. The sizes of LaF_3:Ce,Tb nanoparticles obtained by microwave heating were obviously smaller and more uniform than those prepared by oil bath. Figure 41 shows the product yields at different temperatures from different heating sources. It was found that the yields of the microwave-prepared samples were higher than those of the oil bath prepared samples at each temperature with the highest yield of 72.3% for LaF_3:Ce,Tb nanoparticles and 91.2% for $LaPO_4$:Ce,Tb nanorods. The inset images in Figure 41 indicate the differences in the yield % visualized between samples.

Dahal et al.[1009] investigated the effects of the microwave heating versus conventional heating on the nucleation and growth of nearly monodisperse Rh, Pd, and Pt nanoparticles. They adopted a one-pot synthetic method, which combined the nucleation and growth in a single reaction system via precise control over the precursor addition rate. The microwave heating enabled the convenient preparation of polymer-capped metal nanoparticles with improved monodispersity, morphological control, and higher crystallinity, as compared to samples obtained by the conventional heating under otherwise identical conditions. The fundamental difference in Rh nanoparticle formation was observed during the nucleation stage that was directly dependent on the heating method. The microwave heating led to faster nucleation and also the formation of more uniform nanoparticles as compared to the oil bath. Microwave irradiation was found to provide more uniform seeds for the subsequent crystal growth. Nanoparticle growth kinetics by microwave heating was also different as compared to the conventional heating. The conventional heating generally produced nanostructures with mixed morphologies, while microwave synthesis produced a majority of tetrahedral nanocrystals with sizes of 5−7 nm or larger nanocubes (>8 nm) upon further growth. Rh seeds and larger nanoparticles obtained from microwave-assisted synthesis were more highly crystalline and faceted as compared to their conventionally prepared counterparts.

The overall comparative trends in size of Rh nanostructures prepared by both microwave heating and conventional heating are shown in Figure 42.[1009] The control over particle size as a function of total added $RhCl_3$ precursor was achieved under both modes of heating. The smaller conventionally prepared seeds (Figure 42A, blue data) resulted in accordingly smaller

dx.doi.org/10.1021/cr400366s | Chem. Rev. 2014, 114, 6462−6555

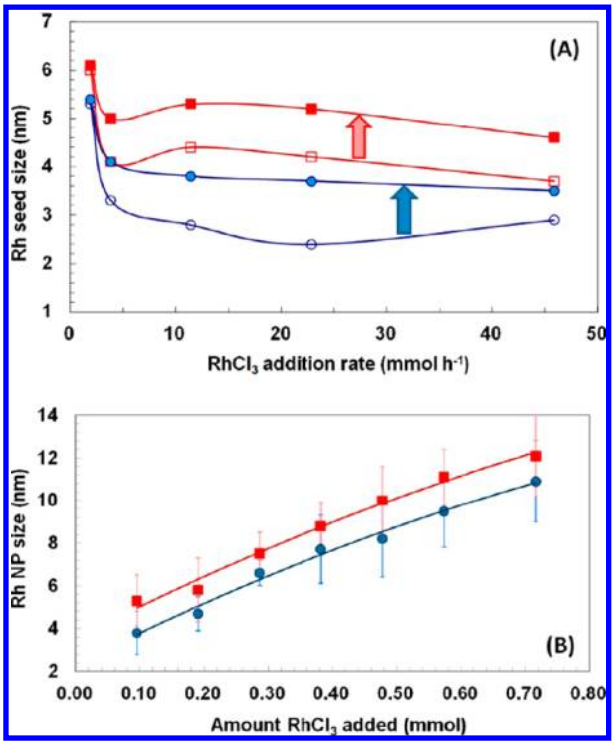

Figure 42. (A) Average sizes of initial Rh seeds (open symbols) and after ripening (solid symbols) as a function of precursor injection rate. (B) Size and standard deviation of Rh nanoparticles as a function of the amount of added $RhCl_3$ precursor. Blue stands for conventional heating; red stands for microwave heating. Reprinted with permission from ref 1009. Copyright 2012 American Chemical Society.

Rh nanoparticles (Figure 42B, blue data) as compared to those of larger microwave-derived seeds (Figure 42A, red data). Microwave-prepared Rh nanoparticles exhibited approximately twice the catalytic activity of similarly sized conventionally prepared nanoparticles in the vapor-phase hydrogenation of cyclohexene. The microwave heating resulted in the complete exchange of PVP capping agent with oleylamine and oleic acid. In contrast, similar ligand exchange was difficult by the conventional heating.

To understand quantitatively which stage of the nucleation or crystal growth is selectively accelerated under microwave irradiation, Jhung et al.[30] synthesized silicalite-1 and VSB-5 molecular sieves by the conventional electric heating (CE) and microwave heating (MW). They considered three cases of acceleration in the microwave synthesis: (1) acceleration both in nucleation and in crystal growth, (2) acceleration in nucleation only, and (3) acceleration in crystal growth only. The syntheses were performed in two steps, that is, MW−MW, MW−CE, CE−MW, and CE−CE (in the order of nucleation−crystal growth). They found that microwave irradiation accelerated not only nucleation but also crystal growth as compared to the conventional heating. However, the effect of microwave irradiation appeared to be much more significant on the nucleation relative to crystal growth (Figure 43). The reaction rates of the nucleation and crystal growth were analyzed by using crystallization curves of silicalite-1 and VSB-5. As shown in Figure 43, the syntheses of silicalite-1 had different induction periods (crystallization time needed to show any crystallinity), different synthesis times to complete the crystallization, and the slopes of crystallinity changed depending on the reaction modes.

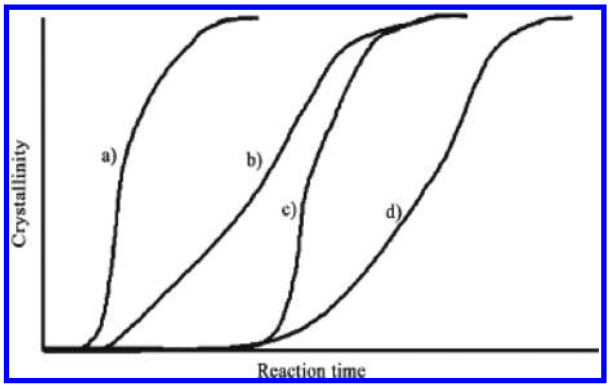

Figure 43. Change of crystallinity of a microporous material with time to show several modes of accelerations: (a) both nucleation and crystallization are accelerated; (b) only nucleation is accelerated; (c) only crystallization is accelerated; and (d) normal synthesis without any acceleration. Reprinted with permission from ref 30. Copyright 2007 Wiley-VCH.

Figure 44 shows the crystallization curves of silicalite-1 prepared under microwave irradiation and/or conventional

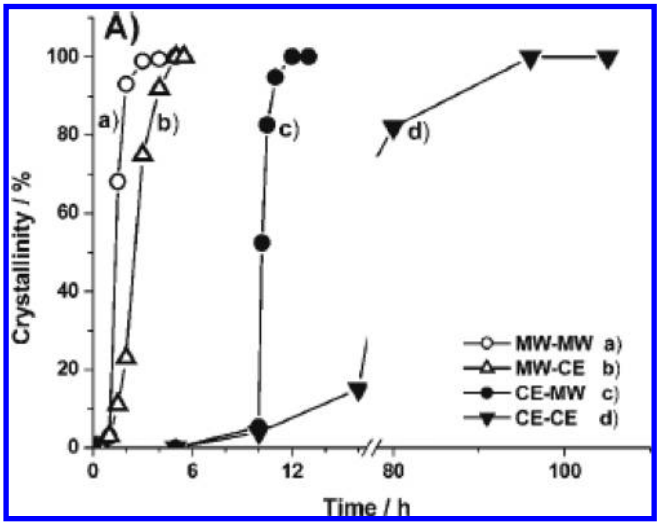

Figure 44. Crystallization curves of silicalite-1 prepared under microwave irradiation (MW) and/or conventional electric heating (CE), showing crystallinity changes depending on the synthesis method and reaction time. Reprinted with permission from ref 30. Copyright 2007 Wiley-VCH.

electric heating, showing crystallinity changes according to the synthesis method and reaction time. The overall synthesis time for the completion of crystallization under microwave irradiation was around 3 h, whereas ~90 h was needed to complete the crystallization with the conventional heating (Figure 44a and d). Therefore, the cumulative degree of acceleration by microwaves was around 30-fold. The slope of the crystallization curve obtained by microwave heating was more steep as compared to that by the conventional heating, indicating that the crystallization stage is accelerated by microwave heating. Irrespective of the first heating method, crystallization under microwave irradiation was quite rapid. However, the crystal growth by the conventional heating depended mainly on the initial heating method. The crystal growth by the conventional heating was quite fast for the sample nucleated by microwave irradiation relative to the very

dx.doi.org/10.1021/cr400366s | Chem. Rev. 2014, 114, 6462−6555

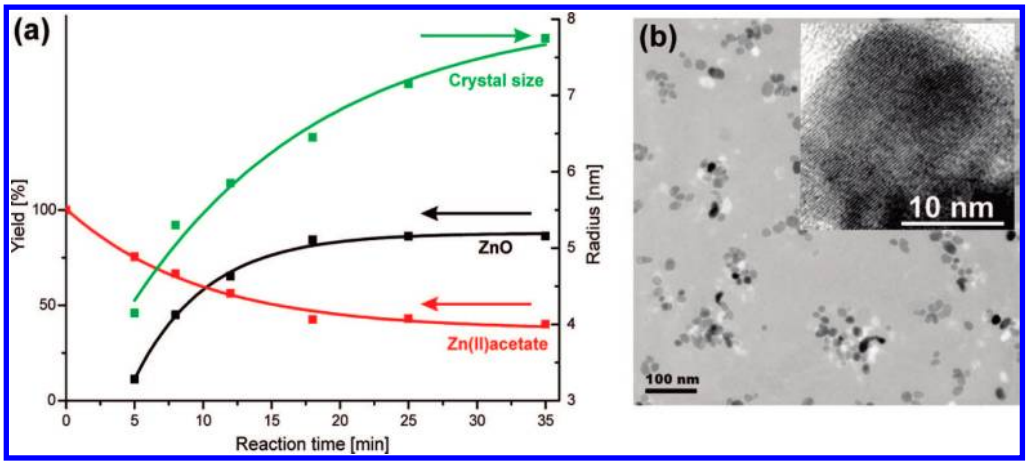

Figure 45. (a) Time-dependent evolution of the crystal size (green curve), yield of ZnO powder (black curve), and zinc acetate concentration (red curve) by microwave heating at 120 °C. (b) TEM overview micrograph of ZnO nanoparticles obtained by microwave heating at 120 °C for 3 min (inset: HRTEM image of one nanoparticle). Reprinted with permission from ref 772. Copyright 2009 American Chemical Society.

slow crystallization of the sample nucleated by the conventional heating. The times needed for crystallization were about 2 and 4−80 h with microwave irradiation and conventional heating, respectively. The nucleation time of silicalite-1 was also reduced from 10 to 1 h by microwave heating, indicating the high efficiency of microwave irradiation in the acceleration of nucleation. Because of the acceleration in both stages, the overall synthesis times for silicalite-1 and VSB-5 decreased by about 30- and 12-fold, respectively, by using microwave heating. The crystal sizes of silicalite-1 and VSB-5 increased in the order of the products synthesized by MW−MW > MW−CE > CE−MW > CE−CE. The rapid crystal growth and small crystal size observed in the synthesis from the microwave-nucleated precursor can be explained in terms of the fact that the microwave-nucleated samples have higher population of nuclei with smaller sizes than the samples nucleated by the conventional heating.

Campelo et al.[922] compared the microwave synthesized metal (Au, Ag, or Pd) nanoparticles supported on mesoporous material SBA-12 with those obtained under the conventional heating under the same conditions (temperature and heating time). They found that the conventional heating preparation led to an extremely low metal loading with a poor dispersion of supported metal nanoparticles, and higher nanoparticle loading was only achieved at relatively long heating times (over 1 h), and uneven distribution and dispersion of metal nanoparticles were also observed. The rapid heating of the reaction mixtures, especially those containing polar solvents (e.g., ethanol and water), by microwaves led to a rapid and almost simultaneous formation of metal nanoparticles with small particle sizes and narrow size distributions at very short reaction times (less than 3 min). Bhattacharya et al.[1010] reported the preparation of aqueous ferrofluids by chemical coprecipitation of iron salts in poly(vinyl alcohol) by both conventional and microwave heating modes. They found that for the same initial constituents, microwave irradiation enhanced the saturation magnetization of the product more than double as compared to that prepared by the conventional heating. Microwave irradiation increased the polydispersity, average particle size, and crystallinity of the product.

Bilecka et al.[772] reported a detailed investigation of the kinetics and thermodynamics in the microwave-assisted synthesis of ZnO nanoparticles from $Zn(CH_3COO)_2$ and benzyl alcohol at temperatures ranging from 120 to 180 °C for 0.5−35 min. They also investigated the organic esterification reaction between acetate and benzyl alcohol, and the formation and growth of ZnO nanoparticles. Monitoring both the formation of the organic species as well as the crystal size of ZnO with time directly correlated the kinetics of the organic side reaction with the growth kinetics of ZnO nanoparticles. The esterification reaction, which is the chemical basis for producing the monomer for ZnO formation, was found to be first order. The growth of ZnO nanoparticles followed the Lifshitz−Slyozov−Wagner model for coarsening, indicating a diffusion-limited process. For comparison, the synthesis of ZnO was also carried out at 120 °C in an oil bath under otherwise identical reaction conditions. As compared to the conventional heating, the microwave irradiation greatly accelerated nanoparticle formation by (a) facilitating the dissolution of the precursor in the solvent, (b) increasing the rate constant for the esterification reaction by 1 order of magnitude, resulting in faster production of monomer and consequently in an earlier nucleation event, and (c) increasing the rate constant k_{growth} for the crystal growth from 3.9 $nm^3\ min^{-1}$ for the conventional heating to 15.4 $nm^3\ min^{-1}$ for the microwave heating.[772]

Figure 45a illustrates the relation between the yield of ZnO powder (black curve), crystal size (green curve), and $Zn(CH_3COO)_2$ concentration (red curve) at 120 °C for different microwave heating times.[772] It took about 5 min of microwave heating at 120 °C to obtain phase-pure ZnO nanoparticles, and the crystal size grew continuously with increasing microwave heating time (Figure 45a, green curve), and $Zn(CH_3COO)_2$ was gradually consumed due to the esterification reaction (Figure 45a, red curve). The concentration of $Zn(CH_3COO)_2$ decreased from the initial concentration C_0 (C_0 = 100%) to about 35−40% within 18 min, then it little changed (Figure 45a, red curve). The yield of ZnO increased with time, but reached a maximum value of about 80% after ∼18 min and then remained almost constant. Comparison of the ZnO yield with $Zn(CH_3COO)_2$ concentration showed an inversely related behavior with comparable kinetics. With decreasing $Zn(CH_3COO)_2$ concentration, the ZnO yield increased, and both values became almost constant after 18 min; that is, the system reached a dynamic equilibrium between the dissolved monomer and the solid ZnO. However, the crystal size of ZnO still increased with microwave heating

dx.doi.org/10.1021/cr400366s | Chem. Rev. 2014, 114, 6462−6555

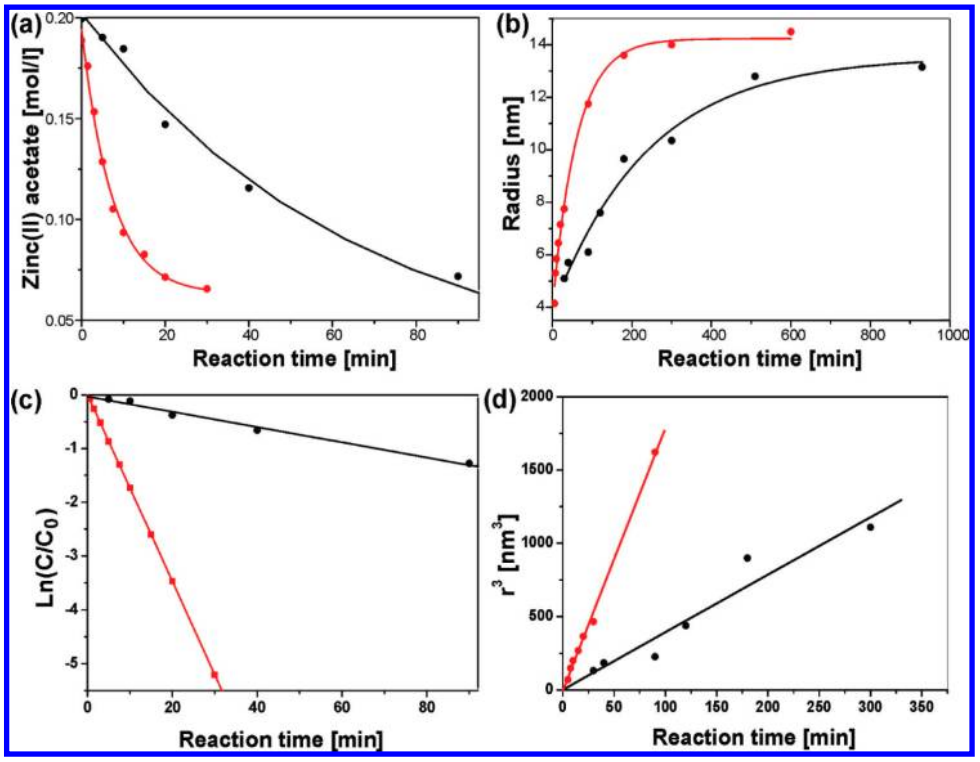

Figure 46. Comparison of benzyl acetate (a,c) and ZnO formation (b,d) by microwave heating (red) and conventional heating (black) at 120 °C. (a) Zinc acetate concentration versus reaction time, (c) corresponding first-order kinetic plot. (b) Radius of ZnO nanocrystals versus reaction time, (d) r^3 versus time according to the Lifshitz–Slyozov–Wagner (LSW) model. Reprinted with permission from ref 772. Copyright 2009 American Chemical Society.

time, indicating that the Ostwald ripening was the only growth mode for longer reaction times. Figure 45b shows a TEM micrograph of ZnO nanoparticles with diameters from 10 to 25 nm obtained by microwave heating at 120 °C for 3 min, and a HRTEM image of a single ZnO nanoparticle exhibiting the single-crystalline nature in structure. Bilecka et al.[772] proposed that the acceleration effect of microwave irradiation is mainly based on kinetic rather than thermodynamic factors, because no experimental indication was found that the activation energy for ester formation or for crystal growth was significantly lowered. It was reported that the activation energy was determined to be 37 kJ mol^{-1} for the benzyl acetate formation, and 60 kJ mol^{-1} for ZnO crystal growth.[772]

For comparison, Bilecka et al.[772] also performed experiments by the conventional heating in an oil bath preheated at 120 °C under otherwise similar conditions, and the obtained experimental results are summarized in Figure 46. The faster dissolution rate of the precursor contributed to the shorter precipitation time of ZnO under microwave irradiation in comparison to the conventional heating. However, microwave irradiation also affected the organic esterification reaction. The change of zinc acetate concentration at 120 °C versus time shows a significant difference between microwave heating (red curve) and conventional heating (black curve) (Figure 46a), which consequently led to different rate constants (Figure 46c). For the conventional heating, the rate constant $k_{esterification}$ was 0.0142 min^{-1}; however, the rate constant was 0.124 min^{-1} for the microwave heating, which corresponds to a kinetic enhancement of almost 1 order of magnitude. Faster esterification also means faster increase in the monomer concentration, suggesting that the nucleation occurs earlier for the microwave-assisted synthesis. In addition to the esterification reaction, the crystal growth of ZnO was greatly enhanced by microwave heating (Figure 46b). The corresponding rate constant k_{growth}, obtained from the LSW analysis, was 15.36 nm^3 min^{-1} for the microwave heating and only 3.9 nm^3 min^{-1} for the conventional heating (Figure 46d), which means that the crystal growth rate under microwave irradiation was about 4 times that by the conventional heating. These experimental results are consistent with the work by Jhung et al.[30] on the microwave-assisted synthesis of microporous materials, which has also shown that microwave irradiation accelerated both the nucleation and the crystal growth with a more obvious effect on the nucleation stage relative to crystal growth.

There have been some conflicting reports on the activation energies for chemical reactions under microwave irradiation, and more careful investigations are needed to clarify this issue in the future. Some papers have reported that the activation energies for microwave-assisted processes are smaller than those by the conventional heating. For example, Lewis et al.[1011] discussed a mechanism based on temperature difference for the microwave-enhanced reaction of imidization in solution. The apparent activation energy for the reaction was reduced from 105 to 55 kJ mol^{-1} when microwave radiation was utilized under the experimental conditions they employed. They proposed a mechanism to explain this enhancement based on the concept of a nonuniform temperature on a molecular scale, rather than a true reduction in the activation energy. They proposed that the pulsed microwave energy would produce effects different from those produced by the continuous microwave irradiation. Brosnan et al.[1012] investigated the sintering kinetics and microstructural evolution of alumina tubes by the conventional heating and microwave heating at

dx.doi.org/10.1021/cr400366s | Chem. Rev. 2014, 114, 6462–6555

Table 2. Calculated Pre-exponential Factors (A) and Activation Energies (E_a) in the Arrhenius Equation $k = A\,e^{-E_a/RT}$ and Activation Free Energy (ΔG) for the Nucleation and Crystal Growth in the Synthesis of Cu_2O Crystals by Three Different Methods[a]

synthesis method	A for nucleation (min^{-1})	E_a for nucleation (kJ mol^{-1})	ΔG for nucleation (kJ mol^{-1})	A for crystal growth (min^{-1})	E_a for crystal growth (kJ mol^{-1})	ΔG for crystal growth (kJ mol^{-1})
ultrasound irradiation	2.72×10^{11}	72.7	91.3	5.32×10^{12}	84.7	94.4
microwave heating	1.36×10^{9}	61.5	94.7	2.92×10^{10}	75.1	99.0
conventional heating	9.23×10^{4}	44.1	103	2.81×10^{6}	58.6	107

[a]The data were collected from ref 1014.

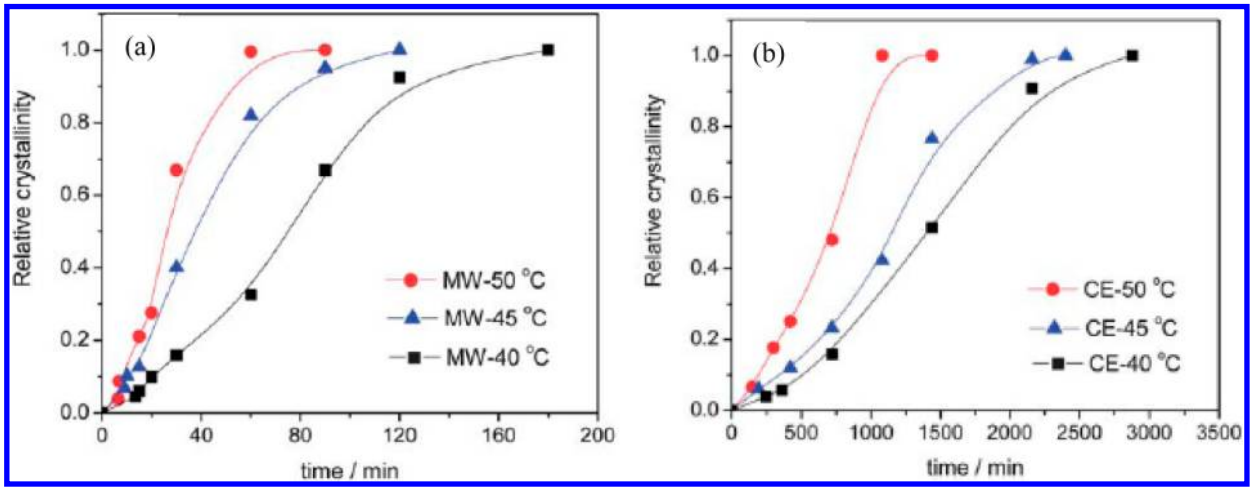

Figure 47. Crystallization curves for the synthesis of Cu_2O crystals by three different methods: (a) microwave heating; (b) conventional heating. Reprinted with permission from ref 1014. Copyright 2011 The Royal Society of Chemistry.

2.45 GHz. With no hold time at the sintering temperature, microwave-sintered samples reached 95% density at 1350 °C versus 1600 °C for conventionally heated samples. The activation energy for microwave sintering was 85 ± 10 kJ mol^{-1}; in comparison, the activation energy for the conventional sintering was 520 ± 14 kJ mol^{-1}. Fang et al.[1013] investigated the kinetic mechanism of the microwave cure of 3,4′-bis[(4-phenylethynyl)phthalimido]diphenyl ether (PEPA-3,4′-ODA) and phenylethynyl-terminated imide oligomer (PETI-5). The microwave cure of PEPA-3,4′-ODA and PETI-5 was investigated using a variable frequency microwave furnace. As compared to the conventional thermal curing rate studies of these two materials, the microwave cure gave much higher rate constants for both. The activation energy of the microwave cure was 68% that of the thermal cure for PEPA-3,4′-ODA, and 51% that of the thermal cure for PETI-5. However, in some reports, the activation energies for microwave-assisted processes were even higher than those by the conventional heating. For example, Haque et al.[1014] reported that the activation energies for the nucleation and crystal growth in the microwave-assisted synthesis of Cu_2O crystals were higher than those by the conventional heating (Table 2). The calculated activation energy for the nucleation of Cu_2O was 61.5 kJ mol^{-1} by the microwave heating and 44.1 kJ mol^{-1} by the conventional heating. In contrast, the activation energy for the crystal growth of Cu_2O crystals was 75.1 kJ mol^{-1} by the microwave heating and 58.6 kJ mol^{-1} by the conventional heating. It was also reported that the activation energies for the microwave-assisted synthesis of porous materials such as metal−organic frameworks and aluminophosphates were higher than those by the conventional heating.[1015]

Haque et al.[1014] compared the effects of the heating methods on the acceleration and yield of Cu_2O crystals. Three different methods including the conventional heating (CE), ultrasound irradiation (US), and microwave heating (MW) were adopted using an aqueous solution containing $CuSO_4{\cdot}5H_2O$, Na_2CO_3, sodium citrate, and PVP. The reaction was carried out at a low temperature (up to 50 °C) to take advantage of low reaction rates for a precise comparison. Cu_2O crystals with a cubic morphology were obtained by ultrasound irradiation and microwave heating; however, a mixture of multipod and truncated octahedra was formed by the conventional heating. Cu_2O crystals obtained by the conventional heating had various sizes and shapes due to concomitant nucleation and crystal growth and long reaction time. The accelerated synthesis with microwaves or ultrasound was explained with the activation energy, pre-exponential factor, and thermodynamic parameters. The rapid microwave-assisted synthesis (acceleration degree was 17−18 times of the conventional heating) was explained by a significant increase in the pre-exponential factor of the Arrhenius equation or decreased activation free energy (ΔG) of the Eyring equation even though the activation energies (E_a) were increased under microwave irradiation. The decreased ΔG was due to the small decrease (or relatively high) in activation entropy (ΔS) rather than low activation enthalpy (ΔH). The activation energy decreased in the order of ultrasound synthesis > microwave synthesis > conventional heating synthesis. They proposed that the acceleration by microwave heating is mainly

dx.doi.org/10.1021/cr400366s | Chem. Rev. 2014, 114, 6462−6555

due to physical effects including hot spots or transient temperature rather than chemical ones.

It was found that the crystallinity of Cu_2O prepared by microwave heating was dependent on the reaction temperature and time.[1014] As shown in Figure 47, the crystallinity of the product changed with the reaction temperature, time, and synthetic methods. The crystallinities of Cu_2O obtained with different methods are compared in Figure 48 at the same reaction temperature of 40 °C. All of the crystallization curves exhibited the typical sigmoid form, which has been widely observed in the syntheses of solid materials. As shown in Figure 47, the fully crystallized Cu_2O was obtained in around 30−90, 60−120, and 1000−3000 min with ultrasound (30−40 °C), microwaves (40−50 °C), and conventional heating (40−50 °C), respectively, showing the synthesis rates were in the order of ultrasound > microwave ≫ conventional heating. The rates for nucleation and crystal growth were evaluated with the time of first appearance of XRD peaks and the slope of crystallization curves of Figure 47, respectively. The crystallization rate was very rapid for the synthesis by both ultrasound irradiation and microwave heating. In contrast, the crystallization rate was very slow for the synthesis by the conventional heating. The crystallization curves of Cu_2O crystals at the same temperature of 40 °C (Figure 48) also indicate the relative crystallization rates of three methods (ultrasound > microwave ≫ conventional heating).

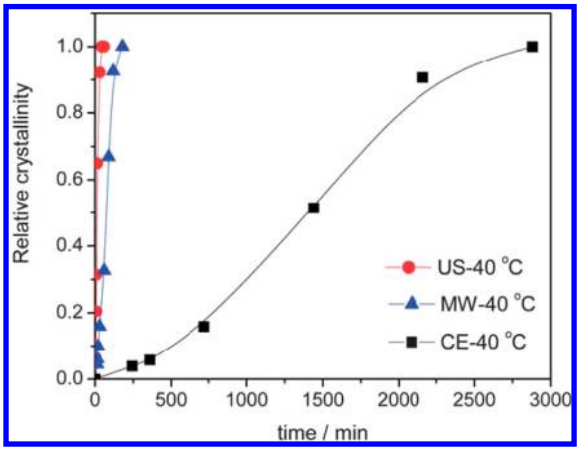

Figure 48. Crystallization curves of Cu_2O crystals synthesized at 40 °C by three different methods. Reprinted with permission from ref 1014. Copyright 2011 The Royal Society of Chemistry.

Haque et al.[1014] compared the product yields by using different methods at the same reaction temperature of 40 °C, as shown in Figure 49a. The yield of the product increased with increasing reaction time or increasing reaction temperature, and the yield changed in the order of ultrasound > microwave > conventional heating. Figure 49b shows that the average particle size of Cu_2O crystals increased with increasing reaction time.

Haque et al.[1015] reported the synthesis of porous materials such as metal−organic frameworks and aluminophosphates by microwave heating and conventional heating at various temperatures for different times to investigate the quantitative acceleration in the microwave-assisted synthesis of porous materials. The acceleration degrees (r_{MW}/r_{CE}) for nucleation and crystal growth by microwave heating were 4.9−32.7 and 20.5−35.9, respectively. There was little effect of the types of porous materials and types of metal ions (Al^{3+}, Cr^{3+}, and V^{4+}) in isotypic metal−organic frameworks on the acceleration degrees in the microwave syntheses of porous materials. Their studies indicated that the free energy (ΔG) of microwave synthesis was lower than that of the conventional synthesis. However, the activation enthalpy (ΔH) and activation entropy (ΔS) were higher for the microwave-assisted synthesis. They proposed that the acceleration by microwaves was mainly due to decreased activation free energy even though the activation energy and activation enthalpy increased. The decreased activation free energy of the microwave synthesis was mainly due to the higher activation entropy of microwave synthesis as compared to that of the conventional synthesis. They proposed that accelerated synthesis with microwaves may be due to changes of relative energies of the intermediates. The relative thermodynamic parameters of microwave and conventional syntheses are summarized in Figure 50. Even though the detailed reasons of the difference in thermodynamic parameters could not be clearly explained, they explained the microwave-accelerated synthesis with a more favorable reaction coordinate (selective heating and changing the reaction profile) or changes of relative energies of the intermediates for high activation entropy with increased randomness.

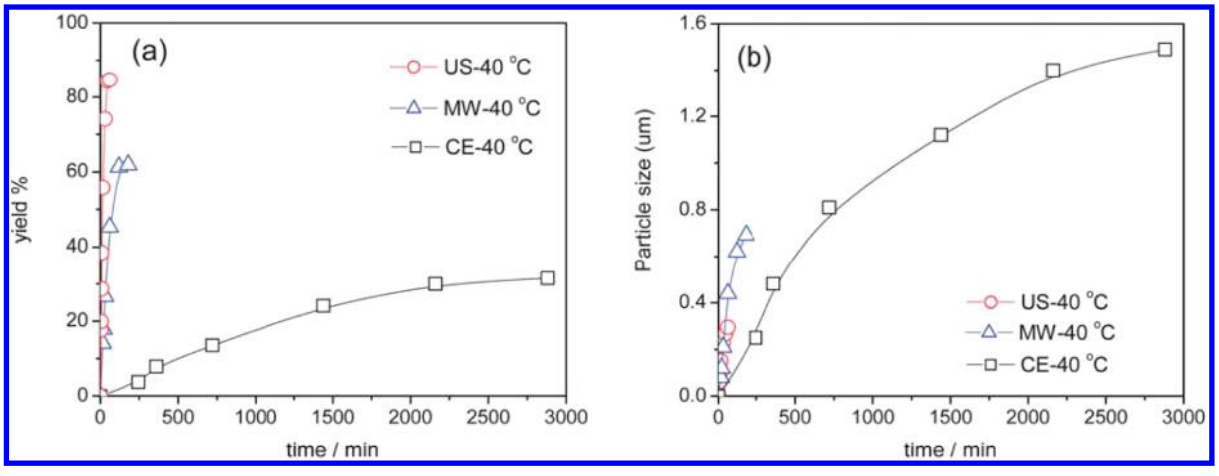

Figure 49. Yields (a) and particle sizes (b) of Cu_2O crystals versus reaction time prepared at 40 °C by three different methods. Reprinted with permission from ref 1014. Copyright 2011 The Royal Society of Chemistry.

dx.doi.org/10.1021/cr400366s | Chem. Rev. 2014, 114, 6462−6555

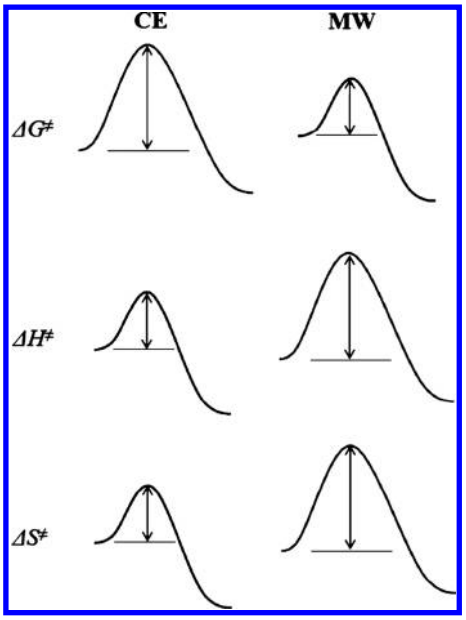

Figure 50. Suggested relative activation free energy, enthalpy, and entropy changes with synthesis methods (CE = conventional heating; MW = microwave heating). Reprinted with permission from ref 1015. Copyright 2011 The American Chemical Society.

Although obvious differences between the microwave heating and conventional heating have been reported in many cases for the preparation of inorganic nanostructures in liquid phase, there have been some reports in which no obvious differences between the microwave heating and conventional heating could be observed. For example, Gutmann et al.[1016] investigated the electromagnetic field effects on 21 selected chemical reactions by comparing the results obtained in microwave-transparent Pyrex vials with the experiments performed in SiC vials at the same reaction temperature. For most of the 21 reactions, the results in terms of the conversion, purity, and product yield using the two different types of vials were virtually identical, indicating that the electromagnetic field had no direct influence on the reaction pathway. Obermayer et al.[54] used a reaction vessel made out of SiC, in combination with a single-mode microwave reactor that allows simultaneous temperature monitoring by external infrared and internal fiber-optic probes. Their experimental setup provided a means to heat a reaction system by a conventional heat transfer mechanism and not by dielectric heating effects, although using microwave irradiation. Eighteen previously reported microwave-assisted organic chemical reactions were investigated in comparison with the conventional heating; however, they did not find any significant differences in terms of the conversion, purity, and product yield between experiments performed in microwave-transparent Pyrex and SiC vials.

Pein et al.[809] investigated the synthesis of $CuInS_2$ nanoparticles using CuI, $InCl_3$, and elemental S in oleylamine as a solvent and capping agent. They carefully carried out the comparative experiments by microwave heating using Pyrex and

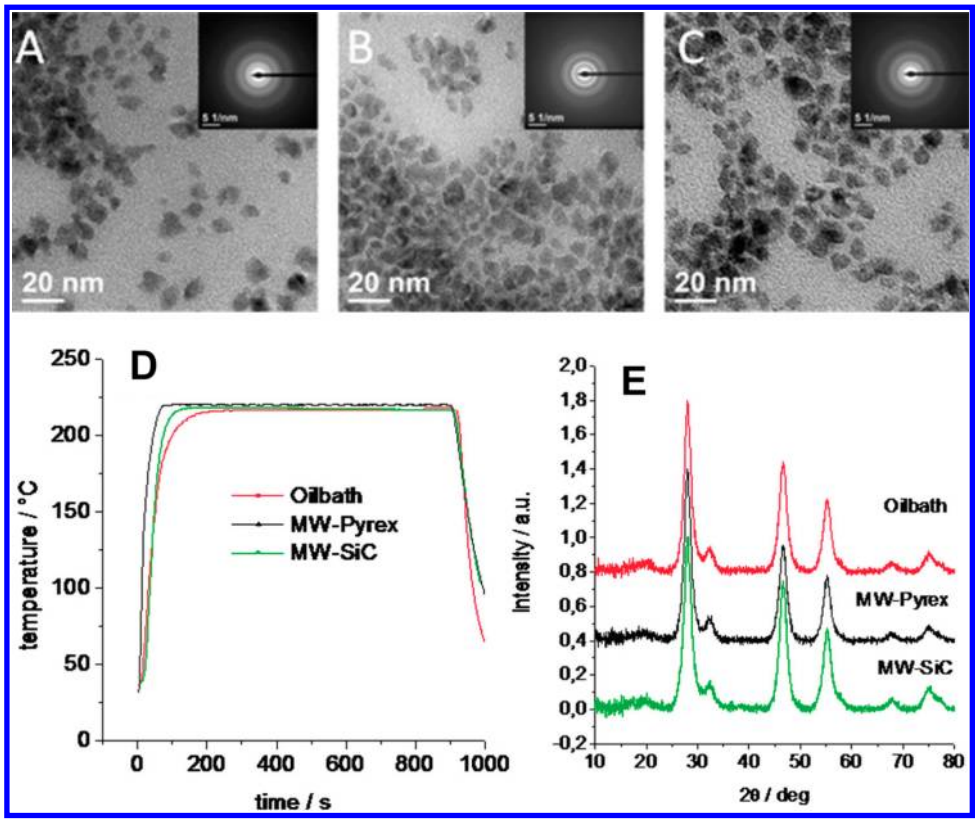

Figure 51. Comparison of $CuInS_2$ nanoparticles synthesized at 220 °C by different heating methods: (A) TEM micrograph and SAED pattern (inset) of the sample obtained by microwave-Pyrex; (B) TEM micrograph and SAED pattern (inset) of the sample obtained by microwave-SiC; (C) TEM micrograph and SAED pattern (inset) of the sample obtained by oil bath; (D) heating profiles of the comparative experiments; and (E) XRD patterns of the samples obtained after 15 min overall reaction time. Reprinted with permission from ref 809. Copyright 2010 The American Chemical Society.

dx.doi.org/10.1021/cr400366s | Chem. Rev. 2014, 114, 6462−6555

SiC vials and conventional heating using SiC vials under otherwise identical reaction conditions. In all cases, the desired final temperature was 220 °C, and the overall heating period (including ramp and hold time) was 15 min. The experiments showed that the samples had the same crystal phase with similar primary crystallite sizes of ~5.4 nm. The TEM micrographs in Figure 51 indicate similar nanoparticle shapes and size distributions in the range between 5 and 10 nm. Both TEM and XRD experiments could not identify significant differences between two heating modes. The only small difference observed was that the microwave-prepared sample had a somewhat higher amount of capping ligand, detected by the thermogravimetric analysis. Carefully executed control experiments, ensuring identical heating and cooling profiles, stirring rates, volumes and concentrations of reactants, and reactor geometries, demonstrated that for the preparation of $CuInS_2$ nanoparticles no differences between the microwave irradiation and conventional heating could be observed.[809]

9. FUTURE PROSPECTS AND CHALLENGES

In summary, as demonstrated in a large number of publications in the literature, the remarkable advantages of the microwave heating technology are rapid volumetric heating, higher chemical reaction rate and selectivity, shorter reaction time, and higher product yield as compared to the conventional heating methods. In many cases, the microwave-assisted syntheses exhibit order-of-magnitude enhancements in chemical reaction rate as compared to the conventional syntheses. As a result, the microwave heating as a novel heat source allows the rapid production of inorganic nanostructured materials in liquid phase, leading to relatively low cost, energy savings, and high efficiency, thus advancing rapidly toward its practical applications. On the other hand, the rich varieties of liquid solvents and their smart combinations will provide a great freedom for the rapid preparation of various nanostructured materials, and more importantly for the control over the chemical composition, structure, size, morphology, and self-assembly, thus greatly expanding the applications of the microwave heating technology in materials science. Therefore, the microwave heating technology has been emerging as an alternative heat source for rapid chemical reactions and materials preparation in minutes, instead of hours or even days usually required by the conventional heating methods. Consequently, the microwave heating technology has been receiving an exponential increase in acceptance, as evidenced by a rapidly increasing number of publications each year. It is expected that the use of the microwave heating technology as an alternative heat source will become more popular in many research laboratories and even in industry. The microwave-assisted rapid preparation of inorganic nanostructures in liquid phase is currently a fast-growing area of research, and the research activities will continue to rapidly expand in the coming years. Although the overwhelming number of microwave-assisted applications are still performed on a laboratory (milliliter) scale, it is expected that this novel technology will be able to scale up for the industrial production in the near future.

However, some challenges still exist and need to be overcome. For example, one major problem is that many published papers did not provide detailed experimental parameters, which are essential for the repeat by other researchers, and the information on the microwave reactors employed and the reaction containers was rarely documented. In some cases, the types of the microwave ovens, typically domestic microwave ovens, were even not mentioned. Many early reports on the microwave-assisted syntheses were carried out in household microwave ovens, and the reproducibility varied with the brand of the instrument, and the size and geometry of the microwave cavity. The microwave heating temperatures were not accurately measured and even not reported in many early published papers. Thus, these reported experiments are difficult to be repeated and compared by other researchers. Therefore, the use of specially designed microwave reactors with the ability to accurately measure and control the temperature is strongly recommended. With the development of the microwave instrumentation technology, together with the reasonable cost and simplicity of its use, researchers now have easy access to commercial microwave reactors with temperature and pressure monitoring by various probes and sensors, built-in magnetic stirring, power control, cooling system, and software operation. It is expected that more microwave-assisted syntheses will be performed using microwave ovens specifically designed for chemical reactions and materials synthesis, which allow precise control of the various experimental parameters and good repeatability. On the other hand, it is strongly suggested that the experimental description in publications for the microwave-assisted synthesis should be as specific and detailed as possible.

Because the mechanisms of the microwave heating are different from those of the conventional heating methods, the mechanisms of the chemical reaction, nucleation, and growth of inorganic nanostructures in liquid phase are also different using different heating methods. Although a large volume of experimental data on microwave-assisted syntheses has been documented in the literature, the detailed mechanisms of the chemical reaction, nucleation, and growth of inorganic nanostructures in liquid phase under microwave irradiation have still not been fully understood, and some important issues such as the nonthermal effects or specific microwave effects under microwave irradiation have not been clearly solved. The existence of nonthermal effects or specific microwave effects under microwave irradiation has been controversial and under intense debate. Therefore, more carefully designed comparative studies between the microwave heating and conventional heating are necessary for further understanding of the microwave heating mechanisms.

Although the comparative studies between the microwave heating and conventional heating are essential for further understanding of the microwave heating mechanisms, many literature reports were based on inaccurate comparisons, which could not reach unequivocal conclusions about microwave effects, leading to some contradictions and controversies in this research field. One of the fundamental difficulties facing all comparative studies between the microwave heating and conventional heating is the discrepancies between different experiments in terms of the microwave field homogeneity (e.g., multimode or single mode microwave oven), size and geometry of microwave cavity and reaction vessel, volume of reaction system, stirring of recation system, microwave power, heating rate, heating temperature, and heating time, etc. Unfortunately, in many cases, the microwave-assisted syntheses were often compared to the experimental data from those that were performed under completely different conditions such as different reaction temperatures and reaction times, and the conclusions drawn from these comparisons are usually inaccurate and speculative. Therefore, it is strongly recom-

dx.doi.org/10.1021/cr400366s | Chem. Rev. 2014, 114, 6462−6555

mended that the comparative studies between the microwave heating and conventional heating should be conducted under exactly identical experimental conditions. However, the challenge is that the rapid and unique temperature profiles of microwave heating are very difficult, if not impossible, to be duplicated by the conventional heating. Therefore, the comparisons of the microwave heating processes with conventional heating ones under the exactly same conditions are inherently challenging.

Some future research trends and directions are expected as follows: (1) the in-depth understanding of the detailed mechanisms of the chemical reaction, nucleation, and growth of inorganic nanostructures in liquid phase under microwave irradiation; (2) carefully designed comparative studies between the microwave heating and conventional heating to clarify some important issues such as the nonthermal effects or specific microwave effects under microwave irradiation, which have been controversial and under intense debate; (3) theoretical and computer simulations of microwave effects and microwave heating mechanisms; (4) research on the microwave-assisted precise control over the chemical composition, structure, size, morphology, and self-assembly of nanostructures; (5) to develop environmentally friendly microwave-assisted synthesis methods at low cost and high efficiency; (6) investigation on scaling up microwave-assisted large-scale production of inorganic nanostructured materials, such as continuous flow microwave synthesis; and (7) investigation on the relationship of structure−property and applications of microwave-prepared nanostructured materials. The realization of these targets will greatly advance microwave chemistry and its wide practical applications in rapid microwave-assisted controlled syntheses of inorganic nanostructured materials in liquid phase, both at the laboratory level and on the industrial scale.

AUTHOR INFORMATION

Corresponding Author

*Tel: +86-21-52412616. Fax: +86-21-52413122. E-mail: y.j.zhu@mail.sic.ac.cn.

Notes

The authors declare no competing financial interest.

Biographies

Ying-Jie Zhu is a full Professor at Shanghai Institute of Ceramics, Chinese Academy of Sciences (CAS). He received his Master degree and Ph.D. at the University of Science and Technology of China (USTC) in 1992 and 1994, respectively. He worked as Assistant Professor and Associate Professor at USTC from 1994 to 1997. He then worked as a Visiting Professor at University of Western Ontario, Canada, from 1997 to 1998. He worked as an Alexander von Humboldt Research Fellow at Fritz-Haber Institut der Max-Planck-Gesellschaft, Germany, from 1998 to 1999. He then worked as a Postdoctoral Fellow at the University of Utah and the University of Delaware, from 1999 to 2002. In 2002, he was selected by the Chinese Academy of Sciences under the Program for Recruiting Overseas Outstanding Talents (Hundred Talents Program), and started to work as a full Professor and a group leader at Shanghai Institute of Ceramics, CAS. He won "Excellence" in the Hundred Talents Program in 2005. He was selected under the Program of Shanghai Subject Chief Scientist in 2007. In 2009, he and his colleagues won the First Class Prize of Natural Sciences of Shanghai (ranked No. 2). He has been working in the research area of microwave-assisted preparation of nanostructured materials for many years. He has published more than 230 peer-reviewed journal papers, and has more than 20 granted patents. He is currently an Editorial Board/Editorial Advisory Board member of six journals. His current main research interests involve nanostructured biomaterials and microwave-assisted preparation of nanostructured materials.

Feng Chen was born in 1981 in Anhui, China. He received his B.S. in Biology from Anhui Normal University in 2005, and received his M.S. in Chemistry under the supervision of Prof. Xiu-Mei Mo from Donghua University in 2008. He then joined the research group of Professor Ying-Jie Zhu at Shanghai Institute of Ceramics, Chinese Academy of Sciences. His current research interest focuses on the microwave-assisted synthesis, properties, and applications of nanostructured materials.

ACKNOWLEDGMENTS

The financial support from the National Natural Science Foundation of China (51172260, 51121064), the National Basic Research Program of China (973 Program, No. 2012CB933600), and the Science and Technology Commission of Shanghai (11nm0506600) is gratefully acknowledged.

ABBREVIATIONS

1-D	one-dimensional
[BMIM][BF_4]	1-*n*-butyl-3-methylimidazolium tetrafluoroborate
BSA	bovine serum albumin
CTAB	cetyltrimethylammonium bromide
DMF	*N*,*N*-dimethylformamide
EDTA	ethylenediaminetetraacetic acid
EG	ethylene glycol
HAP	hydroxyapatite
HMTA	hexamethylenetetramine

P123	poly(ethylene glycol)-block-poly(propylene glycol)-block-poly(ethylene glycol)
PEG	poly(ethylene glycol)
PVP	poly(vinylpyrrolidone)
SAED	selected-area electron diffraction
SDS	sodium dodecyl sulfate
SEM	scanning electron microscopy
TEOS	tetraethyl orthosilicate
TEM	transmission electron microscopy
XRD	X-ray powder diffraction

REFERENCES

(1) Hayes, B. L. *Microwave Synthesis: Chemistry at the Speed of Light*; CEM Publishing: Matthews, 2002.
(2) Bilecka, I.; Niederberger, M. *Nanoscale* **2010**, *2*, 1358.
(3) Dallinger, D.; Kappe, C. O. *Chem. Rev.* **2007**, *107*, 2563.
(4) Tompsett, G. A.; Conner, W. C.; Yngvesson, K. S. *ChemPhysChem* **2006**, *7*, 296.
(5) Ryan, M. A., Tinnesand, M., Eds. *Introduction to Green Chemistry*; American Chemical Society: Washington, DC, 2002.
(6) Patete, J. M.; Peng, X. H.; Koenigsmann, C.; Xu, Y.; Karn, B.; Wong, S. S. *Green Chem.* **2011**, *13*, 482.
(7) Dahl, J. A.; Maddux, B. L. S.; Hutchison, J. E. *Chem. Rev.* **2007**, *107*, 2228.
(8) Komarneni, S.; Roy, R. *Mater. Lett.* **1985**, *3*, 165.
(9) Gedye, R.; Smith, F.; Westaway, K.; Ali, H.; Baldisera, L.; Laberge, L.; Rousell, J. *Tetrahedron Lett.* **1986**, *27*, 279.
(10) Giguere, R. J.; Bray, T. L.; Duncan, S. M.; Majetich, G. *Tetrahedron Lett.* **1986**, *27*, 4945.
(11) Rao, K. J.; Vaidhyanathan, B.; Ganguli, M.; Ramakrishnan, P. A. *Chem. Mater.* **1999**, *11*, 882.
(12) Collins, M. J., Jr. *Future Med. Chem.* **2010**, *2*, 151.
(13) Nadagouda, M. N.; Speth, T. F.; Varma, R. S. *Acc. Chem. Res.* **2011**, *44*, 469.
(14) Tsuji, M.; Hashimoto, M.; Nishizawa, Y.; Kubokawa, M.; Tsuji, T. *Chem.—Eur. J.* **2005**, *11*, 440.
(15) Zhang, X. Y.; Liu, Z. *Nanoscale* **2012**, *4*, 707.
(16) Park, S. E.; Chang, J. S.; Hwang, Y. K.; Kim, D. S.; Jhung, S. H.; Hwang, J. S. *Catal. Surv. Asia* **2004**, *8*, 91.
(17) Baghbanzadeh, M.; Carbone, L.; Cozzoli, P. D.; Kappe, C. O. *Angew. Chem., Int. Ed.* **2011**, *50*, 11312.
(18) Motshekga, S. C.; Pillai, S. K.; Ray, S. S.; Jalama, K.; Krause, R. W. M. *J. Nanomater.* **2012**, *2012*, 691503.
(19) Bogdal, D.; Prociak, A.; Michalowski, S. *Curr. Org. Chem.* **2011**, *15*, 178.
(20) Li, Y. S.; Yang, W. S. *J. Membr. Sci.* **2008**, *316*, 3.
(21) Klinowski, J.; Almeida Paz, F. A.; Silva, P.; Rocha, J. *Dalton Trans.* **2011**, *40*, 321.
(22) Das, S.; Mukhopadhyay, A. K.; Datta, S.; Basu, D. *Bull. Mater. Sci.* **2008**, *31*, 943.
(23) Nehlig, E.; Milosevic, I.; Motte, L.; Guenin, E. *Curr. Org. Chem.* **2013**, *17*, 528.
(24) Nüchter, M.; Ondruschka, B.; Bonrath, W.; Gum, A. *Green Chem.* **2004**, *6*, 128.
(25) Gabriel, C.; Gabriel, S.; Grant, E. H.; Halstead, B. S. J.; Mingos, D. M. P. *Chem. Soc. Rev.* **1998**, *27*, 213.
(26) Mingos, D. M. P.; Baghurst, D. R. *Chem. Soc. Rev.* **1991**, *20*, 1.
(27) Galema, S. A. *Chem. Soc. Rev.* **1997**, *26*, 233.
(28) Schanche, J.-S. *Mol. Diversity* **2003**, *7*, 293.
(29) Kappe, C. O. *Angew. Chem., Int. Ed.* **2004**, *43*, 6250.
(30) Jhung, S. H.; Jin, T. H.; Hwang, Y. K.; Chang, J. S. *Chem.—Eur. J.* **2007**, *13*, 4410.
(31) Horikoshi, S.; Sakai, F.; Kajitani, M.; Abe, M.; Serpone, N. *Chem. Phys. Lett.* **2009**, *470*, 304.
(32) Horikoshi, S.; Abe, H.; Sumi, T.; Torigoe, K.; Sakai, H.; Serpone, N.; Abe, M. *Nanoscale* **2011**, *3*, 1697.
(33) Bogdal, D. *Microwave-Assisted Organic Synthesis-One Hundred Reaction Procedures*; Tetrahedron Organic Chemistry Series; Elsevier: New York, 2005.
(34) Malinger, K. A.; Ding, Y. S.; Sithambaram, S.; Espinal, L.; Gomez, S.; Suib, S. L. *J. Catal.* **2006**, *239*, 290.
(35) Jiang, H. J.; Moon, K. S.; Zhang, Z. Q.; Pothukuchi, S.; Wong, C. P. *J. Nanopart. Res.* **2006**, *8*, 117.
(36) Nyutu, E. K.; Chen, C. H.; Dutta, P. K.; Suib, S. L. *J. Phys. Chem. C* **2008**, *112*, 9659.
(37) Seol, S. K.; Kim, D.; Jung, S.; Hwu, Y. *Mater. Chem. Phys.* **2011**, *131*, 331.
(38) Yang, Y.; Hu, Y. Y.; Xiong, X. H.; Qin, Y. Z. *RSC Adv.* **2013**, *3*, 8431.
(39) Shen, P. K.; Yin, S. B.; Li, Z. H.; Chen, C. *Electrochim. Acta* **2010**, *55*, 7969.
(40) Gedye, R. N.; Smith, F. E.; Westaway, K. C. *Can. J. Chem.* **1988**, *66*, 17.
(41) Gedye, R. N.; Rank, W.; Westaway, K. C. *Can. J. Chem.* **1991**, *69*, 706.
(42) Bonaccorsi, L.; Proverbio, E. *J. Cryst. Growth* **2003**, *247*, 555.
(43) Conner, W. C.; Tompsett, G.; Lee, K.-H.; Yngvesson, K. S. *J. Phys. Chem. B* **2004**, *108*, 13913.
(44) Panzarella, B.; Tompsett, G. A.; Yngvesson, K. S.; Conner, W. C. *J. Phys. Chem. B* **2007**, *111*, 12657.
(45) Komarneni, S.; Katsuki, H. *Ceram. Int.* **2010**, *36*, 1165.
(46) Katsuki, H.; Furuta, S.; Komarneni, S. *Mater. Lett.* **2012**, *83*, 8.
(47) Robinson, J.; Kingman, S.; Irvine, D.; Licence, P.; Smith, A.; Dimitrakis, G.; Obermayer, D.; Kappe, C. O. *Phys. Chem. Chem. Phys.* **2010**, *12*, 4750.
(48) Langa, F.; de la Cruz, P.; de la Hoz, A.; Díaz-Ortiz, A.; Díez-Barra, E. *Contemp. Org. Synth.* **1997**, *4*, 373.
(49) Jacob, J.; Chia, L. H. L.; Boey, F. Y. C. *J. Mater. Sci.* **1995**, *30*, 5321.
(50) Perreux, L.; Loupy, A. *Tetrahedron* **2001**, *57*, 9199.
(51) Kuhnert, N. *Angew. Chem., Int. Ed.* **2002**, *41*, 1863.
(52) de la Hoz, A.; Díaz-Ortiz, Á.; Moreno, A. *Chem. Soc. Rev.* **2005**, *34*, 164.
(53) Godinho, M.; Ribeiro, C.; Longo, E.; Leite, E. R. *Cryst. Growth Des.* **2008**, *8*, 384.
(54) Obermayer, D.; Gutmann, B.; Kappe, C. O. *Angew. Chem., Int. Ed.* **2009**, *48*, 8321.
(55) Washington, A. L.; Strouse, G. F. *J. Am. Chem. Soc.* **2008**, *130*, 8916.
(56) Conner, W. C.; Tompsett, G. A. *J. Phys. Chem. B* **2008**, *112*, 2110.
(57) Leadbeater, N. E.; Torenius, H. M. *J. Org. Chem.* **2002**, *67*, 3145.
(58) Cushing, B. L.; Kolesnichenko, V. L.; O'Connor, C. J. *Chem. Rev.* **2004**, *104*, 3893.
(59) Yoshimura, M.; Byrappa, K. *J. Mater. Sci.* **2008**, *43*, 2085.
(60) Komarneni, S.; Roy, R.; Li, Q. H. *Mater. Res. Bull.* **1992**, *27*, 1393.
(61) Komarneni, S.; Katsuki, H. *Pure Appl. Chem.* **2002**, *74*, 1537.
(62) Rajamathi, M.; Seshadri, R. *Curr. Opin. Solid State Mater. Sci.* **2002**, *6*, 337.
(63) Polshettiwar, V.; Varma, R. S. *Green Chem.* **2010**, *12*, 743.
(64) Craig, D. Q. M. *Dielectric Analysis of Pharmaceutical Systems*; Taylor and Francis, UK, 1995.
(65) Baruwati, B.; Varma, R. S. *ChemSusChem* **2009**, *2*, 1041.
(66) Polshettiwar, V.; Nadagouda, M. N.; Varma, R. S. *Aust. J. Chem.* **2009**, *62*, 16.
(67) Meng, X. K.; Tang, S. C.; Vongehr, S. *J. Mater. Sci. Technol.* **2010**, *26*, 487.
(68) Vargas-Hernandez, C.; Mariscal, M. M.; Esparza, R.; Yacaman, M. J. *Appl. Phys. Lett.* **2010**, *96*, 213115.
(69) Shang, L.; Yang, L. X.; Stockmar, F.; Popescu, R.; Trouillet, V.; Bruns, M.; Gerthsen, D.; Nienhaus, G. U. *Nanoscale* **2012**, *4*, 4155.
(70) Pal, A.; Shah, S.; Devi, S. *Colloids Surf., A* **2007**, *302*, 51.
(71) Kundu, S.; Wang, K.; Liang, H. *J. Phys. Chem. C* **2009**, *113*, 5157.

(72) Uppal, M. A.; Kafizas, A.; Ewing, M. B.; Parkin, I. P. *New J. Chem.* **2010**, *34*, 2906.
(73) Fang, Y.; Ren, Y. P.; Jiang, M. *Colloid Polym. Sci.* **2011**, *289*, 1769.
(74) Arshi, N.; Ahmed, F.; Kumar, S.; Anwar, M. S.; Lu, J. Q.; Koo, B. H.; Lee, C. G. *Curr. Appl. Phys.* **2011**, *11*, S360.
(75) Wang, J.; Wang, Z. X. *Mater. Lett.* **2007**, *61*, 4149.
(76) Mallikarjuna, N. N.; Varma, R. S. *Cryst. Growth Des.* **2007**, *7*, 686.
(77) Aswathy, B.; Suji, S.; Avadhani, G. S.; Aswathy, R.; Suganthi, S.; Sony, G. *J. Mol. Liq.* **2011**, *162*, 155.
(78) Kundu, S.; Liang, H. *J. Nanosci. Nanotechnol.* **2010**, *10*, 746.
(79) Kundu, S.; Liang, H. *Colloids Surf., A* **2008**, *330*, 143.
(80) Kundu, S.; Peng, L. H.; Liang, H. *Inorg. Chem.* **2008**, *47*, 6344.
(81) Lee, J. H.; Hong, S. K.; Kim, J. M.; Ko, W. B. *J. Nanosci. Nanotechnol.* **2011**, *11*, 734.
(82) Sun, X. P.; Luo, Y. L. *Mater. Lett.* **2005**, *59*, 4048.
(83) Zhang, Z. W.; Jia, J.; Ma, Y. Y.; Weng, J.; Sun, Y. A.; Sun, L. P. *MedChemComm* **2011**, *2*, 1079.
(84) He, D. F.; Xiang, Y.; Wang, X.; Yu, X. F. *Mater. Res. Bull.* **2011**, *46*, 2418.
(85) Lee, Y.; Geckeler, K. E. *J. Biomed. Mater. Res., Part A* **2012**, *100A*, 848.
(86) Yue, Y.; Liu, T.-Y.; Li, H.-W.; Liu, Z. Y.; Wu, Y. Q. *Nanoscale* **2012**, *4*, 2251.
(87) Yan, L.; Cai, Y. Q.; Zheng, B. Z.; Yuan, H. Y.; Guo, Y.; Xiao, D.; Choi, M. M. F. *J. Mater. Chem.* **2012**, *22*, 1000.
(88) Kou, J. H.; Varma, R. S. *RSC Adv.* **2012**, *2*, 10283.
(89) Fragoon, A.; Li, J. J.; Zhu, J.; Zhao, J. W. *J. Nanosci. Nanotechnol.* **2012**, *12*, 2337.
(90) Luo, Y. L. *Mater. Lett.* **2007**, *61*, 1873.
(91) Wang, H. J.; Wang, L.; Nemoto, Y.; Suzuki, N.; Yamauchi, Y. *J. Nanosci. Nanotechnol.* **2010**, *10*, 6489.
(92) Li, R. Q.; Wang, C. L.; Bo, F.; Wang, Z. Y.; Shao, H. B.; Xu, S. H.; Cui, Y. P. *ChemPhysChem* **2012**, *13*, 2097.
(93) Kundu, S.; Maheshwari, V.; Niu, S.; Saraf, R. F. *Nanotechnology* **2008**, *19*, 065604.
(94) Sreeram, K. J.; Nidhin, M.; Nair, B. U. *Bull. Mater. Sci.* **2008**, *31*, 937.
(95) Raghunandan, D.; Mahesh, B. D.; Basavaraja, S.; Balaji, S. D.; Manjunath, S. Y.; Venkataraman, A. *J. Nanopart. Res.* **2011**, *13*, 2021.
(96) Liu, F. K.; Huang, P. W.; Chang, Y. C.; Ko, F. H.; Chu, T. C. *J. Mater. Res.* **2004**, *19*, 469.
(97) Luo, Y. L.; Sun, X. P. *Mater. Lett.* **2007**, *61*, 1622.
(98) Liu, F. K.; Huang, P. W.; Chu, T. C.; Ko, F. H. *Mater. Lett.* **2005**, *59*, 940.
(99) Hu, B.; Wang, S. B.; Wang, K.; Zhang, M.; Yu, S. H. *J. Phys. Chem. C* **2008**, *112*, 11169.
(100) Chen, J.; Wang, J.; Zhang, X.; Jin, Y. L. *Mater. Chem. Phys.* **2008**, *108*, 421.
(101) Filippo, E.; Serra, A.; Manno, D. *Colloids Surf., A* **2009**, *348*, 205.
(102) Baruwati, B.; Polshettiwar, V.; Varma, R. S. *Green Chem.* **2009**, *11*, 926.
(103) Liu, S.-H.; Lu, F.; Zhu, J.-J. *Chem. Commun.* **2011**, *47*, 2661.
(104) Filippo, E.; Manno, D.; Buccolieri, A.; Di Giulio, M.; Serra, A. *Superlattices Microstruct.* **2010**, *47*, 66.
(105) Cui, Q.; Zhong, L. B.; Ding, J. B.; Weng, J. *Curr. Nanosci.* **2010**, *6*, 610.
(106) Valodkar, M.; Modi, S.; Pal, A.; Thakore, S. *Mater. Res. Bull.* **2011**, *46*, 384.
(107) Saifuddin, N.; Wong, C. W.; Yasumira, A. A. N. *E-J. Chem.* **2009**, *6*, 61.
(108) Kundu, S.; Wang, K.; Liang, H. *J. Phys. Chem. C* **2009**, *113*, 134.
(109) Chaudhari, P. R.; Masurkar, S. A.; Shidore, V. B.; Kamble, S. P. *Micro Nano Lett.* **2012**, *7*, 646.
(110) Tsuji, M.; Gomi, S.; Maeda, Y.; Matsunaga, M.; Hikino, S.; Uto, K.; Tsuji, T.; Kawazumi, H. *Langmuir* **2012**, *28*, 8845.
(111) Horikoshi, S.; Abe, H.; Torigoe, K.; Abe, M.; Serpone, N. *Nanoscale* **2010**, *2*, 1441.
(112) Mehta, S. K.; Gupta, S. *J. Appl. Electrochem.* **2011**, *41*, 1407.
(113) Zhang, H.; Yin, Y. J.; Hu, Y. J.; Li, C. Y.; Wu, P.; Wei, S. H.; Cai, C. X. *J. Phys. Chem. C* **2010**, *114*, 11861.
(114) Liu, Y.-Q.; Zhang, M.; Wang, F.-X.; Pan, G.-B. *RSC Adv.* **2012**, *2*, 11235.
(115) Pradhan, M.; Sarkar, S.; Sinha, A. K.; Basu, M.; Pal, T. *J. Phys. Chem. C* **2010**, *114*, 16129.
(116) Nishioka, M.; Miyakawa, M.; Daino, Y.; Kataoka, H.; Koda, H.; Sato, K.; Suzuki, T. M. *Ind. Eng. Chem. Res.* **2013**, *52*, 4683.
(117) Zhou, B.; Hong, J. M.; Zhu, J. J. *Mater. Lett.* **2005**, *59*, 3081.
(118) He, Y.; Zhong, Y. L.; Peng, F.; Wei, X. P.; Su, Y. Y.; Lu, Y. M.; Su, S.; Gu, W.; Liao, L. S.; Lee, S.-T. *J. Am. Chem. Soc.* **2011**, *133*, 14192.
(119) Zhong, Y. L.; Peng, F.; Wei, X. P.; Zhou, Y. F.; Wang, J.; Jiang, X. X.; Su, Y. Y.; Su, S.; Lee, S.-T.; He, Y. *Angew. Chem., Int. Ed.* **2012**, *51*, 8485.
(120) Liu, J. W.; Chen, F.; Zhang, M.; Qi, H.; Zhang, C. L.; Yu, S. H. *Langmuir* **2010**, *26*, 11372.
(121) Liu, T.; Zhang, G.; Su, X.; Chen, X. G.; Wang, D. H.; Qin, J. G. *J. Nanosci. Nanotechnol.* **2007**, *7*, 2500.
(122) Gao, F.; Lu, Q. Y.; Meng, X. K.; Komarneni, S. *J. Mater. Sci.* **2008**, *43*, 2377.
(123) Wang, X. H.; Qu, K. G.; Xu, B. L.; Ren, J. S.; Qu, X. G. *J. Mater. Chem.* **2011**, *21*, 2445.
(124) Mitra, S.; Chandra, S.; Patra, P.; Pramanik, P.; Goswami, A. *J. Mater. Chem.* **2011**, *21*, 17638.
(125) Puvvada, N.; Kumar, B. N. P.; Konar, S.; Kalita, H.; Mandal, M.; Pathak, A. *Sci. Technol. Adv. Mater.* **2012**, *13*, 045008.
(126) Wang, Q. L.; Zheng, H. Z.; Long, Y. J.; Zhang, L. Y.; Gao, M.; Bai, W. J. *Carbon* **2011**, *49*, 3134.
(127) Jiang, J.; He, Y.; Li, S. Y.; Cui, H. *Chem. Commun.* **2012**, *48*, 9634.
(128) Jaiswal, A.; Ghosh, S. S.; Chattopadhyay, A. *Chem. Commun.* **2012**, *48*, 407.
(129) Wang, Q.; Liu, X.; Zhang, L. C.; Lv, Y. *Analyst* **2012**, *137*, 5392.
(130) Song, Y. C.; Shi, W.; Chen, W.; Li, X. H.; Ma, H. M. *J. Mater. Chem.* **2012**, *22*, 12568.
(131) Chandra, S.; Das, P.; Bag, S.; Laha, D.; Pramanik, P. *Nanoscale* **2011**, *3*, 1533.
(132) Zhu, H.; Wang, X. L.; Li, Y. L.; Wang, Z. J.; Yang, F.; Yang, X. R. *Chem. Commun.* **2009**, 5118.
(133) Cui, R. J.; Liu, C.; Shen, J. M.; Gao, D.; Zhu, J. J.; Chen, H. Y. *Adv. Funct. Mater.* **2008**, *18*, 2197.
(134) Zhang, M.; Liu, S.; Yin, X. M.; Du, Z. F.; Hao, Q. Y.; Lei, D. N.; Li, Q. H.; Wang, T. H. *Chem.—Asian J.* **2011**, *6*, 1151.
(135) Janowska, I.; Chizari, K.; Ersen, O.; Zafeiratos, S.; Soubane, D.; Da Costa, V.; Speisser, V.; Boeglin, C.; Houlle, M.; Begin, D.; Plee, D.; Ledoux, M. J.; Pham-Huu, C. *Nano Res.* **2010**, *3*, 126.
(136) Choi, B. G.; Park, H.; Yang, M. H.; Jung, Y. M.; Lee, S. Y.; Hong, W. H.; Park, T. J. *Nanoscale* **2010**, *2*, 2692.
(137) Long, J.; Fang, M.; Chen, G. H. *J. Mater. Chem.* **2011**, *21*, 10421.
(138) Vadahanambi, S.; Jung, J.-H.; Oh, I.-K. *Carbon* **2011**, *49*, 4449.
(139) Al-Hazmi, F.; Alnowaiser, F.; Al-Ghamdi, A. A.; Al-Ghamdi, A. A.; Aly, M. M.; Al-Tuwirqi, R. M.; El-Tantawy, F. *Superlattices Microstruct.* **2012**, *52*, 200.
(140) Wang, K. M.; Huang, T.; Liu, H. F.; Zhao, Y. X.; Liu, H. W.; Sun, C. T. *Colloids Surf., A* **2008**, *325*, 21.
(141) Pan, R. J.; Wu, Y. C.; Wang, Q. P.; Hong, Y. *Chem. Eng. J.* **2009**, *153*, 206.
(142) Hu, X. L.; Zhu, Y. J.; Wang, S. W. *Mater. Chem. Phys.* **2004**, *88*, 421.
(143) Unalan, H. E.; Hiralal, P.; Rupesinghe, N.; Dalal, S.; Milne, W. I.; Amaratunga, G. A. J. *Nanotechnology* **2008**, *19*, 255608.
(144) Jing, Z. H.; Zhan, J. H. *Adv. Mater.* **2008**, *20*, 4547.

(145) Wu, W. T.; Shi, L.; Zhu, Q. R.; Wang, Y. S.; Xu, G. Y.; Pang, W. M. *Mater. Lett.* **2008**, *62*, 159.
(146) Thongtem, T.; Phuruangrat, A.; Thongtem, S. *Ceram. Int.* **2010**, *36*, 257.
(147) Phuruangrat, A.; Thongtem, T.; Thongtem, S. *Mater. Lett.* **2009**, *63*, 1224.
(148) Hamedani, N. F.; Mahjoub, A. R.; Khodadadi, A. A.; Mortazavi, Y. *Sens. Actuators, B* **2011**, *156*, 737.
(149) Liu, H.; Zhu, Z. F.; Yang, D.; Sun, H. J. *Mater. Technol.* **2011**, *26*, 62.
(150) Chen, M.; Wang, Z. H.; Han, D. M.; Gu, F. B.; Guo, G. S. *J. Phys. Chem. C* **2011**, *115*, 12763.
(151) Rai, P.; Song, H.-M.; Kim, Y.-S.; Song, M.-K.; Oh, P.-R.; Yoon, J.-M.; Yu, Y.-T. *Mater. Lett.* **2012**, *68*, 90.
(152) Cho, S.; Kim, S.; Kim, N. H.; Lee, U. J.; Jung, S. H.; Oh, E.; Lee, K. H. *J. Phys. Chem. C* **2008**, *112*, 17760.
(153) Cho, S.; Jung, S. H.; Lee, K. H. *J. Phys. Chem. C* **2008**, *112*, 12769.
(154) Kong, X. R.; Duan, Y. Q.; Peng, P.; Qiu, C.; Wu, L. Y.; Liu, L.; Zheng, W. J. *Chem. Lett.* **2007**, *36*, 428.
(155) Wu, D. S.; Han, C. Y.; Wang, S. Y.; Wu, N. L.; Rusakova, I. A. *Mater. Lett.* **2002**, *53*, 155.
(156) Pires, F. I.; Joanni, E.; Savu, R.; Zaghete, M. A.; Longo, E.; Varela, J. A. *Mater. Lett.* **2008**, *62*, 239.
(157) Zhu, J. J.; Zhu, J. M.; Liao, X. H.; Fang, J. L.; Zhou, M. G.; Chen, H. Y. *Mater. Lett.* **2002**, *53*, 12.
(158) Yoshinaga, M.; Kijima, N.; Wakahara, S.; Akimoto, J. *Chem. Lett.* **2011**, *40*, 414.
(159) Jouhannaud, J.; Rossignol, J.; Stuerga, D. *J. Solid State Chem.* **2008**, *181*, 1439.
(160) Krishna, M.; Komarneni, S. *Ceram. Int.* **2009**, *35*, 3375.
(161) Wang, H. E.; Xi, L. J.; Ma, R. G.; Lu, Z. G.; Chung, C. Y.; Bello, I.; Zapien, J. A. *J. Solid State Chem.* **2012**, *190*, 104.
(162) Yang, Y.-L.; Hu, C.-C.; Hua, C.-C. *CrystEngComm* **2011**, *13*, 5638.
(163) Wang, W. W.; Zhu, Y. J.; Ruan, M. L. *J. Nanopart. Res.* **2007**, *9*, 419.
(164) Katsuki, H.; Shiraishi, A.; Komarneni, S.; Moon, W. J.; Toh, S.; Kaneko, K. *J. Ceram. Soc. Jpn.* **2004**, *112*, 384.
(165) Zhang, X. J.; Li, Q. L. *Mater. Lett.* **2008**, *62*, 988.
(166) Qiu, G. H.; Huang, H.; Genuino, H.; Opembe, N.; Stafford, L.; Dharmarathna, S.; Suib, S. L. *J. Phys. Chem. C* **2011**, *115*, 19626.
(167) Hu, X. L.; Yu, J. C. *Adv. Funct. Mater.* **2008**, *18*, 880.
(168) Hu, X. L.; Yu, J. C.; Gong, J. M.; Li, Q.; Li, G. S. *Adv. Mater.* **2007**, *19*, 2324.
(169) Hu, X. L.; Yu, J. C.; Gong, J. M. *J. Phys. Chem. C* **2007**, *111*, 11180.
(170) Xue, B.; Liu, R.; Xu, Z. D.; Zheng, Y. F. *Chem. Lett.* **2008**, *37*, 1058.
(171) Sreeja, V.; Joy, P. A. *Mater. Res. Bull.* **2007**, *42*, 1570.
(172) Hong, R. Y.; Pan, T. T.; Li, H. Z. *J. Magn. Magn. Mater.* **2006**, *303*, 60.
(173) Miao, F.; Hua, W.; Hu, L.; Huang, K. M. *Mater. Lett.* **2011**, *65*, 1031.
(174) Zhou, H. F.; Yi, R.; Li, J. H.; Su, Y.; Liu, X. H. *Solid State Sci.* **2010**, *12*, 99.
(175) Muraliganth, T.; Murugan, A. V.; Manthiram, A. *Chem. Commun.* **2009**, 7360.
(176) Ma, G. B.; Zhou, S. H.; Huang, S. S. *Int. J. Mod. Phys. B* **2005**, *19*, 2841.
(177) Li, L.; Ren, J. C. *Mater. Res. Bull.* **2006**, *41*, 2286.
(178) Lai, T. L.; Lai, Y. L.; Lee, C. C.; Shu, Y. Y.; Wang, C. B. *Catal. Today* **2008**, *131*, 105.
(179) Meher, S. K.; Rao, G. R. *J. Phys. Chem. C* **2011**, *115*, 25543.
(180) Al-Tuwirqi, R.; Al-Ghamdi, A. A.; Aal, N. A.; Umar, A.; Mahmoud, W. E. *Superlattices Microstruct.* **2011**, *49*, 416.
(181) Wang, J. Q.; Niu, B.; Du, G. D.; Zeng, R.; Chen, Z. X.; Guo, Z. P.; Dou, S. X. *Mater. Chem. Phys.* **2011**, *126*, 747.
(182) Liang, Z. H.; Zhu, Y. J. *Chem. Lett.* **2005**, *34*, 214.
(183) Zhu, H. T.; Zhang, C. Y.; Tang, Y. M.; Wang, J. X. *J. Phys. Chem. C* **2007**, *111*, 1646.
(184) Deng, C. H.; Hu, H. M.; Zhu, W. L.; Han, C. L.; Shao, G. Q. *Mater. Lett.* **2011**, *65*, 575.
(185) Chen, G.; Zhou, H. F.; Ma, W.; Zhang, D.; Qiu, G. Z.; Liu, X. H. *Solid State Sci.* **2011**, *13*, 2137.
(186) Volanti, D. P.; Orlandi, M. O.; Andrés, J.; Longo, E. *CrystEngComm* **2010**, *12*, 1696.
(187) Qiu, G. H.; Dharmarathna, S.; Zhang, Y. S.; Opembe, N.; Huang, H.; Suib, S. L. *J. Phys. Chem. C* **2012**, *116*, 468.
(188) Moura, A. P.; Cavalcante, L. S.; Sczancoski, J. C.; Stroppa, D. G.; Paris, E. C.; Ramirez, A. J.; Varela, J. A.; Longo, E. *Adv. Powder Technol.* **2010**, *21*, 197.
(189) Liang, Z. H.; Zhu, Y. J. *Chem. Lett.* **2004**, *33*, 1314.
(190) Yang, L. X.; Zhu, Y. J.; Tong, H.; Wang, W. W.; Cheng, G. F. *J. Solid State Chem.* **2006**, *179*, 1225.
(191) Ai, Z. H.; Zhang, L. Z.; Kong, F. H.; Liu, H.; Xing, W. T.; Qiu, J. R. *Mater. Chem. Phys.* **2008**, *111*, 162.
(192) Du, G. D.; Wang, J. Q.; Guo, Z. P.; Chen, Z. X.; Liu, H. K. *Mater. Lett.* **2011**, *65*, 1319.
(193) Li, Y. L.; Wang, J. J.; Zhang, Y.; Banis, M. N.; Liu, J.; Geng, D. S.; Li, R. Y.; Sun, X. L. *J. Colloid Interface Sci.* **2012**, *369*, 123.
(194) Truong, T. T.; Liu, Y. Z.; Ren, Y.; Trahey, L.; Sun, Y. G. *ACS Nano* **2012**, *6*, 8067.
(195) Huang, H.; Sithambaram, S.; Chen, C. H.; Kithongo, C. K.; Xu, L. P.; Iyer, A.; Garces, H. F.; Suib, S. L. *Chem. Mater.* **2010**, *22*, 3664.
(196) Ming, B. S.; Li, J. L.; Kang, F. Y.; Pang, G. Y.; Zhang, Y. K.; Chen, L.; Xu, J. Y.; Wang, X. D. *J. Power Sources* **2012**, *198*, 428.
(197) Baldassari, S.; Komarneni, S.; Mariani, E.; Villa, C. *J. Am. Ceram. Soc.* **2005**, *88*, 3238.
(198) Baldassari, S.; Komarneni, S.; Mariani, E.; Villa, C. *Mater. Res. Bull.* **2005**, *40*, 2014.
(199) Gressel-Michel, E.; Chaumont, D.; Stuerga, D. *J. Colloid Interface Sci.* **2005**, *285*, 674.
(200) Corradi, A. B.; Bondioli, F.; Focher, B.; Ferrari, A. M.; Grippo, C.; Mariani, E.; Villa, C. *J. Am. Ceram. Soc.* **2005**, *88*, 2639.
(201) Murugan, A. V.; Samuel, V.; Ravi, V. *Mater. Lett.* **2006**, *60*, 479.
(202) Zhang, L. X.; Liu, P.; Su, Z. X. *Mater. Res. Bull.* **2006**, *41*, 1631.
(203) Zhang, P. L.; Yin, S.; Sato, T. *Appl. Catal., B* **2009**, *89*, 118.
(204) Zheng, Y.; Lv, K. L.; Wang, Z. Y.; Deng, K. J.; Li, M. *J. Mol. Catal. A* **2012**, *356*, 137.
(205) Suprabha, T.; Roy, H. G.; Thomas, J.; Kumar, K. P.; Mathew, S. *Nanoscale Res. Lett.* **2009**, *4*, 144.
(206) Ma, G. B.; Zhao, X. N.; Zhu, J. M. *Int. J. Mod. Phys. B* **2005**, *19*, 2763.
(207) Li, L.; Qin, X. M.; Wang, G. B.; Qi, L. M.; Du, G. P.; Hu, Z. J. *Appl. Surf. Sci.* **2011**, *257*, 8006.
(208) Zhang, D. Q.; Li, G. S.; Wang, F.; Yu, J. C. *CrystEngComm* **2010**, *12*, 1759.
(209) Wu, X.; Jiang, Q. Z.; Ma, Z. F.; Fu, M.; Shangguan, W. F. *Solid State Commun.* **2005**, *136*, 513.
(210) Sitthisang, S.; Komarneni, S.; Tantirungrotechai, J.; Noh, Y. D.; Li, H. H.; Yin, S.; Sato, T.; Katsuki, H. *Ceram. Int.* **2012**, *38*, 6099.
(211) Yin, S.; Liu, B.; Sato, T. *Funct. Mater. Lett.* **2008**, *1*, 173.
(212) Glaspell, G.; Panda, A. B.; El-Shall, M. S. *J. Appl. Phys.* **2006**, *100*, 124307.
(213) Manseki, K.; Kondo, Y.; Ban, T.; Sugiura, T.; Yoshida, T. *Dalton Trans.* **2013**, *42*, 3295.
(214) Etacheri, V.; Michlits, G.; Seery, M. K.; Hinder, S. J.; Pillai, S. C. *ACS Appl. Mater. Interface* **2013**, *5*, 1663.
(215) Bondioli, F.; Ferrari, A. M.; Leonelli, C.; Siligardi, C.; Pellacani, G. C. *J. Am. Ceram. Soc.* **2001**, *84*, 2728.
(216) Rizzuti, A.; Leonelli, C.; Corradi, A.; Caponetti, E.; Martino, D. C.; Nasillo, G.; Saladino, M. L. *J. Dispersion Sci. Technol.* **2009**, *30*, 1511.
(217) Bellon, K.; Chaumont, D.; Stuerga, D. *J. Mater. Res.* **2001**, *16*, 2619.

(218) Bondioli, F.; Leonelli, C.; Manfredini, T.; Ferrari, A. M.; Caracoche, M. C.; Rivas, P. C.; Rodríguez, A. M. *J. Am. Ceram. Soc.* **2005**, *88*, 633.
(219) Rizzuti, A.; Corradi, A.; Leonelli, C.; Rosa, R.; Pielaszek, R.; Lojkowski, W. *J. Nanopart. Res.* **2010**, *12*, 327.
(220) Hariharan, V.; Radhakrishnan, S.; Parthibavarman, M.; Dhilipkumar, R.; Sekar, C. *Talanta* **2011**, *85*, 2166.
(221) Sun, Q. J.; Luo, H. M.; Xie, Z. F.; Wang, J. D.; Su, X. T. *Mater. Lett.* **2008**, *62*, 2992.
(222) Phuruangrat, A.; Ham, D. J.; Hong, S. J.; Thongtem, S.; Lee, J. S. *J. Mater. Chem.* **2010**, *20*, 1683.
(223) Sungpanich, J.; Thongtem, T.; Thongtem, S. *Ceram. Int.* **2012**, *38*, 1051.
(224) Wei, G. D.; Qin, W. P.; Zhang, D. S.; Wang, G. F.; Kim, R. J.; Zheng, K. Z.; Wang, L. L. *J. Alloys Compd.* **2009**, *481*, 417.
(225) Corradi, A. B.; Bondioli, F.; Ferrari, A. M.; Manfredini, T. *Mater. Res. Bull.* **2006**, *41*, 38.
(226) Liao, X. H.; Zhu, J. M.; Zhu, J. J.; Xu, J. Z.; Chen, H. Y. *Chem. Commun.* **2001**, 937.
(227) Wang, H.; Zhu, J. J.; Zhu, J. M.; Liao, X. H.; Xu, S.; Ding, T.; Chen, H. Y. *Phys. Chem. Chem. Phys.* **2002**, *4*, 3794.
(228) Dos Santos, M. L.; Lima, R. C.; Riccardi, C. S.; Tranquilin, R. L.; Bueno, P. R.; Varela, J. A.; Longo, E. *Mater. Lett.* **2008**, *62*, 4509.
(229) Araújo, V. D.; Avansi, W.; de Carvalho, H. B.; Moreira, M. L.; Longo, E.; Ribeiro, C.; Bernardi, M. I. B. *CrystEngComm* **2012**, *14*, 1150.
(230) Natile, M. M.; Boccaletti, G.; Glisenti, A. *Chem. Mater.* **2005**, *17*, 6272.
(231) Gao, F.; Lu, Q.; Komarneni, S. *J. Nanosci. Nanotechnol.* **2006**, *6*, 3812.
(232) Bondioli, F.; Ferrari, A. M.; Lusvarghi, L.; Manfredini, T.; Nannarone, S.; Pasquali, L.; Selvaggi, G. *J. Mater. Chem.* **2005**, *15*, 1061.
(233) Prado-Gonjal, J.; Schmidt, R.; Espíndola-Canuto, J.; Ramos-Alvarez, P.; Morán, E. *J. Power Sources* **2012**, *209*, 163.
(234) Zawadzki, M. *J. Alloys Compd.* **2008**, *451*, 297.
(235) de Moura, A. P.; de Oliveira, L. H.; Paris, E. C.; Li, M. S.; Andrés, J.; Varela, J. A.; Longo, E.; Viana Rosa, I. L. *J. Fluoresc.* **2011**, *21*, 1431.
(236) Dai, S. H.; Liu, Y. F.; Lu, Y. N. *J. Colloid Interface Sci.* **2010**, *349*, 34.
(237) Qiu, G.; Dharmarathna, S.; Genuino, H.; Zhang, Y.; Huang, H.; Suib, S. L. *ACS Catal.* **2011**, *1*, 1702.
(238) Siqueira, K. P. F.; Dias, A. *J. Nanopart. Res.* **2011**, *13*, 5927.
(239) Almeida, M. A. P.; Cavalcante, L. S.; Morilla-Santos, C.; Dalmaschio, C. J.; Rajagopal, S.; Li, M. S.; Longo, E. *CrystEngComm* **2012**, *14*, 7127.
(240) Shen, Y. H.; Li, W.; Li, T. H. *Mater. Lett.* **2011**, *65*, 2956.
(241) Luo, Z. J.; Li, H. M.; Xia, J. X.; Zhu, W. S.; Guo, J. X.; Zhang, B. B. *Mater. Lett.* **2007**, *61*, 1845.
(242) Thongtem, T.; Kaowphong, S.; Thongtem, S. *Appl. Surf. Sci.* **2008**, *254*, 7765.
(243) Hu, B.; Wu, L. H.; Liu, S. J.; Yao, H. B.; Shi, H. Y.; Li, G. P.; Yu, S. H. *Chem. Commun.* **2010**, *46*, 2277.
(244) Su, Y. G.; Zhu, B. L.; Guan, K.; Gao, S. S.; Lv, L.; Du, C. F.; Peng, L. M.; Hou, L. C.; Wang, X. J. *J. Phys. Chem. C* **2012**, *116*, 18508.
(245) Xie, H. D.; Shen, D. Z.; Wang, X. Q.; Shen, G. Q. *Mater. Chem. Phys.* **2007**, *103*, 334.
(246) Cao, X.-F.; Zhang, L.; Chen, X.-T.; Xue, Z.-L. *CrystEngComm* **2011**, *13*, 306.
(247) Yao, S. S.; Wei, J. Y.; Huang, B. B.; Feng, S. Y.; Zhang, X. Y.; Qin, X. Y.; Wang, P.; Wang, Z. Y.; Zhang, Q.; Jing, X. Y.; Zhan, J. *J. Solid State Chem.* **2009**, *182*, 236.
(248) Zhang, J. C.; Wang, W.; Li, B. X.; Zhang, X. H.; Zhao, X. D.; Liu, X. Y.; Zhao, M. *Eur. J. Inorg. Chem.* **2012**, 2220.
(249) Letichevsky, Y.; Sominski, L.; Moreno, J. C.; Gedanken, A. *New J. Chem.* **2005**, *29*, 1445.
(250) Wang, J. Q.; Zheng, S. H.; Zeng, R.; Dou, S. X.; Sun, X. D. *J. Am. Ceram. Soc.* **2009**, *92*, 1217.
(251) Zhang, X. L.; Liu, D.; Sang, Y. H.; Liu, H.; Wang, J. Y. *J. Alloys Compd.* **2010**, *502*, 206.
(252) Lehnen, T.; Zopes, D.; Mathur, S. *J. Mater. Chem.* **2012**, *22*, 17732.
(253) Sun, M.; Li, D. Z.; Zhang, W. J.; Chen, Z. X.; Huang, H. J.; Li, W. J.; He, Y. H.; Fu, X. Z. *J. Solid State Chem.* **2012**, *190*, 135.
(254) Conrad, F.; Zhou, Y.; Yulikov, M.; Hametner, K.; Weyeneth, S.; Jeschke, G.; Günther, D.; Grunwaldt, J. D.; Patzke, G. R. *Eur. J. Inorg. Chem.* **2010**, 2036.
(255) Verma, S.; Joy, P. A.; Khollam, Y. B.; Potdar, H. S.; Deshpande, S. B. *Mater. Lett.* **2004**, *58*, 1092.
(256) Komarneni, S.; D'Arrigo, M. C.; Leonelli, C.; Pellacani, G. C.; Katsuki, H. *J. Am. Ceram. Soc.* **1998**, *81*, 3041.
(257) Nyutu, E. K.; Conner, W. C.; Auerbach, S. M.; Chen, C. H.; Suib, S. L. *J. Phys. Chem. C* **2008**, *112*, 1407.
(258) Kim, C. K.; Lee, J. H.; Katoh, S.; Murakami, R.; Yoshimura, M. *Mater. Res. Bull.* **2001**, *36*, 2241.
(259) Lai, Z. Y.; Xu, G. L.; Zheng, Y. L. *Nanoscale Res. Lett.* **2007**, *2*, 40.
(260) Krishnaveni, T.; Kanth, B. R.; Raju, V. S. R.; Murthy, S. R. *J. Alloys Compd.* **2006**, *414*, 282.
(261) Zawadzki, M. *Solid State Sci.* **2006**, *8*, 14.
(262) Conrad, F.; Massue, C.; Küehl, S.; Kunkes, E.; Girgsdies, F.; Kasatkin, I.; Zhang, B. S.; Friedrich, M.; Luo, Y.; Armbrüester, M.; Patzke, G. R.; Behrens, M. *Nanoscale* **2012**, *4*, 2018.
(263) Obata, S.; Kato, M.; Yokoyama, H.; Iwata, Y.; Kikumoto, M.; Sakurada, O. *J. Ceram. Soc. Jpn.* **2011**, *119*, 208.
(264) Wang, L. Y.; Han, Y. Y.; Jia, G.; Zhang, C. M.; Liu, Y. J.; Liu, L.; Wang, C. Z.; Cao, X. G.; Yin, K. W. *J. Nanosci. Nanotechnol.* **2011**, *11*, 5207.
(265) Zhu, X. H.; Yang, Y.; He, K.; Zhu, J. M.; Ye, S.; Zhou, S. H.; Liu, Z. G. *Ferroelectrics* **2010**, *409*, 204.
(266) Zhu, X. H.; Hang, Q. M.; Xing, Z. B.; Yang, Y.; Zhu, J. M.; Liu, Z. G.; Ming, N. B.; Zhou, P.; Song, Y.; Li, Z. S.; Yu, T.; Zou, Z. G. *J. Am. Ceram. Soc.* **2011**, *94*, 2688.
(267) Hong, R. Y.; Wu, Y. J.; Feng, B.; Di, G. Q.; Li, H. Z.; Xu, B.; Zheng, Y.; Wei, D. G. *J. Magn. Magn. Mater.* **2009**, *321*, 1106.
(268) Nissinen, T.; Kiros, Y.; Gasik, M.; Lampinen, M. *Mater. Res. Bull.* **2004**, *39*, 1195.
(269) Katsuki, H.; Komarneni, S. *J. Ceram. Soc. Jpn.* **2011**, *119*, 525.
(270) Jhung, S. H.; Lee, J. H.; Yoon, J. W.; Hwang, Y. K.; Hwang, J. S.; Park, S. E.; Chang, J. S. *Mater. Lett.* **2004**, *58*, 3161.
(271) Zhu, X. H.; Wang, J. Y.; Zhang, Z. H.; Zhu, J. M.; Zhou, S. H.; Liu, Z. G.; Ming, N. B. *J. Am. Ceram. Soc.* **2008**, *91*, 2683.
(272) Pazik, R.; Hreniak, D.; Strek, W. *Mater. Res. Bull.* **2007**, *42*, 1188.
(273) Simões, A. Z.; Moura, F.; Onofre, T. B.; Ramirez, M. A.; Varela, J. A.; Longo, E. *J. Alloys Compd.* **2010**, *508*, 620.
(274) Pazik, R.; Wiglusz, R. J.; Strek, W. *Mater. Res. Bull.* **2009**, *44*, 1328.
(275) Sulaeman, U.; Yin, S.; Sato, T. *Appl. Phys. Lett.* **2010**, *97*, 103102.
(276) Moreira, M. L.; Longo, V. M.; Avansi, W., Jr.; Ferrer, M. M.; Andrés, J.; Mastelaro, V. R.; Varela, J. A.; Longo, É. *J. Phys. Chem. C* **2012**, *116*, 24792.
(277) Zhu, X. H.; Xing, Z. B.; Zhang, Z. H.; Zhu, J. M.; Song, Y.; Zhou, S. H.; Liu, Z. G. *Mater. Lett.* **2010**, *64*, 479.
(278) Sadhana, K.; Praveena, K.; Bharadwaj, S.; Murthy, S. R. *J. Alloys Compd.* **2009**, *472*, 484.
(279) Chou, S. L.; Wang, J. Z.; Liu, H. K.; Dou, S. X. *J. Phys. Chem. C* **2011**, *115*, 16220.
(280) Zhang, J. W.; Wang, Y. A.; Yang, J. J.; Chen, J. M.; Zhang, Z. J. *Mater. Lett.* **2006**, *60*, 3015.
(281) Luo, Z. J.; Li, H. M.; Shu, H. M.; Wang, K.; Xia, J. X.; Yan, Y. S. *Mater. Chem. Phys.* **2008**, *110*, 17.

(282) Sun, Y.; Li, C. S.; Zhang, Z. J.; Ma, X. G.; Wang, L. N.; Wang, Y. Z.; Song, M. Y.; Ma, P. J.; Jiang, L. P.; Guo, Y. M. *Solid State Sci.* **2012**, *14*, 219.
(283) Xie, H. D.; Shen, D. Z.; Wang, X. Q.; Shen, G. Q. *Mater. Chem. Phys.* **2008**, *110*, 332.
(284) Zhang, L.; Cao, X.-F.; Chen, X.-T.; Xue, Z.-L. *CrystEngComm* **2011**, *13*, 2464.
(285) Shi, J. Y.; Liu, G. J.; Wang, N.; Li, C. *J. Mater. Chem.* **2012**, *22*, 18808.
(286) Liang, S. J.; Zhu, S. Y.; Chen, Y.; Wu, W. M.; Wang, X. C.; Wu, L. *J. Mater. Chem.* **2012**, *22*, 2670.
(287) Zhang, H. M.; Liu, J. B.; Wang, H.; Zhang, W. X.; Yan, H. *J. Nanopart. Res.* **2008**, *10*, 767.
(288) Zhu, Z. F.; Du, J.; Li, J. Q.; Zhang, Y. L.; Liu, D. G. *Ceram. Int.* **2012**, *38*, 4827.
(289) Wang, H.; Meng, Y. Q.; Yan, H. *Inorg. Chem. Commun.* **2004**, *7*, 553.
(290) Xu, H. Y.; Wang, H.; Meng, Y. Q.; Yan, H. *Solid State Commun.* **2004**, *130*, 465.
(291) Wang, Q. M.; Zhang, Z. Y.; Zheng, Y. H.; Cai, W. S.; Yu, Y. F. *CrystEngComm* **2012**, *14*, 4786.
(292) Liao, X. H.; Zhu, J. J.; Zhong, W.; Chen, H. Y. *Mater. Lett.* **2001**, *50*, 341.
(293) Milosevic, I.; Jouni, H.; David, C.; Warmont, F.; Bonnin, D.; Motte, L. *J. Phys. Chem. C* **2011**, *115*, 18999.
(294) Wu, L. H.; Yao, H. B.; Hu, B.; Yu, S.-H. *Chem. Mater.* **2011**, *23*, 3946.
(295) Polshettiwar, V.; Baruwati, B.; Varma, R. S. *ACS Nano* **2009**, *3*, 728.
(296) Wang, Y. A.; Yang, J. J.; Zhang, J. W.; Liu, H. J.; Zhang, Z. J. *Chem. Lett.* **2005**, *34*, 1168.
(297) Nosheen, S.; Galasso, F. S.; Suib, S. L. *Langmuir* **2009**, *25*, 7623.
(298) Zhao, Y.; Liao, X. H.; Hong, J. M.; Zhu, J. J. *Mater. Chem. Phys.* **2004**, *87*, 149.
(299) Hu, H. M.; Deng, C. H.; Zhang, K. H.; Yin, P. *Micro Nano Lett.* **2012**, *7*, 464.
(300) He, X. L.; Demchenko, I. N.; Stolte, W. C.; van Buuren, A.; Liang, H. *J. Phys. Chem. C* **2012**, *116*, 22001.
(301) Mu, C. F.; Yao, Q. Z.; Qu, X. F.; Zhou, G. T.; Li, M. L.; Fu, S. Q. *Colloids Surf., A* **2010**, *371*, 14.
(302) Liao, X. H.; Chen, N. Y.; Xu, S.; Yang, S. B.; Zhu, J. J. *J. Cryst. Growth* **2003**, *252*, 593.
(303) Zhu, J. J.; Zhou, M. G.; Xu, J. Z.; Liao, X. H. *Mater. Lett.* **2001**, *47*, 25.
(304) Han, Z. H.; Yang, Q.; Shi, J.; Lu, G. Q.; Lewis, S. W. *Solid State Sci.* **2008**, *10*, 563.
(305) Shao, M. W.; Li, Q.; Kong, L. F.; Yu, W. C.; Qian, Y. T. *J. Phys. Chem. Solids* **2003**, *64*, 1147.
(306) Kundu, S.; Lee, H.; Liang, H. *Inorg. Chem.* **2009**, *48*, 121.
(307) Shao, M. W.; Xu, F.; Peng, Y. Y.; Wu, J.; Li, Q.; Zhang, S. Y.; Qian, Y. T. *New J. Chem.* **2002**, *26*, 1440.
(308) Ni, Y. H.; Ma, X.; Hong, J. M.; Xu, Z. *Mater. Lett.* **2004**, *58*, 2754.
(309) Hu, Y.; Liu, Y.; Qian, H. S.; Li, Z. Q.; Chen, J. F. *Langmuir* **2010**, *26*, 18570.
(310) Zhao, Y.; Hong, J. M.; Zhu, J. J. *J. Cryst. Growth* **2004**, *270*, 438.
(311) Yang, H. M.; Huang, C. H.; Su, X. H.; Tang, A. D. *J. Alloys Compd.* **2005**, *402*, 274.
(312) Mehta, S. K.; Khushboo; Umar, A. *Talanta* **2011**, *85*, 2411.
(313) Poormohammadi-Ahandani, Z.; Habibi-Yangjeh, A. *Physica E* **2010**, *43*, 216.
(314) Xing, R. M.; Liu, S. H.; Tian, S. F. *J. Nanopart. Res.* **2011**, *13*, 4847.
(315) Liao, X. H.; Wang, H.; Zhu, J. J.; Chen, H. Y. *Mater. Res. Bull.* **2001**, *36*, 2339.
(316) Thongtem, T.; Pilapong, C.; Kavinchan, J.; Phuruangrat, A.; Thongtem, S. *J. Alloys Compd.* **2010**, *500*, 195.
(317) Shao, M. W.; Kong, L. F.; Li, Q.; Yu, W. C.; Qian, Y. T. *Inorg. Chem. Commun.* **2003**, *6*, 737.
(318) Zhang, W. J.; Li, D. Z.; Chen, Z. X.; Sun, M.; Li, W. J.; Lin, Q.; Fu, X. Z. *Mater. Res. Bull.* **2011**, *46*, 975.
(319) Zhang, W. J.; Li, D. Z.; Sun, M.; Shao, Y.; Chen, Z. X.; Xiao, G. C.; Fu, X. Z. *J. Solid State Chem.* **2010**, *183*, 2466.
(320) Bensebaa, F.; Durand, C.; Aouadou, A.; Scoles, L.; Du, X.; Wang, D.; Le Page, Y. *J. Nanopart. Res.* **2010**, *12*, 1897.
(321) Apte, S. K.; Garaje, S. N.; Bolade, R. D.; Ambekar, J. D.; Kulkarni, M. V.; Naik, S. D.; Gosavi, S. W.; Baeg, J. O.; Kale, B. B. *J. Mater. Chem.* **2010**, *20*, 6095.
(322) Shin, S. W.; Han, J. H.; Park, C. Y.; Moholkar, A. V.; Lee, J. Y.; Kim, J. H. *J. Alloys Compd.* **2012**, *516*, 96.
(323) Zhu, J. J.; Palchik, O.; Chen, S. G.; Gedanken, A. *J. Phys. Chem. B* **2000**, *104*, 7344.
(324) Gallagher, S. A.; Moloney, M. P.; Wojdyla, M.; Quinn, S. J.; Kelly, J. M.; Gun'ko, Y. K. *J. Mater. Chem.* **2010**, *20*, 8350.
(325) Han, H.; Di Francesco, G.; Maye, M. M. *J. Phys. Chem. C* **2010**, *114*, 19270.
(326) Chu, M. Q.; Shen, X. Y.; Liu, G. J. *Nanotechnology* **2006**, *17*, 444.
(327) Qian, H. F.; Qiu, X.; Li, L.; Ren, J. C. *J. Phys. Chem. B* **2006**, *110*, 9034.
(328) Huang, L.; Han, H. Y. *Mater. Lett.* **2010**, *64*, 1099.
(329) Jiang, L.-W.; Zhou, J.; Yang, X.-Z.; Peng, X.-N.; Jiang, H.; Zhuo, D.-Q.; Chen, L.-D.; Yu, X.-F. *Chem. Phys. Lett.* **2011**, *510*, 135.
(330) Al Juhaiman, L.; Scoles, L.; Kingston, D.; Patarachao, B.; Wang, D. S.; Bensebaa, F. *Green Chem.* **2010**, *12*, 1248.
(331) Li, L.; Qian, H. F.; Ren, J. C. *Chem. Commun.* **2005**, 528.
(332) He, Y.; Lu, H. T.; Sai, L. M.; Lai, W. Y.; Fan, Q. L.; Wang, L. H.; Huang, W. *J. Phys. Chem. B* **2006**, *110*, 13352.
(333) He, Y.; Sai, L. M.; Lu, H. T.; Hu, M.; Lai, W. Y.; Fan, Q. L.; Wang, L. H.; Huang, W. *Chem. Mater.* **2007**, *19*, 359.
(334) Guo, X.; Wang, C. F.; Fang, Y.; Chen, L.; Chen, S. *J. Mater. Chem.* **2011**, *21*, 1124.
(335) He, Y.; Lu, H. T.; Su, Y. Y.; Sai, L. M.; Hu, M.; Fan, C. H.; Wang, L. H. *Biomaterials* **2011**, *32*, 2133.
(336) Duan, J. L.; Song, L. X.; Zhan, J. H. *Nano Res.* **2009**, *2*, 61.
(337) Du, J.; Li, X. L.; Wang, S. J.; Wu, Y. Z.; Hao, X. P.; Xu, C. W.; Zhao, X. *J. Mater. Chem.* **2012**, *22*, 11390.
(338) Song, L. X.; Duan, J. L.; Zhan, J. H. *Mater. Lett.* **2010**, *64*, 1843.
(339) Lee, B. T.; Youn, M. H.; Paul, R. K.; Lee, K. H.; Song, H. Y. *Mater. Chem. Phys.* **2007**, *104*, 249.
(340) Vani, R.; Raja, S. B.; Sridevi, T. S.; Savithri, K.; Devaraj, S. N.; Girija, E. K.; Thamizhavel, A.; Kalkura, S. N. *Nanotechnology* **2011**, *22*, 285701.
(341) Lak, A.; Mazloumi, M.; Mohajerani, M. S.; Zanganeh, S.; Shayegh, M. R.; Kajbafvala, A.; Arami, H.; Sadrnezhaad, S. K. *J. Am. Ceram. Soc.* **2008**, *91*, 3580.
(342) Liu, J. B.; Li, K. W.; Wang, H.; Zhu, M. K.; Yan, H. *Chem. Phys. Lett.* **2004**, *396*, 429.
(343) Liang, T.; Qian, J. C.; Yuan, Y.; Liu, C. S. *J. Mater. Sci.* **2013**, *48*, 5334.
(344) Chen, F.; Huang, P.; Zhu, Y. J.; Wu, J.; Zhang, C. L.; Cui, D. X. *Biomaterials* **2011**, *32*, 9031.
(345) Han, J. K.; Song, H. Y.; Saito, F.; Lee, B. T. *Mater. Chem. Phys.* **2006**, *99*, 235.
(346) Meejoo, S.; Maneeprakorn, W.; Winotai, P. *Thermochim. Acta* **2006**, *447*, 115.
(347) Siddharthan, A.; Seshadri, S. K.; Kumar, T. S. S. *J. Mater. Sci.: Mater. Med.* **2004**, *15*, 1279.
(348) Zhao, X. Y.; Zhu, Y. J.; Chen, F.; Lu, B. Q.; Wu, J. *CrystEngComm* **2013**, *15*, 206.
(349) Wang, K. W.; Zhu, Y. J.; Chen, X. Y.; Zhai, W. Y.; Wang, Q.; Chen, F.; Chang, J.; Duan, Y. R. *Chem.—Asian J.* **2010**, *5*, 2477.
(350) Wang, K. W.; Zhu, Y. J.; Chen, F.; Cheng, G. F.; Huang, Y. H. *Mater. Lett.* **2011**, *65*, 2361.
(351) Escudero, A.; Calvo, M. E.; Rivera-Fernández, S.; de la Fuente, J. M.; Ocaña, M. *Langmuir* **2013**, *29*, 1985.

(352) Zou, Z. Y.; Lin, K. L.; Chen, L.; Chang, J. *Ultrason. Sonochem.* **2012**, *19*, 1174.
(353) Rameshbabu, N.; Kumar, T. S. S.; Prabhakar, T. G.; Sastry, V. S.; Murty, K. V. G. K.; Rao, K. P. *J. Biomed. Mater. Res., Part A* **2007**, *80A*, 581.
(354) André, R. S.; Paris, E. C.; Gurgel, M. F. C.; Rosa, I. L. V.; Paiva-Santos, C. O.; Li, M. S.; Varela, J. A.; Longo, E. *J. Alloys Compd.* **2012**, *531*, 50.
(355) Qi, C.; Tang, Q. L.; Zhu, Y. J.; Zhao, X. Y.; Chen, F. *Mater. Lett.* **2012**, *85*, 71.
(356) Qi, C.; Zhu, Y. J.; Zhao, X. Y.; Lu, B. Q.; Tang, Q. L.; Zhao, J.; Chen, F. *Chem.—Eur. J.* **2013**, *19*, 981.
(357) Qi, C.; Zhu, Y. J.; Chen, F. *Chem.—Asian J.* **2013**, *8*, 88.
(358) Qi, C.; Zhu, Y. J.; Lu, B. Q.; Zhao, X. Y.; Zhao, J.; Chen, F.; Wu, J. *Chem.—Eur. J.* **2013**, *19*, 5332.
(359) Zhao, X. Y.; Zhu, Y. J.; Qi, C.; Chen, F.; Lu, B. Q.; Zhao, J.; Wu, J. *Chem.—Asian J.* **2013**, *8*, 1313.
(360) Zhao, J.; Zhu, Y. J.; Zheng, J. Q.; Chen, F.; Wu, J. *Microporous Mesoporous Mater.* **2013**, *180*, 79.
(361) Umar, A.; Al-Hazmi, F.; Dar, G. N.; Zaidi, S. A.; Al-Tuwirqi, R. M.; Alnowaiserb, F.; Al-Ghamdi, A. A.; Hwang, S. W. *Sens. Actuators, B* **2012**, *166–167*, 97.
(362) Al-Hazmi, F.; Umar, A.; Dar, G. N.; Al-Ghamdi, A. A.; Al-Sayari, S. A.; Al-Hajry, A.; Kim, S. H.; Al-Tuwirqi, R. M.; Alnowaiserb, F.; El-Tantawy, F. *J. Alloys Compd.* **2012**, *519*, 4.
(363) Patra, C. R.; Gedanken, A. *New J. Chem.* **2004**, *28*, 1060.
(364) Ge, S. X.; Zhang, L. Z.; Jia, H. M.; Zheng, Z. *J. Mater. Res.* **2009**, *24*, 2268.
(365) Lai, T. L.; Shu, Y. Y.; Huang, G. L.; Lee, C. C.; Wang, C. B. *J. Alloys Compd.* **2008**, *450*, 318.
(366) Lai, T. L.; Lai, Y. L.; Yu, J. W.; Shu, Y. Y.; Wang, C. B. *Mater. Res. Bull.* **2009**, *44*, 2040.
(367) Ran, S. H.; Zhu, Y. G.; Huang, H. T.; Liang, B.; Xu, J.; Liu, B.; Zhang, J.; Xie, Z.; Wang, Z. R.; Ye, J. H.; Chen, D.; Shen, G. Z. *CrystEngComm* **2012**, *14*, 3063.
(368) Liu, X. H.; Ma, R. Z.; Bando, Y.; Sasaki, T. *Angew. Chem., Int. Ed.* **2010**, *49*, 8253.
(369) Liang, Z. H.; Zhu, Y. J.; Cheng, G. F.; Huang, Y. H. *Can. J. Chem.* **2006**, *84*, 1050.
(370) Morales, J. G.; Carmona, J. G.; Clemente, R. R.; Muraviev, D. *Langmuir* **2003**, *19*, 9110.
(371) Phuruangrat, A.; Thongtem, S.; Thongtem, T. *Ceram. Int.* **2012**, *38*, 4075.
(372) Ma, L.; Chen, W. X.; Zhao, J.; Zheng, Y. F.; Li, X.; Xu, Z. D. *Mater. Lett.* **2007**, *61*, 1711.
(373) Ma, L.; Chen, W. X.; Zheng, Y. F.; Zhao, J.; Xu, Z. D. *Mater. Lett.* **2007**, *61*, 2765.
(374) Ma, L.; Chen, W. X.; Xu, X. Y.; Xu, L. M.; Ning, X. M. *Mater. Lett.* **2010**, *64*, 1559.
(375) Wang, S.; Su, S. Q.; Song, S. Y.; Deng, R. P.; Zhang, H. J. *CrystEngComm* **2012**, *14*, 4266.
(376) Parhi, P.; Kramer, J.; Manivannan, V. *J. Mater. Sci.* **2008**, *43*, 5540.
(377) Schäfer, H.; Ptacek, P.; Voss, B.; Eickmeier, H.; Nordmann, J.; Haase, M. *Cryst. Growth Des.* **2010**, *10*, 2202.
(378) Zhou, H.; Luchini, T. J. F.; Bhaduri, S. B. *J. Mater. Sci.: Mater. Med.* **2012**, *23*, 2831.
(379) Wang, R.; Jiang, H.; Gong, H.; Zhang, J. *Mater. Res. Bull.* **2012**, *47*, 2108.
(380) Li, G. F.; Ding, Y.; Zhang, Y. F.; Lu, Z.; Sun, H. Z.; Chen, R. *J. Colloid Interface Sci.* **2011**, *363*, 497.
(381) Wang, R.; Ye, J. W.; Ning, G. L.; Jiang, H.; Zhou, W. L.; Sun, F. H. *Mater. Lett.* **2012**, *83*, 130.
(382) Yang, G.; Ji, H. M.; Liu, H. D.; Huo, K. F.; Fu, J. J.; Chu, P. K. *J. Nanosci. Nanotechnol.* **2010**, *10*, 980.
(383) Ekthammathat, N.; Thongtem, T.; Phuruangrat, A.; Thongtem, S. *J. Exp. Nanosci.* **2012**, *7*, 616.
(384) Ekthammathat, N.; Thongtem, T.; Phuruangrat, A.; Thongtem, S. *Rare Met.* **2011**, *30*, 572.
(385) Patra, C. R.; Alexandra, G.; Patra, S.; Jacob, D. S.; Gedanken, A.; Landau, A.; Gofer, Y. *New J. Chem.* **2005**, *29*, 733.
(386) Ma, L.; Xu, L. M.; Chen, W. X.; Xu, Z. D. *Mater. Lett.* **2009**, *63*, 1635.
(387) Jin, Y.; Li, C. X.; Xu, Z. H.; Cheng, Z. Y.; Wang, W. X.; Li, G. G.; Lin, J. *Mater. Chem. Phys.* **2011**, *129*, 418.
(388) Du, H. B.; Fang, M.; Xu, W. G.; Meng, X. P.; Pang, W. Q. *J. Mater. Chem.* **1997**, *7*, 551.
(389) Ng, E. P.; Delmotte, L.; Mintova, S. *Green Chem.* **2008**, *10*, 1043.
(390) Qiu, M.; Zhu, L. J.; Zhang, T. T.; Li, H. B.; Sun, Y. G.; Liu, K. *Mater. Res. Bull.* **2012**, *47*, 2437.
(391) Zhang, H. Y.; Hong, J. M.; Ni, Y. H.; Zhou, Y. Y. *CrystEngComm* **2008**, *10*, 1031.
(392) Ma, M. G.; Zhu, Y. J. *J. Nanosci. Nanotechnol.* **2007**, *7*, 4552.
(393) Li, S. Y.; Yang, W.; Chen, M.; Gao, J. Z.; Kang, J. W.; Qi, Y. L. *Mater. Chem. Phys.* **2005**, *90*, 262.
(394) Mahapatra, S.; Nayak, S. K.; Madras, G.; Row, T. N. G. *Ind. Eng. Chem. Res.* **2008**, *47*, 6509.
(395) Zhang, L.; Cao, X. F.; Ma, Y. L.; Chen, X. T.; Xue, Z. L. *New J. Chem.* **2010**, *34*, 2027.
(396) Wu, J.; Zhu, Y. J.; Cheng, G. F.; Huang, Y. H. *Mater. Res. Bull.* **2010**, *45*, 509.
(397) Xie, L. Y.; Wang, J. X.; Hu, Y. H.; Zheng, Z. Y.; Weng, S. X.; Liu, P.; Shi, X. C.; Wang, D. H. *Mater. Chem. Phys.* **2012**, *136*, 309.
(398) Sun, M.; Li, D. Z.; Chen, Y. B.; Chen, W.; Li, W. J.; He, Y. H.; Fu, X. Z. *J. Phys. Chem. C* **2009**, *113*, 13825.
(399) Hu, Y. Y.; Liu, C.; Zhang, Y. H.; Ren, N.; Tang, Y. *Microporous Mesoporous Mater.* **2009**, *119*, 306.
(400) Hu, Y. Y.; Zhang, Y. H.; Tang, Y. *Chem. Commun.* **2010**, *46*, 3875.
(401) Ajayan, P. M.; Schadler, L. S.; Braun, P. V. *Nanocomposite Science and Technology*; Wiley-VCH: Weinheim, 2003.
(402) Belousov, O. V.; Belousova, N. V.; Sirotina, A. V.; Solovyov, L. A.; Zhyzhaev, A. M.; Zharkov, S. M.; Mikhlin, Y. L. *Langmuir* **2011**, *27*, 11697.
(403) Zeng, J. H.; Lee, J. Y.; Zhou, W. J. *Appl. Catal., A* **2006**, *308*, 99.
(404) Liu, S. J.; Huang, C. H.; Huang, C. K.; Hwang, W. S. *Electrochem. Commun.* **2009**, *11*, 1792.
(405) Wu, J.; Hu, F. P.; Hu, X. D.; Wei, Z. D.; Shen, P. K. *Electrochim. Acta* **2008**, *53*, 8341.
(406) Tang, S. C.; Vongehr, S.; Meng, X. K. *J. Phys. Chem. C* **2010**, *114*, 977.
(407) Yu, J. C.; Hu, X. L.; Li, Q.; Zhang, L. Z. *Chem. Commun.* **2005**, 2704.
(408) Deivaraj, T. C.; Chen, W. X.; Lee, J. Y. *J. Mater. Chem.* **2003**, *13*, 2555.
(409) Hwang, B. J.; Kumar, S. M. S.; Chen, C. H.; Monalisa; Cheng, M. Y.; Liu, D. G.; Lee, J. F. *J. Phys. Chem. C* **2007**, *111*, 15267.
(410) Yu, J. C.; Hu, X. L.; Li, Q.; Zheng, Z.; Xu, Y. M. *Chem.—Eur. J.* **2006**, *12*, 548.
(411) Wu, J.; Hu, F.; Shen, P. K.; Li, C. M.; Wei, Z. *Fuel Cells* **2010**, *10*, 106.
(412) Hassan, H. M. A.; Abdelsayed, V.; Khder, A. E. R. S.; AbouZeid, K. M.; Terner, J.; El-Shall, M. S.; Al-Resayes, S. I.; El-Azhary, A. A. *J. Mater. Chem.* **2009**, *19*, 3832.
(413) Zhang, H.; Xu, X. Q.; Gu, P.; Li, C. Y.; Wu, P.; Cai, C. X. *Electrochim. Acta* **2011**, *56*, 7064.
(414) Siamaki, A. R.; Khder, A. E. R. S.; Abdelsayed, V.; El-Shall, M. S.; Gupton, B. F. *J. Catal.* **2011**, *279*, 1.
(415) Zhang, Y. W.; Chang, G. H.; Liu, S.; Tian, J. Q.; Wang, L.; Lu, W. B.; Qin, X. Y.; Sun, X. P. *Catal. Sci. Technol.* **2011**, *1*, 1636.
(416) Chen, S. Q.; Wang, Y.; Ahn, H.; Wang, G. X. *J. Power Sources* **2012**, *216*, 22.
(417) Jasuja, K.; Linn, J.; Melton, S.; Berry, V. *J. Phys. Chem. Lett.* **2010**, *1*, 1853.
(418) Sun, C.-L.; Chang, C.-T.; Lee, H.-H.; Zhou, J. G.; Wang, J.; Sham, T.-K.; Pong, W.-F. *ACS Nano* **2011**, *5*, 7788.

(419) Gu, J. L.; Fan, W.; Shimojima, A.; Okubo, T. *J. Solid State Chem.* **2008**, *181*, 957.
(420) Yu, Y.-T.; Dutta, P. *J. Solid State Chem.* **2011**, *184*, 312.
(421) Kundu, P.; Singhania, N.; Madras, G.; Ravishankar, N. *Dalton Trans.* **2012**, *41*, 8762.
(422) Geng, J.; Song, G.-H.; Jia, X.-D.; Cheng, F.-F.; Zhu, J.-J. *J. Phys. Chem. C* **2012**, *116*, 4517.
(423) Wang, X.; Fan, H. Q.; Ren, P. R. *Colloids Surf., A* **2013**, *419*, 140.
(424) Xiang, Q. J.; Yu, J. G.; Cheng, B.; Ong, H. C. *Chem.—Asian J.* **2010**, *5*, 1466.
(425) Li, X. B.; Wang, L. L.; Lu, X. H. *J. Hazard. Mater.* **2010**, *177*, 639.
(426) Wong, R. M.; Gilbert, D. A.; Liu, K.; Louie, A. Y. *ACS Nano* **2012**, *6*, 3461.
(427) Wang, Y.; Lee, J. Y. *J. Power Sources* **2005**, *144*, 220.
(428) Cho, S.; Jang, J.-W.; Park, H. J.; Jung, D.-W.; Jung, A.; Lee, J. S.; Lee, K.-H. *RSC Adv.* **2012**, *2*, 566.
(429) Hu, X. L.; Yu, J. C. *Chem.—Asian J.* **2006**, *1*, 605.
(430) Murugan, A. V.; Muraliganth, T.; Manthiram, A. *J. Electrochem. Soc.* **2009**, *156*, A79.
(431) Potirak, P.; Kahattha, C.; Pecharapa, W. *J. Nanosci. Nanotechnol.* **2011**, *11*, 11195.
(432) Xiao, Y.; Zhang, Q.; Yan, J.; Wei, T.; Fan, Z. J.; Wei, F. *J. Electroanal. Chem.* **2012**, *684*, 32.
(433) Fan, Z. J.; Qie, Z. W.; Wei, T.; Yan, J.; Wang, S. S. *Mater. Lett.* **2008**, *62*, 3345.
(434) Yan, S. C.; Wang, H. T.; Qu, P.; Zhang, Y.; Xiao, Z. D. *Synth. Met.* **2009**, *159*, 158.
(435) Zhong, C.; Wang, J. Z.; Chen, Z. X.; Liu, H. K. *J. Phys. Chem. C* **2011**, *115*, 25115.
(436) Lu, T.; Pan, L. K.; Li, H. B.; Zhu, G.; Lv, T.; Liu, X. J.; Sun, Z.; Chen, T.; Chua, D. H. C. *J. Alloys Compd.* **2011**, *509*, 5488.
(437) Zhu, X. J.; Zhu, Y. W.; Murali, S.; Stollers, M. D.; Ruoff, R. S. *ACS Nano* **2011**, *5*, 3333.
(438) Yan, J.; Wei, T.; Qiao, W. M.; Shao, B.; Zhao, Q. K.; Zhang, L. J.; Fan, Z. J. *Electrochim. Acta* **2010**, *55*, 6973.
(439) Chen, T. Q.; Pan, L. K.; Liu, X. J.; Yu, K.; Sun, Z. *RSC Adv.* **2012**, *2*, 11719.
(440) Wu, H. Q.; Wang, Q. Y.; Yao, Y. Z.; Qian, C.; Zhang, X. J.; Wei, X. W. *J. Phys. Chem. C* **2008**, *112*, 16779.
(441) Wu, H. Q.; Yao, Y. Z.; Li, W. T.; Zhu, L. L.; Ni, N.; Zhang, X. J. *J. Nanopart. Res.* **2011**, *13*, 2225.
(442) Hu, H. T.; Wang, X. B.; Liu, F. M.; Wang, J. C.; Xu, C. H. *Synth. Met.* **2011**, *161*, 404.
(443) Liu, X. J.; Pan, L. K.; Lv, T.; Zhu, G.; Sun, Z.; Sun, C. Q. *Chem. Commun.* **2011**, *47*, 11984.
(444) Liu, X. J.; Pan, L. K.; Lv, T.; Zhu, G.; Lu, T.; Sun, Z.; Sun, C. Q. *RSC Adv.* **2011**, *1*, 1245.
(445) Shi, Y.; Chou, S.-L.; Wang, J.-Z.; Wexler, D.; Li, H.-J.; Liu, H.-K.; Wu, Y. P. *J. Mater. Chem.* **2012**, *22*, 16465.
(446) Yan, W.; Fan, H. Q.; Yang, C. *Mater. Lett.* **2011**, *65*, 1595.
(447) Al-Tuwirqi, R. M.; Al-Ghamdi, A. A.; Al-Hazmi, F.; Alnowaiser, F.; Al-Ghamdi, A. A.; Aal, N. A.; El-Tantawy, F. *Superlattices Microstruct.* **2011**, *50*, 437.
(448) Prete, F.; Rizzuti, A.; Esposito, L.; Tucci, A.; Leonelli, C. *J. Am. Ceram. Soc.* **2011**, *94*, 3587.
(449) Hu, C. C.; Yang, Y. L.; Lee, T. C. *Electrochem. Solid-State Lett.* **2010**, *13*, A173.
(450) Zhang, Q. Q.; Huang, B. B.; Wang, P.; Zhang, X. Y.; Qin, X. Y.; Wang, Z. Y. *Int. J. Photoenergy* **2012**, *2012*, 461291.
(451) Cho, S.; Kim, S.; Oh, E.; Jung, S. H.; Lee, K. H. *CrystEngComm* **2009**, *11*, 1650.
(452) Shao, M. W.; Li, Q.; Xie, B.; Wu, J.; Qian, Y. T. *Mater. Chem. Phys.* **2003**, *78*, 288.
(453) Hu, Y.; Qian, H.; Liu, Y.; Du, G.; Zhang, F.; Wang, L.; Hu, X. *CrystEngComm* **2011**, *13*, 3438.
(454) Chen, W.; Ruan, H.; Hu, Y.; Li, D. Z.; Chen, Z. X.; Xian, J. J.; Chen, J.; Fu, X. Z.; Shao, Y.; Zheng, Y. *CrystEngComm* **2012**, *14*, 6295.
(455) Yang, W. L.; Liu, Y.; Hu, Y.; Zhou, M. J.; Qian, H. S. *J. Mater. Chem.* **2012**, *22*, 13895.
(456) Wang, Y. Q.; Wang, G. Z.; Wang, H. Q.; Tang, C. J.; Li, J.; Zhang, L. D. *J. Nanosci. Nanotechnol.* **2009**, *9*, 4820.
(457) Cho, S.; Jang, J.-W.; Lee, J. S.; Lee, K.-H. *Nanoscale* **2012**, *4*, 2066.
(458) Rakovich, A. Y.; Stockhausen, V.; Susha, A. S.; Sapra, S.; Rogach, A. L. *Colloids Surf., A* **2008**, *317*, 737.
(459) Jian, W. P.; Zhuang, J. Q.; Zhang, D. W.; Dai, J.; Yang, W. S.; Bai, Y. B. *Mater. Chem. Phys.* **2006**, *99*, 494.
(460) Qian, H. F.; Li, L.; Ren, J. C. *Mater. Res. Bull.* **2005**, *40*, 1726.
(461) Schumacher, W.; Nagy, A.; Waldman, W. J.; Dutta, P. K. *J. Phys. Chem. C* **2009**, *113*, 12132.
(462) He, Y.; Lu, H. T.; Sai, L. M.; Lai, W. Y.; Fan, Q. L.; Wang, L. H.; Huang, W. *J. Phys. Chem. B* **2006**, *110*, 13370.
(463) Sai, L.-M.; Kong, X. Y. *Nanoscale Res. Lett.* **2011**, *6*, 399.
(464) Zhan, H.-J.; Zhou, P.-J.; He, Z.-Y.; Tian, Y. *Eur. J. Inorg. Chem.* **2012**, 2487.
(465) Shen, Y. Y.; Li, L. L.; Lu, Q.; Ji, J.; Fei, R.; Zhang, J. R.; Abdel-Halim, E. S.; Zhu, J.-J. *Chem. Commun.* **2012**, *48*, 2222.
(466) Zhu, D.; Jiang, X. X.; Zhao, C.; Sun, X. L.; Zhang, J. R.; Zhu, J. J. *Chem. Commun.* **2010**, *46*, 5226.
(467) He, Y.; Lu, H. T.; Sai, L. M.; Su, Y. Y.; Hu, M.; Fan, C. H.; Huang, W.; Wang, L. H. *Adv. Mater.* **2008**, *20*, 3416.
(468) Kou, J. H.; Varma, R. S. *ChemSusChem* **2012**, *5*, 2435.
(469) Wu, Z. J.; Ge, S. H.; Zhang, M. H.; Li, W.; Tao, K. Y. *Catal. Commun.* **2008**, *9*, 1432.
(470) Zhu, J. F.; Zhu, Y. J. *J. Phys. Chem. B* **2006**, *110*, 8593.
(471) Zhu, J. F.; Zhu, Y. J.; Ma, M. G.; Yang, L. X.; Gao, L. *J. Phys. Chem. C* **2007**, *111*, 3920.
(472) Kundu, S.; Liang, H. *Langmuir* **2008**, *24*, 9668.
(473) Nadagouda, M. N.; Varma, R. S. *Macromol. Rapid Commun.* **2007**, *28*, 465.
(474) El-Shall, M. S.; Abdelsayed, V.; Khder, A. E. R. S.; Hassan, H. M. A.; El-Kaderi, H. M.; Reich, T. E. *J. Mater. Chem.* **2009**, *19*, 7625.
(475) Khan, A.; El-Toni, A. M.; Alrokayan, S.; Alsalhi, M.; Alhoshan, M.; Aldwayyan, A. S. *Colloids Surf., A* **2011**, *377*, 356.
(476) Nguyen, T. H.; Lee, K. H.; Lee, B. T. *Mater. Sci. Eng., C* **2010**, *30*, 944.
(477) Nadagouda, M. N.; Varma, R. S. *Biomacromolecules* **2007**, *8*, 2762.
(478) You, L.-J.; Xu, S. A.; Ma, W.-F.; Li, D.; Zhang, Y.-T.; Guo, J.; Hu, J. J.; Wang, C.-C. *Langmuir* **2012**, *28*, 10565.
(479) Cho, S.; Lee, B. R.; Kim, H. J.; Park, D. H.; Lee, K. H. *Mater. Lett.* **2009**, *63*, 2025.
(480) Chen, L.; Yuan, C. Z.; Gao, B.; Chen, S. Y.; Zhang, X. G. *J. Solid State Electrochem.* **2009**, *13*, 1925.
(481) Murugan, A. V.; Kwon, C. W.; Campet, G.; Kale, B. B.; Mandale, A. B.; Sainker, S. R.; Gopinath, C. S.; Vijayamohanan, K. *J. Phys. Chem. B* **2004**, *108*, 10736.
(482) Jagtap, M. A.; Kulkarni, M. V.; Apte, S. K.; Naik, S. D.; Kale, B. B. *Mater. Sci. Eng., B* **2010**, *168*, 199.
(483) Hussein, M. Z. B.; Zainal, Z.; Ming, C. Y. *J. Mater. Sci. Lett.* **2000**, *19*, 879.
(484) Guha, A.; Nayar, S.; Thatoi, H. N. *Bioinspiration Biomimetics* **2010**, *5*, 024001.
(485) Tang, Q. L.; Wang, K. W.; Zhu, Y. J.; Chen, F. *Mater. Lett.* **2009**, *63*, 1332.
(486) Soltani, N.; Saion, E.; Hussein, M. Z.; Bahrami, A.; Naghavi, K.; Yunus, R. B. *Chalcogenide Lett.* **2012**, *9*, 265.
(487) Fievet, F.; Lagier, J. P.; Blin, B.; Beaudoin, B.; Figlarz, M. *Solid State Ionics* **1989**, *32/33*, 198.
(488) Tu, W. X.; Lin, H. F. *Chem. Mater.* **2000**, *12*, 564.
(489) Nishioka, M.; Miyakawa, M.; Daino, Y.; Kataoka, H.; Koda, H.; Sato, K.; Suzuki, T. M. *Chem. Lett.* **2011**, *40*, 1327.
(490) Grace, A. N.; Pandian, K. *Mater. Chem. Phys.* **2007**, *104*, 191.
(491) He, B. L.; Chen, Y. X.; Liu, H. F.; Liu, Y. *J. Nanosci. Nanotechnol.* **2005**, *5*, 266.
(492) Yu, W. Y.; Tu, W. X.; Liu, H. F. *Langmuir* **1999**, *15*, 6.

(493) Patel, K.; Kapoor, S.; Dave, D. P.; Mukherjee, T. *J. Chem. Sci.* **2005**, *117*, 311.
(494) Zawadzki, M. *J. Alloys Compd.* **2007**, *439*, 312.
(495) Yu, Y. C.; Zhao, Y. X.; Huang, T.; Liu, H. F. *Mater. Res. Bull.* **2010**, *45*, 159.
(496) Yu, Y. C.; Zhao, Y. X.; Huang, T.; Liu, H. F. *Pure Appl. Chem.* **2009**, *81*, 2377.
(497) Grace, A. N.; Pandian, K. *Colloids Surf., A* **2006**, *290*, 138.
(498) Tsuji, M.; Matsumoto, K.; Tsuji, T.; Kawazumi, H. *Mater. Lett.* **2005**, *59*, 3856.
(499) Tsuji, M.; Miyamae, N.; Hashimoto, M.; Nishio, M.; Hikino, S.; Ishigami, N.; Tanaka, I. *Colloids Surf., A* **2007**, *302*, 587.
(500) Tsuji, M.; Ueyama, D.; Alam, M. J.; Hikino, S. *Chem. Lett.* **2009**, *38*, 478.
(501) Zhu, Y. J.; Hu, X. L. *Chem. Lett.* **2003**, *32*, 1140.
(502) Patel, K.; Kapoor, S.; Dave, D. P.; Mukherjee, T. *Res. Chem. Intermed.* **2006**, *32*, 103.
(503) Nishioka, M.; Miyakawa, M.; Kataoka, H.; Koda, H.; Sato, K.; Suzuki, T. M. *Nanoscale* **2011**, *3*, 2621.
(504) Groisman, Y.; Gedanken, A. *J. Phys. Chem. C* **2008**, *112*, 8802.
(505) Li, D. S.; Komarneni, S. *J. Nanosci. Nanotechnol.* **2010**, *10*, 8035.
(506) Navaladian, S.; Viswanathan, B.; Varadarajan, T. K.; Viswanath, R. P. *Nanotechnology* **2008**, *19*, 045603.
(507) Chen, D. P.; Qiao, X. L.; Qiu, X. L.; Chen, J. G.; Jiang, R. Z. *Nanotechnology* **2010**, *21*, 025607.
(508) Gou, L. F.; Chipara, M.; Zaleski, J. M. *Chem. Mater.* **2007**, *19*, 1755.
(509) Tsuji, M.; Nishizawa, Y.; Matsumoto, K.; Kubokawa, M.; Miyamae, N.; Tsuji, T. *Mater. Lett.* **2006**, *60*, 834.
(510) Tsuji, M.; Matsumoto, K.; Miyamae, N.; Tsuji, T.; Zhang, X. *Cryst. Growth Des.* **2007**, *7*, 311.
(511) Tsuji, M.; Matsumoto, K.; Jiang, P.; Matsuo, R.; Tang, X. L.; Karnarudin, K. S. N. *Colloids Surf., A* **2008**, *316*, 266.
(512) Tsuji, M.; Matsumoto, K.; Jiang, P.; Matsuo, R.; Hikino, S.; Tang, X. L.; Kamarudin, K. S. N. *Bull. Chem. Soc. Jpn.* **2008**, *81*, 393.
(513) Zhao, T.; Fan, J.-B.; Cui, J.; Liu, J.-H.; Xu, X.-B.; Zhu, M.-Q. *Chem. Phys. Lett.* **2011**, *501*, 414.
(514) Kou, J. H.; Varma, R. S. *Chem. Commun.* **2013**, *49*, 692.
(515) Harpeness, R.; Peng, Z.; Liu, X. S.; Pol, V. G.; Koltypin, Y.; Gedanken, A. *J. Colloid Interface Sci.* **2005**, *287*, 678.
(516) Zawadzki, M.; Okal, J. *Mater. Res. Bull.* **2008**, *43*, 3111.
(517) Galletti, A. M. R.; Antonetti, C.; Longo, I.; Capannelli, G.; Venezia, A. M. *Appl. Catal., A* **2008**, *350*, 46.
(518) Zhu, H. T.; Lin, Y. S.; Yin, Y. S. *J. Colloid Interface Sci.* **2004**, *277*, 100.
(519) Zhu, H. T.; Zhang, C. Y.; Yin, Y. S. *Nanotechnology* **2005**, *16*, 3079.
(520) Kawasaki, H.; Kosaka, Y.; Myoujin, Y.; Narushima, T.; Yonezawa, T.; Arakawa, R. *Chem. Commun.* **2011**, *47*, 7740.
(521) Blosi, M.; Albonetti, S.; Dondi, M.; Martelli, C.; Baldi, G. *J. Nanopart. Res.* **2011**, *13*, 127.
(522) Jung, Y.; Son, Y.-H.; Lee, J.-K. *RSC Adv.* **2012**, *2*, 5877.
(523) Cheng, W. T.; Cheng, H. W. *AIChE J.* **2009**, *55*, 1383.
(524) Wada, Y.; Kuramoto, H.; Sakata, T.; Mori, H.; Sumida, T.; Kitamura, T.; Yanagida, S. *Chem. Lett.* **1999**, 607.
(525) Eluri, R.; Paul, B. *Mater. Lett.* **2012**, *76*, 36.
(526) Li, D. S.; Komarneni, S. *J. Am. Ceram. Soc.* **2006**, *89*, 1510.
(527) Liu, X. S.; Meridor, U.; Zhao, P.; Song, G. B.; Frydman, A.; Gedanken, A. *J. Magn. Magn. Mater.* **2006**, *301*, 13.
(528) Xu, W.; Liew, K. Y.; Liu, H. F.; Huang, T.; Sun, C. T.; Zhao, Y. X. *Mater. Lett.* **2008**, *62*, 2571.
(529) Donegan, K. P.; Godsell, J. F.; Tobin, J. M.; O'Byrne, J. P.; Otway, D. J.; Morris, M. A.; Roy, S.; Holmes, J. D. *CrystEngComm* **2011**, *13*, 2023.
(530) Hu, X. L.; Yu, J. C. *Chem. Mater.* **2008**, *20*, 6743.
(531) Zhou, B.; Ren, T.; Zhu, J. J. *Int. J. Mod. Phys. B* **2005**, *19*, 2829.
(532) García, S.; Anderson, R. M.; Celio, H.; Dahal, N.; Dolocan, A.; Zhou, J. P.; Humphrey, S. M. *Chem. Commun.* **2013**, *49*, 4241.
(533) Tsuji, M.; Hikino, S.; Tanabe, R.; Sano, Y. *Chem. Lett.* **2009**, *38*, 860.
(534) Wang, X.; Yue, W. B.; He, M. S.; Liu, M. H.; Zhang, J.; Liu, Z. F. *Chem. Mater.* **2004**, *16*, 799.
(535) Du, J. Q.; Zhang, Y.; Tian, T.; Yan, S. C.; Wang, H. T. *Mater. Res. Bull.* **2009**, *44*, 1347.
(536) Harpeness, R.; Gedanken, A. *J. Mater. Chem.* **2005**, *15*, 698.
(537) Minami, R.; Kitamoto, Y.; Chikata, T.; Kato, S. *Electrochim. Acta* **2005**, *51*, 864.
(538) Köhler, D.; Heise, M.; Baranov, A. I.; Luo, Y.; Geiger, D.; Ruck, M.; Armbrüster, M. *Chem. Mater.* **2012**, *24*, 1639.
(539) Jia, J. C.; Yu, J. C.; Wang, Y. X. J.; Chan, K. M. *ACS Appl. Mater. Interface* **2010**, *2*, 2579.
(540) Guo, X. H.; Li, Y.; Liu, Q. Y.; Shen, W. J. *Chin. J. Catal.* **2012**, *33*, 645.
(541) Zhu, Y. J.; Hu, X. L. *Mater. Lett.* **2004**, *58*, 1234.
(542) Ji, G. B.; Guo, L.; Chang, X. F.; Liu, Y. S.; Pan, L. J.; Shi, Y.; Zheng, Y. L. *Curr. Nanosci.* **2011**, *7*, 254.
(543) Zhu, Y. J.; Hu, X. L. *Chem. Lett.* **2004**, *33*, 760.
(544) Dzido, G.; Jarzebski, A. B. *J. Nanopart. Res.* **2011**, *13*, 2533.
(545) Chefetz, B.; Sominski, L.; Pinchas, M.; Ginsburg, T.; Elmachliy, S.; Tel-Or, E.; Gedanken, A. *J. Phys. Chem. B* **2005**, *109*, 15179.
(546) Zhu, Y. J.; Hu, X. L. *Chem. Lett.* **2003**, *32*, 732.
(547) Zhu, Y. J.; Hu, X. L. *Mater. Lett.* **2004**, *58*, 1517.
(548) Makhluf, S.; Dror, R.; Nitzan, Y.; Abramovich, Y.; Jelinek, R.; Gedanken, A. *Adv. Funct. Mater.* **2005**, *15*, 1708.
(549) Liu, Y.; Hu, Y.; Zhou, M. J.; Qian, H. S.; Hu, X. *Appl. Catal. B: Environ.* **2012**, *125*, 425.
(550) Bhatte, K. D.; Tambade, P.; Fujita, S.; Arai, M.; Bhanage, B. M. *Powder Technol.* **2010**, *203*, 415.
(551) Bhatte, K. D.; Sawant, D. N.; Watile, R. A.; Bhanage, B. M. *Mater. Lett.* **2012**, *69*, 66.
(552) Hu, X. L.; Gong, J. M.; Zhang, L. Z.; Yu, J. C. *Adv. Mater.* **2008**, *20*, 4845.
(553) Liang, Z. H.; Zhu, Y. J.; Cheng, G. F.; Huang, Y. H. *J. Mater. Sci.* **2007**, *42*, 477.
(554) Lojkowski, W.; Gedanken, A.; Grzanka, E.; Opalinska, A.; Strachowski, T.; Pielaszek, R.; Tomaszewska-Grzeda, A.; Yatsunenko, S.; Godlewski, M.; Matysiak, H.; Kurzydowski, K. J. *J. Nanopart. Res.* **2009**, *11*, 1991.
(555) Xiao, W. C.; Gu, H. C.; Li, D.; Chen, D. D.; Deng, X. Y.; Jiao, Z.; Lin, J. *J. Magn. Magn. Mater.* **2012**, *324*, 488.
(556) Cao, S. W.; Zhu, Y. J.; Ma, M. Y.; Li, L.; Zhang, L. *J. Phys. Chem. C* **2008**, *112*, 1851.
(557) Zhang, H.; Zhong, X.; Xu, J. J.; Chen, H. Y. *Langmuir* **2008**, *24*, 13748.
(558) Yang, D. P.; Gao, F.; Cui, D. X.; Yang, M. *Curr. Nanosci.* **2009**, *5*, 485.
(559) Ai, Z. H.; Deng, K. J.; Wan, Q. F.; Zhang, L. Z.; Lee, S. *J. Phys. Chem. C* **2010**, *114*, 6237.
(560) Cao, S. W.; Zhu, Y. J. *J. Phys. Chem. C* **2008**, *112*, 6253.
(561) Yan, S. C.; Shen, K.; Zhang, Y.; Zhang, Y. P.; Xiao, Z. D. *J. Nanosci. Nanotechnol.* **2009**, *9*, 4886.
(562) Bhatt, A. S.; Bhat, D. K.; Tai, C.-w.; Santosh, M. S. *Mater. Chem. Phys.* **2011**, *125*, 347.
(563) Song, X. F.; Gao, L. *J. Am. Ceram. Soc.* **2008**, *91*, 3465.
(564) Lu, Y.; Zhang, L.; Li, J.; Su, Y. D.; Liu, Y.; Xu, Y. J.; Dong, L.; Gao, H. L.; Lin, J.; Man, N.; Wei, P. F.; Xu, W. P.; Yu, S. H.; Wen, L. P. *Adv. Funct. Mater.* **2013**, *23*, 1534.
(565) Staszak, W.; Zawadzki, M.; Okal, J. *J. Alloys Compd.* **2010**, *492*, 500.
(566) Ibrahim, A. M.; Abd El-Latif, M. M.; Mahmoud, M. M. *J. Alloys Compd.* **2010**, *506*, 201.
(567) Solano, E.; Perez-Mirabet, L.; Martinez-Julian, F.; Guzmán, R.; Arbiol, J.; Puig, T.; Obradors, X.; Yañez, R.; Pomar, A.; Ricart, S.; Ros, J. *J. Nanopart. Res.* **2012**, *14*, 1034.
(568) Giri, J.; Sriharsha, T.; Bahadur, D. *J. Mater. Chem.* **2004**, *14*, 875.

(569) Giri, J.; Sriharsha, T.; Asthana, S.; Rao, T. K. G.; Nigam, A. K.; Bahadur, D. *J. Magn. Magn. Mater.* **2005**, *293*, 55.
(570) Palchik, O.; Zhu, J. J.; Gedanken, A. *J. Mater. Chem.* **2000**, *10*, 1251.
(571) Nayak, B. B.; Vitta, S.; Bahadur, D. *Phys. Status Solidi A* **2005**, *202*, 2790.
(572) Thongtem, T.; Phuruangrat, A.; Thongtem, S. *Curr. Appl. Phys.* **2008**, *8*, 189.
(573) Thongtem, T.; Phuruangrat, A.; Thongtem, S. *J. Nanopart. Res.* **2010**, *12*, 2287.
(574) Phuruangrat, A.; Thongtem, T.; Thongtem, S. *J. Phys. Chem. Solids* **2009**, *70*, 955.
(575) Phuruangrat, A.; Thongtem, T.; Thongtem, S. *J. Alloys Compd.* **2009**, *481*, 568.
(576) Thongtem, T.; Phuruangrat, A.; Thongtem, S. *Mater. Lett.* **2008**, *62*, 454.
(577) Phuruangrat, A.; Thongtem, T.; Thongtem, S. *J. Cryst. Growth* **2009**, *311*, 4076.
(578) Wu, L.; Bi, J. H.; Li, Z. H.; Wang, X. X.; Fu, X. Z. *Catal. Today* **2008**, *131*, 15.
(579) Nakamura, T.; Yanagida, S.; Wada, Y. *Res. Chem. Intermed.* **2006**, *32*, 331.
(580) Chen, D.; Shen, G. Z.; Tang, K. B.; Lei, S. J.; Zheng, H. G.; Qian, Y. T. *J. Cryst. Growth* **2004**, *260*, 469.
(581) Patra, C. R.; Odani, A.; Pol, V. G.; Aurbach, D.; Gedanken, A. *J. Solid State Electrochem.* **2007**, *11*, 186.
(582) Thongtem, T.; Phuruangrat, A.; Thongtem, S. *J. Ceram. Process Res.* **2008**, *9*, 335.
(583) Chen, G. C.; Fan, J. B.; Zhao, T.; Xu, X. B.; Zhu, M. Q.; Tang, Z. Y. *J. Nanosci. Nanotechnol.* **2011**, *11*, 7807.
(584) Kavinchan, J.; Thongtem, T.; Thongtem, S. *Mater. Lett.* **2010**, *64*, 2388.
(585) Yang, H. M.; Su, X. H.; Tang, A. D. *Mater. Res. Bull.* **2007**, *42*, 1357.
(586) He, X. B.; Gao, L.; Yang, S. W.; Sun, J. *CrystEngComm* **2010**, *12*, 3413.
(587) Lu, J.; Han, Q. F.; Yang, X. J.; Lu, L. D.; Wang, X. *Mater. Lett.* **2007**, *61*, 2883.
(588) Oliveira, J. F. A.; Milão, T. M.; Araújo, V. D.; Moreira, M. L.; Longo, E.; Bernardi, M. I. B. *J. Alloys Compd.* **2011**, *509*, 6880.
(589) Tai, G. A.; Guo, W. L. *Ultrason. Sonochem.* **2008**, *15*, 350.
(590) Tai, G. A.; Zhou, J. X.; Guo, W. L. *Nanotechnology* **2010**, *21*, 175601.
(591) Chen, D.; Tang, K. B.; Shen, G. Z.; Sheng, J.; Fang, Z.; Liu, X. M.; Zheng, H. G.; Qian, Y. T. *Mater. Chem. Phys.* **2003**, *82*, 206.
(592) Ma, J.; Tai, G. A.; Guo, W. L. *Ultrason. Sonochem.* **2010**, *17*, 534.
(593) Ni, Y. H.; Yin, G.; Hong, J. M.; Xu, Z. *Mater. Res. Bull.* **2004**, *39*, 1967.
(594) Sun, J. Q.; Shen, X. P.; Chen, K. M.; Liu, Q.; Liu, W. *Solid State Commun.* **2008**, *147*, 501.
(595) Wang, Z. Y.; Lou, W. J.; Wang, X. B.; Liu, W. M. *J. Nanosci. Nanotechnol.* **2011**, *11*, 2080.
(596) Thongtem, T.; Phuruangrat, A.; Thongtem, S. *J. Mater. Sci.* **2007**, *42*, 9316.
(597) Liu, X. L.; Zhu, Y. J. *Mater. Lett.* **2011**, *65*, 1089.
(598) Li, M.-L.; Yao, Q.-Z.; Zhou, G.-T.; Qu, X.-F.; Mu, C.-F.; Fu, S.-Q. *CrystEngComm* **2011**, *13*, 5936.
(599) Aup-Ngoen, K.; Thongtem, S.; Thongtem, T. *Mater. Lett.* **2011**, *65*, 442.
(600) Flynn, B.; Wang, W.; Chang, C.-h.; Herman, G. S. *Phys. Status Solidi A* **2012**, *209*, 2186.
(601) Palchik, O.; Kerner, R.; Gedanken, A.; Weiss, A. M.; Slifkin, M. A.; Palchik, V. *J. Mater. Chem.* **2001**, *11*, 874.
(602) Cao, X. B.; Zhao, C.; Lan, X. M.; Yao, D.; Shen, W. J. *J. Alloys Compd.* **2009**, *474*, 61.
(603) Li, M. L.; Yao, Q. Z.; Zhou, G. T.; Fu, S. Q. *CrystEngComm* **2010**, *12*, 3138.
(604) Mehta, R. J.; Karthik, C.; Jiang, W.; Singh, B.; Shi, Y. F.; Siegel, R. W.; Borca-Tasciuc, T.; Ramanath, G. *Nano Lett.* **2010**, *10*, 4417.
(605) Zhao, C.; Cao, X. B.; Lan, X. M. *Mater. Lett.* **2007**, *61*, 5083.
(606) Harpeness, R.; Gedanken, A. *New J. Chem.* **2003**, *27*, 1191.
(607) Harpeness, R.; Gedanken, A.; Weiss, A. M.; Slifkin, M. A. *J. Mater. Chem.* **2003**, *13*, 2603.
(608) Grisaru, H.; Palchik, O.; Gedanken, A.; Palchik, V.; Slifkin, M. A.; Weiss, A. M.; Hacohen, Y. R. *Inorg. Chem.* **2001**, *40*, 4814.
(609) Grisaru, H.; Palchik, O.; Gedanken, A.; Palchik, V.; Slifkin, M. A.; Weiss, A. M. *J. Mater. Chem.* **2002**, *12*, 339.
(610) Grisaru, H.; Palchik, O.; Gedanken, A.; Palchik, V.; Slifkin, M. A.; Weiss, A. M. *Inorg. Chem.* **2003**, *42*, 7148.
(611) Zhou, B.; Ji, Y.; Yang, Y. F.; Li, X. H.; Zhu, J. J. *Cryst. Growth Des.* **2008**, *8*, 4394.
(612) Zhou, B.; Zhao, Y.; Pu, L.; Zhu, J. J. *Mater. Chem. Phys.* **2006**, *96*, 192.
(613) Palchik, O.; Kerner, R.; Gedanken, A.; Palchik, V.; Slifkin, M. A.; Weiss, A. M. *Glass Phys. Chem.* **2005**, *31*, 80.
(614) Dong, G. H.; Zhu, Y. J.; Cheng, G. F.; Ruan, Y. J. *Mater. Lett.* **2012**, *76*, 69.
(615) Mi, C.-C.; Tian, Z.-h.; Han, B.-f.; Mao, C.-b.; Xu, S.-k. *J. Alloys Compd.* **2012**, *525*, 154.
(616) Zhu, X. X.; Zhang, Q. H.; Li, Y. G.; Wang, H. Z. *J. Mater. Chem.* **2010**, *20*, 1766.
(617) Li, F. F.; Li, C. G.; Liu, X. M.; Bai, T. Y.; Dong, W. J.; Zhang, X.; Shi, Z.; Feng, S. H. *Dalton Trans.* **2013**, *42*, 2015.
(618) Zhang, L.; Cao, X.-F.; Chen, X.-T.; Xue, Z.-L. *J. Colloid Interface Sci.* **2011**, *354*, 630.
(619) Li, G. F.; Qin, F.; Yang, H.; Lu, Z.; Sun, H. Z.; Chen, R. *Eur. J. Inorg. Chem.* **2012**, 2508.
(620) Tian, X. Q.; Cheng, C. M.; Qian, L.; Zheng, B. Z.; Yuan, H. Y.; Xie, S. P.; Xiao, D.; Choi, M. M. F. *J. Mater. Chem.* **2012**, *22*, 8029.
(621) Li, L.; Zhu, Y. J.; Ma, M. G. *Mater. Lett.* **2008**, *62*, 4552.
(622) Tipcompor, N.; Thongtem, T.; Phuruangrat, A.; Thongtem, S. *Mater. Lett.* **2012**, *87*, 153.
(623) Ma, M. G.; Zhu, Y. J.; Zhu, J. F.; Cheng, G. F. *Chem. Lett.* **2006**, *35*, 1138.
(624) Kim, D. H.; Kang, J. W.; Jung, I. O.; Im, J. S.; Kim, E. J.; Song, S. J.; Lee, J. S.; Kim, J. J. *Nanosci. Nanotechnol.* **2008**, *8*, 5376.
(625) Muraliganth, T.; Stroukoff, K. R.; Manthiram, A. *Chem. Mater.* **2010**, *22*, 5754.
(626) Phuruangrat, A.; Ekthammathat, N.; Thongtem, T.; Thongtem, S. *J. Phys. Chem. Solids* **2011**, *72*, 176.
(627) Phuruangrat, A.; Thongtem, T.; Thongtem, S. *J. Exp. Nanosci.* **2010**, *5*, 263.
(628) Anumol, E. A.; Kundu, P.; Deshpande, P. A.; Madras, G.; Ravishankar, N. *ACS Nano* **2011**, *5*, 8049.
(629) Tsuji, M.; Nishio, M.; Jiang, P.; Miyamae, N.; Lim, S.; Matsumoto, K.; Ueyama, D.; Tang, X. L. *Colloids Surf., A* **2008**, *317*, 247.
(630) Tsuji, M.; Matsuo, R.; Jiang, P.; Miyamae, N.; Ueyama, D.; Nishio, M.; Hikino, S.; Kumagae, H.; Kamarudin, K. S. N.; Tang, X. L. *Cryst. Growth Des.* **2008**, *8*, 2528.
(631) Tsuji, M.; Nakamura, N.; Ogino, M.; Ikedo, K.; Matsunaga, M. *CrystEngComm* **2012**, *14*, 7639.
(632) Tsuji, M.; Hikino, S.; Matsunaga, M.; Sano, Y.; Hashizume, T.; Kawazumi, H. *Mater. Lett.* **2010**, *64*, 1793.
(633) Zhao, J.; Chen, W. X.; Zheng, Y. F.; Li, X.; Xu, Z. D. *J. Mater. Sci.* **2006**, *41*, 5514.
(634) Song, S. Q.; Wang, Y.; Shen, P. K. *J. Power Sources* **2007**, *170*, 46.
(635) Hu, S.; Xiong, L. P.; Ren, X. B.; Wang, C. B.; Luo, Y. M. *Int. J. Hydrogen Energy* **2009**, *34*, 8723.
(636) Zhao, G. W.; He, J. P.; Zhang, C. X.; Zhou, J. H.; Chen, X.; Wang, T. *J. Phys. Chem. C* **2008**, *112*, 1028.
(637) Zhou, J. H.; He, J. P.; Wang, T.; Sun, D.; Zhao, G. W.; Chen, X.; Wang, D. J.; Di, Z. Y. *J. Mater. Chem.* **2008**, *18*, 5776.
(638) Liu, Z. L.; Hong, L.; Tay, S. W. *Mater. Chem. Phys.* **2007**, *105*, 222.

(639) Guo, Z. J.; Zhu, H.; Zhang, X. W.; Wang, F. H.; Guo, Y. B.; Wei, Y. S. *Bull. Mater. Sci.* **2011**, *34*, 577.
(640) Lebègue, E.; Baranton, S.; Coutanceau, C. *J. Power Sources* **2011**, *196*, 920.
(641) Liu, S.; Wang, L.; Tian, J. Q.; Lu, W. B.; Zhang, Y. W.; Wang, X. D.; Sun, X. P. *J. Nanopart. Res.* **2011**, *13*, 4731.
(642) Kundu, P.; Nethravathi, C.; Deshpande, P. A.; Rajamathi, M.; Madras, G.; Ravishankar, N. *Chem. Mater.* **2011**, *23*, 2772.
(643) Xu, H.; Zeng, L. P.; Xing, S. J.; Xian, Y. Z.; Jin, L. T. *Electrochem. Commun.* **2008**, *10*, 551.
(644) Sakthivel, M.; Schlange, A.; Kunz, U.; Turek, T. *J. Power Sources* **2010**, *195*, 7083.
(645) Gan, Z. B.; Zheng, X. W.; Wei, D. L.; Hu, Q. T.; Zhao, A. H.; Zhang, X.; Li, G. Y. *Superlattices Microstruct.* **2010**, *47*, 705.
(646) Hsieh, C.-T.; Liu, Y.-Y.; Cheng, Y.-S.; Chen, W.-Y. *Electrochim. Acta* **2011**, *56*, 6336.
(647) Liu, X.-s.; Hu, F.; Zhu, D.-r.; Jia, D.-n.; Wang, P.-p.; Ruan, Z.; Cheng, C.-h. *J. Alloys Compd.* **2011**, *509*, 2829.
(648) Zhang, X. J.; Jiang, W.; Song, D.; Liu, J. X.; Li, F. S. *Mater. Lett.* **2008**, *62*, 2343.
(649) Bo, X. J.; Bai, J.; Yang, L.; Guo, L. P. *Sens. Actuators, B* **2011**, *157*, 662.
(650) Liu, Z. L.; Guo, B.; Hong, L.; Lim, T. H. *Electrochem. Commun.* **2006**, *8*, 83.
(651) Tsuji, M.; Kubokawa, M.; Yano, R.; Miyamae, N.; Tsuji, T.; Jun, M. S.; Hong, S.; Lim, S.; Yoon, S. H.; Mochida, I. *Langmuir* **2007**, *23*, 387.
(652) Zhu, H.; Liu, Y. L.; Shen, L. B.; Wei, Y. S.; Guo, Z. J.; Wang, H. J.; Han, K. F.; Chang, Z. R. *Int. J. Hydrogen Energy* **2010**, *35*, 3125.
(653) Liang, Y. M.; Zhang, H. M.; Zhong, H. X.; Zhu, X. B.; Tian, Z. Q.; Xu, D. Y.; Yi, B. L. *J. Catal.* **2006**, *238*, 468.
(654) Sarkar, A.; Murugan, A. V.; Manthiram, A. *Fuel Cells* **2010**, *10*, 375.
(655) Liang, Y. M.; Zhang, H. M.; Tian, Z. Q.; Zhu, X. B.; Wang, X. L.; Yi, B. L. *J. Phys. Chem. B* **2006**, *110*, 7828.
(656) Wang, S. Y.; Wang, X.; Jiang, S. P. *Langmuir* **2008**, *24*, 10505.
(657) Han, D. M.; Guo, Z. P.; Zhao, Z. W.; Zeng, R.; Meng, Y. Z.; Shu, D.; Liu, H. K. *J. Power Sources* **2008**, *184*, 361.
(658) Wang, X. Z.; Xue, H.; Yang, L. J.; Wang, H. K.; Zang, P. Y.; Qin, X. T.; Wang, Y. N.; Ma, Y. W.; Wu, Q.; Hu, Z. *Nanotechnology* **2011**, *22*, 395401.
(659) Hsieh, C.-T.; Liu, Y.-Y.; Chen, W.-Y.; Hsieh, Y.-H. *Int. J. Hydrogen Energy* **2011**, *36*, 15766.
(660) Hu, Q. T.; Gan, Z. B.; Zheng, X. W.; Zhao, A. H.; Zhang, X. *J. Nanopart. Res.* **2011**, *13*, 3191.
(661) Hsieh, C.-T.; Hung, W.-M.; Chen, W.-Y.; Lin, J.-Y. *Int. J. Hydrogen Energy* **2011**, *36*, 2765.
(662) Wu, H. Q.; Cao, P. P.; Li, W. T.; Ni, N.; Zhu, L. L.; Zhang, X. J. *J. Alloys Compd.* **2011**, *509*, 1261.
(663) Courtel, F. M.; Baranova, E. A.; Abu-Lebdeh, Y.; Davidson, I. J. *J. Power Sources* **2010**, *195*, 2355.
(664) Luo, W.; Hu, X. L.; Sun, Y. M.; Huang, Y. H. *ACS Appl. Mater. Interfaces* **2013**, *5*, 1997.
(665) Zhang, M.; Lei, D. N.; Yin, X. M.; Chen, L. B.; Li, Q. H.; Wang, Y. G.; Wang, T. H. *J. Mater. Chem.* **2010**, *20*, 5538.
(666) Chen, Y. X.; Gu, H. C. *Mater. Lett.* **2012**, *67*, 49.
(667) Zhou, L. N.; Zhang, X. B.; Zhao, X. B.; Sun, C. X.; Niu, Q. *J. Alloys Compd.* **2010**, *502*, 329.
(668) Xu, Q. C.; Lin, J. D.; Li, J.; Fu, X. Z.; Liang, Y.; Liao, D. W. *Catal. Commun.* **2007**, *8*, 1881.
(669) Zhang, X. W.; Zhu, H.; Guo, Z. J.; Wei, Y. S.; Wang, F. H. *J. Power Sources* **2011**, *196*, 3048.
(670) Okal, J. *Catal. Commun.* **2010**, *11*, 508.
(671) Guo, G. M.; Yu, B. B.; Yu, P.; Chen, X. *Talanta* **2009**, *79*, 570.
(672) Liu, X. W.; Cao, H. Q.; Yin, J. F. *Nano Res.* **2011**, *4*, 470.
(673) Nishioka, M.; Miyakawa, M.; Kataoka, H.; Koda, H.; Sato, K.; Suzuki, T. M. *Chem. Lett.* **2011**, *40*, 1204.
(674) Guo, Y.; Wang, H. S.; He, C. L.; Qiu, L. J.; Cao, X. B. *Langmuir* **2009**, *25*, 4678.
(675) Sun, Y. M.; Hu, X. L.; Luo, W.; Huang, Y. H. *J. Mater. Chem.* **2012**, *22*, 19190.
(676) Jiang, J.; Zhang, L. Z. *Chem.—Eur. J.* **2011**, *17*, 3710.
(677) Dong, G. H.; Zhu, Y. J. *Chem. Eng. J.* **2012**, *193*, 227.
(678) Zahoor, A.; Qiu, T.; Zhang, J. R.; Li, X. Y. *J. Mater. Sci.* **2009**, *44*, 6054.
(679) Chen, J. Y.; Li, Z. Y.; Chao, D. M.; Zhang, W. J.; Wang, C. *Mater. Lett.* **2008**, *62*, 692.
(680) Liu, S. H.; Lu, F.; Jia, X. D.; Cheng, F. F.; Jiang, L.-P.; Zhu, J.-J. *CrystEngComm* **2011**, *13*, 2425.
(681) Ma, Z.; Yu, J. H.; Dai, S. *Adv. Mater.* **2010**, *22*, 261.
(682) Rogers, R. D.; Seddon, K. R. *Ionic Liquids as Green Solvents-Progress and Prospects*; American Chemical Society: Washington, DC, 2003.
(683) Rogers, R. D.; Seddon, K. R. *Science* **2003**, *302*, 792.
(684) Li, Z. H.; Jia, Z.; Luan, Y. X.; Mu, T. C. *Curr. Opin. Solid State Mater. Sci.* **2008**, *12*, 1.
(685) Zhu, Y. J.; Wang, W. W.; Qi, R. J.; Hu, X. L. *Angew. Chem., Int. Ed.* **2004**, *43*, 1410.
(686) Redel, E.; Walter, M.; Thomann, R.; Vollmer, C.; Hussein, L.; Scherer, H.; Krüger, M.; Janiak, C. *Chem.—Eur. J.* **2009**, *15*, 10047.
(687) Ren, L. Z.; Meng, L. J.; Lu, Q. H.; Fei, Z. F.; Dyson, P. J. *J. Colloid Interface Sci.* **2008**, *323*, 260.
(688) Ren, L. Z.; Meng, L. J.; Lu, Q. H. *Chem. Lett.* **2008**, *37*, 106.
(689) Marquardt, D.; Xie, Z. L.; Taubert, A.; Thomann, R.; Janiak, C. *Dalton Trans.* **2011**, *40*, 8290.
(690) Vollmer, C.; Redel, E.; Abu-Shandi, K.; Thomann, R.; Manyar, H.; Hardacre, C.; Janiak, C. *Chem.—Eur. J.* **2010**, *16*, 3849.
(691) Campbell, P. S.; Lorbeer, C.; Cybinska, J.; Mudring, A.-V. *Adv. Funct. Mater.* **2013**, *23*, 2924.
(692) Safavi, A.; Sedaghati, F.; Shahbaazi, H.; Farjami, E. *RSC Adv.* **2012**, *2*, 7367.
(693) Wang, W. W.; Zhu, Y. J. *Inorg. Chem. Commun.* **2004**, *7*, 1003.
(694) Cao, J. M.; Wang, J.; Fang, B. Q.; Chang, X.; Zheng, M. B.; Wang, H. Y. *Chem. Lett.* **2004**, *33*, 1332.
(695) Zou, H.; Li, Z. H.; Luan, Y. X.; Mu, T. C.; Wang, Q. Z.; Li, L.; Ge, J. H.; Chen, G. W. *Curr. Opin. Solid State Mater. Sci.* **2010**, *14*, 75.
(696) Jacob, D. S.; Bitton, L.; Grinblat, J.; Felner, I.; Koltypin, Y.; Gedanken, A. *Chem. Mater.* **2006**, *18*, 3162.
(697) Pang, J. M.; Luan, Y. X.; Wang, Q. Z.; Du, J. M.; Cai, X. Q.; Li, Z. H. *Colloids Surf., A* **2010**, *360*, 6.
(698) Cao, S. W.; Zhu, Y. J. *Acta Mater.* **2009**, *57*, 2154.
(699) Li, X. Y.; Liu, D. P.; Song, S. Y.; Wang, X.; Ge, X.; Zhang, H. J. *CrystEngComm* **2011**, *13*, 6017.
(700) Xiao, L. S.; Shen, H.; von Hagen, R.; Pan, J.; Belkoura, L.; Mathur, S. *Chem. Commun.* **2010**, *46*, 6509.
(701) Bühler, G.; Thölmann, D.; Feldmann, C. *Adv. Mater.* **2007**, *19*, 2224.
(702) Wang, W. W.; Zhu, Y. J.; Cheng, G. F.; Huang, Y. H. *Mater. Lett.* **2006**, *60*, 609.
(703) Xu, X. D.; Zhang, M.; Feng, J.; Zhang, M. L. *Mater. Lett.* **2008**, *62*, 2787.
(704) Zhu, L.; Chen, Y.; Sun, Y.; Cui, Y.; Liang, M.; Zhao, J.; Li, N. *Cryst. Res. Technol.* **2010**, *45*, 398.
(705) Xia, J. X.; Li, H. M.; Luo, Z. J.; Shi, H.; Wang, K.; Shu, H. M.; Yan, Y. S. *J. Phys. Chem. Solids* **2009**, *70*, 1461.
(706) Yang, L. X.; Zhu, Y. J.; Wang, W. W.; Tong, H.; Ruan, M. L. *J. Phys. Chem. B* **2006**, *110*, 6609.
(707) Ding, K. L.; Miao, Z. J.; Liu, Z. M.; Zhang, Z. F.; Han, B. X.; An, G. M.; Miao, S. D.; Xie, Y. *J. Am. Chem. Soc.* **2007**, *129*, 6362.
(708) Estruga, M.; Domingo, C.; Ayllón, J. A. *Mater. Res. Bull.* **2010**, *45*, 1224.
(709) Goharshadi, E. K.; Samiee, S.; Nancarrow, P. *J. Colloid Interface Sci.* **2011**, *356*, 473.
(710) Cao, S. W.; Zhu, Y. J.; Cheng, G. F.; Huang, Y. H. *J. Hazard. Mater.* **2009**, *171*, 431.
(711) Wang, W. W.; Zhu, Y. J. *Cryst. Growth Des.* **2005**, *5*, 505.
(712) Xu, J. S.; Zhu, Y. J. *CrystEngComm* **2012**, *14*, 2630.

(713) Li, C. X.; Ma, P. A.; Yang, P. P.; Xu, Z. H.; Li, G. G.; Yang, D. M.; Peng, C.; Lin, J. *CrystEngComm* **2011**, *13*, 1003.
(714) Lorbeer, C.; Cybińska, J.; Mudring, A. V. *Cryst. Growth Des.* **2011**, *11*, 1040.
(715) Lorbeer, C.; Cybinska, J.; Mudring, A. V. *Chem. Commun.* **2010**, *46*, 571.
(716) Chen, C.; Sun, L. D.; Li, Z. X.; Li, L. L.; Zhang, J.; Zhang, Y. W.; Yan, C. H. *Langmuir* **2010**, *26*, 8797.
(717) Wu, L. Y.; Lian, J. B.; Sun, G. X.; Kong, X. R.; Zheng, W. J. *Eur. J. Inorg. Chem.* **2009**, 2897.
(718) Zhu, L. J.; Zheng, Y. T.; Hao, T. Y.; Shi, X. X.; Chen, Y. T.; Ou-Yang, J. *Mater. Lett.* **2009**, *63*, 2405.
(719) Song, J. K.; Zheng, M. B.; Yang, Z. J.; Chen, H. Q.; Wang, H. Y.; Liu, J. S.; Ji, G. B.; Zhang, H. Q.; Cao, J. M. *Nanoscale Res. Lett.* **2009**, *4*, 1512.
(720) Shahid, R.; Gorlov, M.; El-Sayed, R.; Toprak, M. S.; Sugunan, A.; Kloo, L.; Muhammed, M. *Mater. Lett.* **2012**, *89*, 316.
(721) Jiang, Y.; Zhu, Y. J. *Chem. Lett.* **2004**, *33*, 1390.
(722) Jiang, Y.; Zhu, Y. J. *J. Phys. Chem. B* **2005**, *109*, 4361.
(723) Jiang, Y.; Zhu, Y. J.; Cheng, G. F. *Cryst. Growth Des.* **2006**, *6*, 2174.
(724) Ji, G. B.; Shi, Y.; Pan, L. J.; Zheng, Y. D. *J. Alloys Compd.* **2011**, *509*, 6015.
(725) Hayakawa, Y.; Nonoguchi, Y.; Wu, H.-P.; Diau, E. W. G.; Nakashima, T.; Kawai, T. *J. Mater. Chem.* **2011**, *21*, 8849.
(726) Bühler, G.; Feldmann, C. *Angew. Chem., Int. Ed.* **2006**, *45*, 4864.
(727) Zharkouskaya, A.; Feldmann, C.; Trampert, K.; Heering, W.; Lemmer, U. *Eur. J. Inorg. Chem.* **2008**, 873.
(728) Cao, S. W.; Zhu, Y. J.; Cui, J. B. *J. Solid State Chem.* **2010**, *183*, 1704.
(729) Wang, W. W.; Zhu, Y. J. *Mater. Res. Bull.* **2005**, *40*, 1929.
(730) Jacob, D. S.; Genish, I.; Klein, L.; Gedanken, A. *J. Phys. Chem. B* **2006**, *110*, 17711.
(731) Liu, Z. M.; Sun, Z. Y.; Han, B. X.; Zhang, J. L.; Huang, J.; Du, J. M.; Miao, S. D. *J. Nanosci. Nanotechnol.* **2006**, *6*, 175.
(732) Guo, D. J. *J. Power Sources* **2010**, *195*, 7234.
(733) Marquardt, D.; Vollmer, C.; Thomann, R.; Steurer, P.; Mülhaupt, R.; Redel, E.; Janiak, C. *Carbon* **2011**, *49*, 1326.
(734) Jia, N.; Li, S. M.; Ma, M. G.; Sun, R. C.; Zhu, L. *Carbohydr. Res.* **2011**, *346*, 2970.
(735) Li, Z. H.; Liu, Z. M.; Zhang, J. L.; Han, B. X.; Du, J. M.; Gao, Y. N.; Jiang, T. *J. Phys. Chem. B* **2005**, *109*, 14445.
(736) Abargues, R.; Gradess, R.; Canet-Ferrer, J.; Abderrafi, K.; Valdés, J. L.; Martínez-Pastor, J. *New J. Chem.* **2009**, *33*, 913.
(737) Pal, A.; Shah, S.; Devi, S. *Mater. Chem. Phys.* **2009**, *114*, 530.
(738) Li, D. S.; Komarneni, S. *J. Nanosci. Nanotechnol.* **2008**, *8*, 3930.
(739) Galletti, A. M. R.; Antonetti, C.; Venezia, A. M.; Giambastiani, G. *Appl. Catal., A* **2010**, *386*, 124.
(740) Nakamura, T.; Tsukahara, Y.; Sakata, T.; Mori, H.; Kanbe, Y.; Bessho, H.; Wada, Y. *Bull. Chem. Soc. Jpn.* **2007**, *80*, 224.
(741) Dar, M. I.; Sampath, S.; Shivashankar, S. A. *J. Mater. Chem.* **2012**, *22*, 22418.
(742) Nakamura, T.; Tsukahara, Y.; Yamauchi, T.; Sakata, T.; Mori, H.; Wada, Y. *Chem. Lett.* **2007**, *36*, 154.
(743) Druzhinina, T.; Hoeppener, S.; Schubert, U. S. *Adv. Funct. Mater.* **2009**, *19*, 2819.
(744) Schneider, J. J.; Hoffmann, R. C.; Engstler, J.; Klyszcz, A.; Erdem, E.; Jakes, P.; Eichel, R. A.; Pitta-Bauermann, L.; Bill, J. *Chem. Mater.* **2010**, *22*, 2203.
(745) Zhao, X. W.; Qi, L. M. *Nanotechnology* **2012**, *23*, 235604.
(746) Gupta, A.; Kumar, S.; Bhatti, H. S. *J. Mater. Sci.: Mater. Electron.* **2010**, *21*, 765.
(747) Wang, H.; Xu, J. Z.; Zhu, J. J.; Chen, H. Y. *J. Cryst. Growth* **2002**, *244*, 88.
(748) Caillot, T.; Aymes, D.; Stuerga, D.; Viart, N.; Pourroy, G. *J. Mater. Sci.* **2002**, *37*, 5153.
(749) Cao, C.-Y.; Qu, J.; Yan, W.-S.; Zhu, J.-F.; Wu, Z.-Y.; Song, W.-G. *Langmuir* **2012**, *28*, 4573.
(750) Bousquet-Berthelin, C.; Stuerga, D. *J. Mater. Sci.* **2005**, *40*, 253.
(751) Bilecka, I.; Djerdj, I.; Niederberger, M. *Chem. Commun.* **2008**, 886.
(752) Jena, A.; Vinu, R.; Shivashankar, S. A.; Madras, G. *Ind. Eng. Chem. Res.* **2010**, *49*, 9636.
(753) Deshmane, C. A.; Jasinski, J. B.; Carreon, M. A. *Microporous Mesoporous Mater.* **2010**, *130*, 97.
(754) Le Houx, N.; Pourroy, G.; Camerel, F.; Comet, M.; Spitzer, D. *J. Phys. Chem. C* **2010**, *114*, 155.
(755) Ren, Y.; Gao, L. *J. Am. Ceram. Soc.* **2010**, *93*, 3560.
(756) Caillot, T.; Pourroy, G.; Stuerga, D. *J. Alloys Compd.* **2011**, *509*, 3493.
(757) Liu, X.-L.; Zhu, Y.-J.; Cheng, G.-F.; Huang, Y.-H. *Mater. Lett.* **2011**, *65*, 343.
(758) Gonzalez-Arellano, C.; Yoshida, K.; Luque, R.; Gai, P. L. *Green Chem.* **2010**, *12*, 1281.
(759) Balu, A. M.; Dallinger, D.; Obermayer, D.; Campelo, J. M.; Romero, A. A.; Carmona, D.; Balas, F.; Yohida, K.; Gai, P. L.; Vargas, C.; Kappe, C. O.; Luque, R. *Green Chem.* **2012**, *14*, 393.
(760) Glaspell, G.; Fuoco, L.; El-Shall, M. S. *J. Phys. Chem. B* **2005**, *109*, 17350.
(761) Bousquet-Berthelin, C.; Chaumont, D.; Stuerga, D. *J. Solid State Chem.* **2008**, *181*, 616.
(762) Pascu, O.; Gich, M.; Herranz, G.; Roig, A. *Eur. J. Inorg. Chem.* **2012**, 2656.
(763) Mahmoud, W. E.; Faidah, A. *J. Eur. Ceram. Soc.* **2012**, *32*, 3537.
(764) Combemale, L.; Caboche, G.; Stuerga, D.; Chaumont, D. *Mater. Res. Bull.* **2005**, *40*, 529.
(765) Feng, X. J.; Sloppy, J. D.; LaTempa, T. J.; Paulose, M.; Komarneni, S.; Bao, N. Z.; Grimes, C. A. *J. Mater. Chem.* **2011**, *21*, 13429.
(766) Hsu, Y. C.; Lin, H. C.; Chen, C. H.; Liao, Y. T.; Yang, C. M. *J. Solid State Chem.* **2010**, *183*, 1917.
(767) Murugan, A. V.; Sonawane, R. S.; Kale, B. B.; Apte, S. K.; Kulkarni, A. V. *Mater. Chem. Phys.* **2001**, *71*, 98.
(768) Ding, T.; Zhu, J. J. *Mater. Sci. Eng., B* **2003**, *100*, 307.
(769) Yang, W. L.; Zhang, L.; Hu, Y.; Zhong, Y. J.; Wu, H. B.; Lou, X. W. *Angew. Chem., Int. Ed.* **2012**, *51*, 11501.
(770) Wang, H.; Zhang, J. R.; Zhu, J. J. *J. Cryst. Growth* **2001**, *233*, 829.
(771) Caillot, T.; Pourroy, G.; Stuerga, D. *J. Solid State Chem.* **2004**, *177*, 3843.
(772) Bilecka, I.; Elser, P.; Niederberger, M. *ACS Nano* **2009**, *3*, 467.
(773) Pascu, O.; Carenza, E.; Gich, M.; Estradé, S.; Peiró, F.; Herranz, G.; Roig, A. *J. Phys. Chem. C* **2012**, *116*, 15108.
(774) Bhosale, M. A.; Bhatte, K. D.; Bhanage, B. M. *Powder Technol.* **2013**, *235*, 516.
(775) Russo, P. A.; Lima, S.; Rebuttini, V.; Pillinger, M.; Willinger, M. G.; Pinna, N.; Valente, A. A. *RSC Adv.* **2013**, *3*, 2595.
(776) Luo, L.; Rossell, M. D.; Xie, D.; Erni, R.; Niederberger, M. *ACS Sustainable Chem. Eng.* **2013**, *1*, 152.
(777) Darmanin, T.; Nativo, P.; Gilliland, D.; Ceccone, G.; Pascual, C.; De Berardis, B.; Guittard, F.; Rossi, F. *Colloids Surf., A* **2012**, *395*, 145.
(778) Vollmer, C.; Thomann, R.; Janiak, C. *Dalton Trans.* **2012**, *41*, 9722.
(779) Lu, Q. Y.; Gao, F.; Komarneni, S. *J. Mater. Res.* **2004**, *19*, 1649.
(780) He, J.; Zhao, X. N.; Zhu, J. J.; Wang, J. *J. Cryst. Growth* **2002**, *240*, 389.
(781) Zhu, J. J.; Wang, H.; Zhu, J. M.; Wang, J. *Mater. Sci. Eng., B* **2002**, *94*, 136.
(782) Liu, X. Y.; Tian, B. Z.; Yu, C. Z.; Tu, B.; Zhao, D. Y. *Chem. Lett.* **2004**, *33*, 522.
(783) Palchik, O.; Kerner, R.; Zhu, Z.; Gedanken, A. *J. Solid State Chem.* **2000**, *154*, 530.
(784) Wu, C. C.; Shiau, C. Y.; Ayele, D. W.; Su, W. N.; Cheng, M. Y.; Chiu, C. Y.; Hwang, B. J. *Chem. Mater.* **2010**, *22*, 4185.
(785) Lee, J. S.; Suryanarayana, I.; Lee, H. Y.; Hwang, Y. K.; Chang, J. S. *J. Nanosci. Nanotechnol.* **2010**, *10*, 303.

(786) Ding, T.; Zhang, J. R.; Long, S.; Zhu, J. J. *Microelectron. Eng.* **2003**, *66*, 46.
(787) Liu, J. S.; Cao, J. M.; Li, Z. Q.; Ji, G. B.; Zheng, M. B. *Mater. Lett.* **2007**, *61*, 4409.
(788) Grisaru, H.; Pol, V. G.; Gedanken, A.; Nowik, I. *Eur. J. Inorg. Chem.* **2004**, 1859.
(789) Kim, D.; Gedanken, A.; Tver'yanovich, Y. S.; Lee, D. W.; Kim, B. K. *Mater. Lett.* **2006**, *60*, 2807.
(790) Wada, Y.; Kobayashi, T.; Yamasaki, H.; Sakata, T.; Hasegawa, N.; Mori, H.; Tsukahara, Y. *Polymer* **2007**, *48*, 1441.
(791) Wada, Y.; Kuramoto, H.; Anand, J.; Kitamura, T.; Sakata, T.; Mori, H.; Yanagida, S. *J. Mater. Chem.* **2001**, *11*, 1936.
(792) Atkins, T. M.; Louie, A. Y.; Kauzlarich, S. M. *Nanotechnology* **2012**, *23*, 294006.
(793) He, R.; Qian, X. F.; Yin, J.; Zhu, Z. K. *J. Cryst. Growth* **2003**, *252*, 505.
(794) Majumder, M.; Karan, S.; Chakraborty, A. K.; Mallik, B. *Spectrochim. Acta, Part A* **2010**, *76*, 115.
(795) Wu, J. L.; Qin, F.; Cheng, G.; Li, H.; Zhang, J. H.; Xie, Y. P.; Yang, H. J.; Lu, Z.; Yu, X. L.; Chen, R. *J. Alloys Compd.* **2011**, *509*, 2116.
(796) Karan, S.; Majumder, M.; Mallik, B. *Photochem. Photobiol. Sci.* **2012**, *11*, 1220.
(797) Cao, X. B.; Zhao, C.; Lan, X. M.; Gao, G. J.; Qian, W. H.; Guo, Y. *J. Phys. Chem. C* **2007**, *111*, 6658.
(798) Liu, S.; Tian, J. Q.; Wang, L.; Sun, X. P. *J. Nanopart. Res.* **2011**, *13*, 4539.
(799) Chen, F.; Zhu, Y. J.; Zhang, K. H.; Wu, J.; Wang, K. W.; Tang, Q. L.; Mo, X. M. *Nanoscale Res. Lett.* **2011**, *6*, 67.
(800) Nguyen, H. L.; Howard, L. E. M.; Giblin, S. R.; Tanner, B. K.; Terry, I.; Hughes, A. K.; Ross, I. M.; Serres, A.; Bürckstümmer, H.; Evans, J. S. O. *J. Mater. Chem.* **2005**, *15*, 5136.
(801) Ferrer, E.; Nater, S.; Rivera, D.; Colon, J. M.; Zayas, F.; Gonzalez, M.; Castro, M. E. *Mater. Res. Bull.* **2012**, *47*, 3835.
(802) Hasegawa, Y.; Okada, Y.; Kataoka, T.; Sakata, T.; Mori, H.; Wada, Y. *J. Phys. Chem. B* **2006**, *110*, 9008.
(803) Liao, X. H.; Zhu, J. J.; Chen, H. Y. *Mater. Sci. Eng., B* **2001**, *85*, 85.
(804) Firth, A. V.; Tao, Y.; Wang, D. S.; Ding, J. F.; Bensebaa, F. *J. Mater. Chem.* **2005**, *15*, 4367.
(805) Dai, Q. L.; Foley, M. E.; Breshike, C. J.; Lita, A.; Strouse, G. F. *J. Am. Chem. Soc.* **2011**, *133*, 15475.
(806) Marx Nirmal, R.; Pandian, K.; Sivakumar, K. *Appl. Surf. Sci.* **2011**, *257*, 2745.
(807) Liu, J.; Xue, D. F. *J. Mater. Chem.* **2011**, *21*, 223.
(808) Wang, Q. B.; Seo, D. K. *Chem. Mater.* **2006**, *18*, 5764.
(809) Pein, A.; Baghbanzadeh, M.; Rath, T.; Haas, W.; Maier, E.; Amenitsch, H.; Hofer, F.; Kappe, C. O.; Trimmel, G. *Inorg. Chem.* **2011**, *50*, 193.
(810) Yang, X.; Xu, J.; Xi, L. J.; Yao, Y. L.; Yang, Q. D.; Chung, C. Y.; Lee, C.-S. *J. Nanopart. Res.* **2012**, *14*, 931.
(811) Yamauchi, T.; Tsukahara, Y.; Yamada, K.; Sakata, T.; Wada, Y. *Chem. Mater.* **2011**, *23*, 75.
(812) Muthuswamy, E.; Iskandar, A. S.; Amador, M. M.; Kauzlarich, S. M. *Chem. Mater.* **2013**, *25*, 1416.
(813) Sarswat, P. K.; Free, M. L. *J. Cryst. Growth* **2013**, *372*, 87.
(814) Borja-Arco, E.; Jiménez Sandoval, O.; Escalante-García, J.; Sandoval-González, A.; Sebastian, P. J. *Int. J. Hydrogen Energy* **2011**, *36*, 103.
(815) Cano, M.; Benito, A.; Maser, W. K.; Urriolabeitia, E. P. *Carbon* **2011**, *49*, 652.
(816) He, R.; Qian, X. F.; Yin, J.; Bian, L. J.; Xi, H. A.; Zhu, Z. K. *Mater. Lett.* **2003**, *57*, 1351.
(817) Sridhar, V.; Jeon, J. H.; Oh, I. K. *Carbon* **2010**, *48*, 2953.
(818) Liao, L. Q.; Zhang, C.; Gong, S. Q. *Macromol. Rapid Commum* **2007**, *28*, 1148.
(819) Liu, Z. L.; Ling, X. Y.; Su, X. D.; Lee, J. Y. *J. Phys. Chem. B* **2004**, *108*, 8234.
(820) Xu, Q.; Zhao, Y.; Xu, J. Z.; Zhu, J. J. *Sens. Actuators, B* **2006**, *114*, 379.
(821) Tang, S. C.; Zheng, Z.; Vongehr, S.; Meng, X. K. *J. Nanopart. Res.* **2011**, *13*, 7085.
(822) Tang, S. C.; Vongehr, S.; Ren, H.; Meng, X. K. *CrystEngComm* **2012**, *14*, 7209.
(823) Shojaee, K.; Edrissi, M.; Izadi, H. *J. Nanopart. Res.* **2010**, *12*, 1439.
(824) Liu, C. J.; Zhang, P.; Tian, F.; Li, W. C.; Li, F.; Liu, W. G. *J. Mater. Chem.* **2011**, *21*, 13163.
(825) Liu, C. J.; Zhang, P.; Zhai, X. Y.; Tian, F.; Li, W. C.; Yang, J. H.; Liu, Y.; Wang, H. B.; Wang, W.; Liu, W. G. *Biomaterials* **2012**, *33*, 3604.
(826) Chen, W. X.; Lee, J. Y.; Liu, Z. L. *Chem. Commun.* **2002**, 2588.
(827) Wang, H. W.; Dong, R. X.; Chang, H. Y.; Liu, C. L.; Chen-Yang, Y. W. *Mater. Lett.* **2007**, *61*, 830.
(828) Liu, Z. L.; Hong, L.; Tham, M. P.; Lim, T. H.; Jiang, H. X. *J. Power Sources* **2006**, *161*, 831.
(829) Zhou, J. H.; He, J. P.; Ji, Y. J.; Dang, W. J.; Liu, X. L.; Zhao, G. W.; Zhang, C. X.; Zhao, J. S.; Fu, Q. B.; Hu, H. P. *Electrochim. Acta* **2007**, *52*, 4691.
(830) Fang, B.; Chaudhari, N. K.; Kim, M. S.; Kim, J. H.; Yu, J. S. *J. Am. Chem. Soc.* **2009**, *131*, 15330.
(831) Zhao, J.; Wang, P.; Chen, W. X.; Liu, R.; Li, X.; Nie, Q. L. *J. Power Sources* **2006**, *160*, 563.
(832) Liu, Z. L.; Gan, L. M.; Hong, L.; Chen, W. X.; Lee, J. Y. *J. Power Sources* **2005**, *139*, 73.
(833) Bian, L. Y.; Wang, Y. H.; Zang, J. B.; Meng, F. W.; Zhao, Y. L. *Int. J. Hydrogen Energy* **2012**, *37*, 1220.
(834) Li, X.; Chen, W. X.; Zhao, J.; Xing, W.; Xu, Z. D. *Carbon* **2005**, *43*, 2168.
(835) Zhang, W. M.; Chen, J.; Swiegers, G. F.; Ma, Z. F.; Wallace, G. G. *Nanoscale* **2010**, *2*, 282.
(836) Chen, W. X.; Zhao, J.; Lee, J. Y.; Liu, Z. L. *Mater. Chem. Phys.* **2005**, *91*, 124.
(837) Hsieh, C. T.; Hung, W. M.; Chen, W. Y. *Int. J. Hydrogen Energy* **2010**, *35*, 8425.
(838) Sharma, S.; Ganguly, A.; Papakonstantinou, P.; Miao, X. P.; Li, M. X.; Hutchison, J. L.; Delichatsios, M.; Ukleja, S. *J. Phys. Chem. C* **2010**, *114*, 19459.
(839) Guo, S. J.; Wen, D.; Zhai, Y. M.; Dong, S. J.; Wang, E. K. *ACS Nano* **2010**, *4*, 3959.
(840) Liao, C.-S.; Liao, C.-T.; Tso, C.-Y.; Shy, H.-J. *Mater. Chem. Phys.* **2011**, *130*, 270.
(841) Wang, S. Y.; Jiang, S. P.; Wang, X. *Electrochim. Acta* **2011**, *56*, 3338.
(842) Hsieh, C. T.; Pan, C.; Chen, W. Y. *J. Power Sources* **2011**, *196*, 6055.
(843) Kim, J. Y.; Kim, K. H.; Park, S. H.; Kim, K. B. *Electrochim. Acta* **2010**, *55*, 8056.
(844) Deshmukh, R. G.; Badadhe, S. S.; Mulla, I. S. *Mater. Res. Bull.* **2009**, *44*, 1179.
(845) Wei, Z. H.; Xing, R. G.; Zhang, X.; Liu, S.; Yu, H. H.; Li, P. C. *ACS Appl. Mater. Interfaces* **2013**, *5*, 598.
(846) Wang, W. W.; Zhu, Y. J. *Curr. Nanosci.* **2007**, *3*, 171.
(847) Zhu, P. L.; Zhang, J. W.; Wu, Z. S.; Zhang, Z. J. *Cryst. Growth Des.* **2008**, *8*, 3148.
(848) Zhang, L.; Zhu, Y. J. *Appl. Phys. A: Mater. Sci. Process.* **2009**, *97*, 847.
(849) Edrissi, M.; Norouzbeigi, R. *J. Mater. Sci.: Mater. Electron.* **2011**, *22*, 328.
(850) Zhao, Y.; Zhu, J. J.; Hong, J. M.; Bian, N. S.; Chen, H. Y. *Eur. J. Inorg. Chem.* **2004**, 4072.
(851) Guo, L. L.; Tong, F.; Liu, H. W.; Yang, H. M.; Li, J. L. *Mater. Lett.* **2012**, *71*, 32.
(852) Lee, J. H.; Hong, S. K.; Ko, W. B. *J. Ind. Eng. Chem.* **2010**, *16*, 564.
(853) Yamamoto, T.; Wada, Y.; Yin, H. B.; Sakata, T.; Mori, H.; Yanagida, S. *Chem. Lett.* **2002**, 964.

(854) Shirke, B. S.; Patil, A. A.; Hankare, P. P.; Garadkar, K. M. *J. Mater. Sci.: Mater. Electron.* **2011**, *22*, 200.
(855) Zawadzki, M. *J. Alloys Compd.* **2008**, *454*, 347.
(856) Hammarberg, E.; Prodi-Schwab, A.; Feldmann, C. *Thin Solid Films* **2008**, *516*, 7437.
(857) Avadhut, Y. S.; Weber, J.; Hammarberg, E.; Feldmann, C.; Schellenberg, I.; Pöttgen, R.; der Günne, J. S. A. *Chem. Mater.* **2011**, *23*, 1526.
(858) Ma, Y. L.; Zhang, L.; Cao, X. F.; Chen, X. T.; Xue, Z. L. *CrystEngComm* **2010**, *12*, 1153.
(859) Li, Z.-Q.; Lin, X.-S.; Zhang, L.; Chen, X.-T.; Xue, Z.-L. *CrystEngComm* **2012**, *14*, 3495.
(860) Jiang, Y.; Zhu, Y. J.; Xu, Z. L. *Mater. Lett.* **2006**, *60*, 2294.
(861) Nekooi, P.; Amini, M. K. *Electrochim. Acta* **2010**, *55*, 3286.
(862) Liu, G.; Zhang, H. M.; Hu, J. W. *Electrochem. Commun.* **2007**, *9*, 2643.
(863) Jiang, Y.; Zhu, Y. J.; Chen, L. D. *Chem. Lett.* **2007**, *36*, 382.
(864) Yao, Q.; Zhu, Y. J.; Chen, L. D.; Sun, Z. L.; Chen, X. H. *J. Alloys Compd.* **2009**, *481*, 91.
(865) Dong, G. H.; Zhu, Y. J.; Chen, L. D. *J. Mater. Chem.* **2010**, *20*, 1976.
(866) Dong, G. H.; Zhu, Y. J.; Chen, L. D. *CrystEngComm* **2011**, *13*, 6811.
(867) Chen, Y. X.; Ji, X. B.; Wang, X. B. *J. Cryst. Growth* **2010**, *312*, 3191.
(868) Qi, R. J.; Zhu, Y. J. *J. Phys. Chem. B* **2006**, *110*, 8302.
(869) Ma, M. G.; Zhu, Y. J.; Chang, J. *J. Phys. Chem. B* **2006**, *110*, 14226.
(870) Rodriguez-Liviano, S.; Aparicio, F. J.; Rojas, T. C.; Hungría, A. B.; Chinchilla, L. E.; Ocaña, M. *Cryst. Growth Des.* **2012**, *12*, 635.
(871) Rodriguez-Liviano, S.; Aparicio, F. J.; Becerro, A. I.; García-Sevillano, J.; Cantelar, E.; Rivera, S.; Hernández, Y.; de la Fuente, J. M.; Ocaña, M. *J. Nanopart. Res.* **2013**, *15*, 1402.
(872) Rodriguez-Liviano, S.; Becerro, A. I.; Alcántara, D.; Grazú, V.; de la Fuente, J. M.; Ocaña, M. *Inorg. Chem.* **2013**, *52*, 647.
(873) Murugan, A. V.; Muraliganth, T.; Manthiram, A. *Electrochem. Commun.* **2008**, *10*, 903.
(874) Harrison, K. L.; Manthiram, A. *Inorg. Chem.* **2011**, *50*, 3613.
(875) Lee, J. M.; Amalnerkar, D. P.; Hwang, Y. K.; Jhung, S. H.; Hwang, J. S.; Chang, J. S. *J. Nanosci. Nanotechnol.* **2007**, *7*, 952.
(876) Zheng, J. Q.; Zhu, Y. J.; Xu, J. S.; Lu, B. Q.; Qi, C.; Chen, F.; Wu, J. *Mater. Lett.* **2013**, *100*, 62.
(877) Yang, X. W.; Zeng, Y. W.; Mo, L. Q.; Han, L. X. *J. Mater. Chem.* **2011**, *21*, 3133.
(878) Marques, V. S.; Cavalcante, L. S.; Sczancoski, J. C.; Alcântara, A. F. P.; Orlandi, M. O.; Moraes, E.; Longo, E.; Varela, J. A.; Li, M. S.; Santos, M. R. M. C. *Cryst. Growth Des.* **2010**, *10*, 4752.
(879) Zhang, L.; Cao, X. F.; Ma, Y. L.; Chen, X. T.; Xue, Z. L. *CrystEngComm* **2010**, *12*, 207.
(880) Walerczyk, W.; Zawadzki, M.; Grabowska, H. *Catal. Lett.* **2011**, *141*, 592.
(881) Bensebaa, F.; Zavaliche, F.; L'Ecuyer, P.; Cochrane, R. W.; Veres, T. *J. Colloid Interface Sci.* **2004**, *277*, 104.
(882) Wang, W. W. *Mater. Chem. Phys.* **2008**, *108*, 227.
(883) Li, Z.-Q.; Lin, X.-S.; Zhang, L.; Chen, X.-T.; Xue, Z.-L. *Mater. Res. Bull.* **2012**, *47*, 2422.
(884) Ding, Y. S.; Xu, L. P.; Chen, C. H.; Shen, X. F.; Suib, S. L. *J. Phys. Chem. C* **2008**, *112*, 8177.
(885) Mi, C. C.; Tian, Z. H.; Cao, C.; Wang, Z. J.; Mao, C. B.; Xu, S. K. *Langmuir* **2011**, *27*, 14632.
(886) Lei, Y. Q.; Pang, M.; Fan, W. Q.; Feng, J.; Song, S. Y.; Dang, S.; Zhang, H. J. *Dalton Trans.* **2011**, *40*, 142.
(887) Liu, G.; Zhang, H. M. *J. Phys. Chem. C* **2008**, *112*, 2058.
(888) Zheng, Q. M.; Cheng, X.; Jao, T.-C.; Weng, F.-B.; Su, A.; Chiang, Y.-C. *Int. J. Hydrogen Energy* **2011**, *36*, 14599.
(889) Huang, M. H.; Li, L. R.; Guo, Y. L. *Electrochim. Acta* **2009**, *54*, 3303.
(890) Zhao, J.; Chen, W. X.; Zheng, Y. F. *Mater. Chem. Phys.* **2009**, *113*, 591.
(891) Chen, F.; Li, C.; Zhu, Y. J.; Zhao, X. Y.; Lu, B. Q.; Wu, J. *Biomater. Sci.* **2013**, *1*, 1074.
(892) Heuser, J. A.; Spendel, W. U.; Pisarenko, A. N.; Yu, C.; Pechan, M. J.; Pacey, G. E. *J. Mater. Sci.* **2007**, *42*, 9057.
(893) Chang, K.; Chen, W.-x.; Li, H.; Li, H. *Electrochim. Acta* **2011**, *56*, 2856.
(894) Yang, L. X.; Zhu, Y. J.; Cheng, G. F. *Mater. Res. Bull.* **2007**, *42*, 159.
(895) Sankar, K. V.; Kalpana, D.; Selvan, R. K. *J. Appl. Electrochem.* **2012**, *42*, 463.
(896) Tu, W. X.; Liu, H. F. *J. Mater. Chem.* **2000**, *10*, 2207.
(897) Jia, F. L.; Wang, F. F.; Lin, Y.; Zhang, L. Z. *Chem.—Eur. J.* **2011**, *17*, 14603.
(898) Hu, L.; Percheron, A.; Chaumont, D.; Brachais, C.-H. *J. Sol-Gel Sci. Technol.* **2011**, *60*, 198.
(899) Cao, S. W.; Zhu, Y. J. *Nanoscale Res. Lett.* **2011**, *6*, 1.
(900) Birkel, A.; Lee, Y.-G.; Koll, D.; Van Meerbeek, X.; Frank, S.; Choi, M. J.; Kang, Y. S.; Char, K.; Tremel, W. *Energy Environ. Sci.* **2012**, *5*, 5392.
(901) Zhang, L.; Zhu, Y. J.; Cao, S. W. *Chem. Lett.* **2008**, *37*, 1002.
(902) Kar, A.; Patra, A. *J. Phys. Chem. C* **2009**, *113*, 4375.
(903) Wilson, G. J.; Will, G. D.; Frost, R. L.; Montgomery, S. A. *J. Mater. Chem.* **2002**, *12*, 1787.
(904) Periyat, P.; Leyland, N.; McCormack, D. E.; Colreavy, J.; Corr, D.; Pillai, S. C. *J. Mater. Chem.* **2010**, *20*, 3650.
(905) Wang, H.-E.; Zheng, L.-X.; Liu, C.-P.; Liu, Y.-K.; Luan, C.-Y.; Cheng, H.; Li, Y. Y.; Martinu, L.; Zapien, J. A.; Bello, I. *J. Phys. Chem. C* **2011**, *115*, 10419.
(906) Zhu, Z. F.; He, Z. L.; Li, J. Q.; Zhou, J. Q.; Wei, N.; Liu, D. G. *J. Mater. Sci.* **2011**, *46*, 931.
(907) Shojaie, A. F.; Loghmani, M. H. *Chem. Eng. J.* **2010**, *157*, 263.
(908) Zhu, J.; Qian, X. F. *J. Solid State Chem.* **2010**, *183*, 1632.
(909) Corradi, A. B.; Bondioli, F.; Ferrari, A. M.; Focher, B.; Leonelli, C. *Powder Technol.* **2006**, *167*, 45.
(910) Xu, L. P.; Ding, Y. S.; Chen, C. H.; Zhao, L. L.; Rimkus, C.; Joesten, R.; Suib, S. L. *Chem. Mater.* **2008**, *20*, 308.
(911) Zhu, Z. F.; Wei, N.; Liu, H.; He, Z. L. *Adv. Powder Technol.* **2011**, *22*, 422.
(912) Lu, Y.; Wang, Y.; Zou, Y. Q.; Jiao, Z.; Zhao, B.; He, Y. Q.; Wu, M. H. *Electrochem. Commun.* **2010**, *12*, 101.
(913) Zhu, J.; Qian, X. F. *Solid State Sci.* **2008**, *10*, 1577.
(914) Peng, Y. P.; Lo, S. L.; Ou, H. H.; Lai, S. W. *J. Hazard. Mater.* **2010**, *183*, 754.
(915) Xie, Y. H.; Yin, S.; Hashimoto, T.; Kimura, H.; Sato, T. *J. Mater. Sci.* **2009**, *44*, 4834.
(916) Lu, C. H.; Bhattacharjee, B.; Chen, S. Y. *J. Alloys Compd.* **2009**, *475*, 116.
(917) Ayele, D. W.; Chen, H.-M.; Su, W.-N.; Pan, C.-J.; Chen, L.-Y.; Chou, H.-L.; Cheng, J.-H.; Hwang, B.-J.; Lee, J.-F. *Chem.—Eur. J.* **2011**, *17*, 5737.
(918) Zhong, S. L.; Lu, Y. H.; Huang, Z. Z.; Wang, S. P.; Chen, J. J. *Opt. Mater.* **2010**, *32*, 966.
(919) Dambournet, D.; Demourgues, A.; Martineau, C.; Pechev, S.; Lhoste, J.; Majimel, J.; Vimont, A.; Lavalley, J. C.; Legein, C.; Buzaré, J. Y.; Fayon, F.; Tressaud, A. *Chem. Mater.* **2008**, *20*, 1459.
(920) Xie, Y. H.; Yin, S.; Yamane, H.; Hashimoto, T.; Machida, H.; Sato, T. *Chem. Mater.* **2008**, *20*, 4931.
(921) Bahadur, N. M.; Watanabe, S.; Furusawa, T.; Sato, M.; Kurayama, F.; Siddiquey, I. A.; Kobayashi, Y.; Suzuki, N. *Colloids Surf., A* **2011**, *392*, 137.
(922) Campelo, J. M.; Conesa, T. D.; Gracia, M. J.; Jurado, M. J.; Luque, R.; Marinas, J. M.; Romero, A. A. *Green Chem.* **2008**, *10*, 853.
(923) Chen, S. Q.; Wang, Y. *J. Mater. Chem.* **2010**, *20*, 9735.
(924) Parker, A.; Marszewski, M.; Jaroniec, M. *ACS Appl. Mater. Interfaces* **2013**, *5*, 1948.
(925) Park, J. C.; Gilbert, D. A.; Liu, K.; Louie, A. Y. *J. Mater. Chem.* **2012**, *22*, 8449.
(926) Bahadur, N. M.; Furusawa, T.; Sato, M.; Kurayama, F.; Siddiquey, I. A.; Suzuki, N. *J. Colloid Interface Sci.* **2011**, *355*, 312.

(927) Siddiquey, I. A.; Furusawa, T.; Sato, M.; Bahadur, N. M.; Suzuki, N. *Mater. Chem. Phys.* **2011**, *130*, 583.
(928) Bahadur, N. M.; Furusawa, T.; Sato, M.; Kurayama, F.; Suzuki, N. *Mater. Res. Bull.* **2010**, *45*, 1383.
(929) Stutz, C.; Bilecka, I.; Thünemann, A. F.; Niederberger, M.; Böerner, H. G. *Chem. Commun.* **2012**, *48*, 7176.
(930) Luo, H. L.; Sheng, J.; Wan, Y. Z. *Mater. Lett.* **2008**, *62*, 37.
(931) Wang, Y. Q.; Wang, G. Z.; Wang, H. Q.; Tang, C. J.; Jiang, Z.; Zhang, L. D. *Chem. Lett.* **2007**, *36*, 674.
(932) Xu, J. S.; Zhu, Y. J. *Mater. Lett.* **2011**, *65*, 2793.
(933) Apte, S. K.; Naik, S. D.; Sonawane, R. S.; Kale, B. B.; Pavaskar, N.; Mandale, A. B.; Das, B. K. *Mater. Res. Bull.* **2006**, *41*, 647.
(934) Limaye, M. V.; Gokhale, S.; Acharya, S. A.; Kulkarni, S. K. *Nanotechnology* **2008**, *19*, 415602.
(935) Li, W. J.; Li, D. Z.; Zhang, W. J.; Hu, Y.; He, Y. H.; Fu, X. Z. *J. Phys. Chem. C* **2010**, *114*, 2154.
(936) Ma, M. G.; Zhu, Y. J. *Mater. Lett.* **2008**, *62*, 2512.
(937) Zhang, L.; Cao, X. F.; Ma, Y. L.; Chen, X. T.; Xue, Z. L. *CrystEngComm* **2010**, *12*, 3201.
(938) Doolittle, J. W.; Dutta, P. K. *Langmuir* **2006**, *22*, 4825.
(939) Chen, Y. X.; He, B. L.; Liu, H. F. *J. Mater. Sci. Technol.* **2005**, *21*, 187.
(940) Tong, X.; Zhao, Y. X.; Huang, T.; Liu, H. F.; Liew, K. Y. *Appl. Surf. Sci.* **2009**, *255*, 9463.
(941) Chen, W. F.; Yan, L. F.; Bangal, P. R. *Carbon* **2010**, *48*, 1146.
(942) Xi, G. C.; He, Y. T.; Zhang, Q.; Xiao, H. Q.; Wang, X.; Wang, C. *J. Phys. Chem. C* **2008**, *112*, 11645.
(943) Thongtem, T.; Jattukul, S.; Phuruangrat, A.; Thongtem, S. *J. Alloys Compd.* **2010**, *491*, 654.
(944) Ma, M. G.; Zhu, Y. J.; Cheng, G. F.; Huang, Y. H. *Mater. Lett.* **2008**, *62*, 507.
(945) Li, Y. F.; Li, H. F.; Cao, R. *J. Am. Ceram. Soc.* **2009**, *92*, 2188.
(946) Li, Y. F.; Li, H. F.; Li, T. H.; Li, G. L.; Cao, R. *Microporous Mesoporous Mater.* **2009**, *117*, 444.
(947) Szeifert, J. M.; Feckl, J. M.; Fattakhova-Rohlfing, D.; Liu, Y. J.; Kalousek, V.; Rathousky, J.; Bein, T. *J. Am. Chem. Soc.* **2010**, *132*, 12605.
(948) Parmar, K. P. S.; Ramasamy, E.; Lee, J.; Lee, J. S. *Chem. Commun.* **2011**, *47*, 8572.
(949) Nyutu, E. K.; Chen, C. H.; Sithambaram, S.; Crisostomo, V. M. B.; Suib, S. L. *J. Phys. Chem. C* **2008**, *112*, 6786.
(950) Opembe, N. N.; King'ondu, C. K.; Espinal, A. E.; Chen, C. H.; Nyutu, E. K.; Crisostomo, V. M.; Suib, S. L. *J. Phys. Chem. C* **2010**, *114*, 14417.
(951) Panda, A. B.; Glaspell, G.; El-Shall, M. S. *J. Phys. Chem. C* **2007**, *111*, 1861.
(952) Caponetti, E.; Martino, D. C.; Leone, M.; Pedone, L.; Saladino, M. L.; Vetri, V. *J. Colloid Interface Sci.* **2006**, *304*, 413.
(953) Shinde, M. D.; Pawar, A. U.; Sreeja, V.; Rane, S.; Potdar, H. S.; Amalnerkar, D. P. *Int. J. Nanotechnol.* **2010**, *7*, 1120.
(954) Amalnerkar, D. P.; Lee, H. Y.; Hwang, Y. K.; Kim, D. P.; Chang, J. S. *J. Nanosci. Nanotechnol.* **2007**, *7*, 4412.
(955) Patra, C. R.; Patra, S.; Gabashvili, A.; Mastai, Y.; Koltypin, Y.; Gedanken, A.; Palchik, V.; Slifkin, M. A. *J. Nanosci. Nanotechnol.* **2006**, *6*, 845.
(956) Yan, S. C.; Wang, H. T.; Zhang, Y. P.; Li, S. C.; Xiao, Z. D. *J. Non-Cryst. Solids* **2008**, *354*, 5559.
(957) Wang, Y.; Ai, X.; Miller, D.; Rice, P.; Topuria, T.; Krupp, L.; Kellock, A.; Song, Q. *CrystEngComm* **2012**, *14*, 7560.
(958) Panigrahi, P. K.; Pathak, A. *Sci. Technol. Adv. Mater.* **2008**, *9*, 045008.
(959) Sun, C.; Gardner, J. S.; Shurdha, E.; Margulieux, K. R.; Westover, R. D.; Lau, L.; Long, G.; Bajracharya, C.; Wang, C. M.; Thurber, A.; Punnoose, A.; Rodriguez, R. G.; Pak, J. J. *J. Nanomater.* **2009**, *2009*, 748567.
(960) Sliem, M. A.; Chemseddine, A.; Bloeck, U.; Fischer, R. A. *CrystEngComm* **2011**, *13*, 483.
(961) Han, D. M.; Song, C. F.; Li, X. Y. *Mater. Chem. Phys.* **2009**, *116*, 41.
(962) Panda, A. B.; Glaspell, G.; El-Shall, M. S. *J. Am. Chem. Soc.* **2006**, *128*, 2790.
(963) Wang, H. Q.; Nann, T. *Nanoscale Res. Lett.* **2011**, *6*, 267.
(964) Wang, H. Q.; Nann, T. *ACS Nano* **2009**, *3*, 3804.
(965) Wang, H. Q.; Tilley, R. D.; Nann, T. *CrystEngComm* **2010**, *12*, 1993.
(966) Quan, Z. W.; Yang, P. P.; Li, C. X.; Yang, J.; Yang, D. M.; Jin, Y.; Lian, H. Z.; Li, H. Y.; Lin, J. *J. Phys. Chem. C* **2009**, *113*, 4018.
(967) Liu, S.; Tian, J. Q.; Wang, L.; Luo, Y. L.; Zhai, J. F.; Sun, X. P. *J. Mater. Chem.* **2011**, *21*, 11726.
(968) Herring, N. P.; Almahoudi, S. H.; Olson, C. R.; El-Shall, M. S. *J. Nanopart. Res.* **2012**, *14*, 1277.
(969) Jiang, Z. Z.; Wang, Z. B.; Chu, Y. Y.; Gu, D. M.; Yin, G. P. *Energy Environ. Sci.* **2011**, *4*, 728.
(970) Herring, N. P.; AbouZeid, K.; Mohamed, M. B.; Pinsk, J.; El-Shall, M. S. *Langmuir* **2011**, *27*, 15146.
(971) Bensebaa, F.; Farah, A. A.; Wang, D. S.; Bock, C.; Du, X. M.; Kung, J.; Le Page, Y. *J. Phys. Chem. B* **2005**, *109*, 15339.
(972) Kate, K. H.; Singh, K.; Khanna, P. K. *Synth. React. Inorg., Met.-Org., Nano-Met. Chem.* **2011**, *41*, 199.
(973) Mohamed, M. B.; AbouZeid, K. M.; Abdelsayed, V.; Aljarash, A. A.; El-Shall, M. S. *ACS Nano* **2010**, *4*, 2766.
(974) Gao, F.; Lu, Q. Y.; Komarneni, S. *Chem. Mater.* **2005**, *17*, 856.
(975) Erten-Ela, S.; Cogal, S.; Icli, S. *Inorg. Chim. Acta* **2009**, *362*, 1855.
(976) Jiang, F. Y.; Wang, C. M.; Fu, Y.; Liu, R. C. *J. Alloys Compd.* **2010**, *503*, L31.
(977) Baruwati, B.; Nadagouda, M. N.; Varma, R. S. *J. Phys. Chem. C* **2008**, *112*, 18399.
(978) Zedan, A. F.; Abdelsayed, V.; Mohamed, M. B.; El-Shall, M. S. *J. Nanopart. Res.* **2013**, *15*, 1312.
(979) Sun, C.; Su, X. T.; Xiao, F.; Niu, C. G.; Wang, J. D. *Sens. Actuators, B* **2011**, *157*, 681.
(980) Rahal, R.; Wankhade, A.; Cha, D.; Fihri, A.; Ould-Chikh, S.; Patil, U.; Polshettiwar, V. *RSC Adv.* **2012**, *2*, 7048.
(981) Tao, Y.; Wang, H.; Xia, Y. P.; Zhang, G. Q.; Wu, H. P.; Tao, G. L. *Mater. Chem. Phys.* **2010**, *124*, 541.
(982) Bondioli, F.; Corradi, A. B.; Ferrari, A. M.; Leonelli, C. *J. Am. Ceram. Soc.* **2008**, *91*, 3746.
(983) Ma, J.; Huang, X.; Cheng, H.; Zhao, Z.; Qi, L. *J. Mater. Sci. Lett.* **1996**, *15*, 1247.
(984) Su, H. P.; Xu, H. Y.; Gao, S. A.; Dixon, J. D.; Aguilar, Z. P.; Wang, A. Y.; Xu, J.; Wang, J. K. *Nanoscale Res. Lett.* **2010**, *5*, 625.
(985) Zhu, M. Q.; Gu, Z.; Fan, J. B.; Xu, X. B.; Cui, J.; Liu, J. H.; Long, F. *Langmuir* **2009**, *25*, 10189.
(986) Song, Q.; Ai, X.; Topuria, T.; Rice, P. M.; Alharbi, F. H.; Bagabas, A.; Bahattab, M.; Bass, J. D.; Kim, H. C.; Scott, J. C.; Miller, R. D. *Chem. Commun.* **2010**, *46*, 4971.
(987) Mehta, R. J.; Zhang, Y. L.; Karthik, C.; Singh, B.; Siegel, R. W.; Borca-Tasciuc, T.; Ramanath, G. *Nat. Mater.* **2012**, *11*, 233.
(988) Sulaeman, U.; Yin, S.; Sato, T. *Appl. Catal., B* **2011**, *105*, 206.
(989) Zhang, L.; Zhu, Y. J. *J. Phys. Chem. C* **2008**, *112*, 16764.
(990) Zhu, Z. F.; Liu, D. G.; Liu, H.; Li, G. J.; Du, J.; He, Z. L. *J. Lumin.* **2012**, *132*, 261.
(991) Dambournet, D.; Demourgues, A.; Martineau, C.; Durand, E.; Majimel, J.; Vimont, A.; Leclerc, H.; Lavalley, J. C.; Daturi, M.; Legein, C.; Buzaré, J. Y.; Fayon, F.; Tressaud, A. *J. Mater. Chem.* **2008**, *18*, 2483.
(992) Wang, D.; Ren, L.; Zhou, X.; Wang, X.-z.; Zhou, J.; Han, Y.; Kang, N. *Nanotechnology* **2012**, *23*, 225705.
(993) Yang, C.; Yang, P. P.; Wang, W. X.; Gai, S. L.; Wang, J.; Zhang, M. L.; Lin, J. *Solid State Sci.* **2009**, *11*, 1923.
(994) Chen, Z. W.; Li, S.; Yan, Y. S. *Chem. Mater.* **2005**, *17*, 2262.
(995) Hu, Q. T.; Gan, Z. B.; Zheng, X. W.; Lin, Q. F.; Xu, B. F.; Zhao, A. H.; Zhang, X. *Superlattices Microstruct.* **2011**, *49*, 537.
(996) Luo, Z. M.; Ma, X. B.; Yang, D. L.; Yuwen, L. H.; Zhu, X. R.; Weng, L. X.; Wang, L. H. *Carbon* **2013**, *57*, 470.
(997) Yang, C. Z.; van der Laak, N. K.; Chan, K.-Y.; Zhang, X. *Electrochim. Acta* **2012**, *75*, 262.

(998) Jeon, S. S.; Kim, C.; Ko, J.; Im, S. S. *J. Phys. Chem. C* **2011**, *115*, 22035.
(999) He, Y. J.; Yang, B. L.; Cheng, G. X.; Pan, H. M. *Powder Technol.* **2003**, *134*, 52.
(1000) Zedan, A. F.; Sappal, S.; Moussa, S.; El-Shall, M. S. *J. Phys. Chem. C* **2010**, *114*, 19920.
(1001) Ziegler, J.; Merkulov, A.; Grabolle, M.; Resch-Genger, U.; Nann, T. *Langmuir* **2007**, *23*, 7751.
(1002) Roy, M. D.; Herzing, A. A.; Lacerda, S. H. D. P.; Becker, M. L. *Chem. Commun.* **2008**, 2106.
(1003) Zhu, L. W.; Chen, P.; Guo, Y.; Song, Y. Y.; Xue, X. D.; Cao, X. B. *Colloids Surf., A* **2010**, *360*, 111.
(1004) He, R.; Qian, X. F.; Yin, J.; Zhu, Z. K. *Chem. Phys. Lett.* **2003**, *369*, 454.
(1005) Olgun, U. *ACS Appl. Mater. Interfaces* **2010**, *2*, 28.
(1006) Cao, C.-Y.; Guo, W.; Cui, Z.-M.; Song, W.-G.; Cai, W. *J. Mater. Chem.* **2011**, *21*, 3204.
(1007) Kijima, N.; Yoshinaga, M.; Awaka, J.; Akimoto, J. *Solid State Ionics* **2011**, *192*, 293.
(1008) Katsuki, H.; Komarneni, S. *J. Am. Ceram. Soc.* **2001**, *84*, 2313.
(1009) Dahal, N.; García, S.; Zhou, J. P.; Humphrey, S. M. *ACS Nano* **2012**, *6*, 9433.
(1010) Bhattacharya, S.; Mallik, D.; Nayar, S. *IEEE Trans. Magn.* **2011**, *47*, 1647.
(1011) Lewis, D. A.; Summers, J. D.; Ward, T. C.; McGrath, J. E. *J. Polym. Sci., Part A* **1992**, *30*, 1647.
(1012) Brosnan, K. H.; Messing, G. L.; Agrawal, D. K. *J. Am. Ceram. Soc.* **2003**, *86*, 1307.
(1013) Fang, X. M.; Hutcheon, R.; Scola, D. A. *J. Polym. Sci., Part A* **2000**, *38*, 2526.
(1014) Haque, E.; Kim, C. M.; Jhung, S. H. *CrystEngComm* **2011**, *13*, 4060.
(1015) Haque, E.; Khan, N. A.; Kim, C. M.; Jhung, S. H. *Cryst. Growth Des.* **2011**, *11*, 4413.
(1016) Gutmann, B.; Obermayer, D.; Reichart, B.; Prekodravac, B.; Irfan, M.; Kremsner, J. M.; Kappe, C. O. *Chem.—Eur. J.* **2010**, *16*, 12182.